The effects of triglycerides and fatty acids on T cells: role in atherosclerosis

Reilly, N.A.

The effects of triglycerides and fatty acids on T cells: role in atherosclerosis

Nathalie Reilly

The effects of triglycerides and fatty acids on T cells: role in atherosclerosis
N. A. Reilly, MSc.

ISBN: 978-94-93391-54-3

The research described in this thesis was supported by the Dutch CardioVascular Alliance (The Dutch Heart Foundation, Dutch Federation of University Medical Centres, the Netherlands Organization for Health Research and Development, and the Royal Netherlands Academy of Sciences) for the GENIUSII project Generating the Best Evidence-Based Pharmaceutical Targets for Atherosclerosis (CVON2011-19 and CVON2017-20).

Financial support by the Dutch Heart Foundation for the publication of this thesis is gratefully acknowledged.

Cover Design: Extended License purchased from stock.adobe.com and adapted from ©MIMOSA - stock.adobe.com by Nathalie Reilly
Printed by Proefschriftspecialist | proefschriftspecialist.nl
Layout and design: Hans Schaapherder, persoonlijkproefschrift.nl

The effects of triglycerides and fatty acids on T cells: role in atherosclerosis

Proefschrift

ter verkrijging van
de graad van doctor aan de Universiteit Leiden,
op gezag van rector magnificus prof.dr.ir H. Bijl,
volgens besluit van het college voor promoties
te verdedigen op woensdag 30 oktober 2024
klokke 14:30 uur

door
Nathalie Amara Reilly
geboren te Amsterdam
in 1992

Promotors:	Prof. dr. B. T. Heijmans Prof. dr. J. W. Jukema
Promotion Commission:	Prof. dr. P. C. N. Rensen Prof. dr. P. E. Slagboom Prof. dr. I. Bot, *Leiden Academic Centre for Drug Research (LACDR)* Dr. J. Van den Bossche, *Amsterdam University Medical Center, location VUMC*

Contents

CHAPTER 1

Introduction

Atherosclerosis

Atherosclerosis is considered to be a lipid-driven immune disease and is the dominant cause of cardiovascular disease (CVD), which is the leading cause of death worldwide[1, 2]. The initiation of atherosclerosis is generally attributed to excess low-density lipoprotein (LDL). This cholesterol laden lipoprotein is able to cross to the inner most layer of the arterial wall, the intima, and can accumulate there[3]. Here, the LDL particles can undergo oxidation which induces a pro-inflammatory response in the endothelial cells that make up part of the arterial intima[4]. The activated endothelial cells release chemokines, chemoattractant cytokines, that attract monocytes to the site. These monocytes mature into macrophages which can take up the accumulated LDL[1]. However, the pro-inflammatory landscape of the intima causes macrophages to upregulate the expression of scavenger receptors and downregulate the expression of cholesterol transporters and in turn, generates foam cell formation[5]. Foam cells are unable to leave the intima and aggregate, contributing to atherosclerotic plaque formation[6]. Plaque formation progresses by the continued accumulation of lipids and cells to the site and the formation of a fibrous cap[1]. As atherosclerosis advances, a necrotic core may develop as clearance of cells that underwent programmed cell death in the plaque fails[7]. Furthermore, advanced plaques may undergo calcification, in which calcium minerals accumulate, hardening the plaque and increasing the risk of rupture[8]. Complications of atherosclerosis arise as the plaque builds up, narrowing the arterial lumen and limiting blood flow[1]. Further complications include plaque rupture and erosion[9, 10]. Both plaque rupture and erosion form thrombi which can be released into the circulation and are the main cause of myocardial infarction and stroke[1].

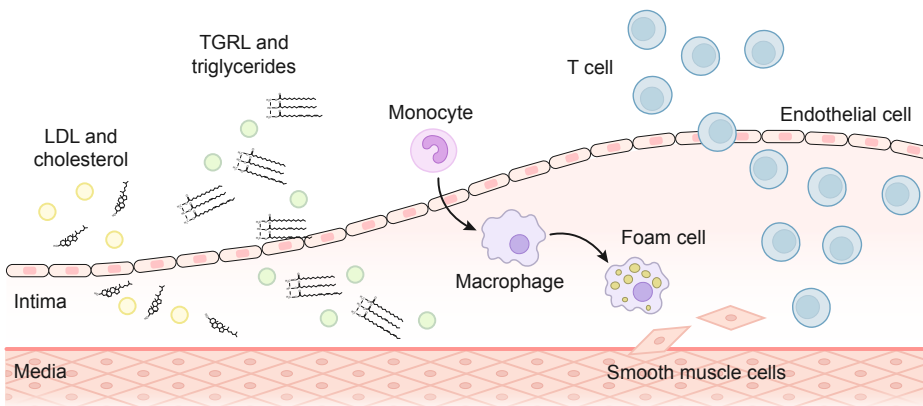

Fig. 1 | Initiation of atherosclerosis pathogenesis. Yellow circles are LDL, green circles are TGRLs, monocytes are in pink, macrophages and foam cells are purple, T cells are blue, endothelial cells are light pink, and smooth muscle cells are light red. Adapted from "Atherosclerosis" by Libby, P. *et. al.*[1].

While much of the pathogenesis of atherosclerosis is classically attributed to macrophages and LDL, it has become increasingly clear that other factors play a crucial role its development. Most notably, triglycerides and T cells have re-emerged as pivotal factors in the pathogenesis of

atherosclerosis[11-14]. Triglycerides are also contained in various lipoproteins such as triglyceride rich lipoproteins (TGRLs), which can cross the arterial intima and aggravate the disease[15]. T cells are attracted into the plaque by the inflammatory response induced by macrophages[11, 12] (Fig. 1). However, the potentially important role of the interaction between these re-emerging risk factors in atherosclerosis remains largely unknown.

T cells

T cells are a component of the adaptive immune system generally found in the lymphatic and circulatory systems in humans. These cells can broadly be split into two categories, $CD4^+$ T cells and $CD8^+$ T cells. T cell function is driven in part by strict metabolic processes that also drive cell fate[16]. Generally speaking, non-activated T cells favor the utilization of β-fatty acid oxidation, whereas activated T cells switch towards utilizing aerobic glycolysis[17, 18]. The main function of T cells is to sense and respond to their environment which, in the circulation, consists of numerous factors including lipids such as triglycerides. However, whether these interactions with lipids in the circulation can have lasting effects on T cells that could impact their function in atherosclerosis remains unknown.

It is known that throughout atherosclerotic development significant numbers of T cells are found in plaques. Specifically, through the use of single cell RNA sequencing and mass spectrometry, it was found that over half of all immune cells present in the atherosclerotic plaque were T cells[19-22]. Furthermore, these studies found that of the T cells present, half were $CD4^+$ and the other half were $CD8^+$ T cells[19] (Fig. 2). Although this technique may selectively favor the survival of T cells over that of other cell types such as macrophages and smooth muscle cells due to the inherent destructiveness of this technique, particularly during the cell isolation phase, the significance of these findings should not be overlooked. Both $CD4^+$ and $CD8^+$ T cells exhibit distinctive characteristics and functions in atherosclerosis[11, 12]. While the role of T cells in atherosclerosis has been studied to some extent, there remains a substantial knowledge gap regarding the mechanisms that govern T cell responses in the plaque and the factors that influence the preferential expression of certain subsets over others.

$CD4^+$ T cells

$CD4^+$ T cells are generally known as helper T cells and are characterized by the expression of both $CD3^+$ and $CD4^+$ on the cell surface. In atherosclerosis, $CD4^+$ T cells generally play a pro-inflammatory role as deficiency of $CD4^+$ T cell was atheroprotective[23] and adoptive transfer of $CD4^+$ T cells was pro-atherogenic[24, 25] in *Apoe*$^{-/-}$ mouse models. $CD4^+$ T cells have multiple functions including activating other immune cells such as B cells and cytotoxic T cells, releasing cytokines, and suppressing immune reactions[26]. Furthermore, upon activation $CD4^+$ T cells can differentiate into subsets, the most well-studied being T helper 1 (T_H1), T helper 2 (T_H2), T helper 17 (T_H17), and T regulatory (T_{reg}) cells[27]. Each subset has a distinguished phenotype, metabolic profile, and plays a different role in disease development and pathogenesis[18, 27, 28] (Fig. 3).

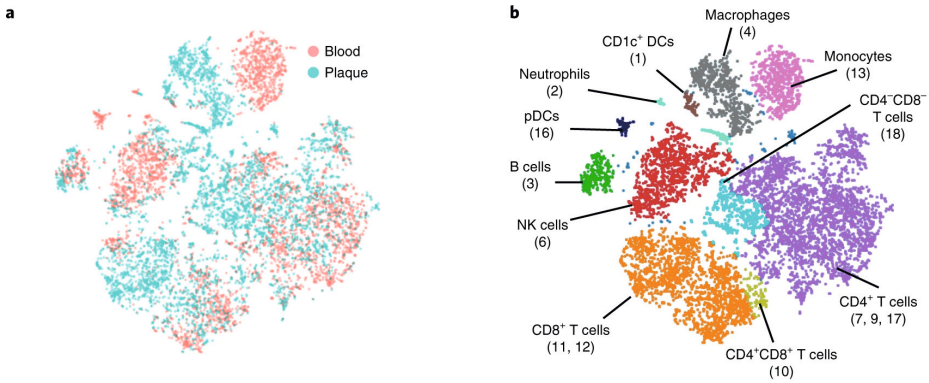

Fig. 2 | Immune cell populations in the blood and atherosclerotic plaque. Adapted from "Single-cell immune landscape of human atherosclerotic plaques" by Fernandez, D. M. *et. al.* showing the proportion of different immune cells in atherosclerotic plaques[19]. Figures are viSNE plots of $CD45^+$ immune cells (n = 9,490) derived from blood and plaque tissue of 15 patients. Clustering is based on the MetaLouvain method. **(a)** Immune cell populations in the blood (red) and in the plaque (blue). **(b)** Immune cell populations as defined by mass cytometry (CyTOF).

T_H1 cells are characterized by the expression of the key transcription factor T-bet, as well as signal transducer and activator of transcription (STAT)1 and STAT4, and generally produce interferon gamma (IFNγ) and tumor necrosis factor alpha (TNFα)[29, 30]. These cells are known to play a strong pro-inflammatory role in atherosclerosis and are the largest $CD4^+$ subset in the plaque[28]. T_H2 cells are characterized by the expression of the key transcription factor GATA3, as well as STAT5 and STAT6, and generally produce interleukin (IL)-4, IL-5, and IL-13[29, 31]. The exact role of T_H2 cells in atherosclerosis has not yet been determined as contradicting results show both pro- and anti-inflammatory effects[28]. However, a subset of T_H2 cells, T_H9 cells[32], have shown to be highly pro-inflammatory in atherosclerotic disease[33-35]. T_H9 cells are characterized by the expression of the transcription factor PU.1 and interferon regulatory factor (IRF)4 and generally produce IL-9[29]. T_H17 cells are characterized by the expression of the key transcription factor RAR related orphan receptor (ROR)γt as well as STAT3, and generally produce IL-17, IL-21, and IL-22[29, 36]. The role of T_H17 cells in atherosclerosis has not yet been defined as both pro- and anti-inflammatory effects have been found[28]. T_{reg} cells are characterized by the expression of the key transcription factor forkhead box P3 (FoxP3) as well as STAT5, and cells generally produce IL-10[29, 37]. T_{regs} are notably anti-inflammatory and atheroprotective[28]. Multiple factors play a role in subset differentiation, such as the surrounding cytokine environment and cellular metabolism, specifically lipid metabolism[27, 38, 39]. Defining how extracellular lipids may influence $CD4^+$ T cell differentiation can aid in understanding T cell responses in atherosclerotic plaques.

$CD8^+$ T cells

$CD8^+$ T cells are generally known as cytotoxic T cells and are characterized by the expression of both $CD3^+$ and $CD8^+$ on the cell surface. While $CD8^+$ T cells don't have defined subsets as $CD4^+$ T cells, they can be broadly divided into cytotoxic and regulatory $CD8^+$ T cells[40]. While the frequency of $CD8^+$ T cells is increased in plaques[19] and in the blood of patients with coronary

artery disease[41], both a pro- as well as an anti-inflammatory role has been found for CD8⁺ T cells in atherosclerosis development and progression[28, 42, 43]. Cytotoxic CD8⁺ T cells have been shown to produce IFNγ, perforin and granzyme B, which may aggravate atherosclerosis[44, 45]. On the other hand, regulatory CD8⁺ T cells may play an atheroprotective role by limiting the accumulation of T_H1 cells and macrophages and stabilizing plaques[46]. Furthermore, immunization with an ApoB- related peptide (p210) has shown an atheroprotective role mediated through CD8⁺ T cells[47, 48]. Overall, CD8⁺ T cells may play an interesting role in atherosclerosis although the exact mechanisms through which these cells induce a pro- or anti-inflammatory effect and whether lipids influence these effects have not yet been studied.

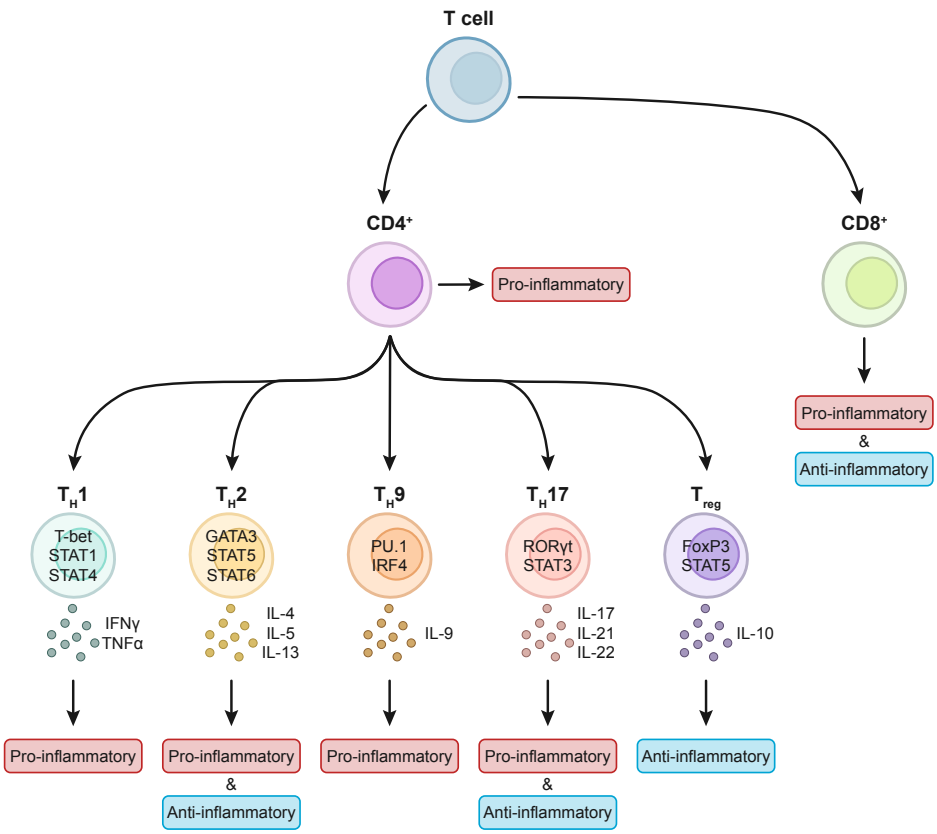

Fig. 3 | Defining transcription factors, cytokines, and role in atherosclerosis pathogenesis of different T cell subsets. T cell subsets are labelled in bold above the cell, main transcription factors are labelled inside of the cells, main cytokines produced are labelled below and to the right of the cell, and the function in atherosclerosis pathogenesis can be found below the main cytokines excreted and is either pro- or anti-inflammatory, or both.

Triglycerides and fatty acids

Triglycerides have re-emerged as a potential risk factor for cardiovascular disease. Population studies showed that increased circulating levels of triglycerides are associated with an increased risk of CVD[49-53] (Fig. 4). Furthermore, this lipid group remains a risk factor for CVD also after accounting for the effect of total cholesterol and high-density lipoprotein (HDL) cholesterol[13, 14]. This can, in part, explain why a residual risk of CVD is still present even in individuals with substantially reduced LDL cholesterol levels[54]. Elevated triglycerides are the characteristic attribute of a lipid disorder called hypertriglyceridemia[55]. This disorder may occur due to primary factors such as one or more mutations in the *LPL*, *APOA5*, or *APOE2* genes, or due to secondary factors such as diabetes, obesity, or excessive alcohol use. As such, hypertriglyceridemia has been linked to a higher risk of CVD, specifically in individuals with moderately elevated triglyceride concentrations (between 2–10 mmol/L)[56, 57]. Hypertriglyceridemia patients with extremely elevated triglyceride concentrations (>13.0mmol/L) often are no longer at risk for CVD because their excessive triglyceride levels get stored in large chylomicron lipoprotein particles that cannot cross the arterial wall[58]. Reduced triglyceride concentrations may protect from atherosclerosis, a characteristic of individuals with hypotriglyceridemia with triglyceride concentrations below 0.3 mmol/L[59]. Individuals with these disorders may offer interesting insights into the effects of elevated or depressed triglycerides on circulating T cells.

The exact contribution of triglycerides in CVD is still widely debated. This is, in part, due to the fact that triglyceride lowering therapies, such as fibrates and niacin, have not demonstrated a convincing benefit for CVD risk[60-64]. Yet, there has been one drug that has shown triglyceride lowering and substantial CVD risk reduction in patients with hypertriglyceridemia, namely icosapent ethyl (IPE)[65-67]. IPE is a highly purified and esterified form of the fatty acid eicosapentaenoic acid (EPA). IPE contains an ethyl group which is cleaved off as the drug is metabolized after ingestion in the human body, exposing cells directly to EPA[68]. The REDUCE-IT trial showed a 25% decrease in primary composite end points and a 26% decrease in secondary composite end points, even when correcting for factors such as the use of mineral oil in the control group[65, 69, 70]. The mechanism of action for this risk reduction remain largely unknown as the beneficial effects observed occurred independently of triglyceride lowering in REDUCE-IT[65], and studies into this research question are thus far limited to model membranes or in whole blood[71-73].

EPA is a polyunsaturated fatty acid, one that has more than one double bond in its carbon chain. Specifically, EPA has 5 double bonds in its 20-carbon chain denoting it as C20:5. Fatty acids may also be saturated, with no double bonds such as palmitic acid (C16:0), or monounsaturated, with one double bond such as oleic acid (C18:1). Palmitic and oleic acid are some of the most common fatty acid in the human circulation[74] and have both been shown to have pro-atherogenic effects[75-79]. Interestingly, triglycerides, which are partially comprised of fatty acids, are hydrolyzed into the fatty acid components inside cells which can be further metabolized and used by the cell[80, 81]. As such, fatty acids may also have a noteworthy influence on T cell function, potentially through changes in cellular metabolism, that could determine T cell effects in atherosclerosis.

However, the exact relationship between different fatty acids, atherosclerosis and T cells has yet to be explored.

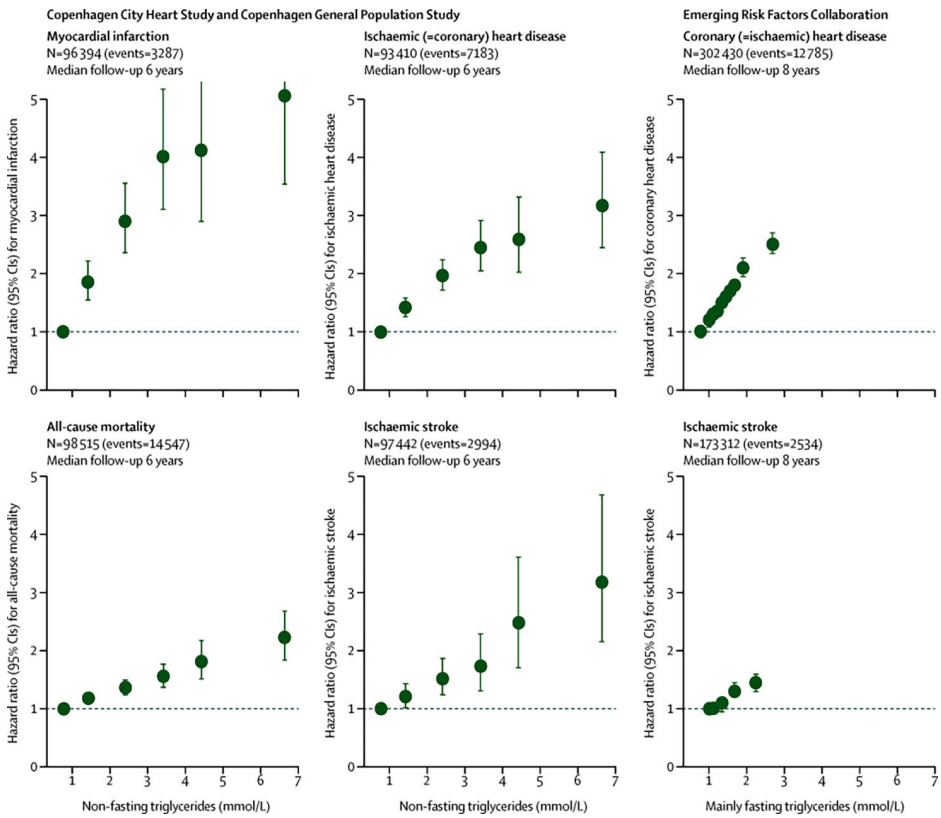

Fig. 4 | Increased hazard ratio with increased non-fasting triglycerides. Adapted from "Triglycerides and cardiovascular disease" by Nordestgaard, B. G. and Varbo, A. showing that increasing triglyceride levels increase the hazard ratio for myocardial infarction, ischemic heart disease, all-cause mortality, and ischemic stroke[56].

Outline of this thesis

This thesis aims to uncover how non-activated T cells can be influenced by triglycerides and fatty acids found in the circulation and whether this interaction can have a lasting effect on T cell function that may influence the role T cells play in atherosclerosis. Particularly, we focus on $CD4^+$ T cells as their role in atherosclerosis has been more well defined and explore the effects of fatty acids and triglycerides from *in vitro* to *in vivo*.

In **Chapter 2** we delve deeper into the role various fatty acids play in atherosclerosis development, how those fatty acids can influence T cell function, and whether the interactions between fatty acids and T cells in the circulation may influence the role T cells play in atherosclerosis. We review the

effects of 14 different fatty acids on four different T cell processes namely, metabolism, activation, proliferation, and differentiation. Indeed, it has been found that fatty acids can influence T cell function post activation and that the effect fatty acids have on T cells, pro- or anti-inflammatory, match the effect that fatty acid is known to have on atherosclerosis. However, interactions between fatty acids and T cells occur prior to atherosclerosis development, in the circulation, where T cells are in a non-activated state. Thus, this chapter concludes by hypothesizing that the interactions that take place between T cells and fatty acids in the circulation may have effects that influence the effect T cells have upon entering the high lipid environment of the atherosclerotic plaque.

In order to test the hypothesis provided in the previous chapter, that is, whether fatty acids can influence non-activated T cells, **Chapter 3** presents a new *in vitro* model to test the effect of fatty acids on non-activated $CD4^+$ T cells and apply it to evaluate the effects of oleic acid. This monounsaturated fatty acid is one of the most abundant fatty acids in the circulation and has been associated with an increased risk of CVD[78]. However, the role of oleic acid on T cells has shown opposing results. To elucidate the effects of oleic acid on $CD4^+$ T cells, we determined changes in gene expression in non-activated cells after exposure and measured phenotypic markers post-activation. Additionally, we test the role cellular metabolism plays in determining functional outcome by exposing the cells to metabolic inhibitors during oleic acid exposure.

Building on this work, in **Chapter 4**, we determine the effects of EPA, palmitic and oleic acid on non-activated $CD4^+$ T cells. In it purified form IPA, EPA was shown to be highly atheroprotective in the influential REDUCE-IT trial. However, the mechanism by which EPA induces anti-inflammatory effects remains unclear. Here, we aim to uncover whether EPA induces an anti-inflammatory transcriptomic profile in non-activated $CD4^+$ T cells, which could aid in explaining the beneficial effects measured in REDUCE-IT. To distinguish the unique effect of EPA on $CD4^+$ T cells, this chapter also compares the results of EPA exposure to two other fatty acids of different saturation, palmitic acid, a saturated fatty acid, and oleic acid, a monounsaturated fatty acid.

The previous chapters use an *in vitro* model to evaluate the effects of fatty acids on non-activated T cells. In **Chapter 5** we move to an *in vivo*, human setting to test whether prolonged exposure to elevated triglycerides, the form in which fatty acids are transported in the circulation, affects $CD4^+$ and $CD8^+$ T cells *in vivo*. Gene expression changes were measured in $CD4^+$ and $CD8^+$ T cells derived from patients with moderate hypertriglyceridemia, in the range that is a risk for CVD. We divide the patient groups into primary moderate, due to genetic mutations, and secondary moderate, due to lifestyle. Additionally, we tested individuals with primary severe hypertriglyceridemia, above the range at risk of CVD, and individuals with primary hypotriglyceridemia, severely depleted triglyceride levels. This was done to test whether the effects on T cells would dissipate when triglycerides are more likely stored in chylomicrons, as is the case in primary severe hypertriglyceridemia, or whether the effects on T cells would be anti-inflammatory in the absence of triglycerides, as is the case in hypotriglyceridemia.

Lastly, all results of this thesis are summarized, connected, and put into context in **Chapter 6**. Here, we discuss the findings and deliberate the implications thereof as well as comment on the future research directions. In sum, the investigations conducted within this thesis have enriched our understanding of the intricate interplay between fatty acids, triglycerides, and their impact on circulating T cells, shedding insights into the pivotal roles these components play in driving the development and advancement of atherosclerosis.

References

1 Libby, P. *et al.* Atherosclerosis. *Nat. Rev. Dis. Primers* **5**, 56, (2019).

2 Causes of Death Collaborators, G. B. D. Global, regional, and national age-sex-specific mortality for 282 causes of death in 195 countries and territories, 1980-2017: a systematic analysis for the Global Burden of Disease Study 2017. *Lancet* **392**, 1736-1788, (2018).

3 Tomkin, G. H. & Owens, D. LDL as a cause of atherosclerosis. *The Open Atherosclerosis & Thrombosis Journal* **5**, 13-21, (2012).

4 Kita, T. *et al.* Role of oxidized LDL in atherosclerosis. *Ann. N. Y. Acad. Sci.* **947**, 199-206, (2001).

5 Chistiakov, D. A., Melnichenko, A. A., Myasoedova, V. A., Grechko, A. V. & Orekhov, A. N. Mechanisms of foam cell formation in atherosclerosis. *J. Mol. Med.* **95**, 1153-1165, (2017).

6 Gui, Y., Zheng, H. & Cao, R. Y. Foam cells in atherosclerosis: novel insights into its origins, consequences, and molecular mechanisms. *Front. Cardiovasc. Med.* **9**, 845942, (2022).

7 Martinet, W., Schrijvers, D. M. & De Meyer, G. R. Necrotic cell death in atherosclerosis. *Basic Res. Cardiol.* **106**, 749-760, (2011).

8 Alexopoulos, N. & Raggi, P. Calcification in atherosclerosis. *Nat. Rev. Cardiol.* **6**, 681-688, (2009).

9 Braganza, D. M. & Bennett, M. R. New insights into atherosclerotic plaque rupture. *Postgrad. Med. J.* **77**, 94–98, (2001).

10 Fahed, A. C. & Jang, I. K. Plaque erosion and acute coronary syndromes: phenotype, molecular characteristics and future directions. *Nat. Rev. Cardiol.* **18**, 724-734, (2021).

11 Ketelhuth, D. F. & Hansson, G. K. Adaptive response of T and B cells in atherosclerosis. *Circ. Res.* **118**, 668-678, (2016).

12 Aukrust, P. *et al.* The complex role of T-cell-based immunity in atherosclerosis. *Curr. Atheroscler. Rep.* **10**, 236–243, (2008).

13 Brunner, D., Altman, S., Loebl, K., Schwartz, S. & Levin, S. Serum cholesterol and triglycerides in patients suffering from ischemic heart disease and in healthy subjects. *Atherosclerosis* **28**, 197-204, (1977).

14 Boullart, A. C., de Graaf, J. & Stalenhoef, A. F. Serum triglycerides and risk of cardiovascular disease. *Biochim. Biophys. Acta* **1821**, 867-875, (2012).

15 Budoff, M. Triglycerides and triglyceride-rich lipoproteins in the causal pathway of cardiovascular disease. *Am. J. Cardiol.* **118**, 138-145, (2016).

16 Makowski, L., Chaib, M. & Rathmell, J. C. Immunometabolism: from basic mechanisms to translation. *Immunol. Rev.* **295**, 5-14, (2020).

17 Chapman, N. M., Boothby, M. R. & Chi, H. Metabolic coordination of T cell quiescence and activation. *Nat. Rev. Immunol.* **20**, 55-70, (2020).

18 MacIver, N. J., Michalek, R. D. & Rathmell, J. C. Metabolic regulation of T lymphocytes. *Annu. Rev. Immunol.* **31**, 259-283, (2013).

19 Fernandez, D. M. *et al.* Single-cell immune landscape of human atherosclerotic plaques. *Nat. Med.* **25**, 1576-1588, (2019).

20 Depuydt, M. A. *et al.* Microanatomy of the human atherosclerotic plaque by single-cell transcriptomics. *Circ. Res.* **127**, 1437-1455, (2020).

21 Winkels, H. *et al.* Atlas of the immune cell repertoire in mouse atherosclerosis defined by single-cell RNA-sequencing and mass cytometry. *Circ. Res.* **122**, 1675-1688, (2018).

22 Cochain, C. *et al.* Single-cell RNA-seq reveals the transcriptional landscape and heterogeneity of aortic macrophages in murine atherosclerosis. *Circ. Res.* **122**, 1661-1674, (2018).

23 Zhou, X., Robertson, A. K., Rudling, M., Parini, P. & Hansson, G. K. Lesion development and response to immunization reveal a complex role for CD4 in atherosclerosis. *Circ. Res.* **96**, 427-434, (2005).

24 Zhou, X., Nicoletti, A., Elhage, R. & Hansson, G. K. Transfer of CD4+ T cells aggravates atherosclerosis in immunodeficient apolipoprotein E knockout mice. *Circulation* **102**, 2919-2922, (2000).

25 Zhou, X., Robertson, A. K., Hjerpe, C. & Hansson, G. K. Adoptive transfer of CD4+ T cells reactive to modified low-density lipoprotein aggravates atherosclerosis. *Arterioscler. Thromb. Vasc. Biol.* **26**, 864-870, (2006).

26 Luckheeram, R. V., Zhou, R., Verma, A. D. & Xia, B. CD4+ T cells: differentiation and functions. *Clin. Dev. Immunol.* **2012**, (2012).

27 Zhu, J., Yamane, H. & Paul, W. E. Differentiation of effector CD4 T cell populations*. *Annu. Rev. Immunol.* **28**, 445-489, (2010).

28 Saigusa, R., Winkels, H. & Ley, K. T cell subsets and functions in atherosclerosis. *Nat. Rev. Cardiol.* **17**, 387-401, (2020).

29 Christie, D. & Zhu, J. Transcriptional regulatory networks for CD4 T cell differentiation. *Curr. Top. Microbiol. Immunol.* **381**, 125-172, (2014).

30 Szabo, S. J., Sullivan, B. M., Peng, S. L. & Glimcher, L. H. Molecular mechanisms regulating Th1 immune responses. *Annu. Rev. Immunol.* **21**, 713-758, (2003).

31 Nakayama, T. *et al.* Th2 cells in health and disease. *Annu. Rev. Immunol.* **35**, 53-84, (2017).

32 Micosse, C. *et al.* Human "Th9" cells are a subpopulation of PPAR-γ+ Th2 cells. *Sci. Immunol.* **4**, 5943, (2019).

33 Li, Q. *et al.* Increased Th9 cells and IL-9 levels accelerate disease progression in experimental atherosclerosis. *Am. J. Transl. Res.* **9**, 1335-1343, (2017).

34 Gregersen, I. *et al.* Increased systemic and local interleukin 9 levels in patients with carotid and coronary atherosclerosis. *PLoS One* **8**, 72769, (2013).

35 Zhang, W. *et al.* IL-9 aggravates the development of atherosclerosis in ApoE2/2 mice. *Cardiovasc. Res.* **106**, 453-464, (2015).

36 Korn, T., Bettelli, E., Oukka, M. & Kuchroo, V. K. IL-17 and Th17 cells. *Annu. Rev. Immunol.* **27**, 485-517, (2009).

37 Savage, P. A., Klawon, D. E. J. & Miller, C. H. Regulatory T cell development. *Annu. Rev. Immunol.* **38**, 421-453, (2020).

38 Gerriets, V. A. & Rathmell, J. C. Metabolic pathways in T cell fate and function. *Trends Immunol.* **33**, 168-173, (2012).

39 Kolan, S. S. *et al.* Cellular metabolism dictates T cell effector function in health and disease. *Scand. J. Immunol.* **92**, 12956, (2020).

40 Zhang, N. & Bevan, M. J. CD8+ T cells: foot soldiers of the immune system. *Immunity* **35**, 161-168, (2011).

41 Bergstrom, I., Backteman, K., Lundberg, A., Ernerudh, J. & Jonasson, L. Persistent accumulation of interferon-γ-producing CD8+CD56+ T cells in blood from patients with coronary artery disease. *Atherosclerosis* **224**, 515-520, (2012).

42 van Duijn, J., Kuiper, J. & Slutter, B. The many faces of CD8+ T cells in atherosclerosis. *Curr. Opin. Lipidol.* **29**, 411-416, (2018).

43 Cochain, C. & Zernecke, A. Protective and pathogenic roles of CD8+ T cells in atherosclerosis. *Basic Res. Cardiol.* **111**, 71, (2016).

44 Kyaw, T. *et al.* Cytotoxic and proinflammatory CD8+ T lymphocytes promote development of vulnerable atherosclerotic plaques in apoE-deficient mice. *Circulation* **127**, 1028-1039, (2013).

45 Seijkens, T. T. P. *et al.* Deficiency of the T cell regulator Casitas B-cell lymphoma-B aggravates atherosclerosis by inducing CD8+ T cell-mediated macrophage death. *Eur. Heart J.* **40**, 372-382, (2019).

46 van Duijn, J. *et al.* CD8+ T-cells contribute to lesion stabilization in advanced atherosclerosis by limiting macrophage content and CD4+ T-cell responses. *Cardiovasc. Res.* **115**, 729-738, (2019).

47 Chyu, K. Y. *et al.* CD8+ T cells mediate the athero-protective effect of immunization with an ApoB-100 peptide. *PLoS One* **7**, 30780, (2012).

48 Honjo, T. *et al.* ApoB-100–Related Peptide Vaccine Protects Against Angiotensin II–Induced Aortic Aneurysm Formation and Rupture. *J. Am. Coll. Cardiol.* **65**, 546–556, (2015).

49 Nordestgaard, B. G., Benn, M., Schnohr, P. & Tybjærg-Hansen, A. Nonfasting triglycerides and risk of myocardial infarction, ischemic heart disease, and death in men and women. *JAMA* **298**, 299–308, (2007).

50 Bauer, R. C., Khetarpal, S. A., Hand, N. J. & Rader, D. J. Therapeutic targets of triglyceride metabolism as informed by human genetics. *Trends Mol. Med.* **22**, 328-340, (2016).

51 Nordestgaard, B. G. Triglyceride-rich lipoproteins and atherosclerotic cardiovascular disease new insights from epidemiology, genetics, and biology. *Circ. Res.* **118**, 547-563, (2016).

52 Toth, P. P. Triglyceride-rich lipoproteins as a causal factor for cardiovascular disease. *Vasc. Health Risk Manag.* **12**, 171-183, (2016).

53 Ference, B. A. *et al.* Association of triglyceride-lowering LPL variants and LDL-C-lowering LDLR variants with risk of coronary heart disease. *JAMA* **321**, 364-373, (2019).

54 Sampson, U. K., Fazio, S. & Linton, M. F. Residual cardiovascular risk despite optimal LDL cholesterol reduction with statins: the evidence, etiology, and therapeutic challenges. *Curr. Atheroscler. Rep.* **14**, 1-10, (2012).

55 Brunzell, J. D. Hypertriglyceridemia. *N. Engl. J. Med.* **357**, 1009-1017, (2007).

56 Nordestgaard, B. G. & Varbo, A. Triglycerides and cardiovascular disease. *Lancet* **384**, 626-635, (2014).

57 Peng, J., Luo, F., Ruan, G., Peng, R. & Li, X. Hypertriglyceridemia and atherosclerosis. *Lipids Health Dis.* **16**, 233, (2017).

58 Nordestgaard, B. G. & Tybjærg-Hansen, A. IDL, VLDL, chylomicrons and atherosclerosis. *Eur. J. Epidemiol.* **8**, 92-98, (1992).

59 Dron, J. S. & Hegele, R. A. Genetics of triglycerides and the risk of atherosclerosis. *Curr. Atheroscler. Rep.* **19**, 31, (2017).

60 The ACCORD Study Group. Effects of intensive blood-pressure control in type 2 diabetes mellitus. *N. Engl. J. Med.* **362**, 1575-1585, (2010).

61 Keech, A. *et al.* Effects of long-term fenofibrate therapy on cardiovascular events in 9795 people with type 2 diabetes mellitus (the FIELD study): randomised controlled trial. *Lancet* **366**, 1849-1861, (2005).

62 Pradhan, A. D. *et al.* Rationale and design of the pemafibrate to reduce cardiovascular outcomes by reducing triglycerides in patients with diabetes (PROMINENT) study. *Am. Heart J.* **206**, 80-93, (2018).

63 The AIM-HIGH Investigators. Niacin in patients with low HDL cholesterol levels receiving intensive statin therapy. *N. Engl. J. Med.* **365**, 2255-2267, (2011).

64 The HPS2-THRIVE Collaborative Group *et al.* Effects of extended-release niacin with laropiprant in high-risk patients. *N. Engl. J. Med.* **371**, 203-212, (2014).

65 Bhatt, D. L. *et al.* Cardiovascular risk reduction with icosapent ethyl for hypertriglyceridemia. *N. Engl. J. Med.* **380**, 11-22, (2019).

66 Bhatt, D. L. *et al.* Effects of icosapent ethyl on total ischemic events from REDUCE-IT. *J. Am. Coll. Cardiol.* **73**, 2791-2802, (2019).

67 Bhatt, D. L. *et al.* Rationale and design of REDUCE-IT: reduction of cardiovascular events with icosapent ethyl-intervention trial. *Clin. Cardiol.* **40**, 138-148, (2017).

68 Wang, X., Verma, S., Mason, R. P. & Bhatt, D. L. The road to approval: a perspective on the role of icosapent ethyl in cardiovascular risk reduction. *Curr. Diab. Rep.* **20**, 65, (2020).

69 Huston, J. *et al.* A critical review of icosapent ethyl in cardiovascular risk reduction. *Am. J. Cardiovasc. Drugs* **23**, 393-406, (2023).

70 Assessment report Vazkepa. *Committee for Medicinal Products for Human Use* **EMA**, (2021).

71 Mason, R. P., Jacob, R. F., Shrivastava, S., Sherratt, S. C. R. & Chattopadhyay, A. Eicosapentaenoic acid reduces membrane fluidity, inhibits cholesterol domain formation, and normalizes bilayer width in atherosclerotic-like model membranes. *Biochim. Biophys. Acta* **1858**, 3131-3140, (2016).

72 Tsunoda, F. *et al.* Effects of oral eicosapentaenoic acid versus docosahexaenoic acid on human peripheral blood mononuclear cell gene expression. *Atherosclerosis* **241**, 400-408, (2015).

73 Vors, C. *et al.* Inflammatory gene expression in whole blood cells after EPA vs. DHA supplementation: results from the ComparED study. *Atherosclerosis* **257**, 116-122, (2017).

74 Bicalho, B., David, F., Rumplel, K., Kindt, E. & Sandra, P. Creating a fatty acid methyl ester database for lipid profiling in a single drop of human blood using high resolution capillary gas chromatography and mass spectrometry. *J. Chromatogr. A* **1211**, 120-128, (2008).

75 Afonso, M. S. *et al.* Dietary interesterified fat enriched with palmitic acid induces atherosclerosis by impairing macrophage cholesterol efflux and eliciting inflammation. *J. Nutr. Biochem.* **32**, 91-100, (2016).

76 Yamagishi, K., Nettleton, J. A., Folsom, A. R. & Investigators, A. S. Plasma fatty acid composition and incident heart failure in middle-aged adults: the Atherosclerosis Risk in Communities (ARIC) Study. *Am. Heart J.* **156**, 965-974, (2008).

77 Wang , L., Folsom, A. R., Eckfeldt, J. H. & Investigators, t. A. S. Plasma fatty acid composition and incidence of coronary heart disease in middle aged adults: the Atherosclerosis Risk in Communities (ARIC) study. *Nutr. Metab. Cardiovasc. Dis.* **13**, 256-266, (2003).

78 Steffen, B. T., Duprez, D., Szklo, M., Guan, W. & Tsai, M. Y. Circulating oleic acid levels are related to greater risks of cardiovascular events and all-cause mortality: The Multi-Ethnic Study of Atherosclerosis. *J. Clin. Lipidol.* **12**, 1404-1412, (2018).

79 Delgado, G. E. *et al.* Individual omega-9 monounsaturated fatty acids and mortality – the Ludwigshafen Risk and Cardiovascular Health Study. *J. Clin. Lipidol.* **11**, 126-135, (2017).

80 Kersten, S. Triglyceride metabolism under attack. *Cell Metab.* **25**, 1209-1210, (2017).

81 Kersten, S. Physiological regulation of lipoprotein lipase. *Biochim. Biophys. Acta* **1841**, 919-933, (2014).

CHAPTER 2

Effects of fatty acids on T cell function: role in atherosclerosis

Nathalie A. Reilly[1,2], Esther Lutgens[3,4,5], Johan Kuiper[6], Bastiaan T. Heijmans[1,8], and J. Wouter Jukema[2,7,8]

[1] *Molecular Epidemiology, Department of Biomedical Data Sciences, Leiden University Medical Centre, Leiden, Netherlands.*
[2] *Department of Cardiology, Leiden University Medical Centre, Leiden, Netherlands.*
[3] *Department of Medical Biochemistry, Amsterdam University Medical Centre, Amsterdam, Netherlands.*
[4] *Institute for Cardiovascular Prevention (IPEK), Ludwig-Maximilians Universität, Munich, Germany.*
[5] *German Centre for Cardiovascular Research (DZHK), partner site Munich Heart Alliance, Munich, Germany.*
[6] *Leiden Academic Centre for Drug Research, Division of Biotherapeutics, Leiden University, Leiden, Netherlands.*
[7] *Netherlands Heart Institute, Utrecht, Netherlands.*
[8] *These authors jointly supervised: Bastiaan T. Heijmans, J. Wouter Jukema.*

Nat Rev Cardiol **18**, *824–837, (2021).*
DOI: 10.1038/s41569-021-00582-9

Abstract

T cells are among the most common cell types present in atherosclerotic plaques and are increasingly being recognized as a central mediator in atherosclerosis development and progression. At the same time, triglycerides and fatty acids have re-emerged as crucial risk factors for atherosclerosis. Triglycerides and fatty acids are important components of the milieu to which the T cell is exposed from the circulation to the plaque, and increasing evidence shows that fatty acids influence T cell function. In this Review, we discuss the effects of fatty acids on four components of the T cell response — metabolism, activation, proliferation and polarization — and the influence of these changes on the pathogenesis of atherosclerosis. We also discuss how quiescent T cells can undergo a type of metabolic reprogramming induced by exposure to fatty acids in the circulation that influences the subsequent functions of T cells after activation, such as in atherosclerotic plaques.

Key points

- Fatty acids in the circulation can affect T cell function.
- Saturated fatty acids generally induce pro-inflammatory responses in T cells, whereas unsaturated fatty acids generally induce anti-inflammatory responses.
- Changes in T cell metabolism underlie the fatty acid-induced alterations in T cell activation, proliferation and polarization.
- Fatty acid-induced alterations in T cell function can in turn influence the development and progression of atherosclerosis.
- Exposure to fatty acids in the circulation leads to metabolic reprogramming of the T cells that might predetermine the subsequent role of the T cell in disease processes.

Glossary

T helper 1 cells (T_H1 cells): A subtype of $CD4^+$ T cell characterized by the expression of the transcription factor T-bet and the production of pro-inflammatory cytokines, such as IFNγ, IL-2 and TNF. T_H1 cells have been shown to be pro-atherogenic.

T helper 2 cells (T_H2 cells): A subtype of $CD4^+$ T cell characterized by the expression of the transcription factor GATA3 and the production of anti-inflammatory cytokines, such as IL-4, IL-5 and IL-13. The role of T_H2 cells in atherosclerosis is not completely clear, although anti-atherogenic properties have been described.

T helper 17 cells (T_H17 cells): A subtype of $CD4^+$ T cell characterized by the expression of the transcription factor RORγt and the production of pro-inflammatory cytokines, such as IL-17A. The role of T_H17 cells in atherosclerosis is undefined because they have been found to have both pro-atherogenic and anti-atherogenic properties.

Regulatory T cells (T_{reg} cells): A subtype of $CD4^+$ T cell characterized by the expression of the transcription factor FOXP3 and the secretion of anti-inflammatory cytokines, such as IL-10 and TGFβ. T_{reg} cells have been shown to have anti-atherogenic functions.

T cell tolerance: The process of eliminating T cells that are reactive to self-antigens. Tolerance can be induced by exposure to high doses of an antigen, which results in deletion or anergy of the T cells that are specific for that antigen.

Triglycerides: Esters formed by a glycerol and three fatty acid groups. High circulating levels of triglycerides have been associated with an increased risk of cardiovascular disease.

Polyunsaturated fatty acid (PUFA): A fatty acid with a carbon chain that contains two or more double bonds. These fatty acids have a primarily anti-atherogenic effect.

Saturated fatty acids (SFAs): Fatty acids with a carbon chain that contains no double bonds. These fatty acids have a primarily pro-atherogenic effect.

Monounsaturated fatty acids (MUFAs): Fatty acids with a carbon chain that contains a single double bond. These fatty acids have both pro-atherogenic and anti-atherogenic effects.

Oxidative phosphorylation: The main form of energy production in quiescent T cells. High amounts of ATP are generated through the uptake of glucose and exogenous fatty acids to ensure cell survival.

Aerobic glycolysis: The main form of energy production in activated T helper cells, in which glucose is actively consumed to produce ATP and the necessary metabolites for cell growth and proliferation.

Introduction

Atherosclerosis is the primary underlying cause of cardiovascular disease (CVD) and is characterized by interactions among lipids, the immune system and the vascular wall[1]. The hallmark of atherosclerosis is lipid accumulation in the arterial intima[1]. Both LDL, laden with cholesterol, and innate immune cells, specifically monocytes and macrophages, have crucial roles in the development of atherosclerosis[2-5]. However, it is increasingly clear that these factors cannot account for the full pathological mechanisms of atherosclerosis.

Atherosclerotic plaques have long been known to contain an adaptive immune component. T cells are an important part of the adaptive immune response and were originally thought to comprise 10% of all cells in the atherosclerotic plaque[6,7]. The functions of T cells and their major subsets, $CD4^+$ T cells and $CD8^+$ cytotoxic T cell, have been extensively studied in this context. $CD4^+$ T cells are the most prominent T cell subtype in atherosclerosis and generally contribute to the development of disease, as observed in studies showing that adoptive transfer of $CD4^+$ T cells aggravates the atherosclerosis in immunodeficient *Apoe*$^{-/-}$ mice[8-12]. $CD4^+$ T cells can be further subdivided into T helper 1 cells (T_H1 cells), T_H2 cells, T_H17 cells and regulatory T cells (T_{reg} cells) (Box 1). T_H1 cells seem to be the predominant T cell subset in atherosclerotic plaques and the most pro-atherogenic subset, whereas T_{reg} cells have anti-atherogenic functions[11,12]. The exact roles of T_H2 cells, T_H17 cells and $CD8^+$ T cells remain unclear because both pro-atherogenic and anti-atherogenic effects have been reported[10-16]. Although the total number of $CD8^+$ T cells is low in early atherosclerotic lesions, the number increases as the disease progresses[10-13].

As techniques to study atherosclerosis have progressed, the importance of T cells in atherosclerosis development and progression has become increasingly clear. A study using optical coherence tomography with simultaneous immunophenotyping by flow cytometry analysis of the culprit atherosclerotic lesion in patients with an acute coronary syndrome showed enrichment of both $CD4^+$ T cells and $CD8^+$ T cells in plaques with intact fibrous caps compared with ruptured plaques[17]. Studies using single-cell RNA sequencing showed that T cells make up about half of the $CD45^+$ leukocytes present in atherosclerotic plaques in both humans and mice[18-20]. Furthermore, analyses with other techniques, such as mass cytometry, have also shown that 30–65% of the leukocytes in atherosclerotic plaques are T cells in both humans and mice[18,19,21]. Although these techniques are fairly destructive during the cell isolation step, favoring the survival of T cells over macrophages and vascular smooth muscle cells, these findings should not be underestimated[21,22]. T cells might have a substantially greater role in the pathogenesis of atherosclerosis than previously conceived.

T cells are designed to sense, interact with and respond to their environment. In the circulation, this environment comprises many factors, including but not limited to other immune cells, the vascular wall, chemokines, cytokines and lipids[23]. In this Review, we focus on the interactions that occur between T cells and circulating lipids that might modulate the immune responses underlying atherosclerosis development and progression[10]. For example, antigens derived from

LDL particles, which are widely associated with atherosclerosis development, are recognized by T cells in atherosclerotic plaques[9, 24, 25]. Moreover, T cell tolerance to LDL can be induced in a T_{reg} cell-mediated manner by continuously exposing *Ldlr*$^{-/-}$ mice to the primary apolipoprotein of LDL, ApoB-100, which leads to a reduction in atherosclerosis[26-29]. However, the precise consequences in atherosclerosis of the T cell interactions with lipids have not yet been elucidated.

A type of circulating lipid with which T cells can interact is triglycerides, which in the past decade have re-emerged as an important risk factor for atherosclerosis[30-33]. The role of triglycerides in CVD is still debated because clinical trials aimed at improving CVD by lowering triglyceride levels in the plasma have had opposing results. The findings of these clinical trials have been summarized previously[34]. Some triglyceride-lowering drugs have been shown to reduce the risk of CVD development[34-36]. The REDUCE-IT trial[37, 38] showed a significant reduction in the risk of adverse cardiovascular events with treatment with the polyunsaturated fatty acid (PUFA) icosapent ethyl, which lowers plasma triglyceride levels, compared with placebo. Triglycerides are composed of fatty acids (FAs) and polar lipids, which are hydrolyzed into their FA components and used as a source of energy production in cells[39, 40]. Triglycerides are incorporated into chylomicrons after intestinal uptake and transported via the mesenteric lymph to the circulation. FAs are essentially the functional components of triglycerides and as such, the development and progression of atherosclerosis is tied to the various FAs present in the circulation. The effect of different FAs on the risk of atherosclerotic CVD ranges from pro-atherosclerotic to anti-atherosclerotic depending on the FA[41-57]. In this Review, we do not provide evidence to close the debate about the role of triglycerides in CVD but instead aim to uncover and clarify the role of FAs in CVD, which might help in the development of future approaches for the treatment and prevention of atherosclerotic CVD.

FAs are ubiquitously present throughout the body and interact with T cells, particularly in T cell-rich lymphatic vessels and the blood circulation[58, 59]. FAs are composed of a carboxyl group with a carbon chain of various lengths. FAs are classified according to the number of double bonds in the carbon chain: saturated fatty acids (SFAs) have no double bonds, monounsaturated fatty acids (MUFAs) have one double bond, and PUFAs have more than one double bond. Of note, the double bonds of naturally occurring FAs are almost always in *cis*[60]. In the context of atherosclerosis, SFAs are generally considered to be pro-atherogenic, whereas MUFAs and PUFAs are considered to be anti-atherogenic. However, some exceptions have been described[61]. For example, higher plasma levels of the MUFA oleic acid have been associated with a higher risk of CVD in humans[42]. The different findings might be explained by the structural and biological differences between FAs in each group, such as in chain length and branching of methyl groups, which are not taken into account in the conventional classification according to the number of double bonds.

Table 1 | Effects of circulating fatty acids on atherosclerosis. Common fatty acids found in the circulation, as measured from a fingertip blood drop from healthy men with the use of an optimized method of capillary gas chromatography separation and mass spectrometry detection[128]. The table includes only the fatty acids discussed in this Review and is not a complete list of all the fatty acids present in the circulation; a full list of fatty acids measured in the blood is provided in REF[128]. MUFA, monounsaturated fatty acid; PUFA, polyunsaturated fatty acid; SFA, saturated fatty acid. As provided in REF[128].

Fatty acid	Common name	Saturation	Carbon chain length	Relative abundance in blood (%)	Pro-atherogenic or anti-atherogenic association	Pro-inflammatory or anti-inflammatory response in T cells
Dodecanoic acid	Lauric acid	SFA	C12:0	0.04	Pro-atherogenic[55, 89]	Pro-inflammatory
Tetradecanoic acid	Myristic acid	SFA	C14:0	0.38	Pro-atherogenic[47, 48]	Pro-inflammatory
Hexadecanoic acid	Palmitic acid	SFA	C16:0	16.28	Pro-atherogenic[43, 48, 94]	Pro-inflammatory
Hexadec-9-enoic acid	Palmitoleic acid	MUFA	C16:1	0.72	Pro-atherogenic[48, 52] and anti-atherogenic[45]	Pro-inflammatory and anti-inflammatory
Octadecanoic acid	Stearic acid	SFA	C18:0	9.41	Pro-atherogenic[48, 53, 94]	Pro-inflammatory
Octadec-9-enoic acid	Oleic acid	MUFA	C18:1 Ω9	13.34	Pro-atherogenic[42, 50, 94]	Pro-inflammatory and anti-inflammatory
11-Octadecenoic acid	Vaccenic acid	MUFA	C18:1 Ω7	1.06	Anti-atherogenic[52, 124]	Anti-inflammatory
Octadecadienoic acid	Linoleic acid	PUFA	C18:2	15.95	Anti-atherogenic[44, 48]	Anti-inflammatory
Octadecatrienoic acid	γ-Linolenic acid	PUFA	C18:3	0.18	Pro-atherogenic[41, 48, 94] and anti-atherogenic[46]	Pro-inflammatory and anti-inflammatory
Eicosanoic acid	Arachidic acid	SFA	C20:0	0.32	Pro-atherogenic[56]	Pro-inflammatory
Eicosatetraenoic acid	Arachidonic acid	PUFA	C20:4	8.16	Pro-atherogenic[57, 107] and anti-atherogenic[41, 48, 94]	Pro-inflammatory
Eicosapentaenoic acid	EPA	PUFA	C20:5	0.63	Anti-atherogenic[37, 38, 51, 54, 80, 105, 108-110, 123]	Anti-inflammatory
Docosahexaenoic acid	DHA	PUFA	C22:6	2.25	Anti-atherogenic[41, 48, 51, 54, 86, 105-110, 123]	Anti-inflammatory
Tetracosanoic acid	Lignoceric acid	SFA	C24:0	2.21	Anti-atherogenic[57]	Pro-inflammatory

In this Review, we describe the role of FAs that are present in the circulation in determining the metabolic and functional responses of T cells and the link to the development and progression of atherosclerosis. FAs are known to affect the pathogenesis of atherosclerosis and the risk of CVD; however, these effects were traditionally assumed to be mediated via differential effects of FAs on LDL cholesterol that thus also affect the LDL to HDL ratio[62]. We now know that FAs also affect other aspects of physiology and CVD risk factors, such as high blood triglyceride levels, inflammation and vascular reactivity. Most research on FAs and inflammation has so far focused on monocytes, macrophages and endothelial cells. However, accumulating evidence shows that FAs also modulate T cell functions and processes. Therefore, understanding the effects of FAs on T cells might be inherent to a better comprehension of the pathogenesis of atherosclerosis.

Fatty acids and T cell responses

T cells are a major cellular component of the atherosclerotic plaque, but before they migrate into the lesion, T cells circulate in the bloodstream and the lymph. T cells spend much of their lifespan in the circulation, therefore, in this Review, we focus on the FA-induced changes that T cells undergo in the blood (although similar processes might occur in other tissues) and the role that these changes have in atherosclerosis development and progression.

In the circulation, T cells are usually in a quiescent or resting state until a strong enough stimulus induces an immune response[63-65]. The response of T cells can be broadly divided into cell activation, proliferation and polarization, coinciding with a change in metabolism[64, 65]. The T cell response is usually initiated by antigen presentation by an antigen-presenting cell, although environmental factors, including but not limited to oxygen tension, glucose availability and FAs, can also influence the T cell response[5, 66-69]. The blood and lymph provide a setting rich in these environmental factors. In this Review, we focus solely on exogenous FAs; that is, FAs that are not being produced by the T cell itself. These FAs are abundant in the circulation and therefore can interact with T cells and influence each part of their response, and the outcomes differ depending on the type of FA to which the cell is exposed (Fig. 1). We discuss the effects of circulating FAs on the main outcomes of each component of the T cell response and the link with atherosclerosis. A comprehensive discussion of the mechanisms by which FAs influence these responses, which can include the formation of lipid rafts, G protein-coupled receptors and epigenetic reprogramming, is beyond the scope of this Review. The sections on each aspect of the T cell response are organized into the effects of specific FAs, from pro-inflammatory to anti-inflammatory effects. Within each inflammatory response, FAs are discussed from SFA to MUFA and PUFA, grouping FAs with similar effects on T cell responses. The potential effects of short-chain FAs, which are derived from the gut microbiota, are not discussed. The effects of the FAs on T cells are then related to the known role in atherosclerosis of each FA or T cell. Only the FAs that have been studied in the context of T cell responses are discussed. Table 1 provides an overview of the discussed FAs, their abundance in the circulation, their proposed effect on atherosclerosis (not including T cell effects) and the proposed effect on atherosclerosis on the basis of the effect of the FA on T cell function.

Box 1 | Polarization of $CD4^+$ T cells.
Polarization is a process that determines the different subsets of the $CD4^+$ T cells and occurs during T cell activation and proliferation. This Review focuses on how fatty acids in the circulation influence the polarization into four $CD4^+$ T cell subsets, T helper 1 (T_H1) cells, T_H2 cells, T_H17 cells and regulatory T (T_{reg}) cells, which are the most extensively studied. T cell subsets are identified by the expression levels of specific surface markers and transcription factors and by the cytokines the cells secrete[129-131]. T_H1, T_H2, T_H17 and T_{reg} cells are defined by the expression of the transcription factors T-bet (also known as TBX21), GATA3, RORγt and FOXP3, respectively[132, 133]. The signature cytokines of T_H1 cells include interferon-γ (IFNγ), IL-2 and tumor necrosis factor (TNF). Those of T_H2 cells are IL-4, IL-5 and IL-13. T_H17 cells secrete IL-17A, and T_{reg} cells produce transforming growth factor-β (TGFβ) and IL-10. Given that IFNγ, IL-2, TNF and IL-17A are considered to be pro-inflammatory cytokines, T_H1 cells and T_H17 cells are generally considered to be pro-inflammatory T cell subsets[134, 135]. IL-4, IL-5, IL-10, IL-13 and TGFβ are generally deemed to be anti-inflammatory and, therefore, T_{reg} cells and T_H2 cells are classified as anti-inflammatory, but in the context of atherosclerosis, the effect of T_H2 cells is unclear[12, 136, 137]. In addition, T_H2 cells cannot be considered to have only anti-inflammatory functions, because these cells have a role in the pathogenesis of inflammatory diseases such as asthma[138].

The proper balance of different T cell subsets is very important for an appropriate and effective immune response. Alterations to this balance can lead to a variety of inflammatory and autoimmune diseases, such as rheumatoid arthritis and type 1 diabetes mellitus[113, 139, 140]. Atherosclerosis is primarily a lipid-driven immunological disease but with a large inflammatory component[113]. Therefore, maintaining a proper balance of T cell subsets is crucial in atherosclerosis as well. Alterations to the balance of T cell subsets occur for several reasons, such as changes in the cytokine milieu or the gut microenvironments[132]. In addition, the effects of circulating fatty acids on T cell activation and proliferation might be linked to the outcome of atherosclerosis. T cell exposure to fatty acids in the circulation might induce changes in T cell polarization, disrupting the T cell subset balance and providing another mechanism for atherosclerosis attenuation or worsening.

Fatty acids and T cell metabolism

T cell metabolism has a crucial role in all stages of the T cell lifespan, from quiescence to polarization, and has been extensively reviewed previously[70]. An overview of T cell metabolism can be found in Box 2. The role of FA metabolism changes substantially throughout these stages, and inappropriate metabolism reprogramming leads to severe skewing of the T cell populations[71] (Fig. 1a; Supp. Table 1). A change in metabolism is the driving force of the T cell immune response and underlies the other three components: activation, proliferation and polarization. Therefore, understanding T cell metabolism and how it can be influenced by circulating FAs is an integral part of understanding the subsequent T cell functional outcomes.

Specific inhibitors of FA metabolism, such as rapamycin, C75 and soraphen A, can modulate T cell polarization[72-75], although T cell metabolism can also be directly influenced by surrounding FAs. For example, external FAs can influence the development of T_H17 cells by modifying T cell metabolism[76]. In mice, deletion of *Acaca*, which encodes acetyl-CoA carboxylase 1 (ACC1), results in a decrease in T_H17 cell numbers, but administration of the pro-atherogenic[42] MUFA oleic acid at high concentrations (100 µmol/l) restores the T_H17 polarization of naive *Acaca*$^{-/-}$ T cells *in vitro*[76]. Lower concentrations of the SFAs myristic acid (30 µmol/l) and lauric acid (10 µmol/l) or the PUFA docosahexaenoic acid (DHA) (1 µmol/l) did not rescue the T_H17 polarization *in vitro*[76]. Whether the type of FA or the difference in concentrations accounts for the observed differences is unclear. A similar study suggested that the inhibition of T_H17 polarization induced by the ACC1 inhibitor soraphen A might be rescued by exposure to sufficient levels of the SFA palmitate, although this hypothesis was not formally tested[74, 75].

Oleic acid can also rescue T cell metabolism reprogramming by restoring the rates of oxidative phosphorylation and aerobic glycolysis in mouse $CD4^+$ T cells treated with the ACC1 inhibitor TOFA *in vitro*[77]. Rates of oxidative phosphorylation and glycolysis were measured by the levels of oxygen and protons, respectively, in the culture medium[77]. Under FA-free conditions, the addition of 100 µmol/l oleic acid restored both oxidative phosphorylation and glycolysis[77]. If $CD4^+$ T cells can use extrinsic FAs as oxidative substrates for energy production to compensate for blocked metabolic pathways, this compensatory process might also occur in atherosclerotic plaques, which could promote the development of pro-inflammatory effector T cell subsets.

Not all supplemented FAs have been shown to rescue T cell metabolism, some alter T cell metabolism and lead to cell death. For example, in C57BL/6 mice, a diet with 12% weight for weight (w/w) of the PUFA linoleic acid resulted in $CD4^+$ T cell death but did not affect $CD8^+$ T cell viability[78]. The $CD4^+$ T cell death might occur through upregulation of FA oxidation and dysregulation of the electron transport chain. Indeed, exposure of $CD4^+$ T cells isolated from transgenic mice with an inducible liver-specific MYC oncogene (which overexpress MYC and are used as a model of non-alcoholic fatty liver disease) to 50 µmol/l of linoleic acid *in vitro* increased the expression of genes encoding proteins involved in FA oxidation, whereas the expression of genes encoding components of the electron transport chain was decreased[78]. These transcriptional changes have a negative effect on T cell function because FAs are actively β-oxidized in the mitochondria, which favors more NADH entering the electron transport chain to produce ATP. However, because the electron transport chain is disrupted, premature leakage of electrons to oxygen can generate the accumulation of reactive oxygen species and lead to cell death or apoptosis[78]. Therefore, linoleic acid might have anti-inflammatory effects by inducing a pro-apoptotic phenotype in $CD4^+$ T cells and reducing this T cell population. Other PUFAs also might induce a pro-apoptotic phenotype in T cells through alterations in T cell metabolism. Exposure of human $CD4^+$ T cells *in vitro* to 50 µmol/l of eicosapentaenoic acid (EPA) or DHA for 48 h led to increased proton leakage associated with mitochondrial respiration[79], a pro-apoptotic signature. Furthermore, the ratio of oxidative phosphorylation to glycolysis was reduced in these cells, which has been linked to suppressed proliferation.

Of note, linoleic acid, EPA and DHA have all been shown to have anti-atherogenic effects in humans, mice and *in vitro* models[41, 44, 80]. However, in humans, the concentrations of these PUFAs in atherosclerotic plaques are lower than in the serum[81]. By contrast, the concentrations of pro-atherogenic SFAs and MUFAs such as oleic acid are similar or higher in human atherosclerotic plaques than in the serum[81]. This observation provides a partial explanation for the skewed polarization towards pro-inflammatory T cell subsets observed in atherosclerotic plaques in humans and animal models[11, 12].

Taken together, these studies provide evidence that external FAs are involved in the metabolic reprogramming of T cells. This metabolic reprogramming underlies the activation, proliferation and polarization of T cells, leading to changes in T cell function that can influence their eventual role in diseases such as atherosclerosis.

Fatty acids and T cell activation

T cell activation is a multifaceted response that follows a complex signaling cascade in the T cell. A detailed description of T cell activation has been provided previously[65]. Briefly, the T cell receptor (TCR) binds to an antigen presented by an antigen-presenting cell to induce a cellular response[82]. Binding of the TCR to an antigen, together with simultaneous stimulation of the CD3 and co-stimulatory molecules leads to the activation of T cells[65]. A summary of the effects of FAs on T cell activation is shown in Fig. 1b and Supp. Table 2.

Remarkably, the SFA palmitic acid can induce T cell activation *in vitro* in the absence of activating antibodies[83]. $CD4^+$ T cells or $CD8^+$ T cells isolated from five individuals without diabetes mellitus and with normal glucose tolerance were exposed to palmitic acid *in vitro*. Activation was then determined across five time points by measuring oxidative stress and the expression of the activation markers CD69, insulin receptor, insulin-like growth factor 1, IL-2, glucose transporter type 4 and insulin receptor substrate 1. Palmitic acid (50 µmol/l and 500 µmol/l) induced time-dependent and concentration-dependent activation of the T cells. This effect was not observed with exposure to the MUFA oleic acid or the PUFAs linoleic acid, linolenic acid and arachidonic acid[83]. Palmitic acid can be categorized as pro-atherogenic[43]. Weaning male *Ldlr*$^{-/-}$ mice fed a diet enriched in an interesterified palmitic acid had greater atherosclerosis burden and lesion area than mice fed high-fat diets enriched in PUFAs, palmitic acid, stearic acid or interesterified stearic acid[43]. The researchers attributed this effect to higher cholesterol accumulation in LDL particles and macrophages, but did not consider the effect that this diet might have had on other immune cells, such as T cells, and how these cells could have affected disease progression[43].

Oleic acid is also generally considered to be pro-atherogenic because elevated levels of oleic acid in the plasma are an independent risk factor for CVD[42]. The effect of oleic acid on T cell activation might contribute to this observation. The proportion of splenic T lymphocytes expressing CD25 (a T cell activation marker) was significantly higher in male Wistar rats fed a diet in which 12%

of the total energy came from a lipid emulsion rich in oleic acid (53%) than in rats fed a diet in which 12% of the total energy came from a lipid emulsion rich in linoleic acid (51%)[84]. The number of $CD25^+$ cells was measured by fluorescence-activated cell sorting and correlated with the oleic acid content in the lipid emulsion, indicating a potential role of this FA in T cell activation[84].

FAs can also decrease T cell activation. In a study in healthy human volunteers, supplementation with the PUFA DHA (nine capsules of 1 g of fish oil enriched in DHA per day over 4 weeks) specifically reduced T cell activation compared with placebo, as measured by a decrease in CD69 expression in T cells. No reduction in the percentage of cells participating in phagocytosis or expressing adhesion molecules was observed in the monocyte or neutrophil fractions of the samples, as measured by fluorescence flow cytometry[85]. DHA is generally classified as anti-atherogenic because dietary intake of DHA has been shown to decrease heart rate, blood pressure and the plasma levels of LDL particles in humans, and high plasma levels of DHA are associated with a lower risk of developing carotid atherosclerotic plaques, all of which are associated with a reduced risk of atherosclerosis development[54, 86]. Understanding the transformative effects of a specific FA on the T cell response and how the FA is related to CVD allows us to begin to link the effects of FAs on T cells to atherosclerosis.

Box 2 | T cell metabolism.

Quiescent T cells

Quiescent T cells have high energetic demands and, therefore, focus their metabolism on ATP generation through oxidative phosphorylation and β-oxidation of fatty acids[63]. These catabolic processes are driven by the uptake of glucose and exogenous fatty acids for mitochondrial metabolism, which is regulated by the AMP-activated protein kinase (AMPK) pathway and the rate-limiting factor carnitine O-palmitoyltransferase 1 (CPT1A), which regulates lipid uptake into the mitochondria[63, 141].

Activated T cells

Activation and proliferation are characterized by rapid expansion of the T cell population for which T cells must produce energy rapidly and simultaneously create the necessary metabolites to sustain growth[142]. Therefore, activated T cells undergo a metabolic switch to the anabolic processes of aerobic glycolysis and fatty acid biosynthesis, known as the Warburg effect[143]. Aerobic glycolysis yields only two ATPs per molecule of glucose instead of the 36 ATPs that are achieved with oxidative phosphorylation. Nevertheless, this metabolic switch is required to produce the necessary metabolites for sustained cell growth and proliferation[63, 141, 142]. The mechanistic target of rapamycin (mTOR) pathway has a crucial role in the metabolic reprogramming of T cells by inducing the expression of genes related to lipid biosynthesis and decreasing the expression of *CPT1A*[77]. Without CPT1A to actively pump lipids into the mitochondria for oxidation and ATP production, the lipids can be conserved for cell growth.

Regulatory T cells
Regulatory T (T_{reg}) cells are almost completely reliant on oxidative phosphorylation and β-oxidation of fatty acids through maintaining the activation of the AMPK pathway and expression of *CPT1A*[141, 144, 145]. However, under conditions of high lipid concentrations, the AMPK pathway is downregulated, gradually impairing T cell function and numbers[146, 147]. This observation potentially explains why advanced atherosclerotic plaques do not contain high numbers of T_{reg} cells and are instead dominated by effector T cells, in both humans and mice[10, 137, 147]. A dyslipidemic environment, as found in atherosclerosis, might promote the polarization into effector T cells and reduce T_{reg} cell polarization[148-151].

Effector T cells
The polarization of effector T cells (T helper 1 (T_H1) cells, T_H2 cells and T_H17 cells) is highly dependent on anabolic metabolism and the mTOR pathway[141]. Inhibition of this pathway eliminates effector T cells in mice[72, 152]. The mTOR pathway comprises two complexes, mTOR complex 1 (mTORC1) and mTORC2. T_H1 and T_H17 cells are dependent on mTORC1, whereas T_H2 cells are dependent on mTORC2[153]. In mice, deletion of *Rheb* (which encodes a protein required for mTORC1 activation) results in the inhibition of T_H1 and T_H17 polarization, whereas deletion of *Rictor* (which encodes a component of mTORC2) results in the inhibition of T_H2 polarization[153]. T_H17 cells are dependent on the hypoxia-inducible factor 1α pathway and *de novo* fatty acid synthesis[154]. Fatty acid synthesis is controlled by the enzymes fatty acid synthase (FASN) and acetyl-CoA carboxylase 1 (ACC1). In mice, knockout of *Fasn* skews T cell polarization towards T_H1 cells, whereas ACC1 inhibition skews polarization towards T_{reg} cells[73-75]. Therefore, subtle changes in T cell metabolism can greatly alter subset polarization.

A detailed overview of T cell metabolism is provided in REF.[70].

Fatty acids and T cell proliferation

A brief growth phase occurs after T cell activation, followed by a rapid expansion of the T cell population, referred to as proliferation[87]. Like activation, this proliferation phase can also be influenced by the interaction with FAs (Fig. 1c; Supp. Table 3). Male C57BL/6 mice fed a chow diet containing 31% crude fat, of which 13.5% was the SFA lauric acid, had increased T cell proliferation without any additional T cell activation compared with mice fed a control chow diet (4.2% crude fat)[88]. In healthy individuals, lauric acid generally comprises only about 0.04% of circulating FAs (Table 1) but, as the previously described study in mice showed, a high intake of this SFA can lead to an increase in T cell proliferation, which might be important when considering that lauric acid makes up approximately 50% of widely consumed products such as coconut oil[89].

T cell proliferation can also be increased by other FAs that are present at higher levels in the circulation. Oleic acid, which comprises about 13% of circulating FAs (Table 1), can also increase the proliferation of T cells *in vitro*. In an *in vitro* study, T cells isolated from healthy men showed a

17% increase in proliferation after exposure to 25 µmol/l oleic acid for 30 h compared with control cells[90]. The addition of 25 µmol/l oleic or linoleic acid to human lymphocytes in the presence of the activator concanavalin A also increased proliferation *in vitro*[91]. An *in vivo* study showed increased proliferation of lymphocytes in male Wistar rats after intraduodenal administration of 5 ml of an oleic acid solution[92]. Similarly, exposure to palmitic acid, palmitoleic acid, stearic acid, oleic acid, linoleic acid or γ-linolenic acid increased the proliferation of activated human $CD4^+$ T cells *in vitro*[93] (Supp. Table 3). Palmitic acid, stearic acid and oleic acid can be considered to be pro-atherogenic, whereas palmitoleic acid, linoleic acid and γ-linolenic acid can be considered to be anti-atherogenic[42-46, 94]. However, all these FAs increase T cell proliferation. These findings might indicate that different T cell subsets proliferate with either a more pro-inflammatory or anti-inflammatory phenotype, thereby leading to atherosclerosis aggravation or amelioration, highlighting the importance of understanding not only the effects of FAs on T cells, but also how they affect atherosclerosis. In addition, the FA concentrations to which T cells are exposed might influence the observed effects on proliferation. In the described studies, T cell proliferation was increased after exposure to 4 µg/ml of the SFAs palmitic acid or stearic acid[93] (Supp. Table 3). However, a decrease in proliferation was found in human lymphocytes *in vitro* after the addition of 50 µmol/l palmitic acid or stearic acid[91], which is equivalent to about 12 µg/ml and 14 µg/ml, respectively. At these concentrations, T cell proliferation was reduced via an IL-2-mediated pathway[91]. Palmitic acid and stearic acid have both been suggested to have pro-atherogenic effects, although this effect might be mediated in a T cell-independent manner[43, 94].

The effect of the MUFA palmitoleic acid on T cell proliferation might also be concentration-dependent. Human $CD4^+$ T cell proliferation *in vitro* was increased after the addition of 2 µg/ml palmitoleic acid[93], as discussed above (Supp. Table 3). However, addition of 25 µmol/l or 50 µmol/l of this MUFA (equivalent to 6 µg/ml and 13 µg/ml, respectively) for 30 h to T lymphocytes *in vitro* induced a 50% decrease in proliferation[90]. These concentrations were not cytotoxic, as evaluated by membrane integrity and phosphatidylserine externalization assays, but induced a decrease in the expression of CD28 (an activation marker) and an increase in the expression of CD95 (which is involved in the initial steps of apoptosis)[90]. The reduction in activation markers and the increase in suppressor markers in the T cells provides a possible explanation for the observed decrease in proliferation[90]. Palmitoleic acid has been suggested to have anti-atherogenic effects[45]. This effect could be mediated through the anti-proliferative effect of this FA on pro-inflammatory T cell subsets and its proliferative effect on anti-inflammatory T cell subsets, which is discussed in more detail in the next section.

The effect of the PUFA γ-linolenic acid might depend on the timing of exposure relative to T cell activation. This FA reduced T cell proliferation in healthy humans *in vivo* 5 h, 24 h and 48 h after a single oral administration of 2.4 g[95]. Furthermore, the addition of 5–25 µg/ml of γ-linolenic acid *in vitro* before, but not during, T cell activation also inhibited proliferation[96]. By contrast, proliferation increased when γ-linolenic acid was added to activated $CD4^+$ T cells from healthy human donors[93]. γ-Linolenic acid is considered to be anti-atherogenic through inhibition of monocyte migration and foam cell formation[46]. However, further investigation of the potential

anti-atherogenic effects of γ-linolenic acid on T cells is warranted. The results discussed here underline the complexity of translating *in vitro* findings to the *in vivo* situation.

Two FAs have been consistently shown to decrease T cell proliferation across different studies, concentrations and time points, namely the PUFAs EPA and DHA. This effect has been shown in several studies involving human, mouse and rat T cells *in vitro* and *in vivo*[79, 91, 97-104]. How exactly these two FAs induce this response is still unknown, although a speculative hypothesis is that inhibition of IL-2 production, which is necessary for proliferation, and alterations in the structure of the cell membrane are involved[79, 91, 97-101]. Both EPA and DHA have been shown in numerous studies to decrease atherosclerosis development in both human and animal models[51, 54, 80, 105-110]. The observation that these FAs decrease T cell proliferation *in vitro* and the capacity of DHA to reduce T cell activation *in vitro* together with the finding that they protect against atherosclerosis development indicate that these FAs, T cells and atherosclerosis reduction might be linked.

FAs are an integral component of T cell proliferation regardless of whether they increase or decrease it. Without FAs, T cell proliferation is inhibited, meaning the T cells cannot replicate owing to a lack of available resources to generate more cells. This inhibition occurs in T cells cultured under FA-free conditions, but the addition of certain FAs rescues the proliferation. Specifically, the addition of 100 µmol/l of oleic acid, myristic acid, palmitic acid or arachidic acid rescued proliferation of $CD4^+$ T cells from humans, BALB/c mice and C57BL/6 mice cultured under FA-free conditions 48 h after activation[77]. By contrast, the addition of 100 µmol/l of lauric acid, palmitoleic acid, linoleic acid, γ-linolenic or lignoceric acid did not rescue proliferation under the same conditions[77]. These results mimic the observed effects of these FAs on atherosclerosis, because oleic acid, myristic acid and palmitic acid have all been found to be pro-atherogenic, whereas palmitoleic acid, linoleic acid and γ-linolenic acid have all been found to be anti-atherogenic in both humans and mice[42-48]. Furthermore, most of the tested SFAs (myristic acid, palmitic acid and arachidic acid) rescued T cell proliferation *in vitro*, whereas most of the unsaturated FAs (palmitoleic acid, linoleic acid and linolenic acid) did not[77]. Discrepancies between the capacity of saturated and unsaturated FAs to rescue T cell proliferation in FA-free conditions further reveals the complexity of the processes by which different FAs alter T cell function and the difficulty in understanding the effects of these interactions on atherosclerosis.

Fatty acid-mediated T cell polarization

Although T cells differentiate in the thymus, activation and polarization of T cells occur later at the site of injury or damage. T cell polarization generates various T cell subsets, of which the $CD4^+$ T cell subsets are discussed in more detail below (Box 1). Different FAs skew the proportions of these populations in distinct directions (Fig. 1d; Supp. Table 4). SFAs generally induce polarization into pro-inflammatory $CD4^+$ T cell subsets. An example is the medium-chain SFA lauric acid. In activated mouse $CD4^+$ T cells *in vitro* under conditions inducing T_H1 or T_H17 polarization, the addition of 250–500 µmol/l of lauric acid increased the populations of pro-inflammatory

T_H1 cells and T_H17 cells by 50% and decreased the population of anti-inflammatory T_{reg} cells by 30%[88]. In human $CD4^+$ T cells *in vitro* under conditions inducing T_H1 or T_H17 polarization, the addition of 250 µmol/l of lauric acid increased the populations of T_H1 and T_H17 cells by 35% and increased the relative expression of *IFNG* and *TNF*, and *IL17A* and *RORC*, respectively. In human $CD4^+$ T cells *in vitro* under conditions inducing T_{reg} cell polarization, the addition of 250 µmol/l of lauric acid decreased the population of T_{reg} cells and decreased the expression of *FOXP3* by 50%[88]. Additionally, male C57BL/6 mice fed a diet rich in either lauric acid or palmitic acid had higher levels of the cytokines interferon-γ (IFNγ) and IL-17A in lamina propria lymphocytes in the small intestine, increased T_H17 cell numbers in the central nervous system, and increased T_H1 cell and T_H17 cell numbers in the spleen compared with mice fed a control diet[88].

Palmitic acid is another SFA that can induce polarization of pro-inflammatory T cell subsets. The addition of 1 mmol/l palmitic acid to human peripheral blood mononuclear cells (PBMCs) that had been activated with anti-CD3 and anti-CD28 *in vitro* increased the proportion of T_H1 and T_H17 populations but decreased the proportion of T_H2 and T_{reg} cell populations, as measured by the expression of the subset-specific transcription factors T-bet (also known as TBX21), RORγt, GATA3 and FOXP3, respectively[111]. Furthermore, similar results were found when PBMCs were exposed to 1 mmol/l of the MUFA oleic acid or to a combination of 1 mmol/l oleic acid plus palmitic acid for 48 h[111]. These results together with the findings discussed in the previous paragraphs indicate that SFAs and some MUFAs promote pro-inflammatory T cell subset polarization and T cell proliferation.

In addition to SFAs and some MUFAs, the PUFA arachidonic acid also elicits pro-inflammatory T cell polarization[112], even though this PUFA is closely related to the anti-inflammatory PUFAs EPA and DHA. Non-obese diabetic (NOD) mice fed a diet enriched in arachidonic acid had increased T_H1 and T_H17 populations and increased levels of IFNγ, tumor necrosis factor (TNF) and IL-17A in the plasma compared with NOD mice fed a control diet[112]. The same study also found a drastically disrupted T_H1 to T_H2 cell balance. Furthermore, this study found that *in vitro* exposure of activated $CD4^+$ T cells from humans or mice to 100 µmol/l or 50 µmol/l arachidonic acid, respectively, for 24 h resulted in an increased proportion of T_H1 and T_H17 populations and IFNγ and IL-17A secretion together with a decrease in the secretion of IL-4[112]. These findings indicate that arachidonic acid mediates pro-inflammatory responses by influencing $CD4^+$ T cell polarization.

Not all MUFAs are strictly pro-inflammatory: palmitoleic acid and oleic acid seem to have mixed pro-inflammatory and anti-inflammatory effects. Palmitoleic acid has partial anti-inflammatory effects on $CD4^+$ T cell polarization by reducing the proportions of T_H1 and T_H17 populations[90]. Cytokine profiling using flow cytometry showed that *in vitro* addition of 25 µmol/l or 50 µmol/l palmitoleic acid to human activated T cells was not cytotoxic but reduced the production of IL-17A, IL-2, IFNγ and TNF[90]. However, these same concentrations of palmitoleic acid also reduced the proportion of the T_{reg} cells from 3.5% to 0.2%[90]. T_{reg} cells have a pivotal role in reducing the inflammatory response and preventing autoimmunity[113]; therefore, a decrease in their population caused by exposure to a specific FA can be interpreted as that FA substantiating pro-inflammatory responses.

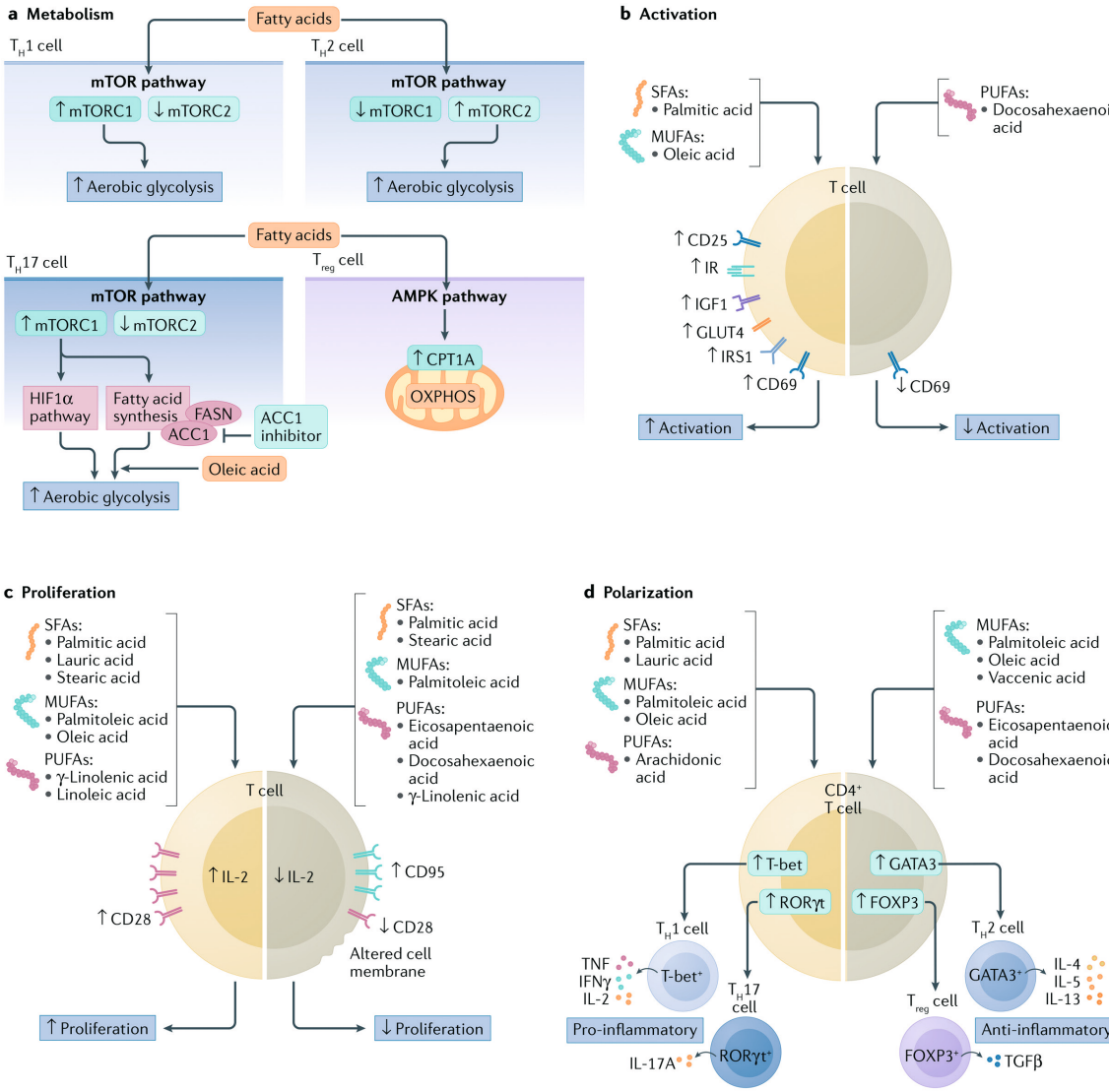

Fig. 1 | Fatty acids alter T cell function by influencing their metabolism, activation, proliferation and polarization. Generally, monounsaturated fatty acids (MUFAs) and polyunsaturated fatty acids (PUFAs) induce anti-inflammatory responses in T cells whereas saturated fatty acid (SFAs) induce pro-inflammatory responses, although some discrepancies have been observed, such as with oleic acid. The yellow background indicates increased activity, such as increased activation and proliferation or a pro-inflammatory response. The grey background indicates decreased activity, such as decreased activation and proliferation or an anti-inflammatory response. **(a)** The metabolism of activated T cells is different depending on the T cell subset. The panel shows the four main subsets of $CD4^+$ T cells. During polarization, the effector T cells T helper 1 (T_H1) cells, T_H2 cells and T_H17 cells switch to aerobic glycolysis, whereas regulatory T (T_{reg}) cells maintain oxidative phosphorylation (OXPHOS). The blockade in T_H17 cell polarization caused by inhibition of the enzyme acetyl-CoA carboxylase 1 (ACC1) can be rescued *in vitro* by the addition of oleic acid. **(b)** Exposure to SFAs or MUFAs induces T cell activation, as measured by increased levels of cell-surface receptors, including insulin receptor (IR), insulin-like growth factor 1 (IGF1), glucose transporter type 4 (GLUT4) and

insulin receptor substrate 1 (IRS1), compared with untreated cells. By contrast, PUFAs inhibit activation, as measured by decreased levels of cell-surface receptors compared with untreated cells. **(c)** Different SFAs, MUFAs and PUFAs differentially increase or decrease T cell proliferation. The effects of fatty acids on proliferation influence the numbers of specific T cell subsets in atherosclerotic plaques, as shown in experimental studies. **(d)** PUFAs generally promote T cell polarization into the anti-inflammatory T cell subsets T_{reg} cells and T_H2 cells. Conversely, SFAs and MUFAs generally promote T cell polarization into pro-inflammatory subsets, such as T_H1 cells and T_H17 cells. The different T cell subsets then produce their signature cytokines, which can be measured for subset identification in experimental studies. See the main text for more information. AMPK, AMP-activated protein kinase; CPT1A, carnitine O-palmitoyltransferase 1; FASN, fatty acid synthase; FOXP3, forkhead box protein P3; GATA3, GATA-binding factor 3; HIF1α, hypoxia-inducible factor 1α; IFNγ, interferon-γ; mTOR, mechanistic target of rapamycin; mTORC, mechanistic target of rapamycin complex; RORγt, nuclear receptor RORγt; T-bet, T-box transcription factor TBX21; TGFβ, transforming growth factor-β; TNF, tumor necrosis factor.

Oleic acid also has partial pro-inflammatory effects, because 50 µmol/l of oleic acid reduced the proportion of T_{reg} cells *in vitro* in a similar fashion to palmitoleic acid[90]. However, oleic acid has also been found to have partial anti-inflammatory effects: the addition of 25 µmol/l and 50 µmol/l oleic acid reduced IFNγ and IL-17A production and increased IL-2, IL-4 and IL-10 production, indicating a partial decrease in T_H1 and T_H17 cells and an increase in T_H2 cells[90].

The above data generally support the classification of palmitoleic acid as being mostly anti-atherogenic, but creates some uncertainty about the findings indicating that oleic acid potentially has pro-atherogenic effects. A study investigating the link between MUFAs and cardiovascular mortality showed a U-shaped association between oleic acid concentrations in erythrocyte membranes and cardiovascular mortality[50]. This observation suggests that oleic acid is associated with cardiovascular mortality only at low and high concentrations in erythrocyte membranes, but less so at medium concentrations, which provides a possible explanation for the occasionally anti-inflammatory effects that oleic acid has on T cell subset polarization. However, the concentrations of oleic acid used in the various studies described above ranged from 25 µmol/l to 1,000 µmol/l, with no clearly distinguishable differences in pro-inflammatory and anti-inflammatory effects based on the concentration used.

Other MUFAs, such as vaccenic acid, have been shown to have solely anti-inflammatory and anti-atherogenic effects. Although the precise mechanism is not yet known, vaccenic acid levels have been inversely correlated with the risk of coronary heart disease in humans[52]. This effect might be mediated by T cells, because male JCR:LA-cp rats fed a diet supplemented with 1.5% w/w vaccenic acid for 3 weeks showed a decreased percentage of T_H cells in both the spleen and mesenteric lymph nodes compared with rats fed a control diet (0% vaccenic acid)[114]. In the same study, splenocytes from lean rats fed the vaccenic acid-supplemented diet produced lower concentrations of IL-2, IL-10 and TNF after *ex vivo* stimulation with the T cell mitogen concanavalin A than splenocytes from lean rats fed the control diet, implying decreased T_H1 cell and T_{reg} cell numbers. By contrast, splenocytes from obese rats produced higher IL-10 levels and lower IL-2 and TNF levels after concanavalin A *ex vivo* stimulation than splenocytes from obese rats fed the control diet. These concentrations were similar to those produced by splenocytes from lean control rats, implying an increase in T_{reg} cell numbers and a normalized number of T_H1 cells[114].

Table 2 | Overview of effects of fatty acids on T cell processes. ↑ and ↓ indicate that the fatty acid had a directed effect on that process. NR, not reported; T_H cell, T helper cell; T_{reg} cell, regulatory T cell.

	T cell process			
Fatty acid	**Metabolism**	**Activation**	**Proliferation**	**Polarization**
Lauric acid	Did not rescue de novo fatty acid synthesis[76]	NR	↑[88] Did not rescue[77]	↑ T_H1 cells[88] ↑ T_H17 cells[88] ↓ T_{reg} cells[88]
Myristic acid	Did not rescue de novo fatty acid synthesis[76]	NR	Rescued[77]	NR
Palmitic acid	NR	↑[83]	↓[91] ↑[93] Rescued[77]	↑ T_H1 cells[88, 111] ↑ T_H17 cells[88, 111] ↓ T_H2 cells[111] ↓ T_{reg} cells[111]
Palmitoleic acid	NR	NR	↓[90] ↑[93] Did not rescue[77]	↓ T_H1 cells[90] ↓ T_H17 cells[90] ↓ T_{reg} cells[90]
Stearic acid	NR	NR	↓[93] ↑[91]	NR
Oleic acid	Rescued de novo fatty acid synthesis[76] Rescued oxidative phosphorylation and glycolysis[77]	↑[84] No effect[83]	↑[90, 92, 93] Rescued[77]	↓[90] and ↑[90, 111] T_H1 cells ↓[90] and ↑[111] T_H17 cells ↓[111] and ↑[90] T_H2 cells ↓ T_{reg} cells[90, 111]
Vaccenic acid	NR	NR	NR	↓ T_H cells[114] ↓ T_H1 cells[116] ↑ T_{reg} cells[114]
Linoleic acid	↑ β-Oxidation[78] ↓ Electron transport chain respiration[78]	No effect[83]	↑[93] Did not rescue[77]	NR
γ-Linolenic acid	NR	No effect[83]	↓[95, 96] ↑[93] Did not rescue[77]	NR
Arachidic acid	NR	NR	Rescued[77]	NR
Arachidonic acid	NR	No effect[83]	NR	↑ T_H1 cells[112] ↑ T_H17 cells[112] ↓ T_H2 cells[112]

[continued on next page]

Table 2 *[continued]*

	T cell process			
Fatty acid	**Metabolism**	**Activation**	**Proliferation**	**Polarization**
Eicosapentaenoic acid	↑ Mitochondrial respiration-associated proton leakage[79]	NR	↓[79, 91, 98-104]	↓ T_H1 cells[112, 118-120] ↓ T_H17 cells[112, 117] ↑[100, 112, 118] or no effect[120] on T_H2 cells ↑[112] or no effect[117] on T_{reg} cells
Docosahexaenoic acid	Did not rescue de novo fatty acid synthesis[76] ↑ Mitochondrial respiration-associated proton leakage[79]	↓[85]	↓[79, 91, 97-104]	↓ T_H1 cells[112, 118-120] ↓ T_H17 cells[112, 117] ↑[100, 112, 118] or no effect[120] on T_H2 cells ↑[112] or no effect[117] on T_{reg} cells
Lignoceric acid	NR	NR	Did not rescue[77]	NR

Another study showed that this effect on cytokine levels was mediated by vaccenic acid and not through its conversion to conjugated linoleic acid[115], which has known anti-inflammatory properties. Human PBMCs exposed *in vitro* to 11 µmol/l, 33 µmol/l or 100 µmol/l of vaccenic acid for 24 h had a >30% reduction in IL-2 and TNF secretion compared with control cells[116]. Gas chromatography analysis showed that vaccenic acid increased in a dose-dependent manner in the lipid fractions of the cells, but conjugated linoleic acid did not. This finding indicates that vaccenic acid, independent of its conversion to conjugated linoleic acid, induces anti-inflammatory effects in T cells[116].

PUFAs such as EPA and DHA have distinct anti-inflammatory properties, increasing the proportion and cytokine levels of anti-inflammatory T_H2 cells and T_{reg} cells and decreasing those of pro-inflammatory T_H1 cells and T_H17 cells, both *in vitro* and *in vivo* in humans and mice[100, 117-120]. In one study, NOD mice fed a diet enriched in EPA and DHA for 20 weeks were used in *in vivo* assays, and in *in vitro* experiments activated $CD4^+$ T cells derived from NOD mice, from four patients with type 1 diabetes mellitus and from five donors without type 1 diabetes were exposed to 50 µmol/l or 100 µmol/l of EPA or DHA for 24 h[112]. DHA and EPA induced an increase in the number of T_H2 cells and T_{reg} cells and a decrease in the pro-inflammatory subsets T_H1 and T_H17. Furthermore, the production of IFNγ and IL-17A decreased and of IL-4 and IL-10 increased[112]. The decrease in total T cell proliferation and simultaneous upregulation of anti-inflammatory cytokines and subsets and downregulation of pro-inflammatory cytokines and subsets induced by EPA and DHA further indicates that these FAs mediate anti-inflammatory and anti-atherogenic immune responses in T cells.

Determining whether a FA is involved in a pro-inflammatory or anti-inflammatory response is straightforward for some FAs. The PUFAs EPA and DHA show anti-inflammatory, anti-proliferative

and anti-atherogenic effects in *in vitro* and *in vivo* studies in both human and mouse T cells[112]. The PUFA arachidonic and the SFA lauric acid both stimulate polarization of pro-inflammatory T cell subsets and induce proliferation[88, 112]. However, not all FAs are as easily classified. Different MUFAs often show contradictory results across different studies that use different concentration or models. For example, the MUFAs palmitoleic acid and oleic acid show both pro-inflammatory and anti-inflammatory effects on T cell polarization as well as pro-proliferative and anti-proliferative effects[90]. These differences might also be attributed to other characteristics of these FAs, such as chain length and methyl groups. Therefore, whereas the effects of PUFAs and SFAs on T cell function and atherosclerosis might be easily determined, the role of MUFAs requires further investigation.

Future directions

Atherosclerosis is a complex disease driven by more than just high cholesterol levels and macrophages. Triglycerides and FAs have an integral role in atherosclerosis development and progression but their mechanisms of action are less well understood. T cells interact with and depend on signals from their environment, of which FAs are particularly important. In this Review, we summarize evidence showing that various FAs can substantially affect T cell function, which might in turn influence the development and progression of atherosclerosis. The metabolism, activation, proliferation and polarization of T cells can each be altered by interactions with specific FAs, as summarized in Fig. 1 and Table 2.

Nonetheless, many unknowns remain about the complex interactions among FAs, T cells and atherosclerosis. The mechanisms through which FAs influence T cell functions remain to be elucidated. In this respect, the formation of lipid rafts or metabolite-sensing G protein-coupled receptors are intriguing areas of research[121, 122]. Moreover, whether FA–T cell interactions are similar in the circulation and in atherosclerotic plaques, whether T cell responses and numbers are related to the FA content in the plaque, and whether FAs can influence T cell responses to antigens or pathogens have not yet been investigated.

The functional changes in T cells induced by FAs might also have a role in ameliorating atherosclerosis. This aspect has been widely studied in various studies on pharmacological interventions, especially with the PUFAs, EPA and DHA derived from fish oil, which have been summarized in a meta-analysis and systematic review[123]. One notable study assessing the effects of EPA supplementation on atherosclerosis is the REDUCE-IT trial[37, 38]. In this trial, men and women with established CVD who received 2 g of a highly purified ethyl ester of EPA twice daily had profound reductions in the risk of cardiovascular death compared with participants receiving placebo[37, 38]. The trial investigators relate the results to the very high concentrations of purified EPA, to the cell membrane stabilization properties of EPA and a change in high-sensitivity C-reactive protein levels. However, the results were independent of normalizing triglyceride levels in patients, indicating that other mechanisms also affected the outcomes[37, 38]. We propose

that T cells might also be a source of the pleiotropic beneficial effects of EPA observed in the REDUCE-IT trial. EPA has been shown to have an anti-inflammatory and suppressive effect on T cells[79, 91, 98-104, 112, 117-120] although this aspect has not yet been studied in relation to the trial outcomes.

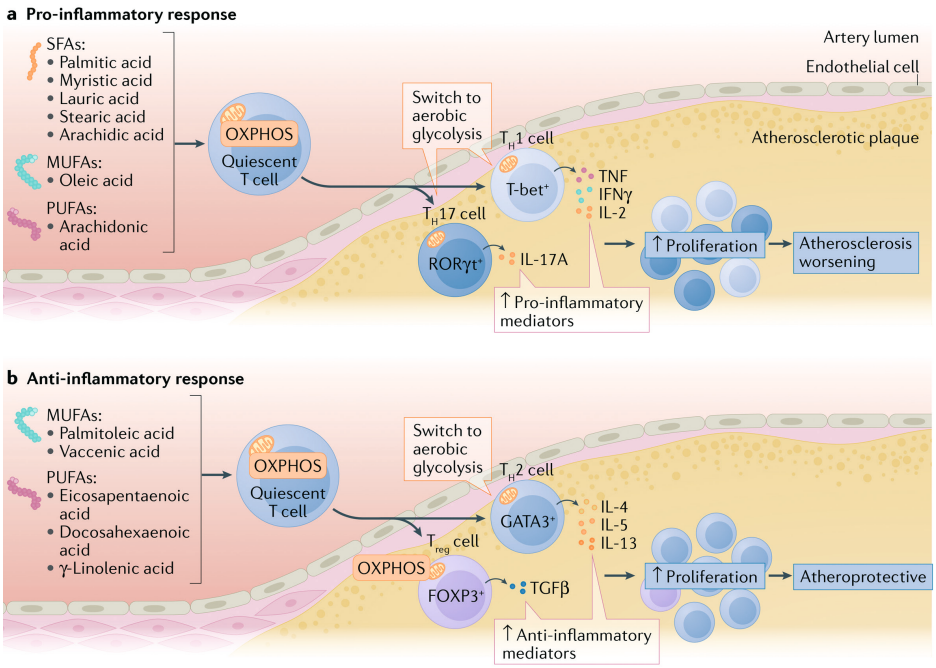

Fig. 2 | Effects of circulating fatty acids on T cell functions in atherosclerosis. Quiescent T cells can take up fatty acids present in the circulation, and the type of fatty acid determines the T cell metabolic switch after the T cell enters the dyslipidemic environment of the atherosclerotic plaque. The metabolic reprogramming in turn influences the polarization and inflammatory response of the T cell. Saturated fatty acids (SFAs) skew the polarization to pro-inflammatory T helper 1 (T_H1) cells and T_H17 cells, which proliferate and secrete pro-inflammatory cytokines, including interferon-γ (IFNγ), IL-2, tumor necrosis factor (TNF) and IL-17A, thereby contributing to worsening of atherosclerosis. **(a)** Monounsaturated fatty acids (MUFAs), such as palmitoleic acid, and polyunsaturated fatty acids (PUFAs), such as docosahexaenoic acid, skew the polarization to anti-inflammatory T_H2 cells and regulatory T (T_{reg}) cells. The T_H2 cells and T_{reg} cells proliferate and secrete anti-inflammatory cytokines, including IL-4, IL-5, IL-13 and transforming growth factor-β (TGFβ), that attenuate atherosclerosis. **(b)** Of note, the MUFA oleic acid and the PUFA arachidonic acid induce polarization into pro-inflammatory T cell subsets. FOXP3, forkhead box protein P3; GATA3, GATA-binding factor 3; OXPHOS, oxidative phosphorylation; RORγt, nuclear receptor RORγt; T-bet, T-box transcription factor TBX21.

SFAs and MUFAs have also been studied in clinical trials on CVD outcomes. The MUFA vaccenic acid has been shown to reduce the risk of CVD in clinical trials, as summarized previously[124]. A meta-analysis of clinical studies investigating the effects of coconut oil, which is rich in the SFA lauric acid, showed that coconut oil intake increases the levels of triglycerides, LDL cholesterol and HDL cholesterol in the plasma compared with intake of other oils[89]. This finding indicates that the consumption of coconut oil, and thereby lauric acid (which makes up around 50% of the FA component of coconut oil), increases the risk of CVD[89]. These studies provide overlapping

results for the effect of dietary FAs on atherosclerosis and what we describe in this Review about the effect of FAs on T cell function. However, T cells were not considered in the discussion of these clinical trials. Therefore, establishing and defining the interactions among atherosclerosis, FAs and T cells will be crucial to our understanding of the pathogenesis of this disease and how it can be prevented and treated.

The concentrations of FAs are higher in atherosclerotic plaques than in the circulation and, therefore, the plaque environment might influence effector T cell functions more strongly[125]. However, if the T cells have already been exposed to high concentrations of FAs, or their precursor triglycerides, in the circulation before migrating into the atherosclerotic plaque, the function of these T cells has probably already been altered. For example, γ-linolenic acid has been shown to inhibit T cell proliferation *in vitro* when added before T cell activation[96]. This inhibition is also likely to occur in individuals with hypertriglyceridemia or obesity and provides a potential link between these conditions and the associated increased risk of developing atherosclerosis[126, 127]. More research is needed to identify the precise effects of secondary exposure of the T cells to FAs in atherosclerotic plaques after the T cells have come into contact with FAs in the circulation.

The effects of FAs in altering T cell metabolism in relation to atherosclerosis development and progression is of particular interest for future investigation. Immunometabolism is highly dependent on FAs, and FAs can influence the T cell immune response. This rapidly evolving area of research could help explain the changes in T cell function induced by FAs by providing substantial insight into the mechanisms that drive these changes. The data reviewed here are in accordance with a mechanism involving T cells undergoing a type of metabolic reprogramming induced by the interactions with FAs in the circulation that might influence the subsequent T cell effects on diseases such as atherosclerosis.

Conclusions

We call for a shift in the focus of atherosclerosis research. FAs and triglycerides have re-emerged as crucial media- tors in the development of atherosclerosis. Furthermore, atherosclerosis development and progression have also been linked to T cells, with these cells making up ≥30% of the leukocytes present in atherosclerotic plaques in both humans and mice. T cells can be functionally altered by FAs through changes in T cell metabolism. This observation suggests that FAs, T cells and atherosclerosis are linked, and this possible association remains to be further elucidated. We propose that the metabolic reprogramming of T cells induced by their interactions with FAs in the circulation influences their subsequent functions in disease states such as atherosclerosis (Fig. 2).

Acknowledgements
The authors' work is supported by the Netherlands CardioVascular Research Initiative (The Dutch Heart Foundation, Dutch Federation of University Medical Centers, the Netherlands

Organization for Health Research and Development, and the Royal Netherlands Academy of Sciences) for the GENIUSII project Generating the Best Evidence-Based Pharmaceutical Targets for Atherosclerosis (CVON2011-19, CVON2017-20) and the Joint Programming Initiative a Healthy Diet for a Healthy Life (JPI HDHL) administered by ZonMW, the Netherlands (grant 529051021).

Author contributions

N.A.R. researched data for the article and wrote the manuscript. B.T.H. and J.W.J. conceived and designed the content of the manuscript. All the authors provided substantial contributions to the discussion of content and reviewed and edited the manuscript before submission.

Competing interests

The authors declare no competing interests.

Review criteria

We conducted a literature search divided into three main strategies. First, we searched for the four T cell responses, metabolism, activation, proliferation and polarization, together with different fatty acid names. Second, we searched for the four T cell responses in combination with the term “atherosclerosis”. Third, we searched fatty acid names in combination with the term “atherosclerosis”. The different T cell subsets ($CD8^+$, $CD4^+$, T_H1, T_H2, T_H17 and T_{reg} cells) were also used as search terms in combination with the groups listed above.

References

1 Schaftenaar, F., Frodermann, V., Kuiper, J. & Lutgens, E. Atherosclerosis: the interplay between lipids and immune cells. *Curr. Opin. Lipidol.* **27**, 209-215, (2016).

2 Barquera, S. *et al.* Global overview of the epidemiology of atherosclerotic cardiovascular disease. *Arch. Med. Res.* **46**, 328-338, (2015).

3 Brown, M. S. & Goldstein, J. L. How LDL receptors influence cholesterol and atherosclerosis. *Sci. Am.* **251**, 58-69, (1984).

4 Brown, M. S. & Goldstein, J. L. A receptor-mediated pathway for cholesterol homeostasis. *Science* **232**, 43-47, (1986).

5 Tabas, I. & Lichtman, A. H. Monocyte-macrophages and T cells in atherosclerosis. *Immunity* **47**, 621-634, (2017).

6 Hansson, G. K., Holm, J. & Jonasson, L. Detection of activated T lymphocytes in the human atherosclerotic plaque. *Am. J. Pathol.* **135**, 169-175, (1989).

7 Jonasson, L., Holm, J., Skalli, O., Bondjers, G. & Hansson, G. K. Regional accumulations of T cells, macrophages, and smooth muscle cells in the human atherosclerotic plaque. *Arteriosclerosis* **6**, 131–138, (1986).

8 Zhou, X., Nicoletti, A., Elhage, R. & Hansson, G. K. Transfer of CD4+ T cells aggravates atherosclerosis in immunodeficient apolipoprotein E knockout mice. *Circulation* **102**, 2919-2922, (2000).

9 Zhou, X., Robertson, A. K., Hjerpe, C. & Hansson, G. K. Adoptive transfer of CD4+ T cells reactive to modified low-density lipoprotein aggravates atherosclerosis. *Arterioscler. Thromb. Vasc. Biol.* **26**, 864-870, (2006).

10 Ketelhuth, D. F. & Hansson, G. K. Adaptive response of T and B cells in atherosclerosis. *Circ. Res.* **118**, 668-678, (2016).

11 Aukrust, P. *et al.* The complex role of T-cell-based immunity in atherosclerosis. *Curr. Atheroscler. Rep.* **10**, 236–243, (2008).

12 Saigusa, R., Winkels, H. & Ley, K. T cell subsets and functions in atherosclerosis. *Nat. Rev. Cardiol.* **17**, 387-401, (2020).

13 Cochain, C. & Zernecke, A. Protective and pathogenic roles of CD8+ T cells in atherosclerosis. *Basic Res. Cardiol.* **111**, 71, (2016).

14 van Duijn, J., Kuiper, J. & Slutter, B. The many faces of CD8+ T cells in atherosclerosis. *Curr. Opin. Lipidol.* **29**, 411-416, (2018).

15 van Duijn, J. *et al.* CD8+ T-cells contribute to lesion stabilization in advanced atherosclerosis by limiting macrophage content and CD4+ T-cell responses. *Cardiovasc. Res.* **115**, 729-738, (2019).

16 Cochain, C. *et al.* CD8+ T cells regulate monopoiesis and circulating Ly6C-high monocyte levels in atherosclerosis in mice. *Circ. Res.* **117**, 244-253, (2015).

17 Leistner, D. M. *et al.* Differential immunological signature at the culprit site distinguishes acute coronary syndrome with intact from acute coronary syndrome with ruptured fibrous cap: results from the prospective translational OPTICO-ACS study. *Eur. Heart J.* **41**, 3549-3560, (2020).

18 Winkels, H. *et al.* Atlas of the immune cell repertoire in mouse atherosclerosis defined by single-cell RNA-sequencing and mass cytometry. *Circ. Res.* **122**, 1675-1688, (2018).

19 Fernandez, D. M. *et al.* Single-cell immune landscape of human atherosclerotic plaques. *Nat. Med.* **25**, 1576-1588, (2019).

20 Depuydt, M. A. *et al.* Microanatomy of the human atherosclerotic plaque by single-cell transcriptomics. *Circ. Res.* **127**, 1437-1455, (2020).

21 Zernecke, A. *et al.* Meta-analysis of leukocyte diversity in atherosclerotic mouse aortas. *Circ. Res.* **127**, 402-426, (2020).

22 Williams, J. W. *et al.* Single cell RNA sequencing in atherosclerosis research. *Circ. Res.* **126**, 1112-1126, (2020).

23 Visscher, M. *et al.* Data processing pipeline for lipid profiling of carotid atherosclerotic plaque with mass spectrometry imaging. *J. Am. Soc. Mass. Spectrom.* **30**, 1790-1800, (2019).

24 Stemme, S. *et al.* T lymphocytes from human atherosclerotic plaques recognize oxidized low density lipoprotein. *Proc. Natl Acad. Sci. USA* **92**, 3893–3897, (1995).

25 Wolf, D. *et al.* Pathogenic autoimmunity in atherosclerosis evolves from initially protective apolipoprotein B100-reactive CD4(+) T-regulatory cells. *Circulation* **142**, 1279-1293, (2020).

26 van Puijvelde, G. H. *et al.* Induction of oral tolerance to oxidized low-density lipoprotein ameliorates atherosclerosis. *Circulation* **114**, 1968-1976, (2006).

27 Klingenberg, R. *et al.* Intranasal immunization with an apolipoprotein B-100 fusion protein induces antigen-specific regulatory T cells and reduces atherosclerosis. *Arterioscler. Thromb. Vasc. Biol.* **30**, 946-952, (2010).

28 Tse, K. *et al.* Atheroprotective vaccination with MHC-II restricted peptides from ApoB-100. *Front. Immunol.* **4**, 493, (2013).

29 Nilsson, J., Wigren, M. & Shah, P. K. Regulatory T cells and the control of modified lipoprotein autoimmunity-driven atherosclerosis. *Trends Cardiovasc. Med.* **19**, 272-276, (2009).

30 McNamara, D. J. Dietary cholesterol and atherosclerosis. *Biochim. Biophys. Acta* **1529**, 310-320, (2000).

31 Talayero, B. G. & Sacks, F. M. The role of triglycerides in atherosclerosis. *Curr. Cardiol. Rep.* **13**, 544-552, (2011).

32 Dron, J. S. & Hegele, R. A. Genetics of triglycerides and the risk of atherosclerosis. *Curr. Atheroscler. Rep.* **19**, 31, (2017).

33 Nordestgaard, B. G. Triglyceride-rich lipoproteins and atherosclerotic cardiovascular disease new insights from epidemiology, genetics, and biology. *Circ. Res.* **118**, 547-563, (2016).

34 Keech, A. C. & Jenkins, A. J. Triglyceride-lowering trials. *Curr. Opin. Lipidol.* **28**, 477-487, (2017).

35 Salakhutdinov, N. F. & Laev, S. S. Triglyceride-lowering agents. *Bioorg. Med. Chem.* **22**, 3551-3564, (2014).

36 Budoff, M. Triglycerides and triglyceride-rich lipoproteins in the causal pathway of cardiovascular disease. *Am. J. Cardiol.* **118**, 138-145, (2016).

37 Bhatt, D. L. *et al.* Cardiovascular risk reduction with icosapent ethyl for hypertriglyceridemia. *N. Engl. J. Med.* **380**, 11-22, (2019).

38 Bhatt, D. L. *et al.* Effects of icosapent ethyl on total ischemic events from REDUCE-IT. *J. Am. Coll. Cardiol.* **73**, 2791-2802, (2019).

39 Kersten, S. Triglyceride metabolism under attack. *Cell Metab.* **25**, 1209-1210, (2017).

40 Kersten, S. Physiological regulation of lipoprotein lipase. *Biochim. Biophys. Acta* **1841**, 919-933, (2014).

41 Ding, D. *et al.* Association between erythrocyte membrane n-3 and n-6 polyunsaturated fatty acids and carotid atherosclerosis: a prospective study. *Atherosclerosis* **298**, 7-13, (2020).

42 Steffen, B. T., Duprez, D., Szklo, M., Guan, W. & Tsai, M. Y. Circulating oleic acid levels are related to greater risks of cardiovascular events and all-cause mortality: The Multi-Ethnic Study of Atherosclerosis. *J. Clin. Lipidol.* **12**, 1404-1412, (2018).

43 Afonso, M. S. *et al.* Dietary interesterified fat enriched with palmitic acid induces atherosclerosis by impairing macrophage cholesterol efflux and eliciting inflammation. *J. Nutr. Biochem.* **32**, 91-100, (2016).

44 Marangoni, F. *et al.* Dietary linoleic acid and human health: focus on cardiovascular and cardiometabolic effects. *Atherosclerosis* **292**, 90-98, (2020).

45 Yang, Z. H. *et al.* Dietary palmitoleic acid attenuates atherosclerosis progression and hyperlipidemia in low-density lipoprotein receptor-deficient mice. *Mol. Nutr. Food Res.* **63**, 1900120, (2019).

46 Gallagher, H. *et al.* Dihomo-γ-linolenic acid inhibits several key cellular processes associated with atherosclerosis. *Biochim. Biophys. Acta Mol. Basis Dis.* **1865**, 2538-2550, (2019).

47 Noto, D. *et al.* Myristic acid is associated to low plasma HDL cholesterol levels in a Mediterranean population and increases HDL catabolism by enhancing HDL particles trapping to cell surface proteoglycans in a liver hepatoma cell model. *Atherosclerosis* **246**, 50-56, (2016).

48 Yamagishi, K., Nettleton, J. A., Folsom, A. R. & Investigators, A. S. Plasma fatty acid composition and incident heart failure in middle-aged adults: the Atherosclerosis Risk in Communities (ARIC) Study. *Am. Heart J.* **156**, 965-974, (2008).

49 Valenzuela, C. A., Baker, E. J., Miles, E. A. & Calder, P. C. Eighteen-carbon trans fatty acids and inflammation in the context of atherosclerosis. *Prog. Lipid Res.* **76**, 101009, (2019).

50 Delgado, G. E. *et al.* Individual omega-9 monounsaturated fatty acids and mortality – the Ludwigshafen Risk and Cardiovascular Health Study. *J. Clin. Lipidol.* **11**, 126-135, (2017).

51 Liu, L. *et al.* Protective role of n6/n3 PUFA supplementation with varying DHA/EPA ratios against atherosclerosis in mice. *J. Nutr. Biochem.* **32**, 171-180, (2016).

52 Djousse, L., Matthan, N. R., Lichtenstein, A. H. & Gaziano, J. M. Red blood cell membrane concentration of cis-palmitoleic and cis-vaccenic acids and risk of coronary heart disease. *Am. J. Cardiol.* **110**, 539-544, (2012).

53 Spigoni, V. *et al.* Stearic acid at physiologic concentrations induces in vitro lipotoxicity in circulating angiogenic cells. *Atherosclerosis* **265**, 162-171, (2017).

54 Kelley, D. S. & Adkins, Y. Similarities and differences between the effects of EPA and DHA on markers of atherosclerosis in human subjects. *Proc. Nutr. Soc.* **71**, 322-331, (2012).

55 Mensink, R. P., Zock, P. L., Kester, A. D. M. & Katan, M. B. Effects of dietary fatty acids and carbohydrates on the ratio of serum total to HDL cholesterol and on serum lipids and apolipoproteins: a meta-analysis of 60 controlled trials. *Am. J. Clin. Nutr.* **77**, 1146-1155, (2003).

56 Polonskaya, Y. V. *et al.* Balance of fatty acids and their correlations with parameters of lipid metabolism and markers of inflammation in men with coronary atherosclerosis. *Bull. Exp. Biol. Med.* **164**, 33-35, (2017).

57 Chung, H. K. *et al.* Plasma phospholipid arachidonic acid and lignoceric acid are associated with the risk of cardioembolic stroke. *Nutr. Res.* **35**, 1001-1008, (2015).

58 Ghoshal, S., Witta, J., Zhong, J., de Villiers, W. & Eckhardt, E. Chylomicrons promote intestinal absorption of lipopolysaccharides. *J. Lipid Res.* **50**, 90-97, (2009).

59 Randolph, G. J. & Miller, N. E. Lymphatic transport of high-density lipoproteins and chylomicrons. *J. Clin. Invest.* **124**, 929-935, (2014).

60 Ratnayake, W. M. & Galli, C. Fat and fatty acid terminology, methods of analysis and fat digestion and metabolism: a background review paper. *Ann. Nutr. Metab.* **55**, 8-43, (2009).

61 Chowdhury, R. *et al.* Association of dietary, circulating, and supplement fatty acids with coronary risk. *Ann. Intern. Med.* **160**, 398-406, (2014).

62 Spady, K. D., Woollett, L. A. & Dietschy, J. M. Regulation of plasma LDL-cholesterol levels by dietary cholesterol and fatty acids. *Annu. Rev. Nutr.* **13**, 355–381, (1993).

63 Chapman, N. M., Boothby, M. R. & Chi, H. Metabolic coordination of T cell quiescence and activation. *Nat. Rev. Immunol.* **20**, 55-70, (2020).

64 Sprent, J. & Surh, C. D. Normal T cell homeostasis: the conversion of naive cells into memory-phenotype cells. *Nat. Immunol.* **12**, 478-484, (2011).

65 Smith-Garvin, J. E., Koretzky, G. A. & Jordan, M. S. T cell activation. *Annu. Rev. Immunol.* **27**, 591-619, (2009).

66 Guermonprez, P., Valladeau, J., Zitvogel, L., Thery, C. & Amigorena, S. Antigen presentation and T cell stimulation by dendritic cells. *Annu. Rev. Immunol.* **20**, 621-667, (2002).

67 Geissmann, F. *et al.* Blood monocytes: distinct subsets, how they relate to dendritic cells, and their possible roles in the regulation of T-cell responses. *Immunol. Cell Biol.* **86**, 398-408, (2008).

68 Ramsay, G. & Cantrell, D. Environmental and metabolic sensors that control T cell biology. *Front. Immunol.* **6**, 99, (2015).

69 Koltsova, E. K. *et al.* Dynamic T cell-APC interactions sustain chronic inflammation in atherosclerosis. *J. Clin. Investig.* **122**, 3114-3126, (2012).

70 Geltink, R. I. K., Kyle, R. L. & Pearce, E. L. Unraveling the complex interplay between T cell metabolism and function. *Annu. Rev. Immunol.* **36**, 461-488, (2018).

71 Howie, D., Ten Bokum, A., Necula, A. S., Cobbold, S. P. & Waldmann, H. The role of lipid metabolism in T lymphocyte differentiation and survival. *Front. Immunol.* **8**, 1949, (2018).

72 Kopf, H., de la Rosa, G. M., Howard, O. M. & Chen, X. Rapamycin inhibits differentiation of Th17 cells and promotes generation of FoxP3+ T regulatory cells. *Int. Immunopharmacol.* **7**, 1819-1824, (2007).

73 Young, K. E., Flaherty, S., Woodman, K. M., Sharma-Walia, N. & Reynolds, J. M. Fatty acid synthase regulates the pathogenicity of Th17 cells. *J. Leukoc. Biol.* **102**, 1229-1235, (2017).

74 Berod, L. *et al.* De novo fatty acid synthesis controls the fate between regulatory T and T helper 17 cells. *Nat. Med.* **20**, 1327-1333, (2014).

75 O'Sullivan, D. & Pearce, E. L. Fatty acid synthesis tips the TH17-Treg cell balance. *Nat. Med.* **20**, 1235-1236, (2014).

76 Endo, Y. *et al.* Obesity drives Th17 cell differentiation by inducing the lipid metabolic kinase, ACC1. *Cell Rep.* **12**, 1042-1055, (2015).

77 Angela, M. *et al.* Fatty acid metabolic reprogramming via mTOR-mediated inductions of PPARγ directs early activation of T cells. *Nat. Commun.* **7**, 13683, (2016).

78 Ma, C. *et al.* NAFLD causes selective CD4+ T lymphocyte loss and promotes hepatocarcinogenesis. *Nature* **531**, 253-257, (2016).

79 Fan, Y. Y. *et al.* Remodelling of primary human CD4+ T cell plasma membrane order by n-3 PUFA. *Br. J. Nutr.* **119**, 163-175, (2018).

80 Borow, K. M., Nelson, J. R. & Mason, R. P. Biologic plausibility, cellular effects, and molecular mechanisms of eicosapentaenoic acid (EPA) in atherosclerosis. *Atherosclerosis* **242**, 357-366, (2015).

81 Stegemann, C. *et al.* Comparative lipidomics profiling of human atherosclerotic plaques. *Circ. Cardiovasc. Genet.* **4**, 232-242, (2011).

82 Cochran, J. R., Cameron, T. O. & Stern, L. J. The relationship of MHC-peptide binding and T cell activation probed using chemically defined MHC class II oligomers. *Immunity* **12**, 241–250, (2000).

83 Stentz, F. B. & Kitabchi, A. E. Palmitic acid-induced activation of human T-lymphocytes and aortic endothelial cells with production of insulin receptors, reactive oxygen species, cytokines, and lipid peroxidation. *Biochem. Biophys. Res. Commun.* **346**, 721-726, (2006).

84 Moussa, M. *et al.* In vivo effects of olive oil-based lipid emulsion on lymphocyte activation in rats. *Clin. Nutr.* **19**, 49-54, (2000).

85 Kew, S. *et al.* Effects of oils rich in eicosapentaenoic and docosahexaenoic acids on immune cell composition and function in healthy humans. *Am. J. Clin. Nutr.* **79**, 674–681, (2004).

86 Steffen, B. T. *et al.* Plasma n-3 and n-6 fatty acids are differentially related to carotid plaque and its progression: the multi-ethnic study of atherosclerosis. *Arterioscler. Thromb. Vasc. Biol.* **38**, 653-659, (2018).

87 Shipkova, M. & Wieland, E. Surface markers of lymphocyte activation and markers of cell proliferation. *Clin. Chim. Acta* **413**, 1338-1349, (2012).

88 Haghikia, A. *et al.* Dietary fatty acids directly impact central nervous system autoimmunity via the small intestine. *Immunity* **43**, 817-829, (2015).

89 Jayawardena, R., Swarnamali, H., Lanerolle, P. & Ranasinghe, P. Effect of coconut oil on cardio-metabolic risk: a systematic review and meta-analysis of interventional studies. *Diabetes Metab. Syndr.* **14**, 2007-2020, (2020).

90 Passos, M. E. *et al.* Differential effects of palmitoleic acid on human lymphocyte proliferation and function. *Lipids Health Dis.* **15**, 217, (2016).

91 Gorjão, R., Cury-Boaventura, M. F., de Lima, T. M. & Curi, R. Regulation of human lymphocyte proliferation by fatty acids. *Cell Biochem. Funct.* **25**, 305-315, (2007).

92 Miura, S. *et al.* Increased proliferative response of lymphocytes from intestinal lymph during long chain fatty acid absorption. *Immunology* **78**, 142-146, (1993).

93 Ioan-Facsinay, A. *et al.* Adipocyte-derived lipids modulate CD4+ T-cell function. *Eur. J. Immunol.* **43**, 1578-1587, (2013).

94 Wang , L., Folsom, A. R., Eckfeldt, J. H. & Investigators, t. A. S. Plasma fatty acid composition and incidence of coronary heart disease in middle aged adults: the Atherosclerosis Risk in Communities (ARIC) study. *Nutr. Metab. Cardiovasc. Dis.* **13**, 256-266, (2003).

95 Rossetti, R. G., Seiler, C. M., DeLuca, P., Laposata, M. & Zurier, R. B. Oral administration of unsaturated fatty acids: effects on human peripheral blood T lymphocyte proliferation. *J. Leukoc. Biol.* **62**, 438-443, (1997).

96 Zurier, R. B., Rossetti, R. G., Seiler, C. M. & Laposata, M. Human peripheral blood T lymphocyte proliferation after activation of the T cell receptor: effects of unsaturated fatty acids. *Prostaglandins Leukot. Essent. Fatty Acids* **60**, 371-375, (1999).

97 Fan, Y. Y., Ly, L. H., Barhoumi, R., McMurray, D. N. & Chapkin, R. S. Dietary docosahexaenoic acid suppresses T cell protein kinase C θ lipid raft recruitment and IL-2 production. *J. Immunol.* **173**, 6151-6160, (2004).

98 Pompos, L. J. & Fritsche, K. L. Antigen-driven murine CD4+ T lymphocyte proliferation and interleukin-2 production are diminished by dietary (n-3) polyunsaturated fatty acids. *J. Nutr.* **132**, 3293–3300, (2002).

99 Ly, L. H., Smith, R., Switzer, K. C., Chapkin, R. S. & McMurray, D. N. Dietary eicosapentaenoic acid modulates CTLA-4 expression in murine CD4+ T-cells. *Prostaglandins Leukot. Essent. Fatty Acids* **74**, 29-37, (2006).

100 Merzouk, S. A. *et al.* N-3 polyunsaturated fatty acids modulate in-vitro T cell function in type I diabetic patients. *Lipids* **43**, 485-497, (2008).

101 Jolly, C. A., Jiang, Y. H., Chapkin, R. S. & McMurray, D. N. Dietary (n-3) polyunsaturated fatty acids suppress murine lymphoproliferation, interleukin-2 secretion, and the formation of diacylglycerol and ceramide. *J. Nutr.* **127**, 37–43, (1997).

102 Collison, L. W., Collison, R. E., Murphy, E. J. & Jolly, C. A. Dietary n-3 polyunsaturated fatty acids increase T-lymphocyte phospholipid mass and acyl-CoA binding protein expression. *Lipids* **40**, 81–87, (2005).

103 McMurray, D. N., Jolly, C. A. & Chapkin, R. S. Effects of dietary n-3 fatty acids on T cell activation and T cell receptor-mediated signaling in a murine model. *J. Infect. Dis.* **182**, S103–S107, (2000).

104 Thies, F. *et al.* Dietary supplementation with γ-linolenic acid or fish oil decreases T lymphocyte proliferation in healthy older humans. *J. Nutr.* **131**, 1918–1927, (2001).

105 Ding, L. *et al.* Eicosapentaenoic acid-enriched phospholipids improve atherosclerosis by mediating cholesterol metabolism. *J. Funct. Foods* **32**, 90-97, (2017).

106 Erkkila, A. T., Matthan, N. R., Herrington, D. M. & Lichtenstein, A. H. Higher plasma docosahexaenoic acid is associated with reduced progression of coronary atherosclerosis in women with CAD. *J. Lipid Res.* **47**, 2814-2819, (2006).

107 Van Noolen, L. *et al.* Docosahexaenoic acid supplementation modifies fatty acid incorporation in tissues and prevents hypoxia induced-atherosclerosis progression in apolipoprotein-E deficient mice. *Prostaglandins Leukot. Essent. Fatty Acids* **91**, 111-117, (2014).

108 de Oliveira Otto, M. C. *et al.* Circulating and dietary omega-3 and omega-6 polyunsaturated fatty acids and incidence of CVD in the multi-ethnic study of atherosclerosis. *J. Am. Heart Assoc.* **2**, 000506, (2013).

109 Chang, C. L. & Deckelbaum, R. J. Omega-3 fatty acids: mechanisms underlying "protective effects" in atherosclerosis. *Curr. Opin. Lipidol.* **24**, 345-350, (2013).

110 Block, R. C., Harris, W. S., Reid, K. J., Sands, S. A. & Spertus, J. A. EPA and DHA in blood cell membranes from acute coronary syndrome patients and controls. *Atherosclerosis* **197**, 821-828, (2008).

111 Hossein zade, A. *et al.* Fatty acids effect on T helper differentiation in vitro. *Int. J. Food Sci. Nutr.* **5**, (2016).

112 Bi, X. *et al.* ω-3 polyunsaturated fatty acids ameliorate type 1 diabetes and autoimmunity. *J. Clin. Invest.* **127**, 1757-1771, (2017).

113 Raphael, I., Nalawade, S., Eagar, T. N. & Forsthuber, T. G. T cell subsets and their signature cytokines in autoimmune and inflammatory diseases. *Cytokine* **74**, 5-17, (2015).

114 Blewett, H. J., Gerdung, C. A., Ruth, M. R., Proctor, S. D. & Field, C. J. Vaccenic acid favourably alters immune function in obese JCR:LA-cp rats. *Br. J. Nutr.* **102**, 526-536, (2009).

115 Reynolds, C. M. & Roche, H. M. Conjugated linoleic acid and inflammatory cell signalling. *Prostaglandins Leukot. Essent. Fatty Acids* **82**, 199-204, (2010).

116 Jaudszus, A. *et al.* Vaccenic acid-mediated reduction in cytokine production is independent of c9,t11-CLA in human peripheral blood mononuclear cells. *Biochim. Biophys. Acta* **1821**, 1316-1322, (2012).

117 Monk, J. M., Hou, T. Y., Turk, H. F., McMurray, D. N. & Chapkin, R. S. n3 PUFAs reduce mouse CD4+ T-cell ex vivo polarization into Th17 cells. *J. Nutr.* **143**, 1501-1508, (2013).

118 Zhang, P., Smith, R., Chapkin, R. S. & McMurray, D. N. Dietary (n-3) polyunsaturated fatty acids modulate murine Th1/Th2 balance toward the Th2 pole by suppression of Th1 development. *J. Nutr.* **135**, 1745–1751, (2005).

119 Zhang, P. *et al.* Dietary fish oil inhibits antigen-specific murine Th1 cell development by suppression of clonal expansion. *J. Nutr.* **136**, 2391–2398, (2006).

120 Switzer, K. C., McMurray, D. N., Morris, J. S. & Chapkin, R. S. (n-3) Polyunsaturated fatty acids promote activation-induced cell death in murine T lymphocytes. *J. Nutr.* **133**, 496–503, (2003).

121 Robinson, G. A., Waddington, K. E., Pineda-Torra, I. & Jury, E. C. Transcriptional regulation of T-cell lipid metabolism: implications for plasma membrane lipid rafts and T-cell function. *Front. Immunol.* **8**, 1636, (2017).

122 Tan, J. K., McKenzie, C., Marino, E., Macia, L. & Mackay, C. R. Metabolite-sensing G protein-coupled receptors–facilitators of diet-related immune regulation. *Annu. Rev. Immunol.* **35**, 371-402, (2017).

123 Wu, G., Ji, Q., Huang, H. & Zhu, X. The efficacy of fish oil in preventing coronary heart disease: A systematic review and meta-analysis. *Medicine* **100**, 27253, (2021).

124 Wang, Y., Jacome-Sosa, M. M., Vine, D. F. & Proctor, S. D. Beneficial effects of vaccenic acid on postprandial lipid metabolism and dyslipidemia: impact of natural trans-fats to improve CVD risk. *Lipid Technol.* **22**, 103-106, (2010).

125 Pettinella, C., Lee, S. H., Cipollone, F. & Blair, I. A. Targeted quantitative analysis of fatty acids in atherosclerotic plaques by high sensitivity liquid chromatography/tandem mass spectrometry. *J. Chromatogr. B* **850**, 168-176, (2007).

126 Rocha, V. Z. & Libby, P. Obesity, inflammation, and atherosclerosis. *Nat. Rev. Cardiol.* **6**, 399-409, (2009).

127 Peng, J., Luo, F., Ruan, G., Peng, R. & Li, X. Hypertriglyceridemia and atherosclerosis. *Lipids Health Dis.* **16**, 233, (2017).

128 Bicalho, B., David, F., Rumplel, K., Kindt, E. & Sandra, P. Creating a fatty acid methyl ester database for lipid profiling in a single drop of human blood using high resolution capillary gas chromatography and mass spectrometry. *J. Chromatogr. A* **1211**, 120-128, (2008).

129 Maecker, H. T., McCoy, J. P. & Nussenblatt, R. Standardizing immunophenotyping for the Human Immunology Project. *Nat. Rev. Immunol.* **12**, 191-200, (2012).

130 McLaughlin, B. E. *et al.* Nine-color flow cytometry for accurate measurement of T cell subsets and cytokine responses. Part I: panel design by an empiric approach. *Cytometry A* **73A**, 400-410, (2008).

131 Leng, S. X. *et al.* ELISA and multiplex technologies for cytokine measurement in inflammation and aging research. *J. Gerontol. A Biol. Sci. Med. Sci.* **63**, 879–884, (2008).

132 Zhou, L., Chong, M. M. & Littman, D. R. Plasticity of CD4+ T cell lineage differentiation. *Immunity* **30**, 646-655, (2009).

133 Zhu, J., Yamane, H. & Paul, W. E. Differentiation of effector CD4 T cell populations*. *Annu. Rev. Immunol.* **28**, 445-489, (2010).

134 Szabo, S. J., Sullivan, B. M., Peng, S. L. & Glimcher, L. H. Molecular mechanisms regulating Th1 immune responses. *Annu. Rev. Immunol.* **21**, 713-758, (2003).

135 Sandquist, I. & Kolls, J. Update on regulation and effector functions of Th17 cells. *F1000 Res.* **7**, 205, (2018).

136 Nakayama, T. *et al.* Th2 cells in health and disease. *Annu. Rev. Immunol.* **35**, 53-84, (2017).

137 Foks, A. C., Lichtman, A. H. & Kuiper, J. Treating atherosclerosis with regulatory T cells. *Arterioscler. Thromb. Vasc. Biol.* **35**, 280-287, (2015).

138 Seumois, G. *et al.* Transcriptional profiling of Th2 cells identifies pathogenic features associated with asthma. *J. Immunol.* **197**, 655-664, (2016).

139 Fournier, C. Where do T cells stand in rheumatoid arthritis? *Jt. Bone Spine* **72**, 527-532, (2005).

140 Roep, B. O. The role of T-cells in the pathogenesis of type 1 diabetes: from cause to cure. *Diabetologia* **46**, 305-321, (2003).

141 MacIver, N. J., Michalek, R. D. & Rathmell, J. C. Metabolic regulation of T lymphocytes. *Annu. Rev. Immunol.* **31**, 259-283, (2013).

142 Vander Heiden, M. G., Cantley, L. C. & Thompson, C. B. Understanding the Warburg effect: the metabolic requirements of cell proliferation. *Science* **324**, 1029-1033, (2009).

143 Warburg, O., Gawehn, K. & Geissler, A. W. Metabolism of leukocytes [German]. *Z. Naturforsch. B* **13B**, 515-516, (1958).

144 Michalek, R. D. *et al.* Cutting edge: distinct glycolytic and lipid oxidative metabolic programs are essential for effector and regulatory CD4+ T cell subsets. *J. Immunol.* **186**, 3299-3303, (2011).

145 Cluxton, D., Petrasca, A., Moran, B. & Fletcher, J. M. Differential regulation of human Treg and Th17 cells by fatty acid synthesis and glycolysis. *Front. Immunol.* **10**, 115, (2019).

146 Fullerton, M. D., Steinberg, G. R. & Schertzer, J. D. Immunometabolism of AMPK in insulin resistance and atherosclerosis. *Mol. Cell Endocrinol.* **366**, 224-234, (2013).

147 Maganto-García, E., Tarrio, M. L., Grabie, N., Bu, D. X. & Lichtman, A. H. Dynamic changes in regulatory T cells are linked to levels of diet-induced hypercholesterolemia. *Circulation* **124**, 185-195, (2011).

148 Ketelhuth, D. F. J. *et al.* Immunometabolism and atherosclerosis: perspectives and clinical significance: a position paper from the Working Group on Atherosclerosis and Vascular Biology of the European Society of Cardiology. *Cardiovasc. Res.* **115**, 1385-1392, (2019).

149 Gistera, A. & Ketelhuth, D. F. J. Lipid-driven immunometabolic responses in atherosclerosis. *Curr. Opin. Lipidol.* **29**, 375-380, (2018).

150 Tomas, L. *et al.* Altered metabolism distinguishes high-risk from stable carotid atherosclerotic plaques. *Eur. Heart J.* **39**, 2301-2310, (2018).

151 Amersfoort, J. *et al.* Diet-induced dyslipidemia induces metabolic and migratory adaptations in regulatory T cells. *Cardiovasc. Res.* **117**, 1309-1324, (2020).

152 Delgoffe, G. M. *et al.* mTOR differentially regulates effector and regulatory T cell lineage commitment. *Immunity* **30**, 832-844, (2009).

153 Delgoffe, G. M. *et al.* The kinase mTOR regulates the differentiation of helper T cells through the selective activation of signaling by mTORC1 and mTORC2. *Nat. Immunol.* **12**, 295-303, (2011).

154 Shi, L. Z. *et al.* HIF1α-dependent glycolytic pathway orchestrates a metabolic checkpoint for the differentiation of TH17 and Treg cells. *J. Exp. Med.* **208**, 1367-1376, (2011).

Supplemental information

Supplementary Table 1 | Overview of fatty acid effects on T cell metabolism. The table shows the findings per fatty acid, listed from shortest to longest chain length and secondly from saturated fatty acid to monounsaturated fatty acid to polyunsaturated fatty acid. Fatty acids used in more than one study are listed in alphabetical order of the first author.

Fatty acid	Author	Model	Study performed *in vitro* or *in vivo*	Concentration of fatty acid used (µmol/l)	Effect on T cell metabolism
Lauric acid	Endo, *et al.*[1]	Mouse	*In vitro*	10	Did not rescue de novo fatty acid synthesis
Myristic acid	Endo, *et al.*[1]	Mouse	*In vitro*	30	Did not rescue de novo fatty acid synthesis
Oleic acid	Angela, *et al.*[2]	Human / mouse	*In vitro*	100	Rescues oxidative phosphorylation and glycolysis
	Endo, *et al.*[1]	Mouse	*In vitro*	100	Rescues de novo fatty acid synthesis
Linoleic acid	Ma, *et al.*[3]	Mouse	*In vitro*	50	↑ β-Oxidation ↓ Electron transport chain
Eicosapentaenoic acid	Fan, *et al.* (2018)[4]	Human	*In vitro*	50	↑ Mitochondrial respiration-associated proton leakage
Docosahexaenoic acid	Endo, *et al.*[1]	Mouse	*In vitro*	1	Did not rescue de novo fatty acid synthesis
	Fan, *et al.* (2018)[4]	Human	*In vitro*	50	↑ Mitochondrial respiration-associated proton leakage

Supplementary Table 2 | Overview of fatty acid effects on T cell activation. ↑ and ↓ indicate the fatty acid had a directed effect on that process. The table shows the findings per fatty acid, listed from shortest to longest chain length and secondly from saturated fatty acid to monounsaturated fatty acid to polyunsaturated fatty acid. Fatty acids used in more than one study are listed in alphabetical order of the first author.

Fatty acid	Author	Model	Study performed *in vitro* or *in vivo*	Concentration of fatty acid used (µmol/l)	Effect on T cell activation
Palmitic acid	Stentz and Kitabchi[5]	Human	*In vitro*	50, 500	↑
Oleic acid	Moussa, et al.[6]	Rat	*In vivo*	12% of diet	↑
	Stentz and Kitabchi[5]	Human	*In vitro*	1, 50, 500	No effect
Linoleic acid	Stentz and Kitabchi[5]	Human	*In vitro*	1, 50, 500	No effect
γ-Linolenic acid	Stentz and Kitabchi[5]	Human	*In vitro*	1, 50, 500	No effect
Arachidonic acid	Stentz and Kitabchi[5]	Human	*In vitro*	1, 50, 500	No effect
Docosahexaenoic acid	Kew, et al.[7]	Human	*In vivo*	1 g capsules nine times daily	↓

Supplementary Table 3 | Overview of fatty acid effects on T cell proliferation. ↑ and ↓ indicate the fatty acid had a directed effect on that process. "Rescued" or "Did not rescue" means the fatty acid could or could not recover that process under fatty-acid-free conditions. The table shows the findings per fatty acid, listed from shortest to longest chain length and secondly from saturated fatty acid to monounsaturated fatty acid to polyunsaturated fatty acid. Fatty acids used in more than one study are listed in alphabetical order of the first author.

Fatty acid	Author	Model	Study performed *in vitro* or *in vivo*	Concentration of fatty acid used (µmol/l)	Effect on T cell proliferation
Lauric acid	Angela, *et al.*[2]	Mouse	*In vitro*	100	Did not rescue
	Haghikia, *et al.*[8]	Mouse	*In vivo*	13.5% of diet	↑
Myristic acid	Angela, *et al.*[2]	Mouse	*In vitro*	100	Rescued
Palmitic acid	Angela, *et al.*[2]	Mouse	*In vitro*	100	Rescued
	Gorjao, *et al.*[9]	Human	*In vitro*	50	↓
	Ioan-Facsinay, *et al.*[10]	Human	*In vitro*	4µg/ml	↑
Palmitoleic acid	Angela, *et al.*[2]	Mouse	*In vitro*	100	Did not rescue
	Ioan-Facsinay, *et al.*[10]	Human	*In vitro*	2.1µg/ml	↑
	Passos, *et al.*[11]	Human	*In vitro*	25, 50	↓
Stearic acid	Gorjao, *et al.*[9]	Human	*In vitro*	50	↓
	Ioan-Facsinay, *et al.*[10]	Human	*In vitro*	4.2µg/ml	↑
Oleic acid	Angela, *et al.*[2]	Human / mouse	*In vitro*	100	Rescued
	Ioan-Facsinay, *et al.*[10]	Human	*In vitro*	17.7µg/ml	↑
	Miura, *et al.*[12]	Rat	*In vivo*	20	↑
	Passos, *et al.*[11]	Human	*In vitro*	25, 50	↑
Linoleic acid	Angela, *et al.*[2]	Mouse	*In vitro*	100	Did not rescue
	Ioan-Facsinay, *et al.*[10]	Human	*In vitro*	18µg/ml	↑
γ-Linolenic acid	Angela, *et al.*[2]	Mouse	*In vitro*	100	Did not rescue
	Ioan-Facsinay, *et al.*[10]	Human	*In vitro*	0.9µg/ml	↑
	Rossetti, *et al.*[13]	Human	*In vivo*	2.4g oral administration	↓
	Zurier, *et al.*[14]	Human	*In vitro*	5-25µg/ml	↓
Arachidic acid	Angela, *et al.*[2]	Mouse	*In vitro*	100	Rescued

[continued on next page]

Supplementary Table 3 *[continued]*

Fatty acid	Author	Model	Study performed *in vitro* or *in vivo*	Concentration of fatty acid used (µmol/l)	Effect on T cell proliferation
Eicosapentaenoic acid	Collison, *et al.*[15]	Rat	*In vivo*	3% safflower oil plus 7% fish oil enriched with EPA/DHA diet	↓
	Fan, *et al.* (2018)[4]	Human	*In vitro*	50	↓
	Gorjao, *et al.*[9]	Human	*In vitro*	25, 50	↓
	Jolly, *et al.*[16]	Mouse	*In vivo*	1% of diet	↓
	Ly, *et al.*[17]	Mouse	*In vivo*	1% of diet	↓
	McMurray, *et al.*[18]	Mouse	*In vivo*	2% of diet	↓
	Merzouk, *et al.*[19]	Human	*In vitro*	15	↓
	Pompos and Fritsche[20]	Mouse	*In vivo*	15.9g per 100g total fatty acids	↓
	Thies *et al.*[21]	Human	*In vivo*	1g capsules nine times daily	↓
Docosahexaenoic acid	Collison, *et al.*[15]	Rat	*In vivo*	3% safflower oil plus 7% fish oil enriched with EPA/DHA diet	↓
	Fan, *et al.* (2004)[22]	Mouse	*In vivo*	4g per 100g fish oil plus 1g per 100g DHA ethyl ester	↓
	Fan, *et al.* (2018)[4]	Human	*In vitro*	50	↓
	Gorjao, *et al.*[9]	Human	*In vitro*	25, 50	↓
	Jolly, *et al.*[16]	Mouse	*In vivo*	1% of diet	↓
	Ly, *et al.*[17]	Mouse	*In vivo*	1% of diet	↓
	McMurray, *et al.*[18]	Mouse	*In vivo*	2% of diet	↓
	Merzouk, *et al.*[19]	Human	*In vitro*	15	↓
	Pompos and Fritsche[20]	Mouse	*In vivo*	12g per 100g total fatty acids	↓
	Thies *et al.*[21]	Human	*In vivo*	720mg capsules nine times daily	↓
Lignoceric acid	Angela, *et al.*[2]	Mouse	*In vitro*	100	Did not rescue

Supplementary Table 4 | Overview of fatty acid effects on T cell polarization. ↑ and ↓ indicate the fatty acid had a directed effect on that process. The table shows the findings per fatty acid, listed from shortest to longest chain length and secondly from saturated fatty acid to monounsaturated fatty acid to polyunsaturated fatty acid. Fatty acids used in more than one study are listed in alphabetical order of the first author. T_H cell, T helper cell; T_{reg} cell, regulatory T cell.

Fatty acid	Author	Model	Study performed *in vitro* or *in vivo*	Concentration of fatty acid used (µmol/l)	Effect on T cell proliferation
Lauric acid	Haghikia, *et al.*[8]	Mouse	*In vivo*	13.5% of diet	↑ T_H1 / ↑ T_H17
	Haghikia, *et al.*[8]	Mouse	*In vitro*	250-500	↑ T_H1 / ↑ T_H17 / ↓ T_{reg}
	Haghikia, *et al.*[8]	Human	*In vitro*	250	↑ T_H1
Palmitic acid	Haghikia, *et al.*[8]	Mouse	*In vivo*	150 mmol/l	↑ T_H1 / ↑ T_H17
	Hossein zade, *et al.*[23]	Human	*In vitro*	1 mmol/l	↑ T_H1 / ↑ T_H17 / ↓ T_H2 / ↓ T_{reg}
Palmitoleic acid	Passos, *et al.*[11]	Human	*In vitro*	25, 50	↓ T_H1 / ↓ T_H17 / ↓ T_{reg}
Oleic acid	Hossein zade, *et al.*[23]	Human	*In vitro*	1 mmol/l	↑T_H1 / ↑ T_H17 / ↓ T_H2 / ↓ T_{reg}
	Passos, *et al.*[11]	Human	*In vitro*	25, 50	↑ and ↓ T_H1 / ↓ T_H17 / ↑ T_H2 / ↓ T_{reg}
Vaccenic acid	Blewett, *et al.*[24]	Rat	*In vivo*	1.5 w/w	↓ T helper / ↑ T_{reg}
	Jaudszus, *et al.*[25]	Human	*In vitro*	100	↓ T_H1
Arachidonic acid	Bi, *et al.*[26]	Mouse	*In vivo*	10% of diet	↑ T_H1 / ↑ T_H17
	Bi, *et al.*[26]	Mouse	*In vitro*	50	↑ T_H1 / ↑ T_H17 / ↓ T_H2
	Bi, *et al.*[26]	Human	*In vitro*	100	↑ T_H1 / ↑ T_H17 / ↓ T_H2

[continued on next page]

Supplementary Table 4 *[continued]*

Fatty acid	Author	Model	Study performed *in vitro* or *in vivo*	Concentration of fatty acid used (µmol/l)	Effect on T cell proliferation
Eicosapentaenoic acid	Bi, *et al.*[26]	Mouse	*In vivo*	10% of diet	↓ T_H1 / ↓ T_H17 / ↑ T_H2 / ↑ T_{reg}
	Bi, *et al.*[26]	Mouse	*In vitro*	50	↓ T_H1 / ↓ T_H17 / ↑ T_H2 / ↑ T_{reg}
	Bi, *et al.*[26]	Human	*In vitro*	100	↓ T_H1 / ↓ T_H17 / ↑ T_H2 / ↑ T_{reg}
	Merzouk, *et al.*[19]	Human	*In vitro*	15	↑ T_H2
	Monk, *et al.*[27]	Mouse	*Ex vivo*	1% of diet	↓ T_H17 / no effect T_{reg}
	Switzer, *et al.*[28]	Mouse	*In vitro*	20 g/kg menhaden fish oil	↓ T_H1 / no effect T_H2
	Zhang, *et al.* (2005)[29]	Mouse	*In vitro*	1% corn oil + 4% fish oil diet	↓ T_H1 / ↑ T_H2
	Zhang, *et al.* (2006)[30]	Mouse	*In vitro*	1% corn oil + 4% fish oil diet	↓ T_H1
Docosahexaenoic acid	Bi, *et al.*[26]	Mouse	*In vivo*	10% of diet	↓ T_H1 / ↓ T_H17 / ↑ T_H2 / ↑ T_{reg}
	Bi, *et al.*[26]	Mouse	*In vitro*	50	↓ T_H1 / ↓ T_H17 / ↑ T_H2 / ↑ T_{reg}
	Bi, *et al.*[26]	Human	*In vitro*	100	↓ T_H1 / ↓ T_H17 / ↑ T_H2 / ↑ T_{reg}
	Merzouk, *et al.*[19]	Human	*In vitro*	15	↑ T_H2
	Monk, *et al.*[27]	Mouse	*Ex vivo*	1% of diet	↓T_H17 / no effect T_{reg}
	Switzer, *et al.*[28]	Mouse	*In vitro*	20 g/kg menhaden fish oil	↓ T_H1 / no effect T_H2
	Zhang, *et al.* (2005)[29]	Mouse	*In vitro*	1% corn oil + 4% fish oil diet	↓ T_H1 / ↑ T_H2
	Zhang, *et al.* (2006)[30]	Mouse	*In vitro*	1% corn oil + 4% fish oil diet	↓ T_H1

References

1 Endo, Y. *et al.* Obesity drives Th17 cell differentiation by inducing the lipid metabolic kinase, ACC1. *Cell Rep.* **12**, 1042-1055, (2015).

2 Angela, M. *et al.* Fatty acid metabolic reprogramming via mTOR-mediated inductions of PPARγ directs early activation of T cells. *Nat. Commun.* **7**, 13683, (2016).

3 Ma, C. *et al.* NAFLD causes selective CD4+ T lymphocyte loss and promotes hepatocarcinogenesis. *Nature* **531**, 253-257, (2016).

4 Fan, Y. Y. *et al.* Remodelling of primary human CD4+ T cell plasma membrane order by n-3 PUFA. *Br. J. Nutr.* **119**, 163-175, (2018).

5 Stentz, F. B. & Kitabchi, A. E. Palmitic acid-induced activation of human T-lymphocytes and aortic endothelial cells with production of insulin receptors, reactive oxygen species, cytokines, and lipid peroxidation. *Biochem. Biophys. Res. Commun.* **346**, 721-726, (2006).

6 Moussa, M. *et al.* In vivo effects of olive oil-based lipid emulsion on lymphocyte activation in rats. *Clin. Nutr.* **19**, 49-54, (2000).

7 Kew, S. *et al.* Effects of oils rich in eicosapentaenoic and docosahexaenoic acids on immune cell composition and function in healthy humans. *Am. J. Clin. Nutr.* **79**, 674–681, (2004).

8 Haghikia, A. *et al.* Dietary fatty acids directly impact central nervous system autoimmunity via the small intestine. *Immunity* **43**, 817-829, (2015).

9 Gorjão, R., Cury-Boaventura, M. F., de Lima, T. M. & Curi, R. Regulation of human lymphocyte proliferation by fatty acids. *Cell Biochem. Funct.* **25**, 305-315, (2007).

10 Ioan-Facsinay, A. *et al.* Adipocyte-derived lipids modulate CD4+ T-cell function. *Eur. J. Immunol.* **43**, 1578-1587, (2013).

11 Passos, M. E. *et al.* Differential effects of palmitoleic acid on human lymphocyte proliferation and function. *Lipids Health Dis.* **15**, 217, (2016).

12 Miura, S. *et al.* Increased proliferative response of lymphocytes from intestinal lymph during long chain fatty acid absorption. *Immunology* **78**, 142-146, (1993).

13 Rossetti, R. G., Seiler, C. M., DeLuca, P., Laposata, M. & Zurier, R. B. Oral administration of unsaturated fatty acids: effects on human peripheral blood T lymphocyte proliferation. *J. Leukoc. Biol.* **62**, 438-443, (1997).

14 Zurier, R. B., Rossetti, R. G., Seiler, C. M. & Laposata, M. Human peripheral blood T lymphocyte proliferation after activation of the T cell receptor: effects of unsaturated fatty acids. *Prostaglandins Leukot. Essent. Fatty Acids* **60**, 371-375, (1999).

15 Collison, L. W., Collison, R. E., Murphy, E. J. & Jolly, C. A. Dietary n-3 polyunsaturated fatty acids increase T-lymphocyte phospholipid mass and acyl-CoA binding protein expression. *Lipids* **40**, 81–87, (2005).

16 Jolly, C. A., Jiang, Y. H., Chapkin, R. S. & McMurray, D. N. Dietary (n-3) polyunsaturated fatty acids suppress murine lymphoproliferation, interleukin-2 secretion, and the formation of diacylglycerol and ceramide. *J. Nutr.* **127**, 37–43, (1997).

17 Ly, L. H., Smith, R., Switzer, K. C., Chapkin, R. S. & McMurray, D. N. Dietary eicosapentaenoic acid modulates CTLA-4 expression in murine CD4+ T-cells. *Prostaglandins Leukot. Essent. Fatty Acids* **74**, 29-37, (2006).

18 McMurray, D. N., Jolly, C. A. & Chapkin, R. S. Effects of dietary n-3 fatty acids on T cell activation and T cell receptor-mediated signaling in a murine model. *J. Infect. Dis.* **182**, S103–S107, (2000).

19 Merzouk, S. A. *et al.* N-3 polyunsaturated fatty acids modulate in-vitro T cell function in type I diabetic patients. *Lipids* **43**, 485-497, (2008).

20 Pompos, L. J. & Fritsche, K. L. Antigen-driven murine CD4+ T lymphocyte proliferation and interleukin-2 production are diminished by dietary (n-3) polyunsaturated fatty acids. *J. Nutr.* **132**, 3293–3300, (2002).

21 Thies, F. *et al.* Dietary supplementation with γ-linolenic acid or fish oil decreases T lymphocyte proliferation in healthy older humans. *J. Nutr.* **131**, 1918–1927, (2001).

22 Fan, Y. Y., Ly, L. H., Barhoumi, R., McMurray, D. N. & Chapkin, R. S. Dietary docosahexaenoic acid suppresses T cell protein kinase C θ lipid raft recruitment and IL-2 production. *J. Immunol.* **173**, 6151-6160, (2004).

23 Hossein zade, A. *et al.* Fatty acids effect on T helper differentiation in vitro. *Int. J. Food Sci. Nutr.* **5**, (2016).

24 Blewett, H. J., Gerdung, C. A., Ruth, M. R., Proctor, S. D. & Field, C. J. Vaccenic acid favourably alters immune function in obese JCR:LA-cp rats. *Br. J. Nutr.* **102**, 526-536, (2009).

25 Jaudszus, A. *et al.* Vaccenic acid-mediated reduction in cytokine production is independent of c9,t11-CLA in human peripheral blood mononuclear cells. *Biochim. Biophys. Acta* **1821**, 1316-1322, (2012).

26 Bi, X. *et al.* ω-3 polyunsaturated fatty acids ameliorate type 1 diabetes and autoimmunity. *J. Clin. Invest.* **127**, 1757-1771, (2017).

27 Monk, J. M., Hou, T. Y., Turk, H. F., McMurray, D. N. & Chapkin, R. S. n3 PUFAs reduce mouse CD4+ T-cell ex vivo polarization into Th17 cells. *J. Nutr.* **143**, 1501-1508, (2013).

28 Switzer, K. C., McMurray, D. N., Morris, J. S. & Chapkin, R. S. (n-3) Polyunsaturated fatty acids promote activation-induced cell death in murine T lymphocytes. *J. Nutr.* **133**, 496–503, (2003).

29 Zhang, P., Smith, R., Chapkin, R. S. & McMurray, D. N. Dietary (n-3) polyunsaturated fatty acids modulate murine Th1/Th2 balance toward the Th2 pole by suppression of Th1 development. *J. Nutr.* **135**, 1745–1751, (2005).

30 Zhang, P. *et al.* Dietary fish oil inhibits antigen-specific murine Th1 cell development by suppression of clonal expansion. *J. Nutr.* **136**, 2391–2398, (2006).

CHAPTER 3

Oleic acid triggers metabolic rewiring of T cells poising them for T helper 9 differentiation

Nathalie A. Reilly,[1,7] Friederike Sonnet,[2] Koen F. Dekkers,[1] Joanneke C. Kwekkeboom,[3] Lucy Sinke,[1] Stan Hilt,[1] Hayat M. Suleiman,[1] Marten A. Hoeksema,[4] Hailiang Mei,[5] Erik W. van Zwet,[6] Bart Everts,[2] Andreea Ioan-Facsinay,[3] J. Wouter Jukema,[7,8] and Bastiaan T. Heijmans[1]

[1] *Molecular Epidemiology, Department of Biomedical Data Sciences, Leiden, the Netherlands.*
[2] *Leiden University Center for Infectious Diseases (LUCID), Leiden, the Netherlands.*
[3] *Department of Rheumatology Leiden University Medical Center, Leiden, the Netherlands.*
[4] *Department of Medical Biochemistry, Amsterdam UMC, location University of Amsterdam, Amsterdam, the Netherlands.*
[5] *Sequencing Analysis Support Core, Department of Biomedical Data Sciences, Leiden, the Netherlands.*
[6] *Medical Statistics, Department of Biomedical Data Sciences, Leiden, the Netherlands.*
[7] *Department of Cardiology, Leiden University Medical Center, Leiden, the Netherlands.*
[8] *Netherlands Heart Institute, Utrecht, the Netherlands.*

iScience **27**, *(2024).*
DOI: 10.1016/j.isci.2024.109496

Abstract

T cells are the most common immune cells in atherosclerotic plaques, and the function of T cells can be altered by fatty acids. Here, we show that pre-exposure of $CD4^+$ T cells to oleic acid, an abundant fatty acid linked to cardiovascular events, upregulates core metabolic pathways and promotes differentiation into interleukin-9 (IL-9)-producing cells upon activation. RNA sequencing of non-activated T cells reveals that oleic acid upregulates genes encoding key enzymes responsible for cholesterol and fatty acid biosynthesis. Transcription footprint analysis links these expression changes to the differentiation toward T_H9 cells, a pro-atherogenic subset. Spectral flow cytometry shows that pre-exposure to oleic acid results in a skew toward IL-9^+-producing T cells upon activation. Importantly, pharmacological inhibition of either cholesterol or fatty acid biosynthesis abolishes this effect, suggesting a beneficial role for statins beyond cholesterol lowering. Taken together, oleic acid may affect inflammatory diseases like atherosclerosis by rewiring T cell metabolism.

Highlights

- Non-activated T cells upregulate metabolism-related genes in response to oleic acid.
- The expression changes link to PU.1, a key transcription factor of T helper 9 cells.
- Upon activation, preexposure leads to a skew toward interleukin-9-producing cells.
- Inhibition of cholesterol or fatty acid biosynthesis abolishes this effect.

Graphical abstract

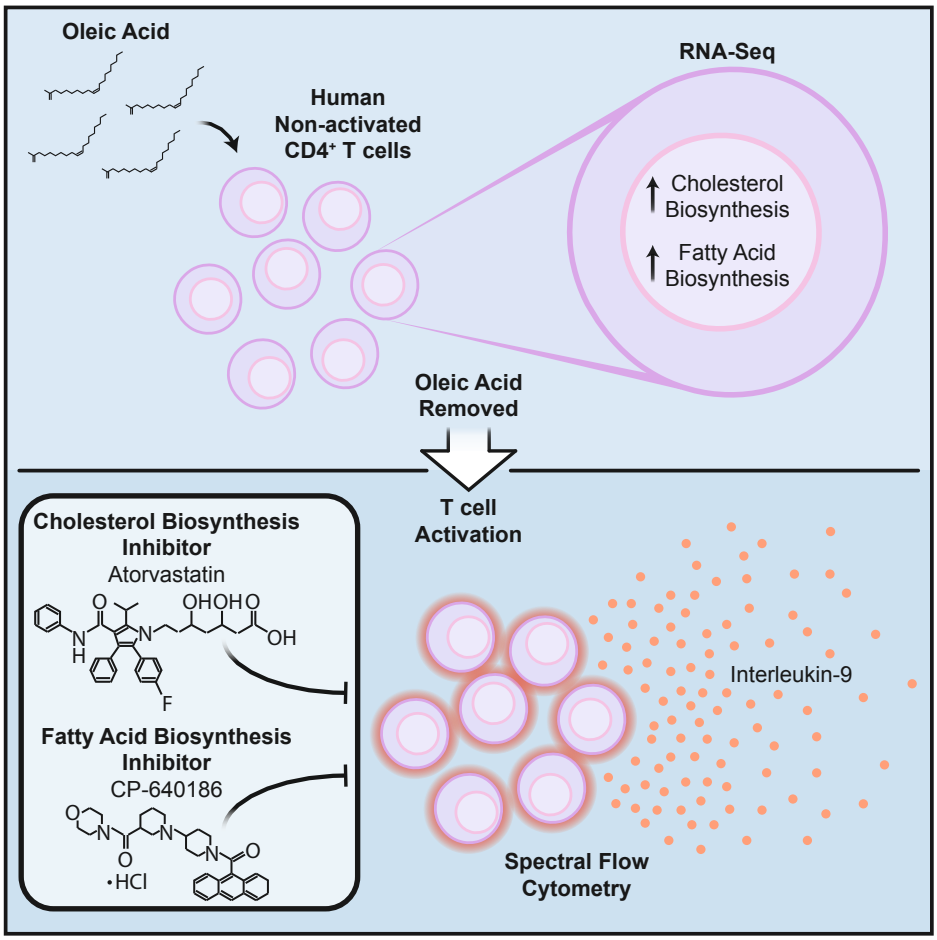

Introduction

Atherosclerosis is the primary underlying cause of cardiovascular disease and is driven by the interactions between the immune system, lipids, and the vascular wall[1, 2]. Recent single-cell RNA sequencing (RNA-seq) and mass cytometry studies showed that T cells make up the majority of immune cells in atherosclerotic plaques, half of which are $CD4^+$ T cells[3-6]. This indicates that the role of $CD4^+$ T cells in atherosclerosis is much greater than previously recognized[7-9]. Lipids and in particular fatty acids are known to have a major influence on the function of $CD4^+$ T cells[2]. While previous research evaluated the effect of fatty acids on $CD4^+$ T cell function during or after activation[2, 10-13], interactions between fatty acids and $CD4^+$ T cells relevant for atherosclerosis can already occur in the circulation, when the cells are in a non-activated state[2]. While the impact of these interactions has not been studied, they may skew the differentiation toward pro- or anti-inflammatory subsets[8, 14] once the $CD4^+$ T cells infiltrate atherosclerotic plaques or other disease sites such as rheumatoid arthritis and become activated[2, 15].

Fatty acids affect $CD4^+$ T cells in multiple ways ranging from activation and proliferation to differentiation[2]. It is thought that these effects are largely mediated by changes in metabolism[16]. In a non-activated state, like in the circulation, $CD4^+$ T cells rely on oxidative phosphorylation and β-oxidation of fatty acids for energy production[17, 18]. However, upon activation, $CD4^+$ T cells switch their metabolism to fatty acid biosynthesis and aerobic glycolysis to support cell growth and proliferation, reminiscent of the Warburg effect[18-20]. Importantly, the generation of specific T cell subset populations is associated with this metabolic reprogramming[10, 21-26]. The generally pro-inflammatory[14, 27, 28] T helper 1 (T_H1) and T helper 17 (T_H17) cells, but also T helper 2 (T_H2) cells that can be both pro- and anti-inflammatory, rely on pathways of aerobic glycolysis upon activation[29-35]. In contrast, the generally anti-inflammatory regulatory T (T_{reg}) cells mainly remain reliant on oxidative phosphorylation even after activation, indicating that the metabolic state of the cell may influence T cell effects in disease[18, 22, 23, 34]. Therefore, fatty acid-mediated metabolic reprogramming of $CD4^+$ T cells may affect the initiation and progression of atherosclerosis by skewing $CD4^+$ T cells toward a pro- or anti-inflammatory phenotype.

In this study, we characterized the effects of oleic acid on non-activated $CD4^+$ T cell function. Oleic acid is a monounsaturated fatty acid that is of particular interest since it is one of the most abundant fatty acids in the circulation[36], is independently associated with an increased risk of cardiovascular events[37, 38], and has been reported to elicit both pro- and anti-inflammatory effects on $CD4^+$ T cells[10-12, 39-43]. To do so, we performed RNA-sequencing on non-activated $CD4^+$ T cells exposed to oleic acid at 5 different time points. Furthermore, we performed spectral cytometry post-activation for various $CD4^+$ T cell markers. We find that oleic acid exposure leads to a metabolic reprogramming and generates a profile that becomes skewed toward T_H2, T_H17, and, notably, T_H9 $CD4^+$ T cells after activation. This skewed profile post-activation is blocked by the addition of metabolic inhibitors during the initial oleic acid exposure.

STAR Methods

Key resources table

REAGENT or RESOURCE	SOURCE	IDENTIFIER
Antibodies		
Anti-human CD4 MicroBeads - lyophilized	Miltenyi Biotec	Cat#130-097-048; RRID:AB_2889919
Anti-human CD3; PE; Isotype Mouse; Clone SK7	BD Biosciences	Cat#345765; RRID:AB_2868796
Anti-human CD4; APC; Isotype Mouse; Clone SK3	BD Biosciences	Cat#345771; RRID:AB_2868799
Anti-human CD8; FITC; Isotype Mouse; Clone HIT8a	BD Biosciences	Cat#555634; RRID:AB_395996
Anti-human CD14; PEcy7; Isotype Mouse; Clone M5E2	BD Biosciences	Cat#557742; RRID:AB_396848
Dynabeads™ Human T-Activator CD3/CD28 for T Cell Expansion and Activation	Thermo Fisher Scientific	Cat#11161D; RRID:AB_2916088
Anti-human CD38; APC/Fire™ 810; Isotype Mouse; Clone HB-7	BioLegend	Cat#356643; RRID:AB_2860936
Anti-human CD8; Pacific Orange™; Isotype Mouse; Clone 3B5	Thermo Fisher Scientific	Cat#MHCD0830; RRID:AB_10372066
Anti-human CD25; BUV563; Isotype Mouse; Clone 2A3	BD Biosciences	Cat#612918; RRID:AB_2870203
Anti-human CD45RA; BUV496; Isotype Mouse; Clone 5H9	BD Biosciences	Cat#741182; RRID:AB_2870749
Anti-human CD45RO; BUV805; Isotype Mouse; Clone UCHL1	BD Biosciences	Cat#748367; RRID:AB_2872786
Anti-human CD4; cFluor® YG584; Isotype Mouse; Clone SK3	Cytek Biosciences	Cat#R7-20042
Anti-human CD3; BUV395; Isotype Mouse; Clone UCHT1	BD Biosciences	Cat#563546; RRID:AB_2744387
Anti-human CD27; APC-H7; Isotype Mouse; Clone M-T271	BD Biosciences	Cat#560222; RRID:AB_1645474
Anti-human CD279 (PD-1); BV750; Isotype Mouse; Clone EH12.1	BD Biosciences	Cat#747446; RRID:AB_2872125
Anti-human CD127; R718; Isotype Mouse; Clone HIL-7R-M21	BD Biosciences	Cat#566967; RRID:AB_2869977

[continued on next page]

Key resources table *[continued]*

REAGENT or RESOURCE	SOURCE	IDENTIFIER
Anti-human CD197 (CCR7); Brilliant Violet 785™; Isotype Mouse; Clone G043H7	BioLegend	Cat#353230; RRID:AB_2561371
Anti-human TNF; PE-Cy™7; Isotype Mouse; Clone MAb11	BD Biosciences	Cat#557647; RRID:AB_396764
Anti-human IL-17A; Pacific Blue™; Isotype Mouse; Clone BL168	BioLegend	Cat#512312; RRID:AB_961392
Anti-human IL-5; APC; Isotype Rat; Clone TRFK5	BioLegend	Cat#504306; RRID:AB_315329
Anti-human IL-4; BUV737; Isotype Rat; Clone MP4-25D2	BD Biosciences	Cat#612835; RRID:AB_2870157
Anti-human IFN-γ; BV650; Isotype Mouse; Clone 4S.B3	BD Biosciences	Cat#563416; RRID:AB_2738193
Anti-human IL-13; BV711; Isotype Rat; Clone JES10-5A2	BD Biosciences	Cat#564288; RRID:AB_2738731
Anti-human IL-9; PE; Isotype Mouse; Clone MH9A4	BioLegend	Cat#507605; RRID:AB_315487
Anti-human IL-10; PerCP-eFluor™ 710; Isotype Rat; Clone JES3-9D7	Thermo Fisher Scientific	Cat#46-7108-42; RRID:AB_2573833
Anti-human CD152; PE-Cy™5; Isotype Mouse; Clone BNI3	BD Biosciences	Cat#555854; RRID:AB_396177
Anti-human IL-21; Alexa Fluor® 647; Isotype Mouse; Clone 3A3-N2.1	BD Biosciences	Cat#560493; RRID:AB_1645421
Anti-human T-bet; KIRAVIA Blue 520™; Isotype Mouse; Clone 4B10	BioLegend	Cat#644838; RRID:AB_2888710
Anti-human FOXP3; PE/Dazzle™ 594; Isotype Mouse; Clone 206D	BioLegend	Cat#320126; RRID:AB_2564024
Anti-human IL-22; Vio® B515; Isotype Human; Clone REA466	Miltenyi Biotec	Cat#130-108-096; RRID:AB_2652431
Anti-human GATA3; BV421; Isotype Mouse; Clone L50-823	BD Biosciences	Cat#563349; RRID:AB_2738152
CompBeads Anti-Mouse Ig, κ/Negative Control Compensation Particles Set	BD Biosciences	Cat#552843; RRID:AB_10051478
CompBeads Anti-Rat Ig, κ/Negative Control Compensation Particles Set	BD Biosciences	Cat#552844; RRID:AB_10055784
MACS® Comp Bead Kit, anti-REA	Miltenyi Biotec	Cat#130-104-693

[continued on next page]

Key resources table *[continued]*

REAGENT or RESOURCE	SOURCE	IDENTIFIER
Biological Samples		
Primary Human $CD4^+$ T cells isolated from buffy coats	Sanquin, Amsterdam, The Netherlands	N/A
Chemicals, Peptides, and Recombinant Proteins		
1% paraformaldehyde	Apotheek LUMC	Cat#120810-001
Fetal Calf Serum	Bodinco BDC	Cat#16941
Dulbecco's Modified Eagle's Medium - high glucose	Sigma-Aldrich	Cat#D5796
Penicillin-Streptomycin	Lonza	Cat#DE17-602E
GlutaMAX™ Supplement	Thermo Fisher Scientific	Cat#35050038
Recombinant Human IL-2	PeproTech	Cat#200-02
CryoSure-Dimethyl Sulfoxide	WAK-Chemie Medical GmbH	Cat#WAK-DMSO-10
Oleic Acid	Sigma-Aldrich	Cat#O1383
HPLC Grade Ethanol	Thermo Fisher Scientific	Cat#64-17-5
Bovine Serum Albumin	Sigma-Aldrich	Cat#A7030
TaqMan™ Fast Advanced Master Mix	Thermo Fisher Scientific	Cat#4444557
Atorvastatin	Sigma-Aldrich	Cat#PHR1422
CP 640,186	Sanbio	Cat#17691-5
RPMI 1640, HEPES, no glutamine	Thermo Fisher Scientific	Cat#42401
Fetal Calf Serum	Serana	Cat#S-FBS-SA-015
Phorbol 12-myristate 13-acetate	Sigma-Aldrich	Cat#P8139
Ionomycin	Sigma-Aldrich	Cat#I0634
Brefeldin A	Sigma-Aldrich	Cat#B7651
LIVE/DEAD™ Fixable Blue Dead Cell Stain	Thermo Fisher Scientific	Cat#L34962

[continued on next page]

Key resources table *[continued]*

REAGENT or RESOURCE	SOURCE	IDENTIFIER
Bovine Serum Albumin Fraction V	Merck	Cat#10735086001
UltraPure™ 0.5M EDTA, pH 8.0	Thermo Fisher Scientific	Cat#15575020
Brilliant Stain Buffer	BD Biosciences	Cat#563794
Critical Commercial Assays		
Quick-DNA/RNA Microprep Plus Kit	Zymo Research	Cat#D7005
Qubit™ RNA, Broad Range (BR), Assay Kits	Thermo Fisher Scientific	Cat#Q10210
Agilent RNA 6000 Nano Kit	Agilent	Cat#5067-1511
Transcriptor First Strand cDNA Synthesis Kit	Roche	Cat#04897030001
Truseq Stranded mRNA Library Prep	Illumina	Cat#20020595
Ribo Zero Gold rRNA Depletion Kit	Illumina	Cat#20037135
eBioscience™ Foxp3 / Transcription Factor Staining Buffer Set	Thermo Fisher Scientific	Cat#00-5523-00
Deposited Data		
Count data of RNA-sequencing	Gene Expression Omnibus repository, GEO	GSE231458
Oligonucleotides		
CPT1A	Thermo Fisher Scientific	Cat#4331182; Assay ID Hs00912671_m1
RPL13A	Thermo Fisher Scientific	Cat#4448892; Assay ID Hs03043887_gH
SDHA	Thermo Fisher Scientific	Cat#4453320; Assay ID Hs00188166_m1
Software and Algorithms		
RStudio	RStudio, Inc.	v4.2.2
BD FACSDiva™ Software	BD Biosciences	v8.0.2
SpectroFlo® Software	Cytek Biosciences	v2.2.0.3
OMIQ	Dotmatics	N/A
BioRender	BioRender	N/A

Resource availability

Materials availability

This study did not generate new unique reagents.

Data and code availability

- RNA sequencing data generated in this study have been deposited at Gene Expression Omnibus repository, accession, GEO, and are publicly available as of the date of publication. Accession numbers are listed in the key resources table.
- This paper does not report original code.
- Any additional information required to reanalyze the data reported in this paper is available from the lead contact upon request.

Experimental model and study participant details

$CD4^+$ T cell isolation and culture conditions

To obtain non-activated $CD4^+$ T cells, peripheral blood mononuclear cells (PBMCs) were isolated from buffy coats of anonymous blood bank donors (Sanquin, Amsterdam, The Netherlands) by Ficoll paque (Apotheek LUMC, 97902861) gradient centrifugation. The sex of the cells could not be determined due to the anonymity of the donors. However, RNA sequencing showed that, of 9 donors sequenced, 8 were female and 1 was male, which was accounted for during the statistical analysis by correcting for donor effect. Next, $CD4^+$ T cells were purified from the PBMCs using lyophilized human anti-$CD4^+$ magnetically labeled microbeads (Miltenyi Biotec, 130-097-048) scaling the manufacturer's instructions to 1/5 of the recommended volumes. $CD4^+$ T cell authentication and purity was assessed on an LSR-II instrument at the Leiden University Medical Center Flow Cytometry Core Facility (https://www.lumc.nl/research/facilities/fcf/) with the BD FACSDiva™ v8.0.2 software (BD Biosciences). Cells were stained with anti-CD3-PE (BD Biosciences, 345765; RRID:AB_2868796), anti-CD4-APC (BD Biosciences, 345771; RRID: AB_2868799), anti-CD8-FITC (BD Biosciences, 555634; RRID:AB_395996), and anti-CD14-PEcy7 (BD Biosciences, 557742; RRID:AB_396848) and resuspended in 1% paraformaldehyde (Apotheek LUMC, 120810-001) to fix the cells prior to acquisition. Purity was >98% for all donors.

Prior to oleic acid exposure,~$8*10^7$ isolated cells were cultured overnight to allow the cells to return to a resting state after the stress of the isolation procedure. This was done in T75 flasks (Greiner Bio-One, 658-175) at a density of ~$2.5*10^6$ cells/mL in 5% fetal calf serum (FCS) (Bodinco BDC, 16941) DMEM (Dulbecco's Modified Eagle's Serum (Sigma-Aldrich, D5796), 1% Pen-Strep (Lonza, DE17-602E), 1% GlutaMAX-1 (100x) (Thermo Fisher Scientific, 35050-038)) medium supplemented with 50 IU/mL IL-2 (PeproTech, 200-02) and incubated at 37°C under 5% CO_2. To keep the cells in a non-activated state, no additional stimulus was added. Any $CD4^+$ T cells not used directly after the isolation were kept in DMEM supplemented with 30% FCS, 1% Pen-Strep, 1% GlutaMAX-1, and 20% Dimethyl Sulfoxide (DMSO) (WAK-Chemie Medical GmbH, WAK-DMSO-10) medium, and stored in liquid nitrogen.

Next, non-activated $CD4^+$ T cells were cultured with or without oleic acid for 0.5, 3, 24, 48, or 72 hours at 37°C under 5% CO_2. To this end, $CD4^+$ T cells from each donor were plated in a 24 wells plate (density of ~$4*10^6$ cells/well) in 2mL 5% FCS DMEM for each time point, one exposed to oleic acid, one to the solvent control, and one to the negative control. Cells were cultured in medium containing FCS to ensure cell viability during culture and to be more comparable to physiological conditions of the circulation where other lipids are also present. Oleic acid (Sigma-Aldrich, O1383) was dissolved in HPLC grade ethanol (Thermo Fisher Scientific, 64-17-5) to a final concentration of 30,000µg/mL and complexed to fatty acid-free (FAF) bovine serum albumin (BSA) (Sigma-Aldrich, A7030) in a 2% FAF BSA DMEM mixture (Dulbecco's Modified Eagle's Serum, 2% FAF BSA, 1% Pen-Strep, 1% GlutaMAX-1 (100x)) to a final concentration of 150µg/mL. Complexing oleic acid mimics physiological conditions as fatty acids are also bound to albumin in the human circulation[68]. Oleic acid was further diluted to the final concentrations of 10, 20, 30, and 50µg/mL. The concentrations tested were determined based on a literature search[10-12, 42-46]. For the solvent control samples, HPLC grade ethanol was diluted in 2% FAF BSA DMEM in the same volume as to dilute oleic acid to 150µg/mL and added to the wells. For the negative control samples, 2% FAF BSA DMEM was added directly to the wells with no additional solvent. The amount of 2% FAF BSA DMEM added to the wells was equal for each condition to keep the volumes equivalent. To assess the additional oleic acid stimulus to the non-activated $CD4^+$ T cells due to FCS in the culture medium, an FCS sample was measured via the Shotgun Lipidomics Assistant (SLA) method[69] to estimate the fraction of oleic acid in the sample. The sample was prepped as previously described[70] but with two modifications, a starting volume of 25µL FCS and 600µL MTBE was added instead of 575µL during the first extraction. After exposure, the cells were flash frozen in liquid nitrogen and stored at -80°C until further use. Cell viability was measured via trypan blue staining (Sigma-Aldrich, T8154).

Spectral cytometry cell prep and activation

To study the effect of oleic acid pre-exposure on $CD4^+$ T cell subset development, cells from 8 out of 9 donors that were previously analyzed using RNA-seq were thawed from liquid nitrogen; 1 donor could not be studied further because too few cells were available. Cells were cultured overnight to allow the cells to return to a resting state after the stress of the thawing, in T75 flasks at a density of ~$2.5*10^6$ cells/mL in 5% FCS DMEM medium supplemented with 50 IU/mL IL-2 at 37°C under 5% CO_2. To keep the cells in a non-activated state, no additional stimulus was added. Following overnight incubation, the cells were divided into 2 conditions, oleic acid and solvent exposed, and plated in a 24 wells plate (density of ~$4*10^6$ cells/well) in 2mL 5% FCS DMEM. The oleic acid and solvent solution were prepared as stated previously, with one modification. To ensure that there was no effect of the solvent on T cell differentiation, the HPLC grade EtOH was evaporated before dissolving the oleic acid in 2% FAF BSA DMEM medium. The HPLC grade EtOH was also evaporated before adding the 2% FAF BSA DMEM medium in the solvent exposed condition, rendering it essentially the same as the negative control. These solutions were each added to the respective wells, where the final concentration of the oleic acid exposed conditions equaled 30µg/mL. The $CD4^+$ T cells were cultured for 48h at 37°C under 5% CO_2.

To ensure that the effect on $CD4^+$ T cell differentiation was due to oleic acid pre-exposure, all medium of each condition was replaced by 5% FCS medium after 48h of exposure, before initiating the activation. Cell viability and diameter were first measured by Via1-Cassette™ (Chemometec, 941-0012) on a NucleoCounter® NC-200™ (Chemometec, 900-0200) and found to be > 90% for each condition. Then, 2 million cells were harvested by flash freezing in liquid nitrogen for *in vitro* model confirmation by RT-qPCR. The remaining cells were plated in a round bottom 96 wells plate (Corning Incorporated, 3799), at a density of 100,000 cells/well, and were activated for 72h using Dynabeads™ Human T-Activator CD3/CD28 for T Cell Expansion and Activation (Thermo Fisher Scientific, 11161D; RRID:AB_2916088) according to the manufacturer's instructions at 37°C under 5% CO_2. Half the cells from each exposure were activated and the other half was left in the non-activated state. Subsequently, the cells from each pre-exposure and activation state were pooled in Eppendorf tubes and the beads were magnetically removed from the activated cells. Cell viability and diameter were measured by Via1-Cassette™ after 72h. Cells were then used for T cell subset identification described in more detail below. All centrifugation steps were performed at 1500 rpm at room temperature.

Inhibitor culture conditions and activation

To study whether the effect of oleic acid pre-exposure on $CD4^+$ T cell subset development could be prevented by metabolic inhibitors, cells from 3 out of 8 donors that were previously analyzed for subset development were thawed from liquid nitrogen; 5 donors could not be studied further because too few cells were available. Cells were cultured overnight to allow the cells to return to a resting state after the stress of the thawing, in T75 flasks at a density of ~$2.5*10^6$ cells/mL in 5% FCS DMEM medium supplemented with 50 IU/mL IL-2 at 37°C under 5% CO_2. To keep the cells in a non-activated state, no additional stimulus was added. Following overnight incubation, the cells were divided into 5 conditions, solvent, oleic acid, oleic acid + atorvastatin (Sigma-Aldrich, PHR1422), oleic acid + CP-640186 (Sanbio, 17691-5), and oleic acid + atorvastatin + CP-640186 exposed, and plated in a 24 wells plate (density of ~$4*10^6$ cells/well) in 2mL 5% FCS DMEM. The oleic acid and solvent solution were prepared as stated previously, with HPLC grade EtOH evaporation. These solutions were each added to the respective wells, where the final concentration of the oleic acid exposed conditions equaled 30µg/mL. Atorvastatin and CP-640186 were added to the respective wells at a concentration of 10µM and 20µM, respectively. The $CD4^+$ T cells were cultured for 48h at 37°C under 5% CO_2.

To ensure that the effect on $CD4^+$ T cell differentiation was due to oleic acid and inhibitor pre-exposure, all medium of each condition was replaced by 5% FCS medium after 48h of exposure, before initiating the activation. Cell viability and diameter were first measured by Via1- Cassette™ on a NucleoCounter® NC-200™ and found to be > 90% for each condition. Then, ~0.5-1.5 million cells were harvested by flash freezing in liquid nitrogen for *in vitro* model confirmation by RT-qPCR. The remaining cells were plated in a round bottom 96 wells plate, at a density of 100,000 cells/well, and were activated for 72h using Dynabeads™ Human T-Activator CD3/CD28 for T Cell Expansion and Activation according to the manufacturer's instructions at 37°C under 5% CO_2. Subsequently, the cells from each pre-exposure were pooled in Eppendorf tubes and the beads

were magnetically removed. Cell viability and diameter were measured by Via1-Cassette™ after 72h. Cells were then used for T cell subset identification described in more detail below. All centrifugation steps were performed at 1500 rpm at room temperature.

Method details

RNA isolation

To isolate total RNA for RNA sequencing and RT-qPCR, RNA was extracted from the cell samples using the Zymo Quick-DNA/RNA Microprep Plus Kit (Zymo Research, D7005) according to manufacturer's instructions. The RNA was quantified using a Qubit® 2.0 Fluorometer (Q32866) with the Qubit® RNA BR Assay Kit (Thermo Fisher Scientific, Q10211) according to manufacturer's instructions. RNA integrity (RIN) values of the samples were on average 8.40 SE 0.14 as determined using an Agilent 2100 Bioanalyzer Instrument (G2939BA) with the Agilent RNA 6000 Nano Reagents (5067-1511). RNA was divided into two samples and stored at -80°C, 1µg for RNA sequencing and the rest for cDNA synthesis and RT-qPCR measurements.

Real time-quantitative PCR

To measure the expression of *CPT1A* in all the cell samples, cDNA was synthesized with 200ng of the stored RNA using the Transcriptor First Strand cDNA Synthesis Kit (Roche, 04897030001) according to the manufacturer's instructions. Quantitative real time PCR's for *CPT1A* (Thermo Fisher Scientific, 4331182; Assay ID: Hs00912671_m1) were performed using the TaqMan™ Fast Advanced Master Mix (Thermo Fisher Scientific, 4444557) with 10ng cDNA per reaction on a QuantStudio 6 Real-Time PCR system (Applied Biosystems). All RT-qPCR reactions were performed in triplicate and outliers were removed if the Ct value measured differed more than 0.5% from the mean. Relative gene expression levels (-ΔCt) were calculated using the average of Ct values of *RPL13A* (Thermo Fisher Scientific, 4448892; Assay ID: Hs03043887_gH) and *SDHA* (Thermo Fisher Scientific, 4453320; Assay ID: Hs00188166_m1) as internal controls[71]. The fold change was determined using the $2^{-\Delta\Delta Ct}$ method, using the negative control as the reference. All statistical analyses were performed in R. Data are expressed as mean of the relative fold change and standard error. The reported P values were determined by applying a paired two-tailed student's T test. P values < 0.05 were considered to be statistically significant.

RNA sequencing

RNA sequencing (RNA-seq) was performed to determine the differences in the transcriptome of oleic acid versus solvent exposed non-activated $CD4^+$ T cells across time. 1µg of total RNA from each of the samples was sent for sequencing (Macrogen, Amsterdam, NL), each with a concentration above 20ng/µL in 50µL solution. RNA-seq libraries were prepared from 200ng RNA using the Illumina Truseq stranded mRNA library prep (Illumina, 20020595) after depletion of ribosomal RNA with Ribo Zero Gold (Illumina, 20037135). Both whole-transcriptome amplification and sequencing library preparations were performed in two 96-well plates with half the samples each, to reduce assay-to-assay variability. Quality control steps were included to determine total RNA quality and quantity, the optimal number of PCR preamplification cycles, and fragment size

selection. No samples were eliminated from further downstream steps. Barcoded libraries were pooled and equally divided across two lanes to ensure an equal distribution of all the samples across the two lanes. Barcoded libraries were sequenced to a read depth of 30 million reads using the Novaseq 6000 (Illumina) to generate 100 base pair paired-end reads.

Spectral cytometry

Prior to FACS analysis, cells were washed in RPMI 1640 medium (Thermo Fisher Scientific, 42401), supplemented with 100U/mL penicillin, 100µg/mL streptomycin, 1mM pyruvate, 2mM glutamate, and 10% FCS (Serana, S-FBS-SA-015), and adjusted to a concentration of $1x10^6$ cells/mL. Cells were then resuspended in 100µL RPMI + 10% FCS and stimulated for 4h with Phorbol 12-myristate 13-acetate (PMA; 100ng/mL, Sigma-Aldrich, P8139) and ionomycin (1µg/mL, Sigma-Aldrich, I0634) at 37°C under 5% CO_2 to promote cytokine production[72]. After 2h of stimulation, 10µg/mL of the protein transport inhibitor Brefeldin A (Sigma-Aldrich, B7651) was added.

After stimulation, the cells were washed twice in phosphate-buffered saline (PBS), stained for viable cells with LIVE/DEAD™ Fixable Blue (Thermo Fisher Scientific, L34962) for 30min at room temperature, then washed twice in fluorescence-activated cell sorting (FACS) buffer (PBS supplemented with 0.5% BSA (Merck, 10735086001) and 2mM EDTA (Thermo Fisher Scientific, 15575020)). The antibody surface cocktail consisted of 11 markers, anti-CD38-APC-Fire810 (BioLegend, 356643; RRID:AB_2860936), anti-CD8-Pacific Orange (Thermo Fisher Scientific, MHCD0830; RRID:AB_10372066), anti-CD25-BUV563 (BD Biosciences, 612918; RRID:AB_2870203), anti-CD45RA-BUV496 (BD Biosciences, 741182; RRID:AB_2870749), anti-CD45RO-BUV805 (BD Biosciences, 748367; RRID:AB_2872786), anti-CD4-cFluor® YG584 (Cytek Biosciences, SKU R7-20041), anti-CD3-BUV395 (BD Biosciences, 563546; RRID:AB_2744387), anti-CD27-APC-H7 (BD Biosciences, 560222; RRID: AB_1645474), anti-PD1-BV750 (BD Biosciences, 747446; RRID:AB_2872125), anti-CD127-R718 (BD Biosciences, 566967; RRID:AB_2869977), and anti-CCR7-BV785 (BioLegend, 353230; RRID:AB_2561371). For the spectral cytometry of the inhibitor experiment, the same surface cocktail was used except for the CD8 marker. The antibody surface cocktail was prepared in FACS buffer containing 20% Brilliant Stain Buffer Plus (BD Biosciences, 563794) was added to the cells and incubated for 30min at room temperature. Cells were then washed twice in FACS buffer and afterwards fixed and permeabilized with the Fixation/Permeabilization solution from the eBioscience™ FoxP3 / Transcription Factor Staining Buffer Set (Thermo Fisher Scientific, 00-5523-00) according to the manufacturer's instructions for 30min at 4°C. Subsequently, cells were washed twice with the Permeabilization buffer from the eBioscience™ FoxP3 / Transcription Factor Staining Buffer Set before being stained with the intracellular/intranuclear antibody cocktail for 30min at 4°C. The intracellular/intranuclear antibody cocktail consisted of 14 markers, anti-TNF-PE-Cy7 (BD Biosciences, 557647; RRID:AB_396764), anti-IL-17A-Pacific Blue (BioLegend, 512312; RRID:AB_961392), anti-IL-5-APC (BioLegend, 504306; RRID:AB_315329), anti-IL-4-BUV737 (BD Biosciences, 612835; RRID:AB_2870157), anti-IFN-γ-BV650 (BD Biosciences, 563416; RRID:AB_2738193), anti-IL-13-BV711 (BD Biosciences, 564288; RRID:AB_2738731), anti-IL-9-PE (BioLegend, 507605; RRID: AB_315487), anti-IL-10-PerCP-eFluor™ 710 (Thermo Fisher Scientific, 46-7108-42; RRID:AB_2573833), anti-CD152-PE-Cy5 (BD Biosciences, 555854; RRID:AB_396177),

anti-IL-21-Alexa Fluor® 647 (BD Biosciences, 560493; RRID:AB_1645421), anti-T-bet-KIRAVIA Blue 520™ (BioLegend, 644838; RRID:AB_2888710), anti-FOXP3-PE/Dazzle™ 594 (BioLegend, 320126; RRID:AB_2564024), anti-IL-22-Vio® B515 (Miltenyi Biotec, 130-108-096; RRID:AB_2652431), and anti-GATA3-BV421 (BD Biosciences, 563349; RRID:AB_2738152). For the spectral cytometry of the inhibitor experiment, the same intracellular/intranuclear antibody cocktail was used except for the IL-5 marker. Lastly, cells were washed with eBioscience™ Permeabilization buffer followed by another wash in FACS buffer. All centrifugation steps before fixation were performed at 300x g at room temperature and after fixation at 800x g at 4°C. Single-stain reference controls were either cells or UltraComp eBeads™ (CompBeads Anti-Mouse Ig, κ/Negative Control Compensation Particles Set (BD Biosciences; 552843; RRID:AB_10051478); CompBeads Anti-Rat Ig, κ/Negative Control Compensation Particles Set (BD Biosciences; 552844; RRID:AB_10055784), or MACS® Comp Bead Kit, anti-REA (Miltenyi Biotec; 130-104-693)). Cells were used as unstained reference control. All reference controls underwent the same protocol as the fully stained samples, including washes, buffers used, and fixation and permeabilization steps.

For acquisition, cells were resuspended in FACS buffer and acquired on a 5L-Cytek Aurora instrument at the Leiden University Medical Center Flow Cytometry Core Facility with the SpectroFlo® v2.2.0.3 software (Cytek Biosciences). Data was manually gated in OMIQ (Dotmatics, 2023). All statistical analyses were performed in R. Data are expressed as mean of the relative fold change and standard error. The reported P values were determined by applying a paired two-tailed student's T test. Differences with $P_{FDR} < 0.05$ (Benjamini-Hochberg) were considered to be significant.

Quantification and statistical analysis

Statistical analyses

All statistical analyses were performed in R (v4.2.2). Statistical details per experiment can be found in the "Method details" section of the "STAR Methods" as well as in the (supplemental) figure and table legends. A detailed description of the methods used to analyze the RNA sequencing data can be found below in the section "RNA Sequencing Analysis". For the analysis of all other experiments, the results are presented as mean ± SEM values. The reported P values were determined by applying a paired two-tailed student's T test between control and oleic acid exposed samples. Differences with $P_{FDR} < 0.05$ (Benjamini-Hochberg) were considered to be significant.

RNA sequencing analysis

RNA-seq reads were processed using the BioWDL RNAseq pipeline (v3.0.0) developed at LUMC (http://zenodo.org/record/3713261#.ZF98HdJBw5k). Quality controls were performed using FastQC (v0.11.7) and MultiQC (v1.7). Cleaned reads were aligned to the human reference genome GRCh38 using STAR aligner (v2.7.3a). Gene count table was generated using Htseq-count (v0.11.2) with Ensembl gene annotation version 99. Based on Ensembl gene biotype annotation, we included only protein coding genes for further downstream analysis (19,916 genes in total). We used the Bioconductor package *DESeq2*[73] (v1.40.1) to test whether oleic acid had an effect on gene expression at any time point. *DESeq2* fits a generalized linear model (GLM) assuming the

negative binomial distribution for the counts. The model expresses the logarithm of the average of the counts in terms of one of more predictors. In this case, we compared two models: The first "null" model has only timepoint (as a categorical variable with 5 levels) and subject identifier as predictors. By including the subject identifier in the model, we account for the dependence between measurements within the same subject. The second "alternative" model also includes the interaction between phenotype (oleic acid as a numerical measurement) and timepoint. We compare the fit of the two models with a likelihood ratio test. As part of the *DESeq2* process lowly expressed genes were automatically removed, resulting in 12,932 analyzed genes[73]. The Benjamini-Hochberg procedure was used to correct for multiple testing and a false discovery rate (FDR) < 0.05 was considered statistically significant.

Next, to identify distinct gene expression patterns in the data, unsupervised K means clustering was performed on the differentially expressed genes using the *factoextra*[74] package (v1.0.7). The number of clusters, *k*, was chosen using the elbow, silhouette, and gap-statistic method. Heatmaps were constructed using *ComplexHeatmap*[75] (v2.14.0) by plotting the log2FoldChange of the DEGs at each time point.

The identified clusters were then mapped for pathway enrichment. 10 human pathway databases (BioPlanet 2019, WikiPathways 2019 Human, KEGG 2019 Human, Elsevier Pathway Collection, BioCarta 2015, Reactome 2016, HumanCyc 2016, NCI-Nature 2016, Panther 2016 and MSigDB Hallmark 2020) were queried using gene symbols, with 430 of 544 queried genes present in at least 1 database. The identified clusters were then mapped for pathway enrichment using *clusterProfiler*[76] (v4.6.2) with the background set to 12,932 expressed genes in the $CD4^+$ T cells based on *DESeq2* filtering. Multiple testing using the Benjamini-Hochberg method at 5% FDR was performed over the combined results from the 10 databases. Pathways that included highly similar gene sets were grouped (Jaccard index > 0.7) and only the most significantly enriched pathway per group was retained. Furthermore, using the UniProt IDs of the enriched genes, the Path-MAP function of the PathBank database[77] was used to visualize the list of matching components within specific canonical pathways. *De novo* motif analysis on promotors of differentially regulated genes was performed using HOMER[78].

Results

Establishing a model to study the effect of oleic acid on non-activated $CD4^+$ T cells

Prior to studying the effect of oleic acid on non-activated $CD4^+$ T cells, we evaluated various experimental conditions in order to establish an *in vitro* exposure model. Cells were cultured in medium containing fetal calf serum (FCS) to ensure cell viability during culture, and oleic acid was complexed to BSA to model physiological conditions of the circulation. The cellular response to oleic acid was assessed by measuring cell viability and the expression of *CPT1A*. The *CPT1A* gene encodes the long-chain fatty acid transporter carnitine palmitoyl transferase 1a, a rate-limiting enzyme in the metabolic process of β-fatty acid oxidation. First, three different

types of culturing conditions for non-activated $CD4^+$ T cells were compared: 5% FCS medium with oleic acid bound to fatty acid-free (FAF) BSA, 5% FCS medium with oleic acid diluted in 5% FCS medium, and FAF medium with oleic acid bound to FAF BSA. However, the latter two conditions led to either undissolved oleic acid or a low cell viability (Supp. Fig. 1a). The first condition produced the largest *CPT1A* response while maintaining a high cell viability (Supp. Fig. 1), presumably because oleic acid bound to BSA and the presence of FCS may be a better approximation of physiological conditions. In addition, various oleic acid concentrations used in previous studies were evaluated[10-12, 42-46]. A concentration of 30 µg/mL was observed to result in the highest *CPT1A* upregulation (9.83-fold, SE 5.60) while maintaining cell viability (84.36%, SE 0.49%; Supp. Fig. 1). Importantly, this concentration is lower than the typical oleic acid concentration in the human circulation (85–904 µg/mL)[47]. The solvent control, ethanol, did not influence the results and was thus used as the control condition for the following analyses (Supp. Fig. 2). Finally, we measured the oleic acid concentration in the medium due to the addition of 5% FCS. This concentration was 0.26 µg/mL of free oleic acid and 4.39 µg/mL oleic acid as components of larger molecules including cholesterol esters and sphingolipids.

Transcriptomic analysis of oleic acid-exposed non-activated $CD4^+$ T cells

In order to identify the molecular features that define the effect of oleic acid exposure on non-activated $CD4^+$ T cells *in vitro*, we exposed nonactivated $CD4^+$ T cells to 30 µg/mL oleic acid for 0.5, 3, 24, 48, or 72 h (n = 9; Fig. 1a). First, we measured *CPT1A* expression and found that its expression consistently increased over time indicating a robust response to oleic acid exposure across donors, while *CPT1A* expression did not change under control conditions (Fig. 1b and Supp. Fig. 2b). Next, we analyzed the transcriptome of non-activated $CD4^+$ T cells after oleic acid exposure using RNA-seq. Oleic acid induced differential expression of 544 genes ($P_{FDR} < 0.05$) that clustered into 310 upregulated genes and 234 downregulated genes (Fig. 1c and Supp. Fig. 3, and Supp. Tables 1a and b). There was no statistical evidence for further subdivisions of the two clusters, for example, in fast- and slow-responding genes.

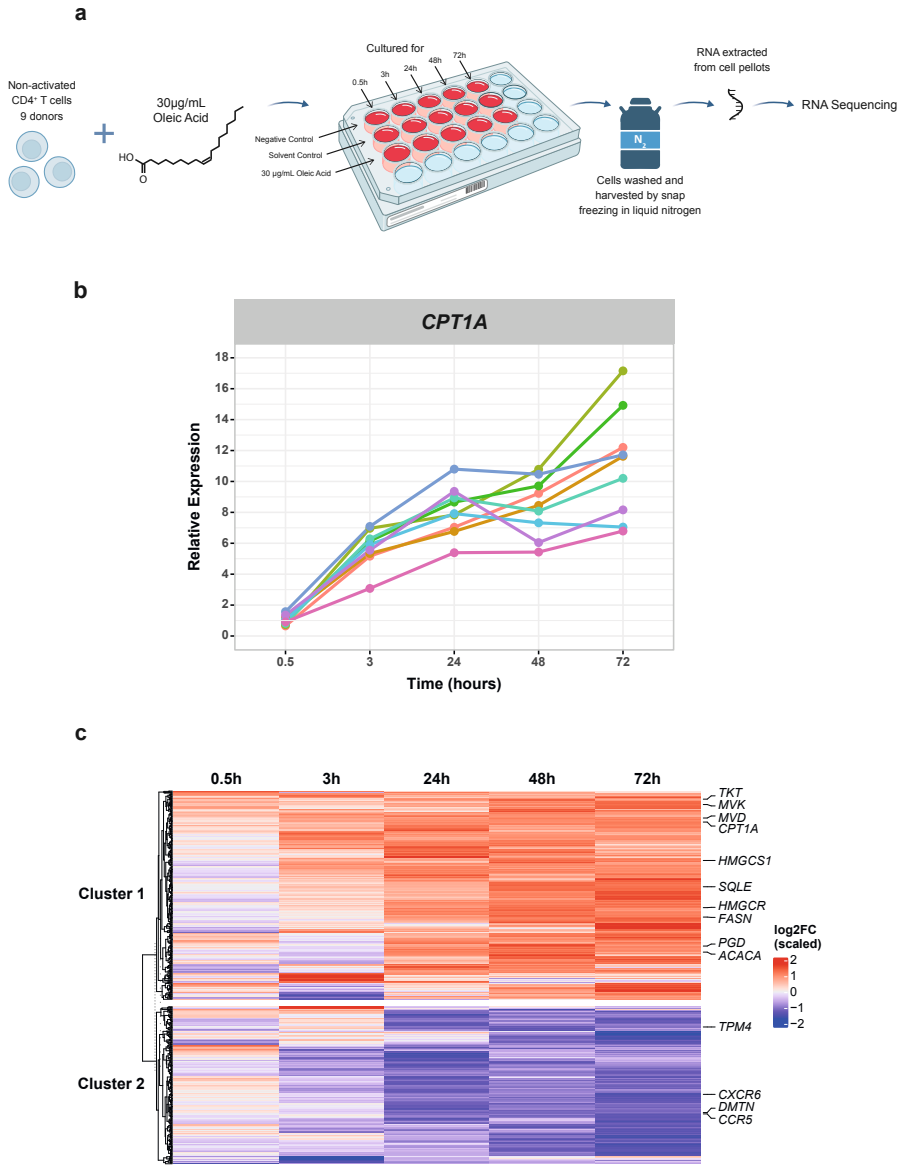

Fig. 1 | Oleic acid exposure in non-activated CD4⁺ T cells induces changes in transcriptomics. (a) Experimental setup for RNA sequencing of oleic acid-exposed non-activated CD4⁺ T cells, n = 9. **(b)** Line plot showing the relative expression of ***CPT1A*** per donor across time as a confirmation of the ***in vitro*** model by RT-qPCR. Values are colored by donor across time. On average ***CPT1A*** was upregulated 1.03 SE 0.10-fold at 0.5 h, 5.73 SE 0.40-fold at 3 h, 8.08 SE 0.53-fold at 24 h, 8.39 SE 0.62-fold at 48 h, and 11.09 SE 1.16-fold at 72 h as compared to the solvent control, n = 9. **(c)** Differentially expressed genes (DEGs) in oleic acid-exposed non-activated CD4⁺ T cells across time as compared to the solvent control. Heatmap obtained from the ***DESeq2*** analysis resulting in 544 DEGs ($P_{FDR} < 0.05$). DEGs were plotted across time to show the genes expression as log2FoldChange at each time point. Unsupervised K-means clustering indicated 2 clusters. Cluster 1 contains 310 of the DEGs, which are generally upregulated and are represented in red, and cluster 2 contains 234 of the DEGs, which are generally downregulated and are represented in blue. Genes of interest are labeled, n = 9.

We first examined the functions of the 310 genes that were upregulated in non-activated $CD4^+$ T cells by oleic acid exposure. We inspected the top differentially expressed genes (Supp. Fig. 3a and Supp. Table 1a). The top differentially expressed gene was *CPT1A* highlighting the involvement of β-fatty acid oxidation. In addition, we found an increased expression of *HMGCR* (3-hydroxy-3-methyl-glutaryl-coenzyme A [CoA] reductase), encoding the rate-limiting enzyme for cholesterol biosynthesis, and *ACACA* (acetyl-coenzyme A carboxylase 1), encoding the rate-limiting enzyme of fatty acid biosynthesis. Furthermore, transcripts of several aerobic glycolysis-related genes, such as *TKT* and *PGD*, were upregulated (Supp. Fig. 3a and Supp. Table 1a). A formal analysis of enriched biological processes among all 310 upregulated genes confirmed the involvement of metabolism. In particular, cholesterol biosynthesis ($P_{FDR} < 0.001$), homeostasis ($P_{FDR} < 0.001$), and signaling of mTORC1 ($P_{FDR} < 0.001$), a key complex of mechanistic target of rapamycin (mTOR) which aids in the switch toward aerobic glycolysis and fatty acid biosynthesis, were enriched (Fig. 2a). Mapping the upregulated genes to canonical metabolic pathways further supported a specific metabolic rewiring of oleic acid-exposed non-activated $CD4^+$ T cells (Fig. 2b). First, oleic acid can first be catabolized through beta oxidation to produce acetyl-CoA, which can then be used as a starting point for cholesterol and fatty acid biosynthesis. In addition to *CPT1A*, we found 4 out of 15 enzymes in b-fatty acid oxidation (including *SLC25A20*, *ACADVL*, and *ACAA2*) and 2 out of 15 enzymes in the aerobic glycolysis pathway to be upregulated (*TKT* and *PGD*; Fig. 2b, Supp. Fig. 4 and 5). Remarkably, on top of *HMGCR*, 15 out of 20 enzymes involved in cholesterol biosynthesis were upregulated in our gene set, including several key rate-limiting genes (such as *HMGCS1*, *SQLE*, *MVD*, and *MVK*). More specifically, 9/11 components of the mevalonate, 6/9 of the Bloch, and 6/9 of the Kandutsch-Russell pathway, together responsible for cholesterol biosynthesis, were upregulated (Fig. 2b and Supp. Fig. 6). The upregulated gene set also included *ACACA* and *FASN* that encode the two enzymes that together are responsible for the 37 reactions making up fatty acid biosynthesis (Fig. 2b and Supp. Fig. 7). Of note, the genes *ACACA* and *FASN* have been implicated in the differentiation toward T_H17 cells, a highly pro-inflammatory subset of $CD4^+$ T cells[46]. Furthermore, aerobic glycolysis and cholesterol and fatty acid biosynthesis are the hallmark metabolic processes of activated T cells and suggest that non-activated $CD4^+$ T cells undergo a metabolic reprogramming upon oleic acid exposure that may poise the cells for a different response to activation.

We then examined the functions of the 234 genes that were downregulated in non-activated $CD4^+$ T cells by oleic acid exposure. We first inspected the top differentially expressed genes (Supp. Fig. 3b and Supp. Table 1b). Among the top downregulated genes, decreased expression of *CXCR6* and *CCR5*, important chemokine receptors in the T cell immune response, was measured. Moreover, expression of *TPM4*, encoding actin-binding proteins involved in the cytoskeleton, and *DMTN*, encoding an actin-binding and bundling protein that stabilizes the actin cytoskeleton, was also downregulated. A formal analysis of the enriched biological processes among all 234 downregulated genes revealed a wide variety of different pathways. In line with the genes observed among the top downregulated genes, this included processes involved in immune response (*CCR2*, *CCR8*, *HLA-DRA*, *SLC2A1*) ($P_{FDR} < 0.001$) and actin cytoskeleton organization (*ACTB*, *RAC2*, *ARPC2*, *IQGAP1*) ($P_{FDR} < 0.001$) (Fig. 2c). In addition, processes involved in chemotaxis

(P_{FDR} < 0.001), chemokine and cytokine signaling (P_{FDR} < 0.001), and Rho GTPase regulation (P_{FDR} < 0.001) were also downregulated (Fig. 2c). Overall, these data point to a broad yet aspecific downregulation of genes in oleic acid-exposed non-activated $CD4^+$ T cells, perhaps to cope with the influx of the fatty acid.

Next, we investigated whether specific transcription factors may underlie the differential expression observed by testing the enrichment of transcription factor binding motifs in upregulated vs. downregulated genes. The top motifs enriched among upregulated genes included key transcription factors PU.1, EGR1, BHLHE40, and SREBP1 (Fig. 2d). Notably, PU.1 is the key transcription factor for the development of T_H9 cells. BHLHE40 has been linked to T_H17 development and pathogenicity in autoimmune encephalomyelitis suggesting an additional possible preference toward T_H17 differentiation post-activation[48, 49]. Furthermore, EGR1 and SREBP1 are involved in either the activation of Tbet or fatty acid and cholesterol biosynthesis, respectively[50, 51]. These data further support the notion that oleic acid-exposed non-activated $CD4^+$ T cells may be poised to differentiate toward T_H9 and T_H17 T cell subsets after activation.

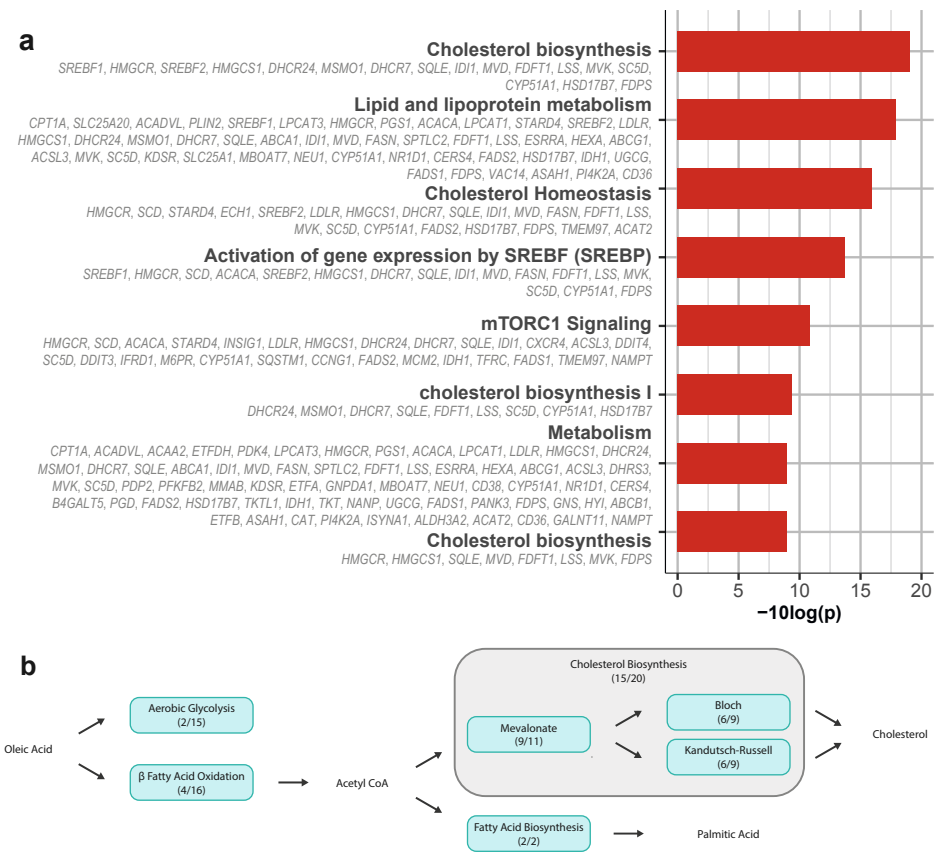

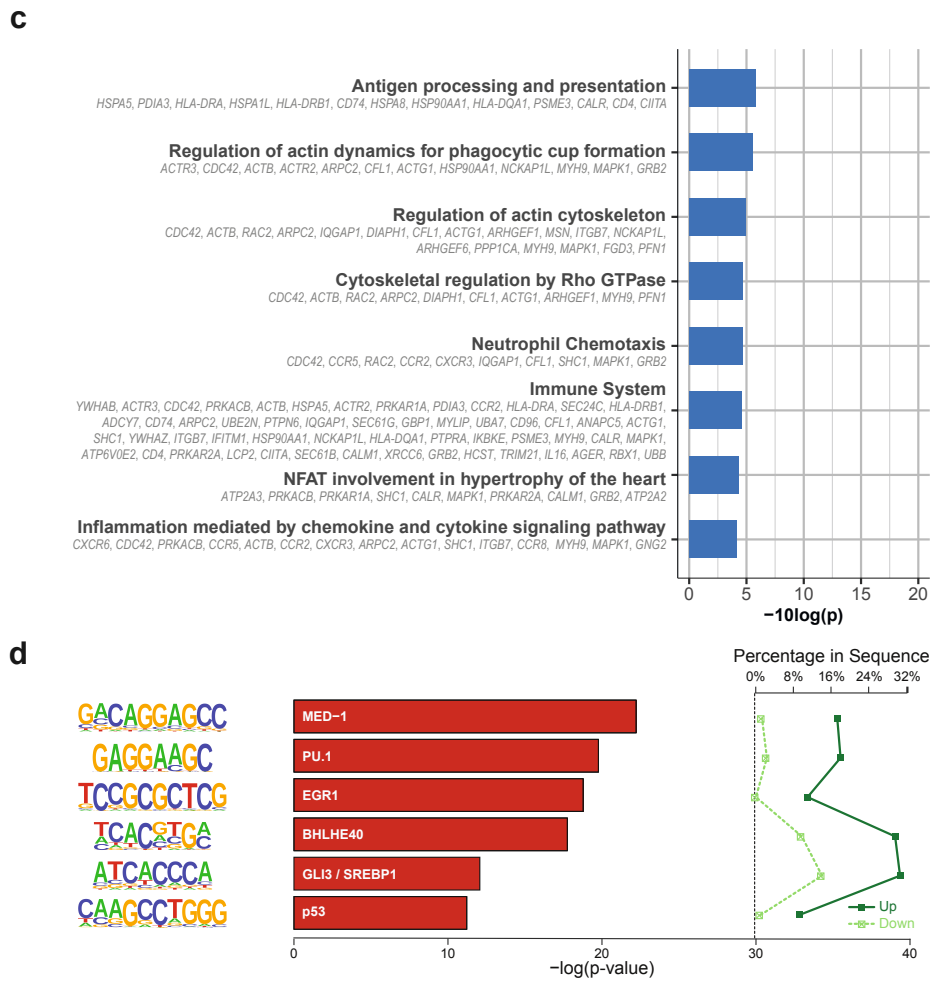

Fig. 2 | Up- and downregulated pathways and transcription factors in oleic acid-exposed non-activated CD4⁺ T cells. (a) Pathway enrichment analysis of cluster 1 DEGs generated using *clusterProfiler* using 10 human pathway databases. Top 8 enrichments are shown. **(b)** Illustration of canonical pathway map of oleic acid metabolism by non-activated CD4⁺ T cells exposed to oleic acid. Blue boxes indicate metabolic pathways with the number of genes present in that particular pathway from cluster 1 of the RNA sequencing. Cholesterol biosynthesis can be divided into 3 separate pathways indicated by the surrounding gray rectangle. **(c)** Pathway enrichment analysis of cluster 2 DEGs generated using *clusterProfiler* using 10 human pathway databases. Top 8 enrichments are shown. **(d)** *De novo* motif analysis on promoters of up- versus down-regulated genes. Enrichment of transcription factor binding motifs was performed using HOMER. 6 motifs are shown with supplementing information on p value, percentage of genes in upregulated gene set and percentage of genes in downregulated gene set, transcription factor name, -log(p value), and percentage in sequence.

Oleic acid induced CD4⁺ T cell phenotypes after activation

To determine the functional impact of the transcriptomic changes identified, we characterized the phenotypes of CD4⁺ T cells that were pre-exposed to oleic acid or control conditions and subsequently activated in the absence of oleic acid. To this end, non-activated CD4⁺ T cells of 8

out of 9 donors, for whom sufficient cells were available, were again exposed to 30 µg/mL oleic acid (Fig. 3a). The effect of exposure was confirmed by an upregulation of *CPT1A* (Supp. Fig. 8a); cell viability was high (>90%), and there was no difference in diameter between cells exposed to oleic acid and control (Supp. Fig. 8b–e).

First, we examined phenotypes after oleic acid exposure without activation (Supp. Fig. 9 and Supp. Table 1c). We observed decreased frequencies of $CD127^{low}CD25^{hi}FoxP3^+$ and $CD27^+$ $CD4^+$ T cells in response to oleic acid pre-exposure ($P_{FDR} < 0.05$; Fig. 3b). In non-activated cells, the $CD127^{low}CD25^{hi}FoxP3^+$ population is representative of T_{reg} cells, and thus the decreased frequencies in the non-activated cells are in line with the lower *FOXP3* expression observed in the RNA-seq analysis. Increased frequencies of interleukin (IL)-5^+ cells were also observed ($P_{FDR} < 0.05$; Fig. 3c) These data suggest that the oleic acid-induced changes in gene expression are reflected in consistent functional characteristics of the $CD4^+$ T cells without activation.

Activation of the $CD4^+$ T cells led to an increased cell size irrespective of pre-exposure to oleic acid (Fig. 3d). In contrast, the expression of surface and intracellular markers was influenced by exposure to oleic acid prior to activation (Supp. Fig. 10 and Supp. Table 1d). Pre-exposure to oleic acid resulted in a higher proportion of IL-9^+ cells ($P_{FDR} < 0.01$) as compared to the control (Fig. 3e). Additional analysis showed that IL-9 was not co-expressed with other T_H2-associated cytokines (Supp. Table 1e). This aligns with our finding that a large percentage of upregulated genes mapped to a PU.1 motif (Fig. 2d), the key transcription factor controlling T_H9 differentiation. Furthermore, increased frequencies of IL-$17A^+$ cells were observed after pre-exposure to oleic acid as compared with control conditions ($P_{FDR} < 0.05$). As IL-17A is mainly produced by T_H17 cells, it was hypothesized that other T_H17-associated cytokines, such as IL-21, may also have been upregulated. Indeed, IL-21^+ cells were increased in frequency ($p < 0.05$), but this effect was no longer significant after correction for multiple testing ($P_{FDR} < 0.08$). This aligns with our finding that a large percentage of upregulated genes mapped to the BHLHE40 motif (Fig. 2d) involved in T_H17 differentiation[48, 49]. Activated $CD4^+$ T cells showed increased frequencies of $CD127^{low}CD25^{hi}FoxP3^+$ and $GATA3^+$ and decreased frequencies of $CD27^+$ and $CD38^+$ cells in response to oleic acid pre-exposure ($P_{FDR} < 0.05$; Fig. 3f). However, FoxP3 can be expressed on activated conventional T cells without a suppressor function[52]; therefore, we are unable to differentiate whether the increased proportion of $CD127^{low}CD25^{hi}FoxP3^+$ cells post-activation is due to increased differentiation toward T_{reg} or an artifact of T cell activation. GATA3 is the key transcription factor involved in T_H2 differentiation, and, as such, frequencies of T_H2-related cytokines IL-5^+ and IL-13^+ were increased ($P_{FDR} < 0.05$; Fig. 3e). Finally, we observed that the effect of oleic acid on differentiation is not secondary to a differential proliferative capacity ($p > 0.92$; Supp. Fig. 11). Together, these data indicate that the metabolic changes in non-activated $CD4^+$ cells upon oleic acid exposure skew the cells toward producing more cytokines characteristic of T_H9, T_H17, and T_H2 subsets upon activation.

In order to reinforce our findings, we repeated the spectral cytometry analysis with 8 independent donors. The effect of oleic acid exposure was confirmed by an upregulation of *CPT1A* (Supp. Fig. 12a). Cell viability was high (>78%), and there was no difference in diameter between cells

exposed to oleic acid and control (Supp. Fig. 12b–e). Without activation, the phenotypes of oleic acid-exposed $CD4^+$ T cells showed increased frequencies of both $IL\text{-}17A^+$ ($P_{FDR} < 0.05$) and $TNF\alpha^+$ cells ($P_{FDR} < 0.05$; Supp. Fig. 13a, b, and 14; Supp. Table 1f). After activation, the phenotypes of oleic acid-exposed $CD4^+$ T cells showed an increased frequency of $IL\text{-}9^+$ ($P_{FDR} < 0.05$) and $GATA3^+$ ($P_{FDR} < 0.05$) cells as well as decreased frequencies of $CD38^+$ cells ($P_{FDR} < 0.05$; Supp. Fig. 13c, d, and 15, and Supp. Table 1g). These findings in non-activated and activated cells confirm results of our experiment and substantiate that oleic acid exposure in non-activated $CD4^+$ cells poised the cells toward producing more cytokines representative of T_H9 cells post-activation.

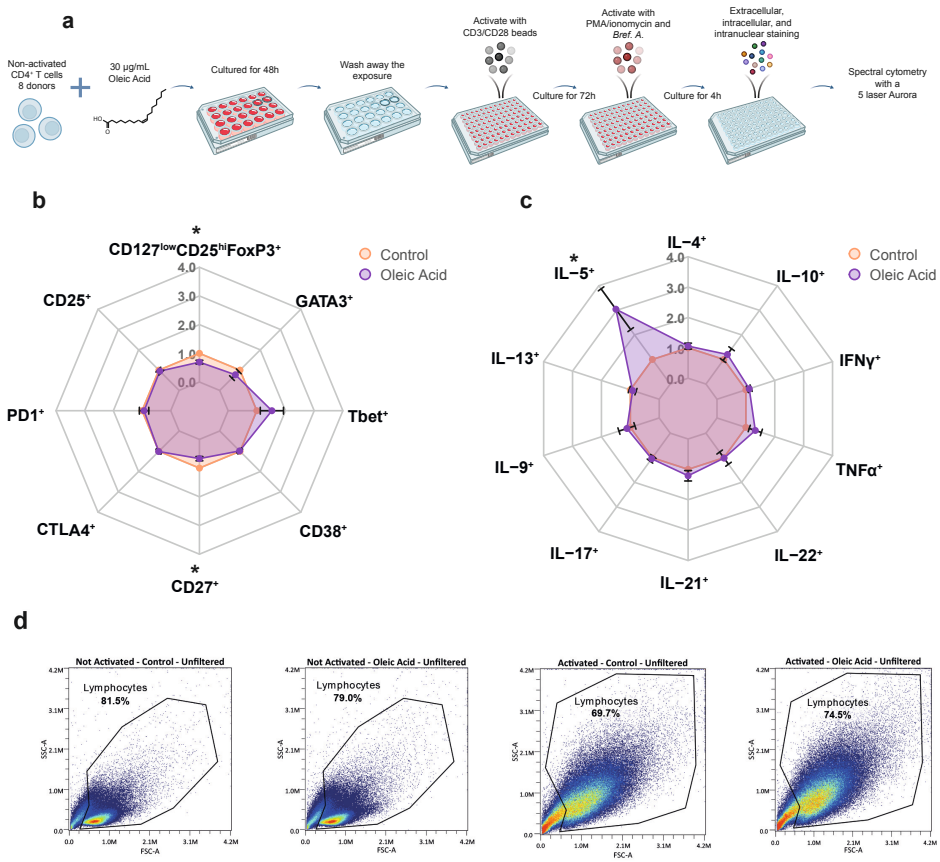

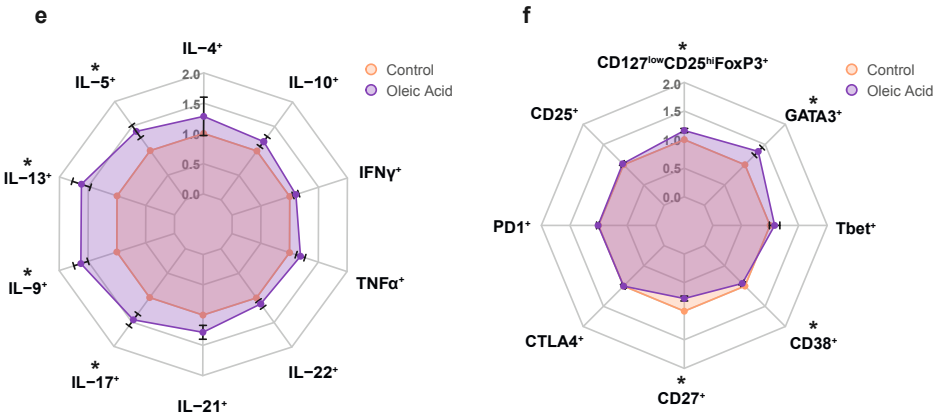

Fig. 3 | Oleic acid pre-exposure leads to changes in expression of extracellular markers, transcription factors, and intracellular cytokines. (*) $P_{FDR} < 0.05$, n = 8. **(a)** Experimental setup for spectral cytometry measurements of oleic acid-exposed non-activated $CD4^+$ T cells for 48 h with and without activation for 72 h post-exposure. **(b)** Radar plot of various $CD4^+$ T cell external markers and transcription factors expressed in $CD4^+$ T cells after 48 h of oleic acid exposure or control followed by 72 h of rest and 4 h stimulus with PMA/ionomycin. Values are expressed as fold change and standard error relative to control. **(c)** Radar plot of various $CD4^+$ T cell internal cytokines expressed in $CD4^+$ T cells after 48 h of oleic acid exposure or control followed by 72 h of rest and 4 h stimulus with PMA/ionomycin. Values are expressed as fold change and standard error relative to control. **(d)** Forward and side scatter of activated vs. non-activated and control vs. oleic acid pre-exposed $CD4^+$ T cells. Large differences in cell shape between the non-activated and activated state were observed, but little difference in cell shape between pre-exposure to control or oleic acid was found. Non-activated control exposed cells are on the far left, non-activated oleic acid-exposed cells are on the center left, activated control-exposed cells are on the center right, and activated oleic acid-exposed cells are on the far right. **(e)** Radar plot of various $CD4^+$ T cell internal cytokines expressed in $CD4^+$ T cells after 48 h of oleic acid exposure or control followed by 72 h of activation with CD3/CD28 activation beads and 4 h additional stimulus with PMA/ionomycin. Values are expressed as fold change and standard error relative to control. **(f)** Radar plot of various $CD4^+$ T cell external markers and transcription factors expressed in $CD4^+$ T cells after 48 h of oleic acid exposure or control followed by 72 h of activation with CD3/CD28 activation beads and 4 h additional stimulus with PMA/ionomycin. Values are expressed as fold change and standard error relative to control.

Oleic acid induced $CD4^+$ T cell phenotypes blocked by metabolic inhibitors

We next determined whether induction of this profile, reminiscent of an increase differentiation toward T_H9, T_H17, and T_H2 subsets, was dependent on an upregulation of cholesterol and fatty acid biosynthesis in line with our RNA-seq data. We inhibited cholesterol synthesis with atorvastatin, targeting 3-hydroxy-3-methylglutaryl (HMG)-CoA reductase (HMGCR), and fatty acid synthesis with CP-640186, targeting both ACC1 and ACC2 (*ACACA* and *ACACB*). To this end, non-activated $CD4^+$ T cells of 3 out of 8 donors, for whom sufficient cells were available, were again exposed to control conditions, oleic acid only, oleic acid +10 µM atorvastatin, oleic acid +20 µM CP-640186, or oleic acid and both atorvastatin and CP-640186 for 48 h. The effect of oleic acid exposure was confirmed by an upregulation of *CPT1A* (Supp. Fig. 16a). Cell viability was high (>88%), and there was no difference in diameter between cells exposed to control, oleic acid, or oleic acid + inhibitors (Supp. Fig. 16b–e).

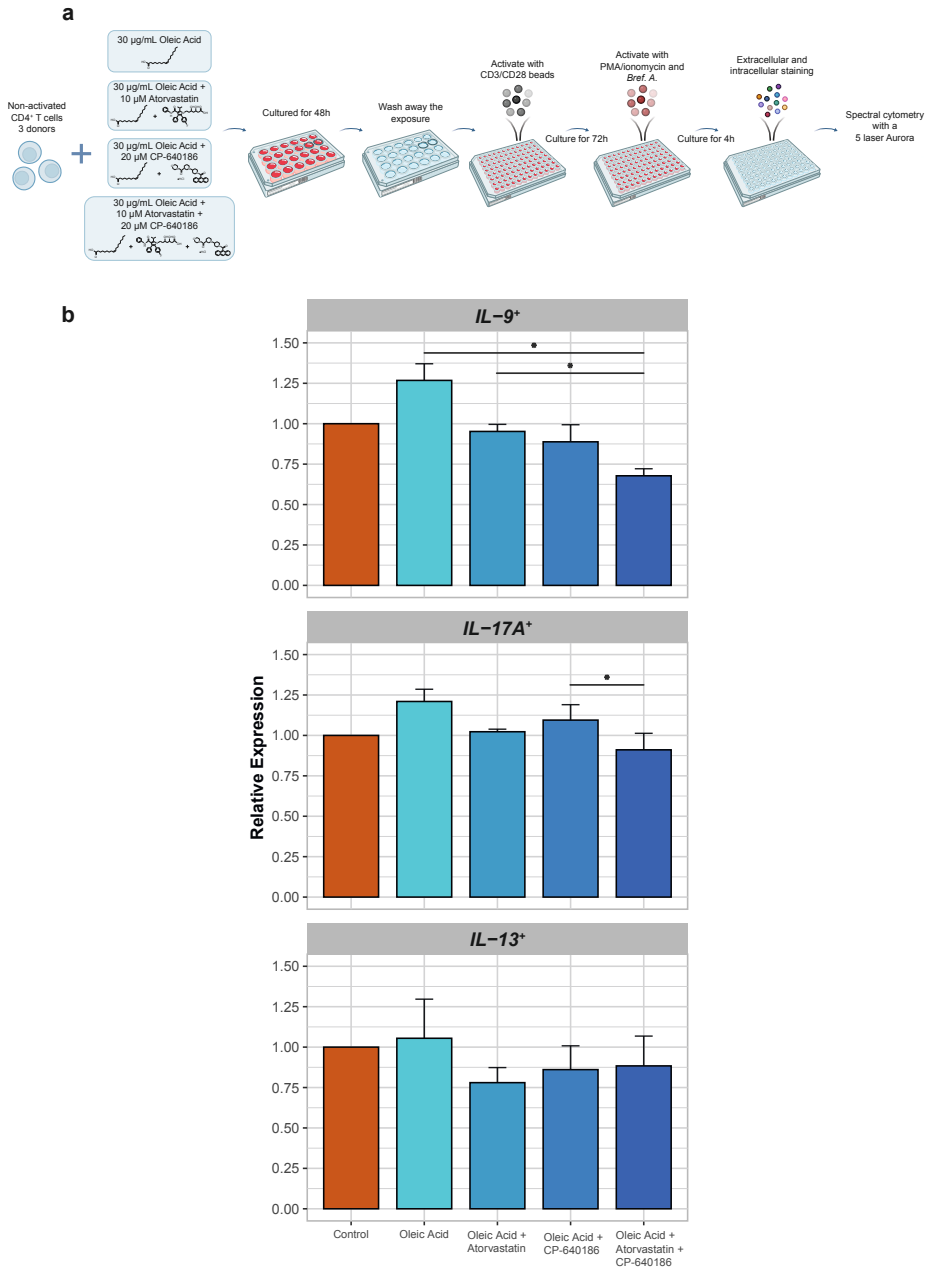

Fig. 4 | Metabolic inhibitors prevent oleic acid pre-exposure-induced changes in expression of IL-9, IL-17A, and IL-13. (*) $p < 0.05$, $n = 3$. **(a)** Experimental setup for spectral cytometry measurements of oleic acid + inhibitor exposed non-activated $CD4^+$ T cells for 48 h with activation for 72 h postexposure. **(b)** Bar plot of IL-9, IL-17A, and IL-13 expression in $CD4^+$ T cell after 48 h of control, oleic acid, oleic acid + atorvastatin, oleic acid + CP-640186, or oleic acid + atorvastatin + CP-640186 exposure followed by 72 h of activation with CD3/CD28 activation beads and 4 h additional stimulus with PMA/ionomycin. Values are expressed as fold change and standard error relative to control.

Subsequently, both oleic acid and the inhibitors were washed away and the pre-exposed $CD4^+$ T cells were activated. We evaluated the expression of one key marker for each subset: IL-9 for T_H9, IL-17A for T_H17, and IL-13 for T_H2 cells (Fig. 4a and Supp. Fig. 17). Remarkably, the ability of oleic acid to increase frequencies of IL-9^+ cells was inhibited by both atorvastatin and CP-640186 (Fig. 4b and Supp. Table 1h). Although similar trends were observed for frequencies of IL-$17A^+$ and IL-13^+ cells, these effects were not statistically significant (Fig. 4b). These data indicate that oleic acid promotes the differentiation to in particular IL-9^+-producing T cells via upregulation of cholesterol and fatty acid biosynthesis.

Discussion

T cells are known to respond to fatty acids[2]. Using an *in vitro* model, we show that sub-physiological concentrations of oleic acid can already influence $CD4^+$ T cells when in a non-activated state by upregulating the expression of genes that encode enzymes involved in core metabolic pathways responsible for cholesterol biosynthesis, fatty acid biosynthesis, and aerobic glycolysis. These metabolic processes are hallmarks of activated T cells[53]. Indeed, upon activation, $CD4^+$ T cells pre-exposed to oleic acid are characterized by increased production of cytokines, including IL-9, IL-17A, IL-5, and IL-13, indicative of a preferential differentiation toward the pro-inflammatory T helper subsets T_H9 as well as T_H17 and T_H2, which can have both pro- and anti-inflammatory effects. Interestingly, this effect is abolished in particular for IL-9^+-producing cells by blocking the cholesterol or the fatty acid biosynthesis pathways during the initial exposure to oleic acid. Our findings imply that increased fatty acid levels in the circulation can rewire the metabolism of non-activated T cells and poise them to particularly differentiate toward T_H9 cells, for example, when the cells infiltrate diseased tissues, including atherosclerotic plaques, and become activated.

Our results showed that cholesterol biosynthesis was the primary transcriptionally upregulated pathway in oleic acid-exposed non-activated $CD4^+$ T cells (15 out of 20 genes). This upregulation is of particular interest because of this pathway's role in producing the necessary metabolites required for T cell activation[54]. Cholesterol biosynthesis is upregulated in activated T cells to support membrane production, cell signaling through the formation of lipid rafts, and prenylation of signaling proteins[55]. Additionally, intracellular cholesterol sensing has also been found to play a role in T cell differentiation, particularly toward pro-inflammatory subsets. For example, sterols were found to bind the T_H17 transcription factor RORγt and could promote its activity[56]. Thus, the upregulation of gene expression in the cholesterol biosynthesis pathway due to oleic acid exposure may be indicative of a metabolic reprogramming of the non-activated $CD4^+$ T cells toward an activated state and may lead to the differentiation toward pro-inflammatory subsets post-activation.

Additionally, expression of the two genes comprising the de novo fatty acid biosynthesis pathway was upregulated (*ACACA* and *FASN*). Together, cholesterol and fatty acid biosynthesis comprise part of the process known as lipogenesis, the synthesis of novel lipids in a cell. Lipogenesis is

induced by the activation of the transcription factor SREBP1, which was associated with the upregulated transcripts in our RNA-seq data. Enrichment analysis of our transcripts also revealed upregulated genes in mTORC1 signaling, which is known to induce the activation of SREBP1[57]. Although this effect is usually insulin dependent, obesity and overfeeding have been shown to hyperactivate mTORC1[58]. Thus, it is possible that oleic acid alone could induce the activation of mTORC1, which in turn activates SREBP1, leading to lipogenesis and expression of cholesterol and fatty acid biosynthesis-related genes.

Fatty acid biosynthesis has also been related to the development of T_H17 cells[17, 32]. Specifically, the mRNA expression of genes *ACACA*, encoding for acetyl-CoA carboxylase 1 (ACC1), and *FASN*, encoding fatty acid synthase, was increased in our dataset. These genes are key determinants in the development of the pro-inflammatory subset T_H17 cells over the anti-inflammatory subset T_{reg} cells[22, 31, 39, 46, 59]. Correspondingly, *FOXP3*, the key transcription factor of T_{reg} cells, was downregulated in oleic acid-exposed non-activated $CD4^+$ T cells. Upregulated transcripts were found to be associated with the transcription factor PU.1. PU.1 is the key transcription factor in the development of T_H9 cells. This subset is a highly pro-inflammatory subset related to T_H2 cells[60]. This further supports the idea that oleic acid exposure leads to a cellular metabolic reprogramming that could promote the development of pro-inflammatory T cell subsets, specifically T_H9, and possibly also T_H17 and T_H2 cells. These results indicate that oleic acid-exposed non-activated $CD4^+$ T cells were upregulating genes involved in metabolism to initiate/prepare for the selective differentiation into T_H9/T_H17/T_H2 cells post-activation. Moreover, the metabolic processes being enhanced due to oleic acid exposure hint that the cells may preferentially differentiate toward T_H9, T_H17, and T_H2 cells upon activation.

Importantly, we provide evidence that the oleic acid-induced metabolic rewiring underpins the observed enhanced T_H9, T_H17, and T_H2 differentiation as exposing non-activated $CD4^+$ T cells to oleic acid in combination with cholesterol or fatty acid synthesis inhibitors decreased the frequencies of IL-9^+, IL-$17A^+$, and IL-13^+ cells. While the role of T_H17 and T_H2 cells in atherosclerosis has not been resolved, these cell types have been identified as pro-inflammatory in other diseases such as autoimmune encephalomyelitis and allergy, respectively[35, 61]. In contrast, T_H9 cells have been implicated in atherosclerosis pathogenesis[62-64]. Additionally, statins have been hypothesized to have protective effects independent of cholesterol reduction[65]; our study hints that effect of statins on T cell responses could contribute to this protective role.

Immune-lipid interactions occur in the circulation, which is a complex environment comprising many factors that can affect T cell function prior to their recruitment to disease site like the atherosclerotic plaque[66]. Fatty acids are a significant component of this environment and have been found to exert their effect not only on atherosclerosis but also on T cell function[2]. Our model was designed to determine the effect of oleic acid exposure on non-activated $CD4^+$ T cells. Here, we focus solely on the interaction between oleic acid and $CD4^+$ T cells and thus make no claim to what effects this fatty acid might have in relation to atherosclerotic cardiovascular disease as a component of more complex lipids, like olive oil. Our study only focuses on oleic acid as

it was shown to have both pro- and anti-inflammatory effects on T cells in previous studies[10-12, 39-43]. Circulating levels of oleic acid have been found to be related to pro-atherogenic effects[37, 38], and oleic acid is one of the most abundant fatty acids in the human circulation[36]. However, this does not preclude any effects *in vivo* or of other types of fatty acids on non-activated T cells.

Taken together, our results suggest that oleic acid can rewire the metabolism of non-activated $CD4^+$ T cells, as they exist in the circulation. This metabolic rewiring induces a preferential differentiation in particular toward T_H9 cell types following activation. Since T_H9 cell have proatherogenic effects[62-64] and we show that the oleic acid-induced differentiation into T_H9 cells can be inhibited by statins, our study indicates a new route by which fatty acids can contribute to atherosclerosis through modifiable effects on the immune system.

Limitations of the study

Although our experiments show that non-activated $CD4^+$ T cells exposed to oleic acid undergo distinct changes in the expression of genes encoding key enzymes constituting core metabolic pathways, and that subsequent activation of pre-exposed cells results in a differentiation that is skewed toward IL-9^+- producing T cells, our study used an *in vitro* model to establish these relationships and lacked an in-depth functional and mechanistic characterization of the metabolic changes involved. First, studies *in vivo* will be required to determine the relevance of our findings to the etiology of inflammatory diseases including atherosclerosis. Second, additional functional support for the occurrence of metabolic rewiring by oleic acid as implied by our results will be important. However, it will be challenging to assay functional effects. The T cells exposed to oleic acid were in a non-activated state and hence are unlikely to display functional differences in cell metabolism. Metabolic pathways are involved in the differentiation of $CD4^+$ T cells into specific subsets, and functional metabolic differences in T cells generally emerge only post-activation. Cell-subtype-specific and single-cell approaches can be informative to overcome the limitations of the bulk sequencing and spectrometry experiments as we performed in this study[18], including flow cytometry-based methods to functionally profile energy metabolism[67], mass spectrometry, and proteomics. Nevertheless, pharmacological inhibition of fatty acid and cholesterol metabolism in non-activated T cells abolished the oleic acid-induced skew toward IL-9^+-producing T cells upon activation, supporting our overall interpretation that metabolism is mechanistically involved in the effects we observed.

Acknowledgements

The authors' work is supported by the Dutch Cardiovascular Alliance (The Dutch Heart Foundation, Dutch Federation of University Medical Centers, the Netherlands Organization for Health Research and Development, and the Royal Netherlands Academy of Sciences) for the GENIUSI and GENIUSII projects Generating the Best Evidence-Based Pharmaceutical Targets for Atherosclerosis (CVON2011-19, CVON2017-20, respectively) and the Joint Programming Initiative A healthy diet for a healthy life (JPI HDHL) administered by ZonMW, the Netherlands (grant 529051021).

Author contributions

B.T.H. and J.W.J. conceived the project. N.A.R. designed and conducted the experiments, analyzed the results, and drafted the manuscript. F.S. designed and analyzed the spectral flow cytometry experiments. K.F.D. designed the *in vitro* model and analyzed the RNA-seq data. J.C.K. and H.M.S. designed the *in vitro* model. L.S. helped with the data analysis. S.H. designed the functional assays. M.A.H. performed and analyzed the transcription factor footprint analysis. H.M. aligned the RNA-seq data. E.W.v.Z. conceived the statistical model used in the analysis of the RNA sequencing. B.E. conceived and interpreted the functional assays and spectral flow cytometry data. A.I.-F. conceived and designed the *in vitro* model. All authors contributed to the writing of the manuscript.

Competing interests

The authors declare no competing interests.

References

1 Schaftenaar, F., Frodermann, V., Kuiper, J. & Lutgens, E. Atherosclerosis: the interplay between lipids and immune cells. *Curr. Opin. Lipidol.* **27**, 209-215, (2016).

2 Reilly, N. A., Lutgens, E., Kuiper, J., Heijmans, B. T. & Wouter Jukema, J. Effects of fatty acids on T cell function: role in atherosclerosis. *Nat. Rev. Cardiol.* **18**, 824–837, (2021).

3 Winkels, H. *et al.* Atlas of the immune cell repertoire in mouse atherosclerosis defined by single-cell RNA-sequencing and mass cytometry. *Circ. Res.* **122**, 1675-1688, (2018).

4 Fernandez, D. M. *et al.* Single-cell immune landscape of human atherosclerotic plaques. *Nat. Med.* **25**, 1576-1588, (2019).

5 Depuydt, M. A. *et al.* Microanatomy of the human atherosclerotic plaque by single-cell transcriptomics. *Circ. Res.* **127**, 1437-1455, (2020).

6 Zernecke, A. *et al.* Meta-analysis of leukocyte diversity in atherosclerotic mouse aortas. *Circ. Res.* **127**, 402-426, (2020).

7 Ketelhuth, D. F. & Hansson, G. K. Adaptive response of T and B cells in atherosclerosis. *Circ. Res.* **118**, 668-678, (2016).

8 Saigusa, R., Winkels, H. & Ley, K. T cell subsets and functions in atherosclerosis. *Nat. Rev. Cardiol.* **17**, 387-401, (2020).

9 Zhou, X., Robertson, A. K., Hjerpe, C. & Hansson, G. K. Adoptive transfer of CD4+ T cells reactive to modified low-density lipoprotein aggravates atherosclerosis. *Arterioscler. Thromb. Vasc. Biol.* **26**, 864-870, (2006).

10 Angela, M. *et al.* Fatty acid metabolic reprogramming via mTOR-mediated inductions of PPARγ directs early activation of T cells. *Nat. Commun.* **7**, 13683, (2016).

11 Ioan-Facsinay, A. *et al.* Adipocyte-derived lipids modulate CD4+ T-cell function. *Eur. J. Immunol.* **43**, 1578-1587, (2013).

12 Hossein zade, A. *et al.* Fatty acids effect on T helper differentiation in vitro. *Int. J. Food Sci. Nutr.* **5**, (2016).

13 Bi, X. *et al.* ω-3 polyunsaturated fatty acids ameliorate type 1 diabetes and autoimmunity. *J. Clin. Invest.* **127**, 1757-1771, (2017).

14 Raphael, I., Nalawade, S., Eagar, T. N. & Forsthuber, T. G. T cell subsets and their signature cytokines in autoimmune and inflammatory diseases. *Cytokine* **74**, 5-17, (2015).

15 Grivel, J. C. *et al.* Activation of T lymphocytes in atherosclerotic plaques. *Arterioscler. Thromb. Vasc. Biol.* **31**, 2929-2937, (2011).

16 Geltink, R. I. K., Kyle, R. L. & Pearce, E. L. Unraveling the complex interplay between T cell metabolism and function. *Annu. Rev. Immunol.* **36**, 461-488, (2018).

17 Chapman, N. M., Boothby, M. R. & Chi, H. Metabolic coordination of T cell quiescence and activation. *Nat. Rev. Immunol.* **20**, 55-70, (2020).

18 MacIver, N. J., Michalek, R. D. & Rathmell, J. C. Metabolic regulation of T lymphocytes. *Annu. Rev. Immunol.* **31**, 259-283, (2013).

19 Warburg, O., Gawehn, K. & Geissler, A. W. Metabolism of leukocytes [German]. *Z. Naturforsch. B* **13B**, 515-516, (1958).

20 Vander Heiden, M. G., Cantley, L. C. & Thompson, C. B. Understanding the Warburg effect: the metabolic requirements of cell proliferation. *Science* **324**, 1029-1033, (2009).

21 Howie, D., Ten Bokum, A., Necula, A. S., Cobbold, S. P. & Waldmann, H. The role of lipid metabolism in T lymphocyte differentiation and survival. *Front. Immunol.* **8**, 1949, (2018).

22 Cluxton, D., Petrasca, A., Moran, B. & Fletcher, J. M. Differential regulation of human Treg and Th17 cells by fatty acid synthesis and glycolysis. *Front. Immunol.* **10**, 115, (2019).

23 Michalek, R. D. *et al.* Cutting edge: distinct glycolytic and lipid oxidative metabolic programs are essential for effector and regulatory CD4+ T cell subsets. *J. Immunol.* **186**, 3299-3303, (2011).

24 Fullerton, M. D., Steinberg, G. R. & Schertzer, J. D. Immunometabolism of AMPK in insulin resistance and atherosclerosis. *Mol. Cell Endocrinol.* **366**, 224-234, (2013).

25 Maganto-García, E., Tarrio, M. L., Grabie, N., Bu, D. X. & Lichtman, A. H. Dynamic changes in regulatory T cells are linked to levels of diet-induced hypercholesterolemia. *Circulation* **124**, 185-195, (2011).

26 Delgoffe, G. M. *et al.* mTOR differentially regulates effector and regulatory T cell lineage commitment. *Immunity* **30**, 832-844, (2009).

27 Korn, T., Bettelli, E., Oukka, M. & Kuchroo, V. K. IL-17 and Th17 cells. *Annu. Rev. Immunol.* **27**, 485-517, (2009).

28 Zhu, J., Yamane, H. & Paul, W. E. Differentiation of effector CD4 T cell populations*. *Annu. Rev. Immunol.* **28**, 445-489, (2010).

29 Delgoffe, G. M. *et al.* The kinase mTOR regulates the differentiation of helper T cells through the selective activation of signaling by mTORC1 and mTORC2. *Nat. Immunol.* **12**, 295-303, (2011).

30 Shi, L. Z. *et al.* HIF1α-dependent glycolytic pathway orchestrates a metabolic checkpoint for the differentiation of TH17 and Treg cells. *J. Exp. Med.* **208**, 1367-1376, (2011).

31 Young, K. E., Flaherty, S., Woodman, K. M., Sharma-Walia, N. & Reynolds, J. M. Fatty acid synthase regulates the pathogenicity of Th17 cells. *J. Leukoc. Biol.* **102**, 1229-1235, (2017).

32 Berod, L. *et al.* De novo fatty acid synthesis controls the fate between regulatory T and T helper 17 cells. *Nat. Med.* **20**, 1327-1333, (2014).

33 O'Sullivan, D. & Pearce, E. L. Fatty acid synthesis tips the TH17-Treg cell balance. *Nat. Med.* **20**, 1235-1236, (2014).

34 Gerriets, V. A. & Rathmell, J. C. Metabolic pathways in T cell fate and function. *Trends Immunol.* **33**, 168-173, (2012).

35 Nakayama, T. *et al.* Th2 cells in health and disease. *Annu. Rev. Immunol.* **35**, 53-84, (2017).

36 Bicalho, B., David, F., Rumplel, K., Kindt, E. & Sandra, P. Creating a fatty acid methyl ester database for lipid profiling in a single drop of human blood using high resolution capillary gas chromatography and mass spectrometry. *J. Chromatogr. A* **1211**, 120-128, (2008).

37 Steffen, B. T., Duprez, D., Szklo, M., Guan, W. & Tsai, M. Y. Circulating oleic acid levels are related to greater risks of cardiovascular events and all-cause mortality: The Multi-Ethnic Study of Atherosclerosis. *J. Clin. Lipidol.* **12**, 1404-1412, (2018).

38 Delgado, G. E. *et al.* Individual omega-9 monounsaturated fatty acids and mortality – the Ludwigshafen Risk and Cardiovascular Health Study. *J. Clin. Lipidol.* **11**, 126-135, (2017).

39 Endo, Y. *et al.* Obesity drives Th17 cell differentiation by inducing the lipid metabolic kinase, ACC1. *Cell Rep.* **12**, 1042-1055, (2015).

40 Moussa, M. *et al.* In vivo effects of olive oil-based lipid emulsion on lymphocyte activation in rats. *Clin. Nutr.* **19**, 49-54, (2000).

41 Miura, S. *et al.* Increased proliferative response of lymphocytes from intestinal lymph during long chain fatty acid absorption. *Immunology* **78**, 142-146, (1993).

42 Stentz, F. B. & Kitabchi, A. E. Palmitic acid-induced activation of human T-lymphocytes and aortic endothelial cells with production of insulin receptors, reactive oxygen species, cytokines, and lipid peroxidation. *Biochem. Biophys. Res. Commun.* **346**, 721-726, (2006).

43 Passos, M. E. *et al.* Differential effects of palmitoleic acid on human lymphocyte proliferation and function. *Lipids Health Dis.* **15**, 217, (2016).

44 Verlengia, R. *et al.* Effect of arachidonic acid on proliferation, cytokines production and pleiotropic genes expression in Jurkat cells - a comparison with oleic acid. *Life Sci.* **73**, 2939-2951, (2003).

45 Gorjão, R., Cury-Boaventura, M. F., de Lima, T. M. & Curi, R. Regulation of human lymphocyte proliferation by fatty acids. *Cell Biochem. Funct.* **25**, 305-315, (2007).

46 Endo, Y. *et al.* ACC1 determines memory potential of individual CD4+ T cells by regulating de novo fatty acid biosynthesis. *Nat. Metab.* **1**, 261-275, (2019).

47 Abdelmagid, S. A. *et al.* Comprehensive profiling of plasma fatty acid concentrations in young healthy Canadian adults. *PLoS One* **10**, 0116195, (2015).

48 Lin, C. C. *et al.* IL-1-induced Bhlhe40 identifies pathogenic T helper cells in a model of autoimmune neuroinflammation. *J. Exp. Med.* **213**, 251-271, (2016).

49 Nechanitzky, R. *et al.* Cholinergic control of Th17 cell pathogenicity in experimental autoimmune encephalomyelitis. *Cell Death Differ.* **30**, 407-416, (2023).

50 Kidani, Y. *et al.* Sterol regulatory element-binding proteins are essential for the metabolic programming of effector T cells and adaptive immunity. *Nat. Immunol.* **14**, 489-499, (2013).

51 Shin, H. J., Lee, J. B., Park, S. H., Chang, J. & Lee, C. W. T-bet expression is regulated by EGR1-mediated signaling in activated T cells. *Clin. Immunol.* **131**, 385-394, (2009).

52 Allan, S. E. *et al.* Activation-induced FOXP3 in human T effector cells does not suppress proliferation or cytokine production. *Int. Immunol.* **19**, 345-354, (2007).

53 Cai, F., Jin, S. & Chen, G. The effect of lipid metabolism on CD4+ T cells. *Mediators Inflamm.* **2021**, 6634532, (2021).

54 Smith-Garvin, J. E., Koretzky, G. A. & Jordan, M. S. T cell activation. *Annu. Rev. Immunol.* **27**, 591-619, (2009).

55 Shyer, J. A., Flavell, R. A. & Bailis, W. Metabolic signaling in T cells. *Cell Res.* **30**, 649-659, (2020).

56 Santori, F. R. *et al.* Identification of natural RORγ ligands that regulate the development of lymphoid cells. *Cell Metab.* **21**, 286-298, (2015).

57 Laplante, M. & Sabatini, D. M. An emerging role of mTOR in lipid biosynthesis. *Curr. Biol.* **19**, 1046-1052, (2009).

58 Khamzina, L., Veilleux, A., Bergeron, S. & Marette, A. Increased activation of the mammalian target of rapamycin pathway in liver and skeletal muscle of obese rats: possible involvement in obesity-linked insulin resistance. *Endocrinology* **146**, 1473-1481, (2005).

59 Sun, L., Fu, J. & Zhou, Y. Metabolism controls the balance of Th17/T-regulatory cells. *Front. Immunol.* **8**, 1632, (2017).

60 Angkasekwinai, P. & Dong, C. IL-9-producing T cells: potential players in allergy and cancer. *Nat Rev Immunol* **21**, 37-48, (2021).

61 Schnell, A., Littman, D. R. & Kuchroo, V. K. Th17 cell heterogeneity and its role in tissue inflammation. *Nat. Immunol.* **24**, 19-29, (2023).

62 Zhang, W. *et al.* IL-9 aggravates the development of atherosclerosis in ApoE2/2 mice. *Cardiovasc. Res.* **106**, 453-464, (2015).

63 Gregersen, I. *et al.* Increased systemic and local interleukin 9 levels in patients with carotid and coronary atherosclerosis. *PLoS One* **8**, 72769, (2013).

64 Li, Q. *et al.* Increased Th9 cells and IL-9 levels accelerate disease progression in experimental atherosclerosis. *Am. J. Transl. Res.* **9**, 1335-1343, (2017).

65 Oesterle, A., Laufs, U. & Liao, J. K. Pleiotropic effects of statins on the cardiovascular system. *Circ. Res.* **120**, 229-243, (2017).

66 Visscher, M. *et al.* Data processing pipeline for lipid profiling of carotid atherosclerotic plaque with mass spectrometry imaging. *J. Am. Soc. Mass. Spectrom.* **30**, 1790-1800, (2019).

67 Argüello, R. J. *et al.* SCENITH: a flow cytometry-based method to functionally profile energy metabolism with single-cell resolution. *Cell Metab.* **32**, 1063-1075, (2020).

68 van der Vusse, G. J. Albumin as fatty acid transporter. *Drug Metab. Pharmacokinet.* **24**, 300-307, (2009).

69 Su, B. *et al.* A DMS shotgun lipidomics workflow application to facilitate high-throughput, comprehensive lipidomics. *J. Am. Soc. Mass Spectrom.* **32**, 2655-2663, (2021).

70 Ghorasaini, M. *et al.* Congruence and complementarity of differential mobility spectrometry and NMR spectroscopy for plasma lipidomics. *Metabolites* **12**, 1030, (2022).

71 Ledderose, C., Heyn, J., Limbeck, E. & Kreth, S. Selection of reliable reference genes for quantitative real-time PCR in human T cells and neutrophils. *BMC Res. Notes* **4**, 427, (2011).

72 Mandala, W., Harawa, V., Munyenyembe, A., Soko, M. & Longwe, H. Optimization of stimulation and staining conditions for intracellular cytokine staining (ICS) for determination of cytokine-producing T cells and monocytes. *Curr. Res. Immunol.* **2**, 184-193, (2021).

73 Love, M. I., Huber, W. & Anders, S. Moderated estimation of fold change and dispersion for RNA-seq data with DESeq2. *Genome Biol.* **15**, 550, (2014).

74 Kassambara, A. & Mundt, F. Extract and visualize the results of multivariate data analyses. (2020).

75 Gu, Z., Eils, R. & Schlesner, M. Complex heatmaps reveal patterns and correlations in multidimensional genomic data. *Bioinformatics* **32**, 2847-2849, (2016).

76 Yu, G., Wang, L. G., Han, Y. & He, Q. Y. clusterProfiler: an R package for comparing biological themes among gene clusters. *OMICS* **16**, 284-287, (2012).

77 Wishart, D. S. *et al.* PathBank: a comprehensive pathway database for model organisms. *Nucleic Acids Res.* **48**, 470-478, (2020).

78 Heinz, S. *et al.* Simple combinations of lineage-determining transcription factors prime cis-regulatory elements required for macrophage and B cell identities. *Mol. Cell* **38**, 576-589, (2010).

Supplemental information

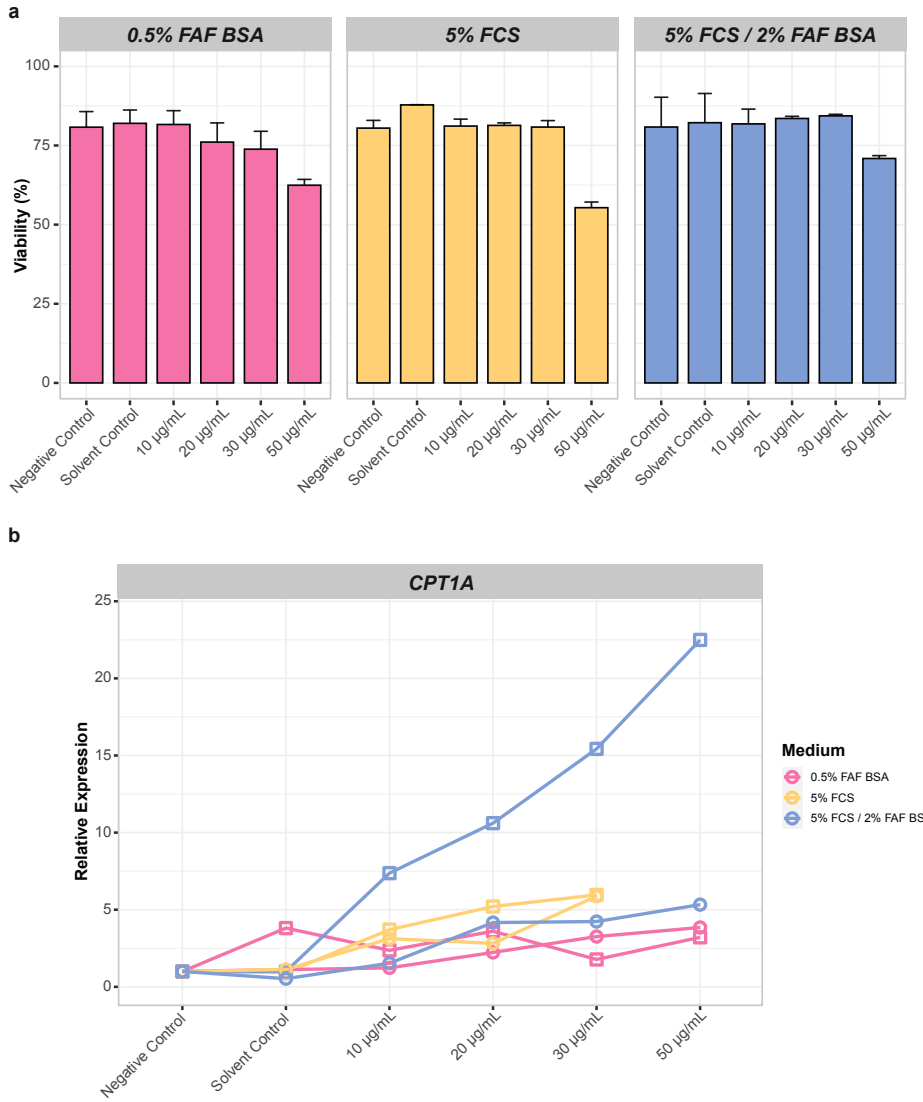

Supplemental Fig. 1 | Determination of culture medium type and concentration of oleic acid to use in the *in vitro* model by viability and *CPT1A* expression. Three different medium types were tested. First, cells cultured in and oleic acid dissolved in FAF BSA only. Second, cells cultured in and oleic acid dissolved in 5% FCS only. Third, cells cultured in 5% FCS and oleic acid dissolved in FAF BSA. Non-activated $CD4^+$ T cells were exposed to 10, 20, 30, or 50µg/mL oleic acid for 48 h. Conditions are labelled by color. The greatest upregulation while maintaining cell viability occurred at 30µg/mL oleic acid in the 5% FCS / 2% FAF BSA medium combination, n = 2. **(a)** Bar plot showing the average cell viability and standard error in percent, as determined by trypan blue staining, for 2 donors for each medium and concentration tested after 48 h exposure. For FAF BSA medium only, the average viability was 80.79 SE 4.93% at negative control, 82.00

SE 4.22% at solvent control, 81.64 SE 4.37% at 10µg/mL, 76.07 SE 6.07% at 20µg/mL, 73.84 SE 5.66% at 30µg/mL, and 62.45 SE 1.84% at 50µg/mL. For 5% FCS medium only, the average viability was 80.49 SE 2.44% at negative control, 87.82 SE 0.06% at solvent control, 81.14 SE 2.19% at 10µg/mL, 81.35 SE 0.79% at 20µg/mL, 80.83 SE 2.04% at 30µg/mL, and 55.36 SE 1.79% at 50µg/mL. For the combination of 5% FCS and FAF BSA, the average cell viability was 80.84 SE 9.41% at negative control, 82.20 SE 9.23% at solvent control, 81.82 SE 43.68% at 10µg/mL, 83.54 SE 0.68% at 20µg/mL, 84.36 SE 0.49% at 30µg/mL, and 70.90 SE 0.90% at 50µg/mL. The solvent control had no effect on $CD4^+$ T cell viability as expected. Oleic acid had no effect on $CD4^+$ T cell viability until 50µg/mL. **(b)** Line plot showing the relative expression of ***CPT1A***, as determined by RT-qPCR, per donor for each medium and concentration tested after 48 h exposure. Data is shown relative to the negative control condition. As expected, the solvent was not found to have any effect on ***CPT1A*** expression, in any of the medium types tested (3.81 fold for FAF BSA only, 1.02 SE 0.11 fold for 5% FCS only, and 0.76 SE 0.23 fold for the combination of 5% FCS and FAF BSA). No RNA was extracted from the second donor in the solvent control condition making the mean only the mean of the first donor and therefore also no SE could be calculated. For FAF BSA medium only, on average, oleic acid exposure caused ***CPT1A*** to be upregulated 1.80 SE 0.57 fold at 10µg/mL, 2.92 SE 0.69 fold at 20µg/mL, and 2.52 SE 0.74 fold at 30µg/mL, and 3.53 SE 0.32 fold at 50µg/mL. ***CPT1A*** expression increased inconsistently, most likely due to insufficient nutrients (often supplied by FCS) for the cells to survive and behave as they normally would. For 5% FCS medium only, on average, oleic acid exposure caused ***CPT1A*** to be upregulated 3.42 SE 0.29 fold at 10µg/mL, 4.01 SE 1.19 fold at 20µg/mL, and 5.92 SE 0.04 fold at 30µg/mL. Oleic acid exposure increased the expression of ***CPT1A*** gradually with increasing concentrations until 50µg/mL where the lack of albumin bound oleic acid became toxic and the cells died, making it impossible to extract sufficient quality RNA for RT-qPCR analysis. For the combination of 5% FCS and FAF BSA, on average, oleic acid exposure caused ***CPT1A*** to be upregulated 4.45 SE 2.92 fold at 10µg/mL, 7.39 SE 3.22 fold at 20µg/mL, 9.83 SE 5.60 fold at 30µg/mL, and 13.91 SE 8.58 fold at 50µg/mL. Oleic acid exposure increased the expression of ***CPT1A*** gradually with increasing concentrations.

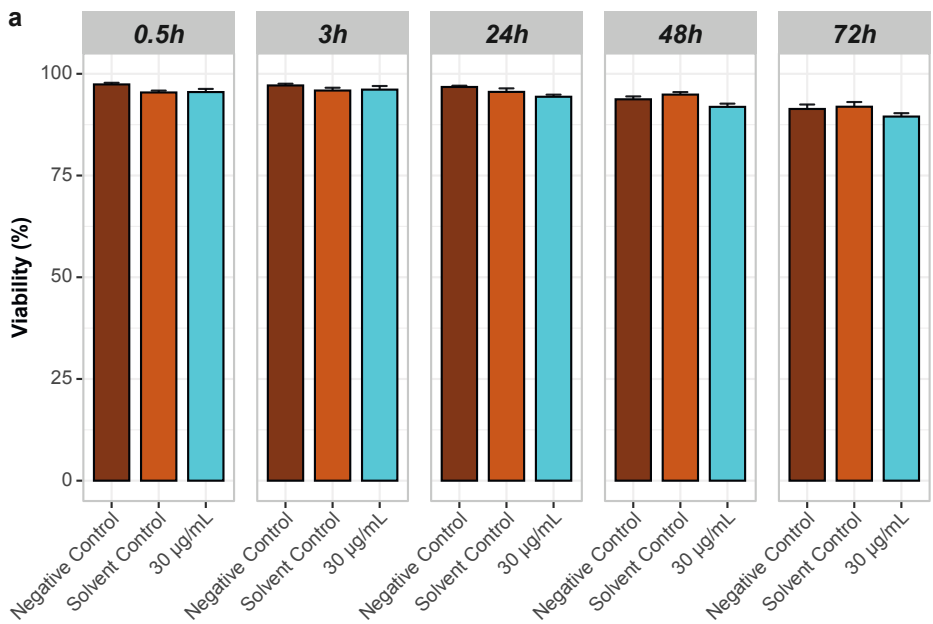

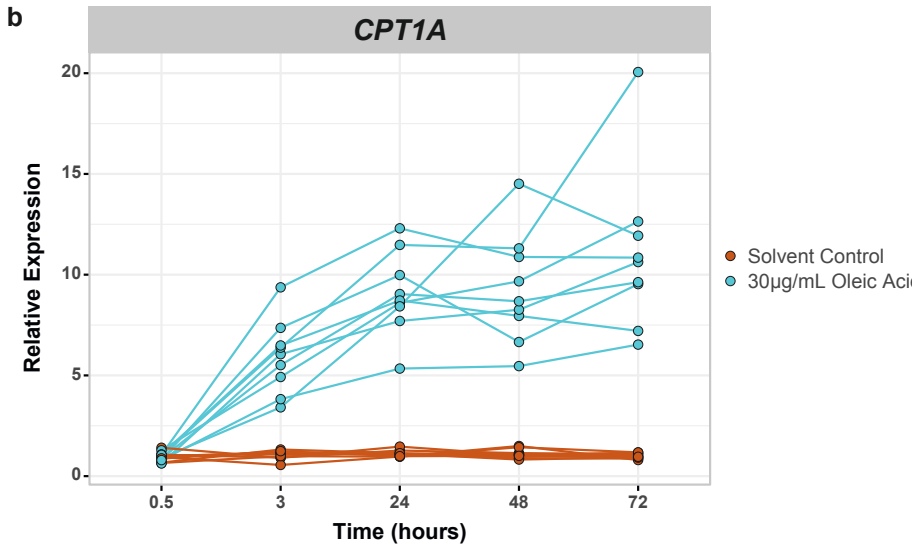

Supplemental Fig. 2 | Verification of *in vitro* model prior to RNA sequencing by viability and *CPT1A* expression. (a) Bar plot showing the average cell viability and standard error in percent, as determined by trypan blue exclusion. On average the cell viability of the negative control exposed cells was 97.4 SE 0.4% at 0.5h, 97.1 SE 0.4% at 3h, 96.8 SE 0.3% at 24h, 93.7 SE 0.7% at 48h, and 91.4 SE 1.1% at 72h. On average the cell viability of the solvent control exposed cells was 95.4 SE 0.5% at 0.5h, 95.9 SE 0.7% at 3h, 95.6 SE 0.9% at 24h, 94.9 SE 0.6% at 48h, and 91.9 SE 1.2% at 72h. On average the cell viability of the oleic acid exposed cells was 95.5 SE 0.8% at 0.5h, 96.1 SE 0.9% at 3h, 94.4 SE 0.5% at 24h, 91.8 SE 0.8% at 48h, and 89.4 SE 0.8% at 72h. Thus, neither the controls nor the exposure had an effect on $CD4^+$ T cell viability, as expected, n = 9. **(b)** Line plot showing the relative expression of ***CPT1A*** per donor across time by RT-qPCR confirming the effect of oleic acid on $CD4^+$ T cells in the ***in vitro*** model and the absence of an effect of solvent. Values are colored by exposure across time. In solvent control exposed samples, there was no effect on ***CPT1A*** expression with a relative expression of 1.0 SE 0.07 fold at 0.5h, 1.0 SE 0.08 fold at 3h, 1.1 SE 0.05 fold at 24h, 1.1 SE 0.08 fold at 48h, and 1.0 SE 0.04 fold at 72h as compared to the negative control. In oleic acid exposed samples, on average ***CPT1A*** was upregulated 0.9 SE 0.07 fold at 0.5h, 5.9 SE 0.61 fold at 3h, 9.1 SE 0.68 fold at 24h, 9.3 SE 0.90 fold at 48h, and 11.0 SE 1.30 fold at 72h as compared to the negative control. The solvent control has no effect gene expression and can therefore be used as a comparison for the differential gene expression analysis, n = 9.

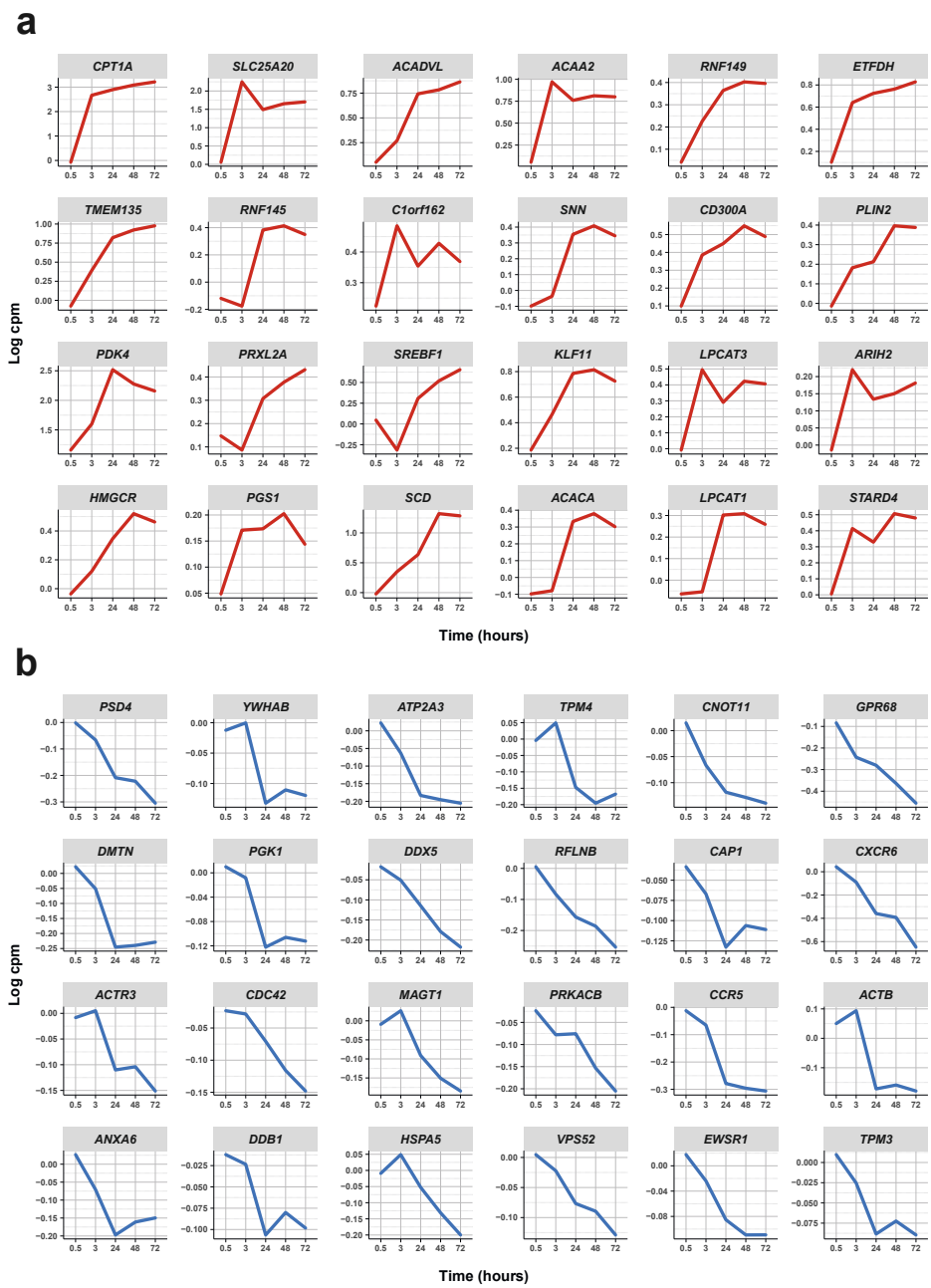

Supplemental Fig. 3 | Top differentially expressed genes from cluster 1 and 2. (a) Cluster 1 differentially expressed genes. Line plots showing mean expression values (read counts) of indicated genes from cluster 1 across time analyzed by RNA-Seq. **(b)** Cluster 2 differentially expressed genes. Line plots showing mean expression values (read counts) of indicated genes from cluster 2 across time analyzed by RNA-Seq.

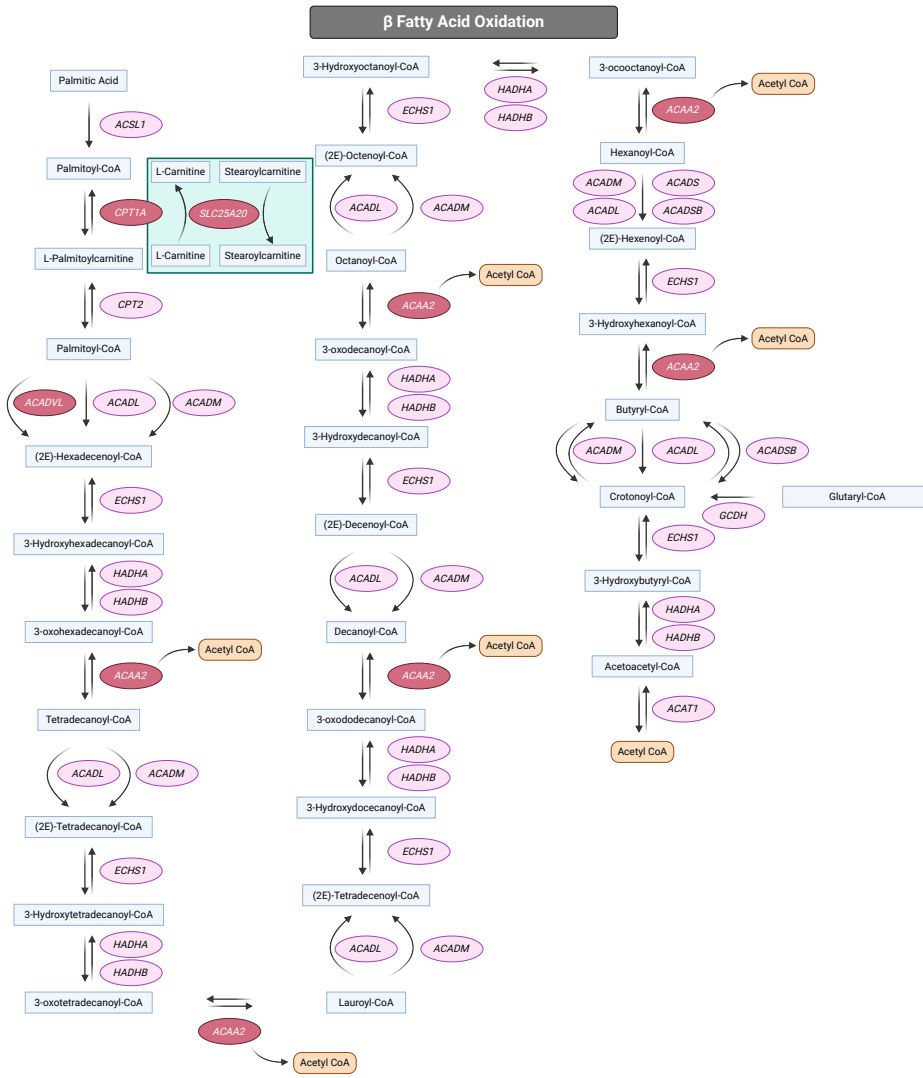

Supplemental Fig. 4 | Visualization of the Path-MAP identified overlap of differentially expressed genes within the β fatty acid oxidation pathway. Overall, a total of 4 out of 16 enzymes involved in the β fatty acid oxidation were upregulated in our oleic acid exposed non-activated $CD4^+$ T cells. Compounds are in blue boxes, enzymes not differentially expressed in the RNA sequencing data are in light pink ovals, enzymes present in the RNA sequencing data are in red ovals, the arrows indicate the direction of movement of the process. Visualization created in BioRender.com.

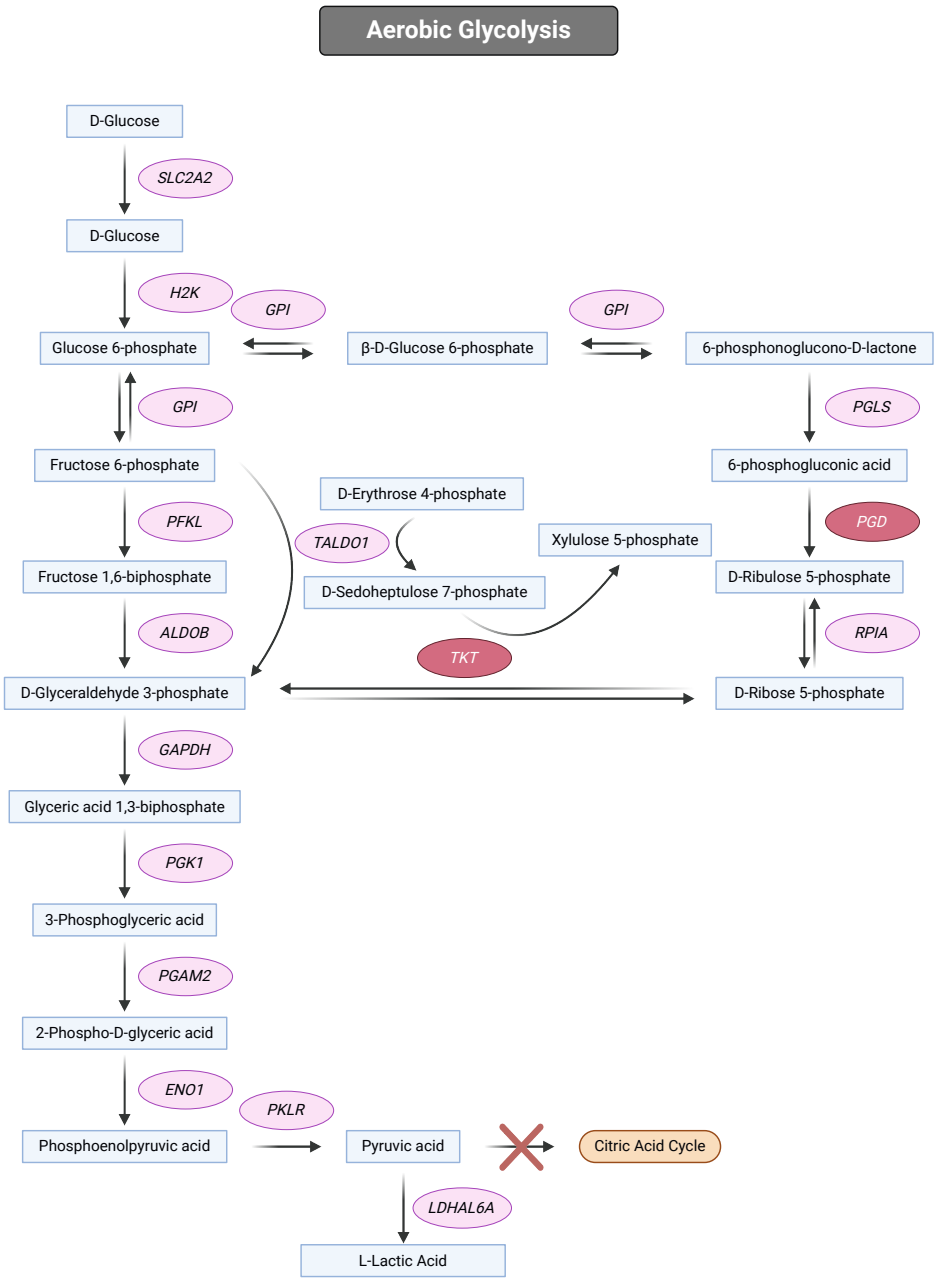

Supplemental Fig. 5 | Visualization of the Path-MAP identified overlap of differentially expressed genes within the aerobic glycolysis pathway. Overall, a total of 2 out of 15 enzymes involved in aerobic glycolysis were upregulated in our oleic acid exposed non-activated $CD4^+$ T cells. Compounds are in blue boxes, enzymes not differentially expressed in the RNA sequencing data are in light pink ovals, enzymes present in the RNA sequencing data are in red ovals, the arrows indicate the direction of movement of the process. Visualization created in BioRender.com.

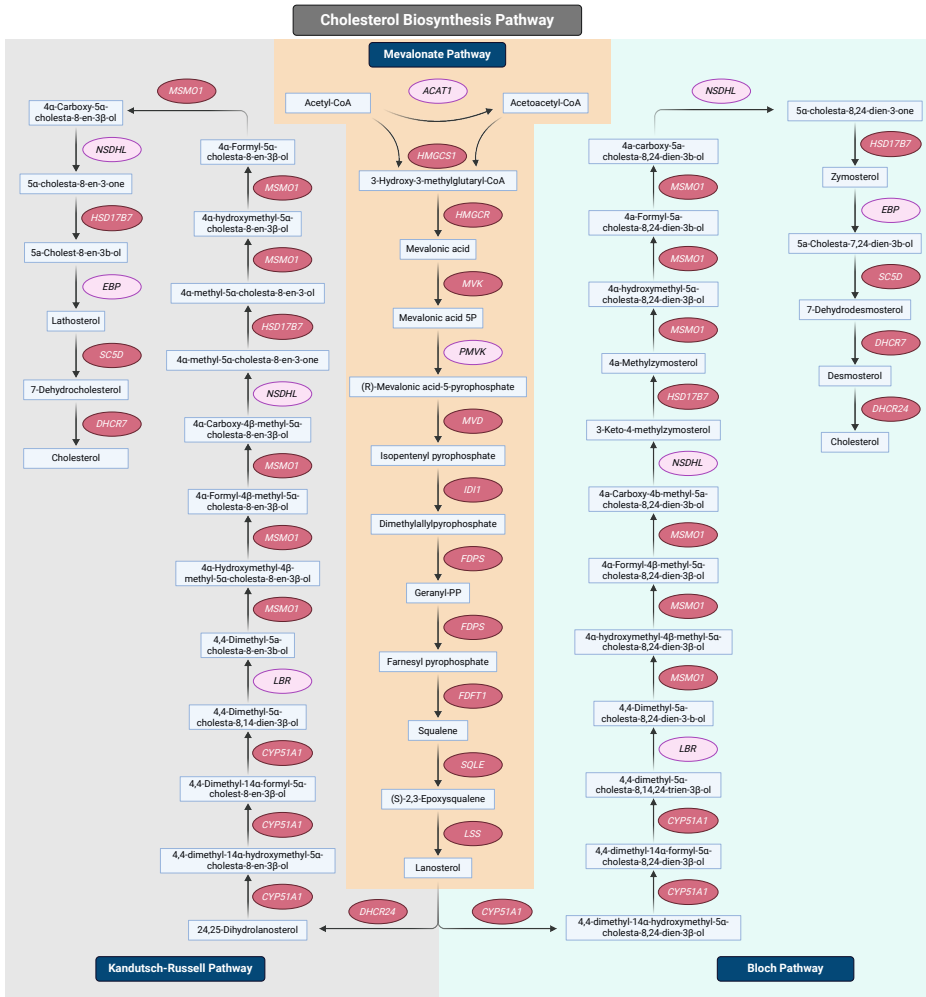

Supplemental Fig. 6 | Visualization of the Path-MAP identified overlap of differentially expressed genes within the cholesterol biosynthesis pathway. Path-MAP showed an overlap between 9 of 11 enzymes within the mevalonate pathway, 6 out of 9 enzymes within the Bloch Pathway, and 6 of 9 enzymes within the Kandutch-Russel Pathway. Overall, a total of 15 out of 20 enzymes involved in cholesterol biosynthesis were upregulated in our oleic acid exposed non-activated $CD4^+$ T cells. Compounds are in blue boxes, enzymes not differentially expressed in the RNA sequencing data are in light pink ovals, enzymes present in the RNA sequencing data are in red ovals, the arrows indicate the direction of movement for cholesterol production, the orange background indicates enzymes and compounds involved in the mevalonate pathway, the grey background indicates enzymes and compounds involved in the Kandutch-Russell pathway, and the light green background indicates enzymes and compounds involved in the Bloch pathway. Visualization created in BioRender.com.

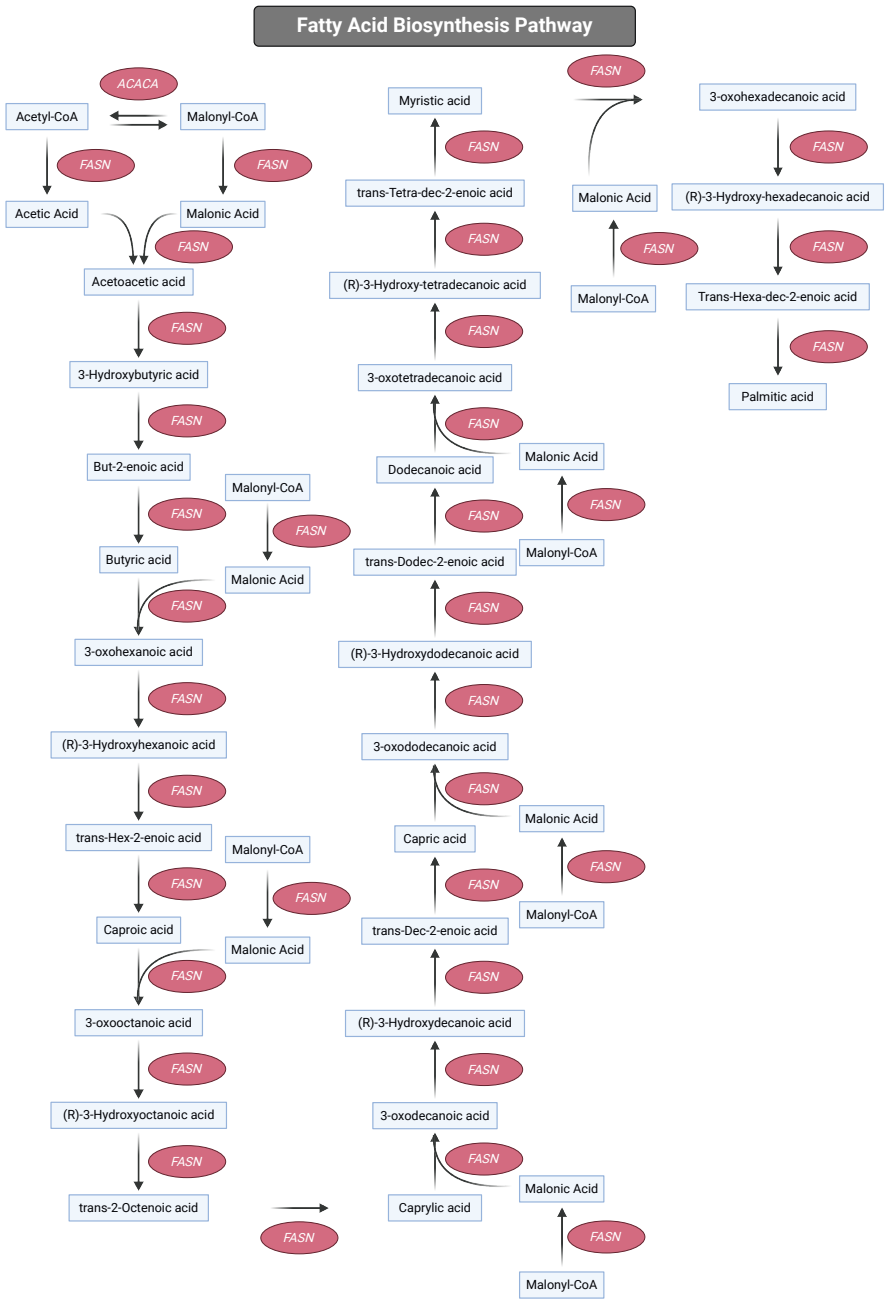

Supplemental Fig. 7 | Visualization of the Path-MAP identified overlap of differentially expressed genes within the fatty acid biosynthesis pathway. Overall, a total of 2 out of 2 enzymes involved in fatty acid biosynthesis were upregulated in our oleic acid exposed non-activated $CD4^+$ T cells. Compounds are in blue boxes, enzymes not differentially expressed in the RNA sequencing data are in light pink ovals, enzymes present in the RNA sequencing data are in red ovals, the arrows indicate the direction of movement for fatty acid production. Visualization created in BioRender.com.

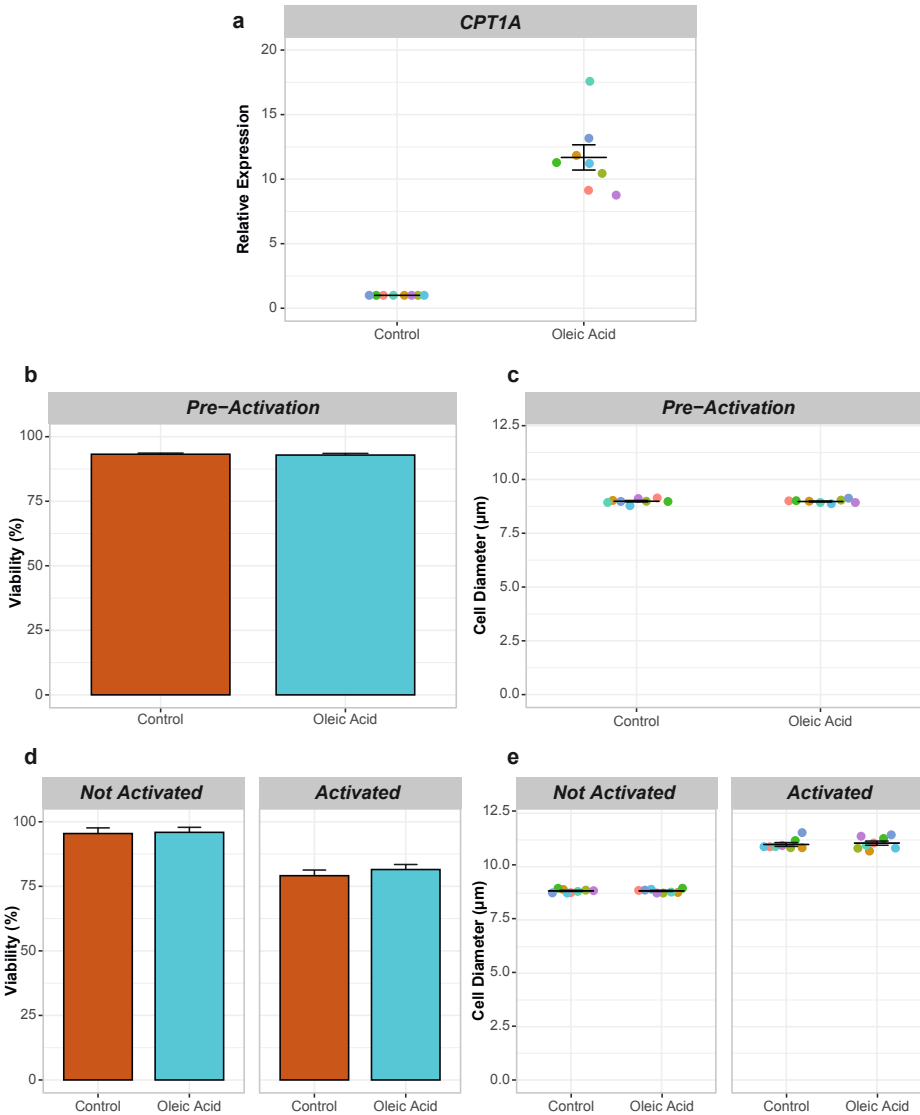

Supplemental Fig. 8 | Verification of viability, cell diameter and *CPT1A* expression post-exposure and post-activation for spectral cytometry. (a) Dot plot showing the relative expression of *CPT1A* per donor after 48h of oleic acid exposure as a confirmation of the *in vitro* model by RT-qPCR. Values are colored by donor and shown relative to the control condition. On average *CPT1A* expression of 30µg/mL oleic acid exposed cells was upregulated by 11.68 SE 0.98 fold after 48h ($p < 0.0001$), n =8. **(b)** Bar plot showing the average cell viability and standard error in percent, as determined by Via1-Cassette™ on a NucleoCounter® NC-200™. On average the cell viability of control exposed cells was 93.21 SE 0.43% and of oleic acid exposed cells was 92.89 SE 0.64%. Thus, The solvent control had no effect on $CD4^+$ T cell viability, as expected, at 48h. Thus, there was no effect on $CD4^+$ T cell viability after 48h exposure, n =8. **(c)** Dot plot showing the average cell diameter and standard error in µm, as determined by Via1-Cassette™ on a NucleoCounter® NC-200™. On average the cell diameter of control exposed cells was 8.99 SE 0.04µm and of oleic acid exposed was 8.98 SE 0.03µm. Thus, there was no effect on $CD4^+$ T cell diameter after 48h exposure, n =8. **(d)** Bar plot showing the average cell viability and standard error in percent, as determined by Via1-Cassette™ on a NucleoCounter®

NC-200™. Left plot shows the cell viability for non-activated cells and right plot shows the cell viability for activated cells. On average, the cell viability of control pre-exposed non-activated cells was 95.45 SE 2.19% and for 30µg/mL oleic acid pre-exposed non-activated cells was 95.91 SE 1.95% after 72h. The cell viability of control pre-exposed activated cells was 79.13 SE 2.19% and for 30µg/mL oleic acid pre-exposed activated cells was 81.51 SE 1.95% after 72h activation with CD3-CD28 beads. Thus, there was no effect on $CD4^+$ T cell viability between the different pre-exposures. However, activation did affect $CD4^+$ T cell viability, where the activated cells were less viable than the not activated cells, n =8. **(e)** Dot plot showing the average cell diameter and standard error in µm, as determined by Via1-Cassette™ on a NucleoCounter® NC-200™. Left plot shows the cell diameter for non-activated cells and right plot shows the cell diameter for activated cells. On average, the cell diameter of control pre-exposed non-activated cells was 8.86 SE 0.03 µm and for 30µg/mL oleic acid pre-exposed non-activated cells was 8.86 SE 0.03µm after 72h. The cell diameter of control pre-exposed activated cells was 11.04 SE 0.09µm and for 30µg/mL oleic acid pre-exposed activated cells was 11.10 SE 0.10µm after 72h activation with CD3-CD28 beads. Thus, there was no effect on $CD4^+$ T cell diameter between the different pre-exposures. However, activation did affect $CD4^+$ T cell diameter, where the activated cells were larger than the not activated cells, n =8.

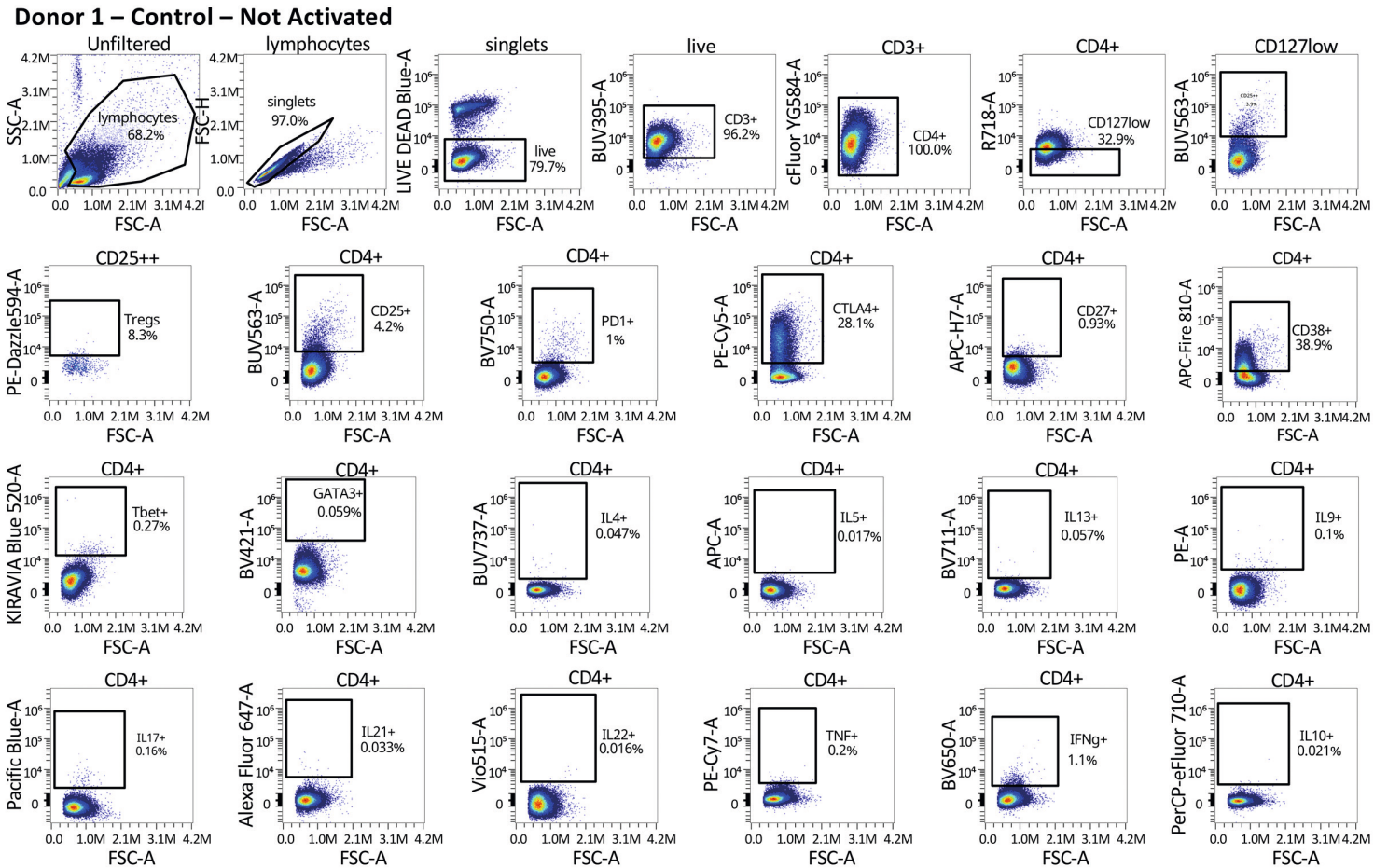
Donor 1 – Control – Not Activated
Unfiltered
SSC-A
FSC-H
FSC-A
lymphocytes
68.2%
lymphocytes
singlets
97.0%
singlets
LIVE DEAD Blue-A
live
79.7%
live
BUV395-A
CD3+
96.2%
CD3+
cFluor YG584-A
CD4+
100.0%
CD4+
R718-A
CD127low
32.9%
CD127low
BUV563-A
CD25++
PE-Dazzle594-A
Tregs
8.3%
CD4+
BUV563-A
CD25+
4.2%
CD4+
BV750-A
PD1+
1%
CD4+
PE-Cy5-A
CTLA4+
28.1%
CD4+
APC-H7-A
CD27+
0.93%
CD4+
APC-Fire 810-A
CD38+
38.9%
CD4+
KIRAVIA Blue 520-A
Tbet+
0.27%
CD4+
BV421-A
GATA3+
0.059%
CD4+
BUV737-A
IL4+
0.047%
CD4+
APC-A
IL5+
0.017%
CD4+
BV711-A
IL13+
0.057%
CD4+
PE-A
IL9+
0.1%
CD4+
Pacific Blue-A
IL17+
0.16%
CD4+
Alexa Fluor 647-A
IL21+
0.033%
CD4+
Vio515-A
IL22+
0.016%
CD4+
PE-Cy7-A
TNF+
0.2%
CD4+
BV650-A
IFNg+
1.1%
CD4+
PerCP-eFluor 710-A
IL10+
0.021%
CD4+
FSC-A

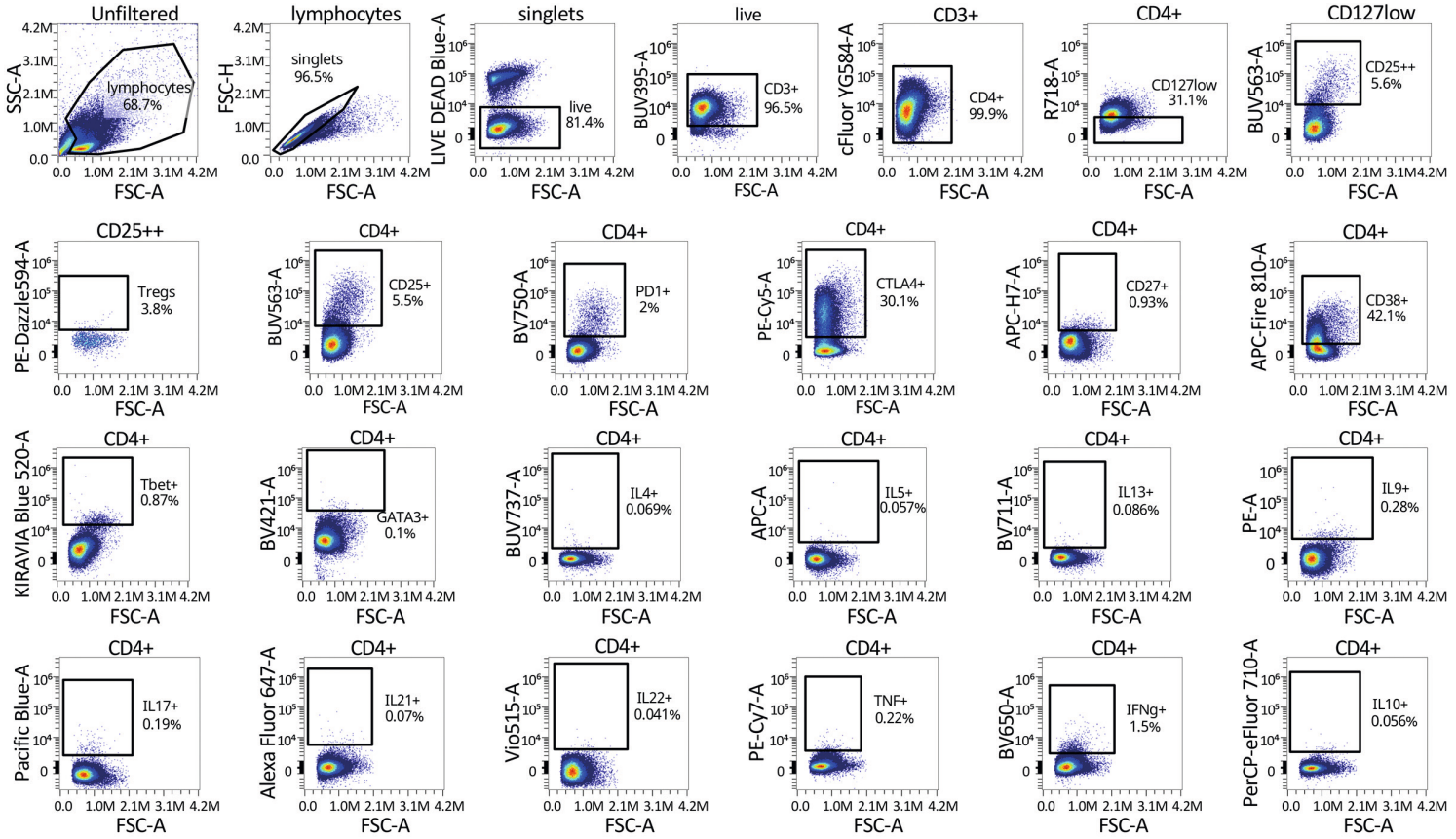

Supplemental Fig. 9 (partial) | Gating strategy for the primary spectral cytometry analysis of non-activated CD4⁺ T cells pre-exposed to oleic acid, n = 8. Gating strategy is the same for all 8 donors analyzed and includes gates set for all markers measured in the panel. Gating strategy for one donor and both exposures are shown here, the rest of the figure can be found in the online supplement: https://doi.org/10.1016/j.isci.2024.109496.

Donor 1 – Control – Activated
Unfiltered
Lymphocytes
73.6%
SSC-A
FSC-A
Lymphocytes
Singlets
97.1%
FSC-H
FSC-A
Singlets
Live
76.8%
LIVE DEAD Blue-A
FSC-A
Live
CD3+CD4+
99.1%
BUV395-A
cFluor YG584-A
CD3+CD4+
CD127low
4.6%
R718-A
FSC-A
CD127low
CD25++
68.9%
BUV563-A
FSC-A
CD25++
Tregs
7.1%
PE-DazzleI594-A
FSC-A
CD3+CD4+
CD25+
72.2%
BUV563-A
FSC-A
CD3+CD4+
PD1+
60.4%
BV750-A
FSC-A
CD3+CD4+
CTLA4+
66.5%
PE-Cy5-A
FSC-A
CD3+CD4+
CD27+
14.6%
APC-H7-A
FSC-A
CD3+CD4+
CD38+
52.3%
APC-Fire 810-A
FSC-A
CD3+CD4+
Tbet+
0.42%
KIRAVIA Blue 520-A
FSC-A
CD3+CD4+
GATA3+
0.63%
BV421-A
FSC-A
CD3+CD4+
IL4+
0.018%
BUV737-A
FSC-A
CD3+CD4+
IL5+
0.023%
APC-A
FSC-A
CD3+CD4+
IL13+
0.059%
BV711-A
FSC-A
CD3+CD4+
IL9+
0.68%
PE-A
FSC-A
CD3+CD4+
IL17A+
0.29%
Pacific Blue-A
FSC-A
CD3+CD4+
IL21+
0.21%
Alexa Fluor 647-A
FSC-A
CD3+CD4+
IL22+
0.12%
Vio515-A
FSC-A
CD3+CD4+
TNF+
0.65%
PE-Cy7-A
FSC-A
CD3+CD4+
IFNg+
2.8%
BV650-A
FSC-A
CD3+CD4+
IL10+
0.12%
PerCP-eFluor 710-A
FSC-A

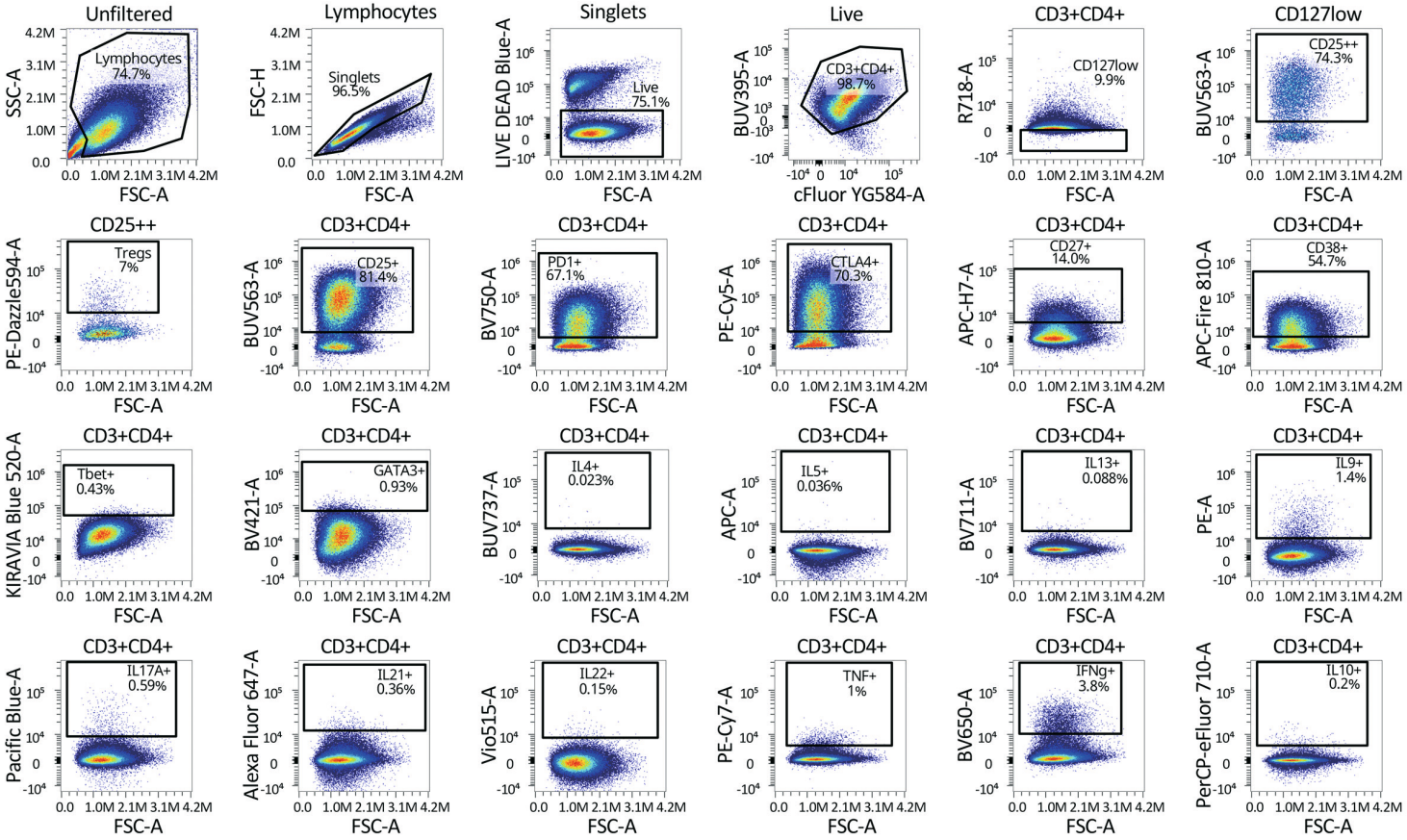

Supplemental Fig. 10 (partial) | Gating strategy for the primary spectral cytometry analysis of activated CD4⁺ T cells pre-exposed to oleic acid, n = 8. Gating strategy is the same for all 8 donors analyzed and includes gates set for all markers measured in the panel. Gating strategy for 2 different donors and exposures are shown here, the rest of the figure can be found in the online supplement: https://doi.org/10.1016/j.isci.2024.109496.

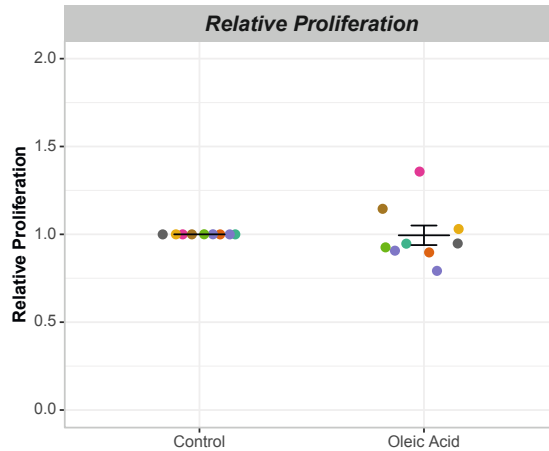

Supplemental Fig. 11 | Relative proliferation post-activation of oleic acid pre-exposed CD4⁺ T cells. Dot plot showing the relative proliferation, as determined by ^{3}H incorporation, per donor after 48h exposure to control or 30µg/mL oleic acid, where the solvent was completely evaporated prior to addition to the cells, and subsequent activation by CD3/CD28 activation beads for 72h. ^{3}H was added post 72h activation and cells were left to proliferate for 18h. Data is shown relative to the Control condition. Points are colored by donor with mean and standard error. No difference in proliferative capacity was observed between the oleic acid and control pre-exposed conditions. On average the relative proliferation of oleic acid exposed cells was 0.99 SE 0.06 ($p > 0.92$), $n = 9$.

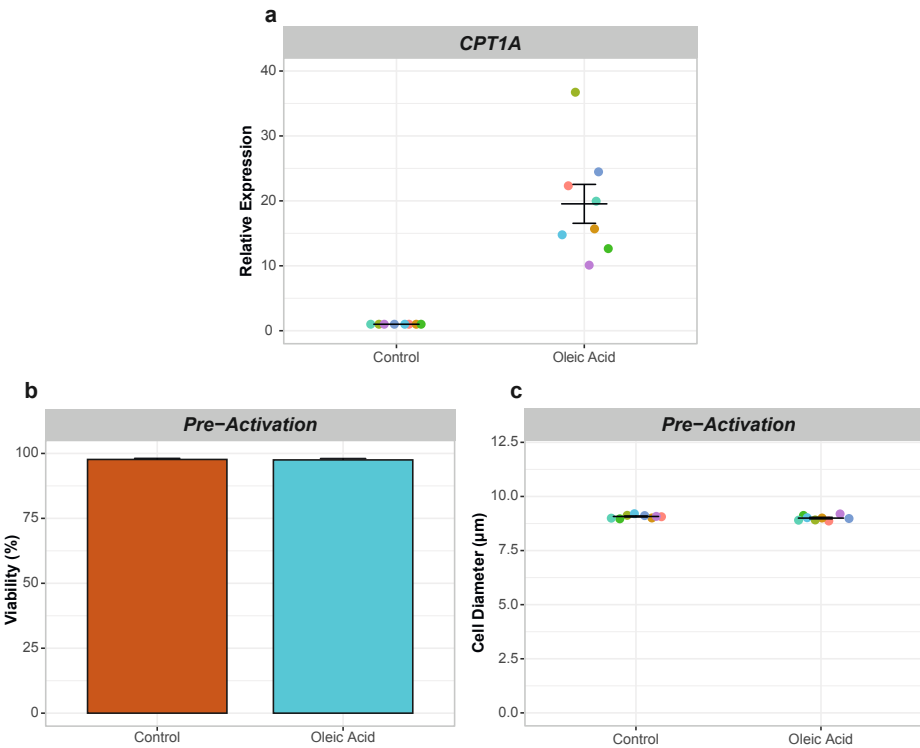

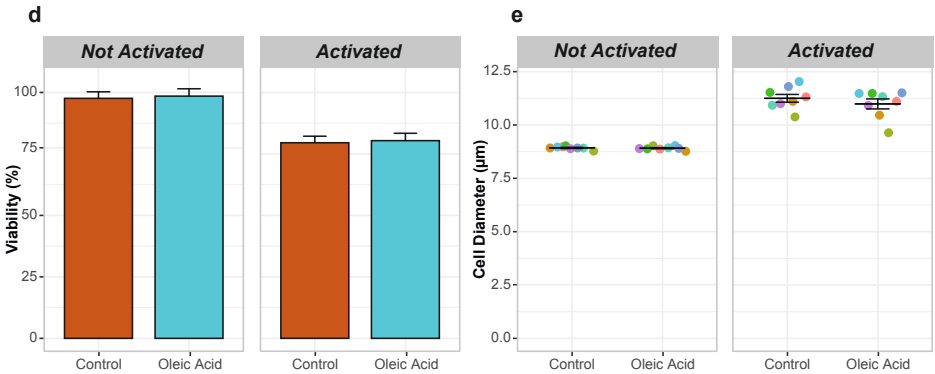

Supplemental Fig. 12 | Verification of viability, cell diameter and *CPT1A* expression post-exposure and post-activation for spectral cytometry. (a) Dot plot showing the relative expression of ***CPT1A*** per donor after 48h of oleic acid exposure as a confirmation of the ***in vitro*** model by RT-qPCR. Values are colored by donor and shown relative to the control condition. On average ***CPT1A*** expression of 28µg/mL oleic acid exposed cells was upregulated by 19.5 SE 3.00 fold after 48h ($p < 0.0001$), n = 8. **(b)** Bar plot showing the average cell viability and standard error in percent, as determined by Via1-Cassette™ on a NucleoCounter® NC-200™. On average the cell viability of control exposed cells was 93.21 SE 0.43% and of oleic acid exposed cells was 92.89 SE 0.64%. Thus, The solvent control had no effect on $CD4^+$ T cell viability, as expected, at 48h. Thus, there was no effect on $CD4^+$ T cell viability after 48h exposure, n = 8. **(c)** Dot plot showing the average cell diameter and standard error in µm, as determined by Via1-Cassette™ on a NucleoCounter® NC-200™. On average the cell diameter of control exposed cells was 8.99 SE 0.04µm and of oleic acid exposed was 8.98 SE 0.03µm. Thus, there was no effect on $CD4^+$ T cell diameter after 48h exposure, n = 8. **(d)** Bar plot showing the average cell viability and standard error in percent, as determined by Via1-Cassette™ on a NucleoCounter® NC-200™. Left plot shows the cell viability for non-activated cells and right plot shows the cell viability for activated cells. On average, the cell viability of control pre-exposed non-activated cells was 95.45 SE 2.19% and for 28µg/mL oleic acid pre-exposed non-activated cells was 95.91 SE 1.95% after 72h. The cell viability of control pre-exposed activated cells was 79.13 SE 2.19% and for 28µg/mL oleic acid pre-exposed activated cells was 81.51 SE 1.95% after 72h activation with CD3-CD28 beads. Thus, there was no effect on $CD4^+$ T cell viability between the different pre-exposures. However, activation did affect $CD4^+$ T cell viability, where the activated cells were less viable than the not activated cells, n = 8. **(e)** Dot plot showing the average cell diameter and standard error in µm, as determined by Via1-Cassette™ on a NucleoCounter® NC-200™. Left plot shows the cell diameter for non-activated cells and right plot shows the cell diameter for activated cells. On average, the cell diameter of control pre-exposed non-activated cells was 8.86 SE 0.03 µm and for 28µg/mL oleic acid pre-exposed non-activated cells was 8.86 SE 0.03µm after 72h. The cell diameter of control pre-exposed activated cells was 11.04 SE 0.09µm and for 28µg/mL oleic acid pre-exposed activated cells was 11.10 SE 0.10µm after 72h activation with CD3-CD28 beads. Thus, there was no effect on $CD4^+$ T cell diameter between the different pre-exposures. However, activation did affect $CD4^+$ T cell diameter, where the activated cells were larger than the not activated cells, n = 8.

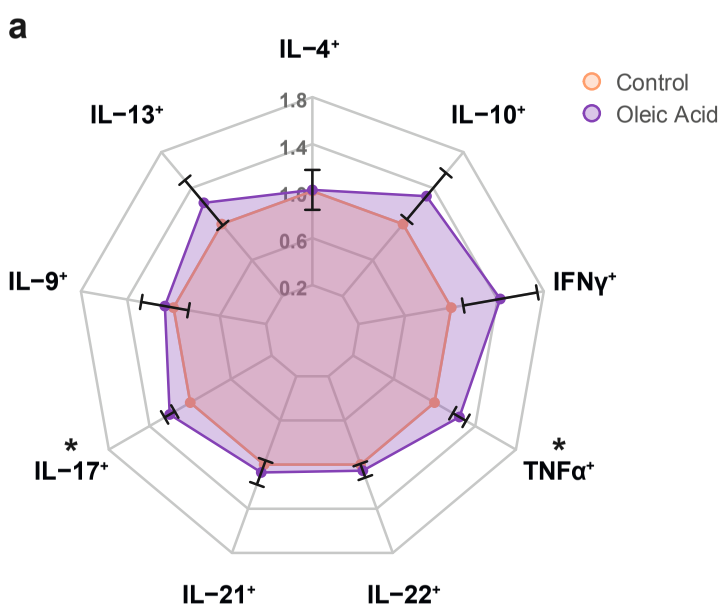
a
IL−4+
IL−10+
IFNγ+
*
TNFα+
IL−22+
IL−21+
*
IL−17+
IL−9+
IL−13+
1.8
1.4
1.0
0.6
0.2
Control
Oleic Acid

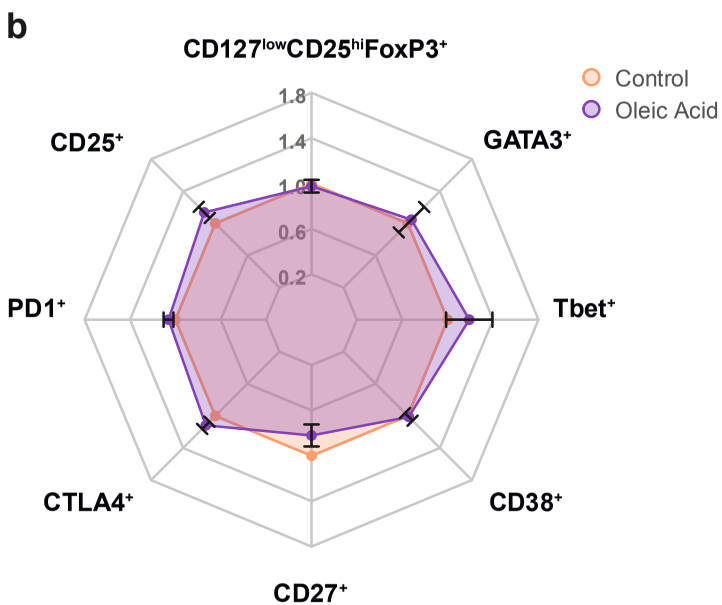
b
CD127lowCD25hiFoxP3+
GATA3+
Tbet+
CD38+
CD27+
CTLA4+
PD1+
CD25+
1.8
1.4
1.0
0.6
0.2
Control
Oleic Acid

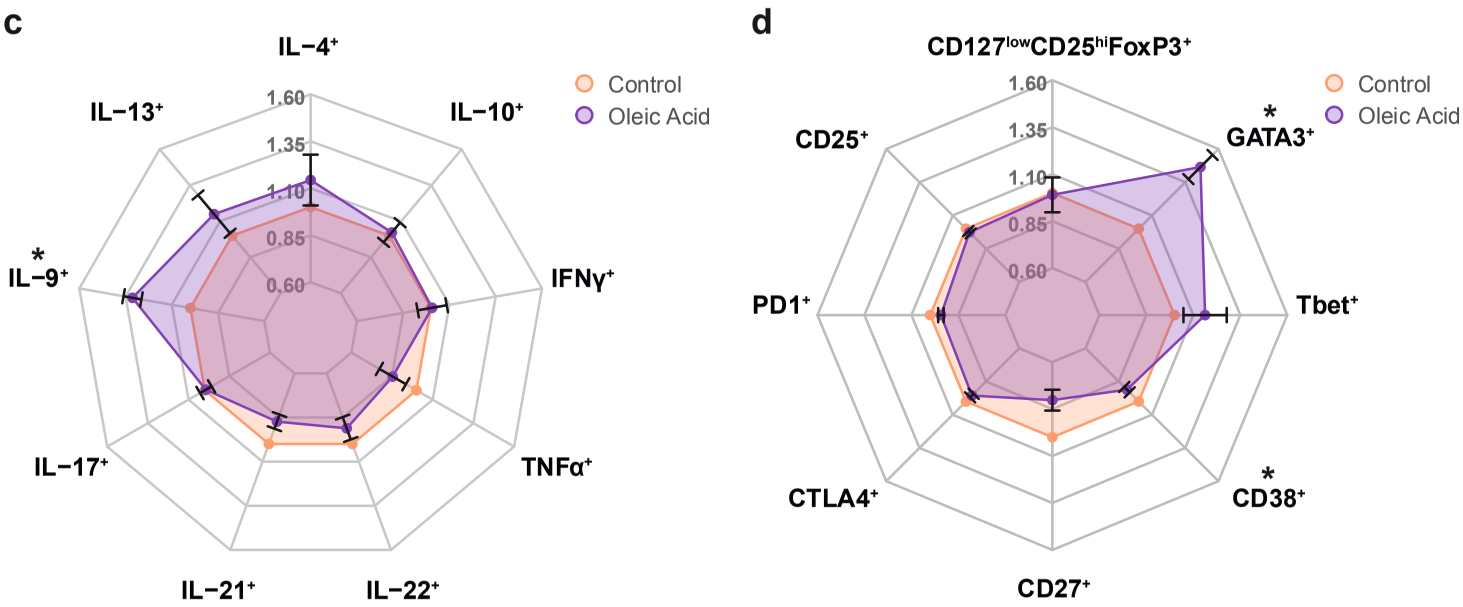

Supplemental Fig. 13 | Oleic acid pre-exposure leads to changes in expression of extracellular markers, transcription factors, and intracellular cytokines. (*) $P_{FDR} < 0.05$, n = 8. **(a)** Radar plot of various $CD4^+$ T cell internal cytokines expressed in $CD4^+$ T cells after 48h of oleic acid exposure or control followed by 72h of rest and 4h stimulus with PMA/ionomycin. Values are expressed as fold change and standard error relative to control. **(b)** Radar plot of various $CD4^+$ T cell external markers and transcription factors expressed in $CD4^+$ T cells after 48h of oleic acid exposure or control followed by 72h of rest and 4h stimulus with PMA/ionomycin. Values are expressed as fold change and standard error relative to control. **(c)** Radar plot of various $CD4^+$ T cell internal cytokines expressed in $CD4^+$ T cells after 48h of oleic acid exposure or control followed by 72h of activation with CD3/CD28 activation beads and 4h additional stimulus with PMA/ionomycin. Values are expressed as fold change and standard error relative to control. **(d)** Radar plot of various $CD4^+$ T cell external markers and transcription factors expressed in $CD4^+$ T cells after 48h of oleic acid exposure or control followed by 72h of activation with CD3/CD28 activation beads and 4h additional stimulus with PMA/ionomycin. Values are expressed as fold change and standard error relative to control.

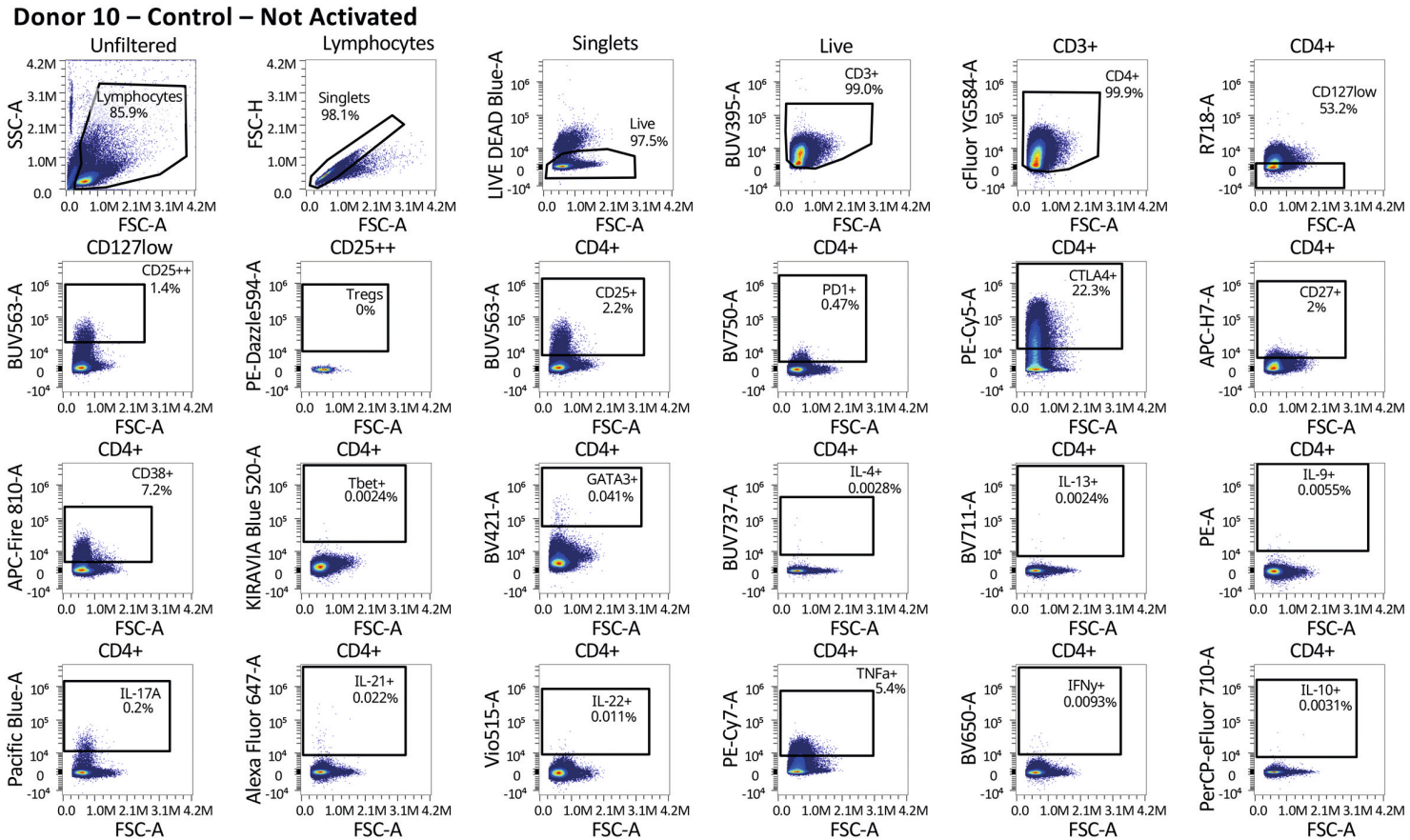
Donor 10 – Control – Not Activated
Unfiltered
Lymphocytes
85.9%
Lymphocytes
Singlets
98.1%
Singlets
Live
97.5%
Live
CD3+
99.0%
CD3+
CD4+
99.9%
CD4+
CD127low
53.2%
CD127low
CD25++
1.4%
CD25++
Tregs
0%
CD4+
CD25+
2.2%
CD4+
PD1+
0.47%
CD4+
CTLA4+
22.3%
CD4+
CD27+
2%
CD4+
CD38+
7.2%
CD4+
Tbet+
0.0024%
CD4+
GATA3+
0.041%
CD4+
IL-4+
0.0028%
CD4+
IL-13+
0.0024%
CD4+
IL-9+
0.0055%
CD4+
IL-17A
0.2%
CD4+
IL-21+
0.022%
CD4+
IL-22+
0.011%
CD4+
TNFa+
5.4%
CD4+
IFNy+
0.0093%
CD4+
IL-10+
0.0031%
SSC-A
FSC-H
LIVE DEAD Blue-A
BUV395-A
cFluor YG584-A
R718-A
BUV563-A
PE-Dazzle594-A
BUV563-A
BV750-A
PE-Cy5-A
APC-H7-A
APC-Fire 810-A
KIRAVIA Blue 520-A
BV421-A
BUV737-A
BV711-A
PE-A
Pacific Blue-A
Alexa Fluor 647-A
Vio515-A
PE-Cy7-A
BV650-A
PerCP-eFluor 710-A
FSC-A

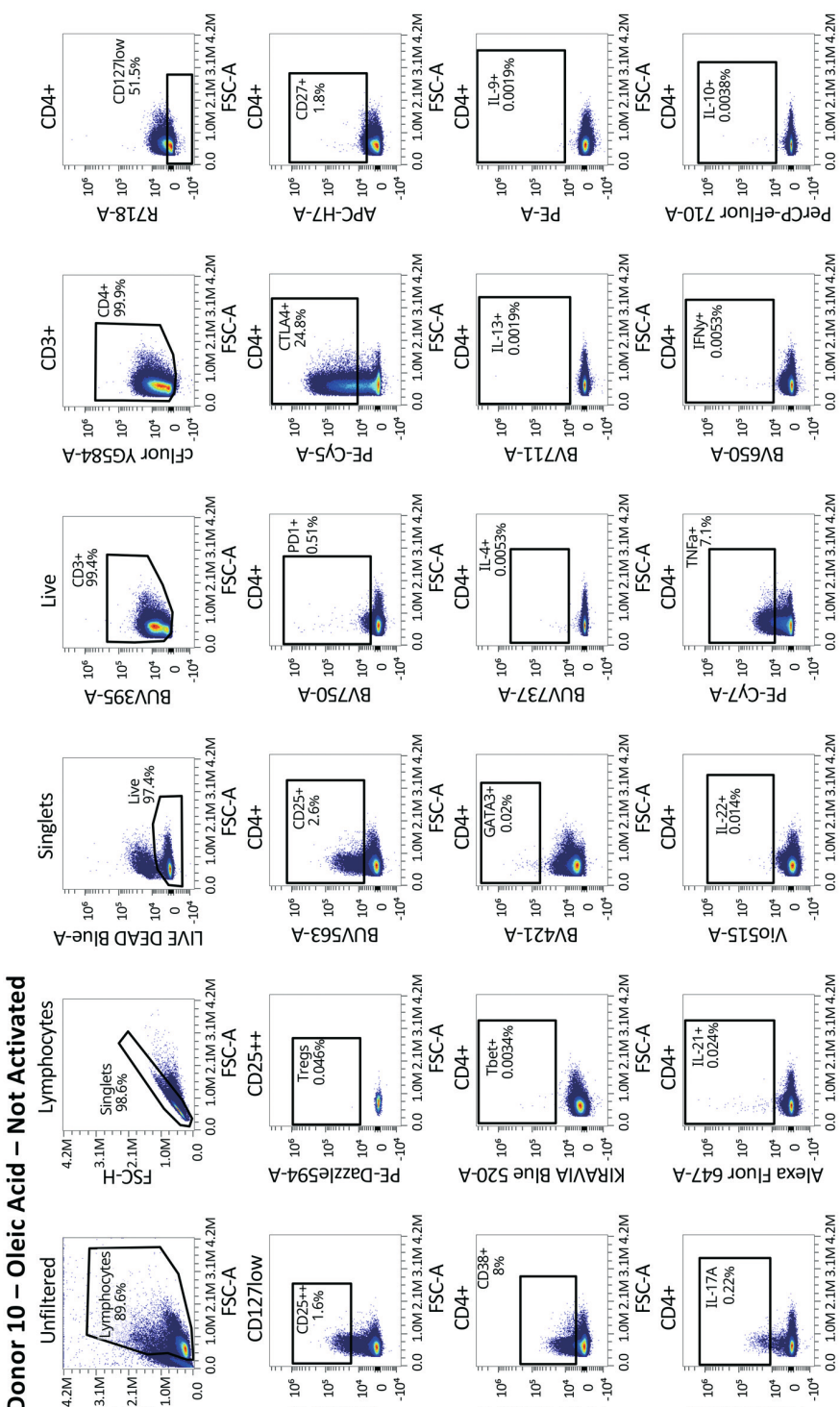

Supplemental Fig. 14 (partial) | Gating strategy for the second spectral cytometry analysis of non-activated CD4⁺ T cells pre-exposed to oleic acid from 8 independent donors, n = 8. Gating strategy is the same for all 8 independent donors analyzed and includes gates set for all markers measured in the panel. Gating strategy for 2 different donors and exposures are shown here, the rest of the figure can be found in the online supplement: https://doi.org/10.1016/j.isci.2024.109496.

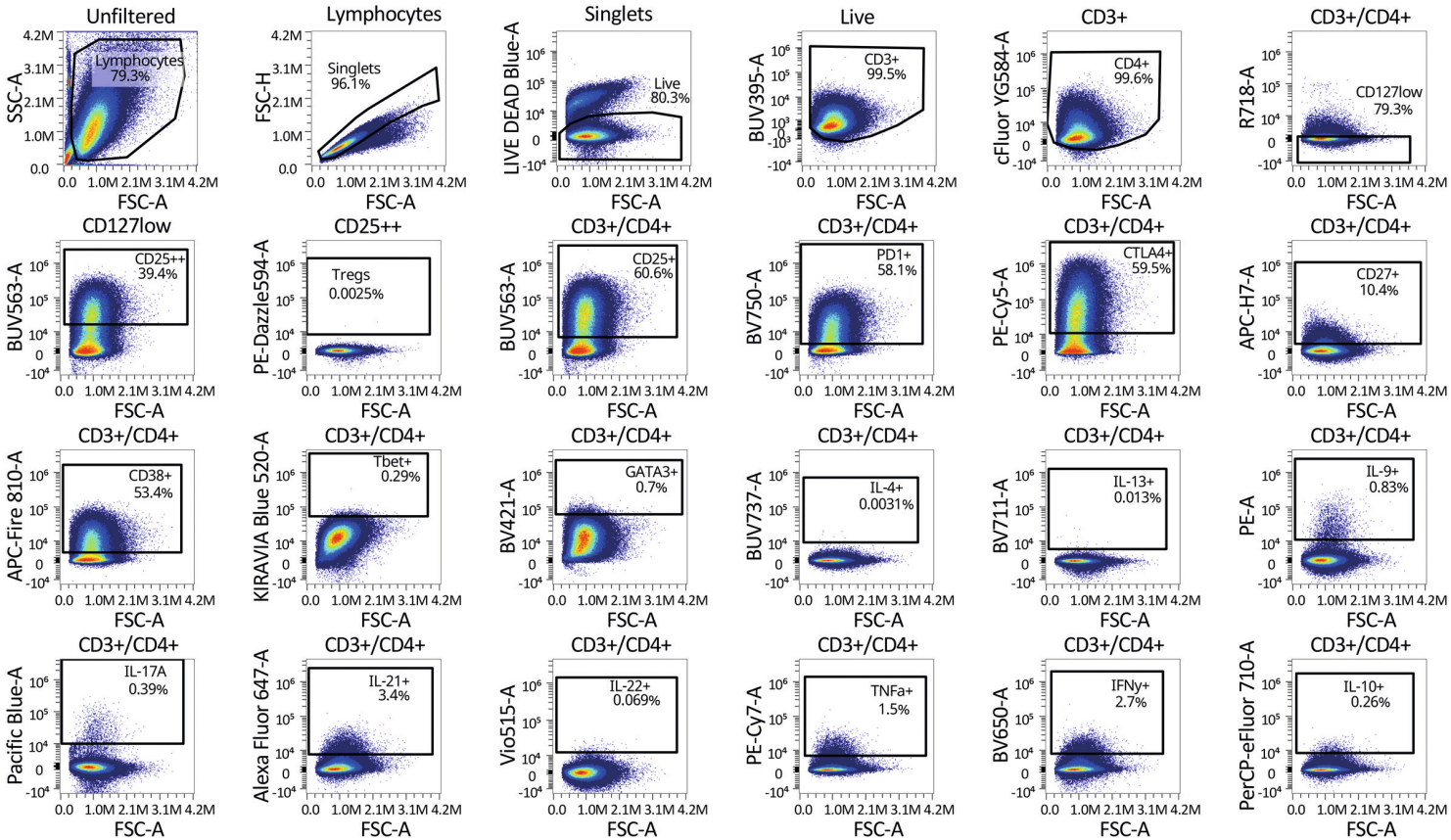
Donor 10 – Control – Activated
Unfiltered
Lymphocytes
79.3%
SSC-A
FSC-A
Lymphocytes
Singlets
96.1%
FSC-H
FSC-A
Singlets
Live
80.3%
LIVE DEAD Blue-A
FSC-A
Live
CD3+
99.5%
BUV395-A
FSC-A
CD3+
CD4+
99.6%
cFluor YG584-A
FSC-A
CD3+/CD4+
CD127low
79.3%
R718-A
FSC-A
CD127low
CD25++
39.4%
BUV563-A
FSC-A
CD25++
Tregs
0.0025%
PE-Dazzle594-A
FSC-A
CD3+/CD4+
CD25+
60.6%
BUV563-A
FSC-A
CD3+/CD4+
PD1+
58.1%
BV750-A
FSC-A
CD3+/CD4+
CTLA4+
59.5%
PE-Cy5-A
FSC-A
CD3+/CD4+
CD27+
10.4%
APC-H7-A
FSC-A
CD3+/CD4+
CD38+
53.4%
APC-Fire 810-A
FSC-A
CD3+/CD4+
Tbet+
0.29%
KIRAVIA Blue 520-A
FSC-A
CD3+/CD4+
GATA3+
0.7%
BV421-A
FSC-A
CD3+/CD4+
IL-4+
0.0031%
BUV737-A
FSC-A
CD3+/CD4+
IL-13+
0.013%
BV711-A
FSC-A
CD3+/CD4+
IL-9+
0.83%
PE-A
FSC-A
CD3+/CD4+
IL-17A
0.39%
Pacific Blue-A
FSC-A
CD3+/CD4+
IL-21+
3.4%
Alexa Fluor 647-A
FSC-A
CD3+/CD4+
IL-22+
0.069%
Vio515-A
FSC-A
CD3+/CD4+
TNFa+
1.5%
PE-Cy7-A
FSC-A
CD3+/CD4+
IFNy+
2.7%
BV650-A
FSC-A
CD3+/CD4+
IL-10+
0.26%
PerCP-eFluor 710-A
FSC-A

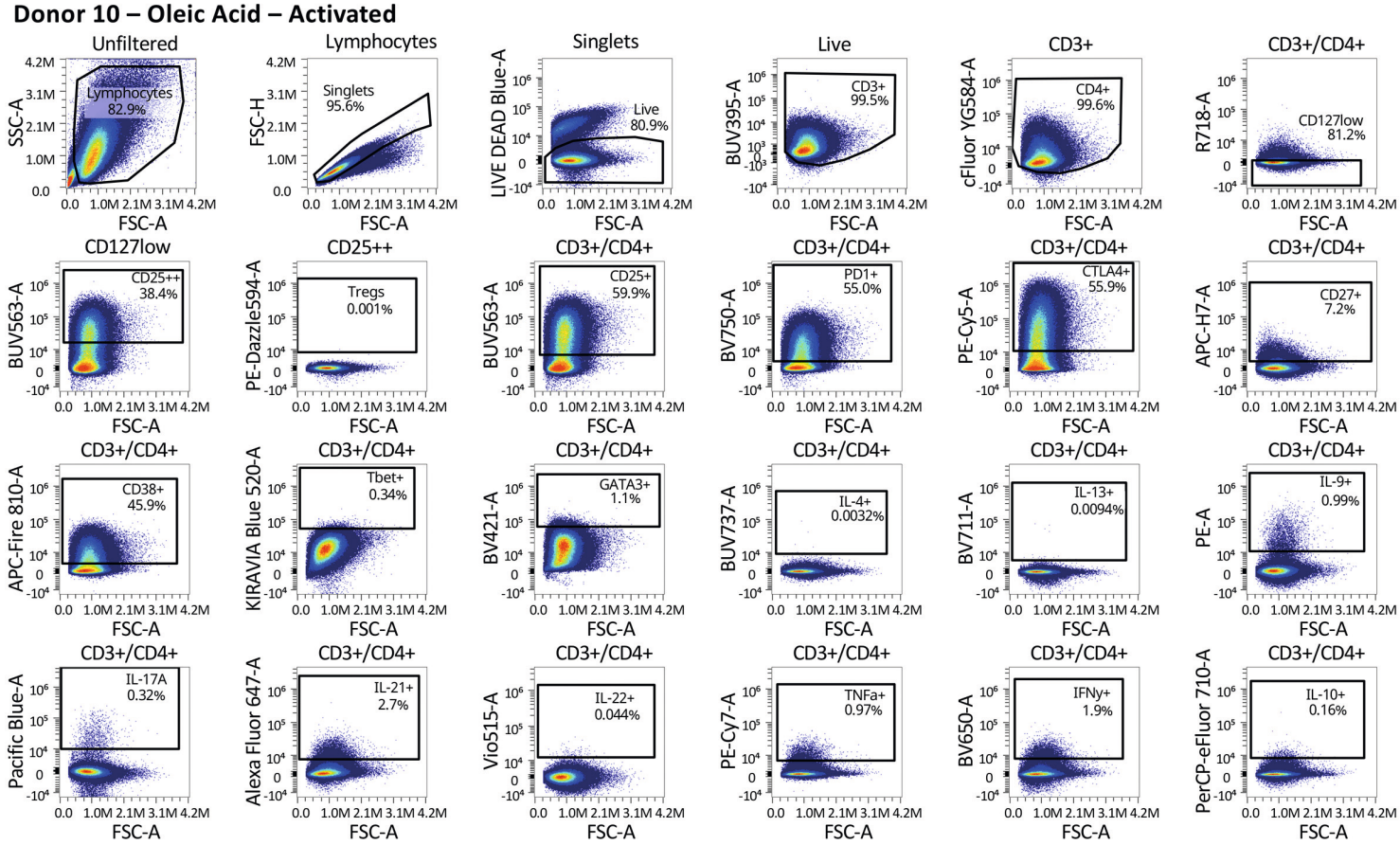

Supplemental Fig. 15 (partial) | Gating strategy for the second spectral cytometry analysis of activated $CD4^+$ T cells pre-exposed to oleic acid from 8 independent donors, n = 8. Gating strategy is the same for all 8 independent donors analyzed and includes gates set for all markers measured in the panel. Gating strategy for 2 different donors and exposures are shown here, the rest of the figure can be found in the online supplement: https://doi.org/10.1016/j.isci.2024.109496.

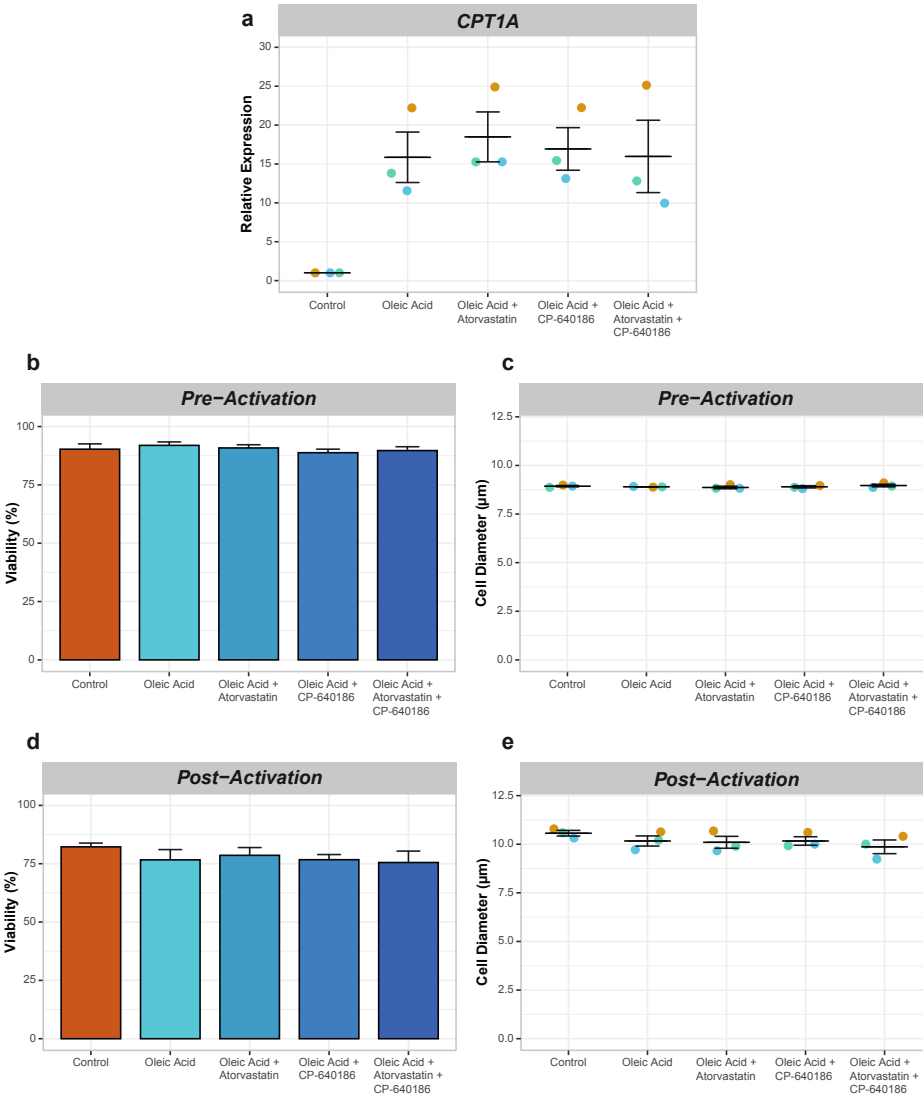

Supplemental Fig. 16 | Verification of viability, cell diameter and *CPT1A* expression post-exposure and post-activation for spectral cytometry with metabolic inhibitors. (a) Dot plot showing the relative expression of *CPT1A* per donor after 48h of oleic acid exposure, with or without inhibitors added as a confirmation of the ***in vitro*** model by RT-qPCR. Values are colored by donor and shown relative to the control condition. On average *CPT1A* was upregulated 15.86 SE 3.24 fold when exposed to oleic acid, 18.48 SE 3.21 fold when exposed to oleic acid + atorvastatin, 16.93 SE 2.74 fold when exposed to oleic acid + CP-640186, and 15.97 SE 4.65 fold when exposed to oleic acid + atorvastatin + CP-640186. Atorvastatin is an HMGCR inhibitor, blocking cholesterol biosynthesis, and CP-640186 is an ACC inhibitor, blocking fatty acid biosynthesis. As CPT1A is a part of the fatty acid oxidation pathway there was no influence of the inhibitors on *CPT1A* expression, n = 3. **(b)** Bar plot showing the average cell viability and standard error in percent, as determined by Via1-Cassette™ on a NucleoCounter® NC-200™. On average the cell viability of control exposed cells was 90.30 SE 2.27%, oleic acid exposed cells was 91.93 SE 1.48%, oleic acid + atorvastatin exposed cells was 90.83 SE 1.37%, oleic acid + CP-640186 exposed cells was 88.80 SE 1.50%, and oleic acid + atorvastatin + CP-640186 exposed cells was

89.70 SE 2.86% at 48h. Thus, there was no effect on $CD4^+$ T cell viability after 48h exposure, n = 3. **(c)** Dot plot showing the average cell diameter and standard error in µm, as determined by Via1-Cassette™ on a NucleoCounter® NC-200™. On average the cell diameter of control exposed cells was 8.93 SE 0.03µm, oleic acid exposed cells was 8.90 SE 0.0µm, oleic acid + atorvastatin exposed cells was 8.87 SE 0.07µm, oleic acid + CP-640186 exposed cells was 8.90 SE 0.0µm, and oleic acid + atorvastatin + CP-640186 exposed cells was 8.97 SE 0.07µm after 48h exposure. Thus, there was no effect on $CD4^+$ T cell diameter after 48h exposure, n = 3. **(d)** Bar plot showing the average cell viability and standard error in percent, as determined by Via1-Cassette™ on a NucleoCounter® NC-200™ after 72h activation with CD3-CD28 activation beads. On average the cell viability of control exposed cells was 82.23 SE 1.62%, oleic acid exposed cells was 76.67 SE 7.61%, oleic acid + atorvastatin exposed cells was 78.60 SE 3.33%, oleic acid + CP-640186 exposed cells was 76.73 SE 2.20%, and oleic acid + atorvastatin + CP-640186 exposed cells was 75.53 SE 4.88% after 72h activation. Thus, there was no effect on $CD4^+$ T cell viability after 72h activation between the different conditions. However, the cells were slightly less viable after activation than before activation, n = 3. **(e)** Dot plot showing the average cell diameter and standard error in µm, as determined by Via1-Cassette™ on a NucleoCounter® NC-200™. On average the cell diameter of control exposed cells was 10.57 SE 0.15µm, oleic acid exposed cells was 10.17 SE 0.26µm, oleic acid + atorvastatin exposed cells was 10.10 SE 0.31µm, oleic acid + CP-640186 exposed cells was 10.17 SE 0.22µm, and oleic acid + atorvastatin + CP-640186 exposed cells was 9.87 SE 0.61µm after 72h activation. Thus, there was no effect on $CD4^+$ T cell diameter after 48h exposure. However, the cells were larger after activation than before activation as was expected, n = 3.

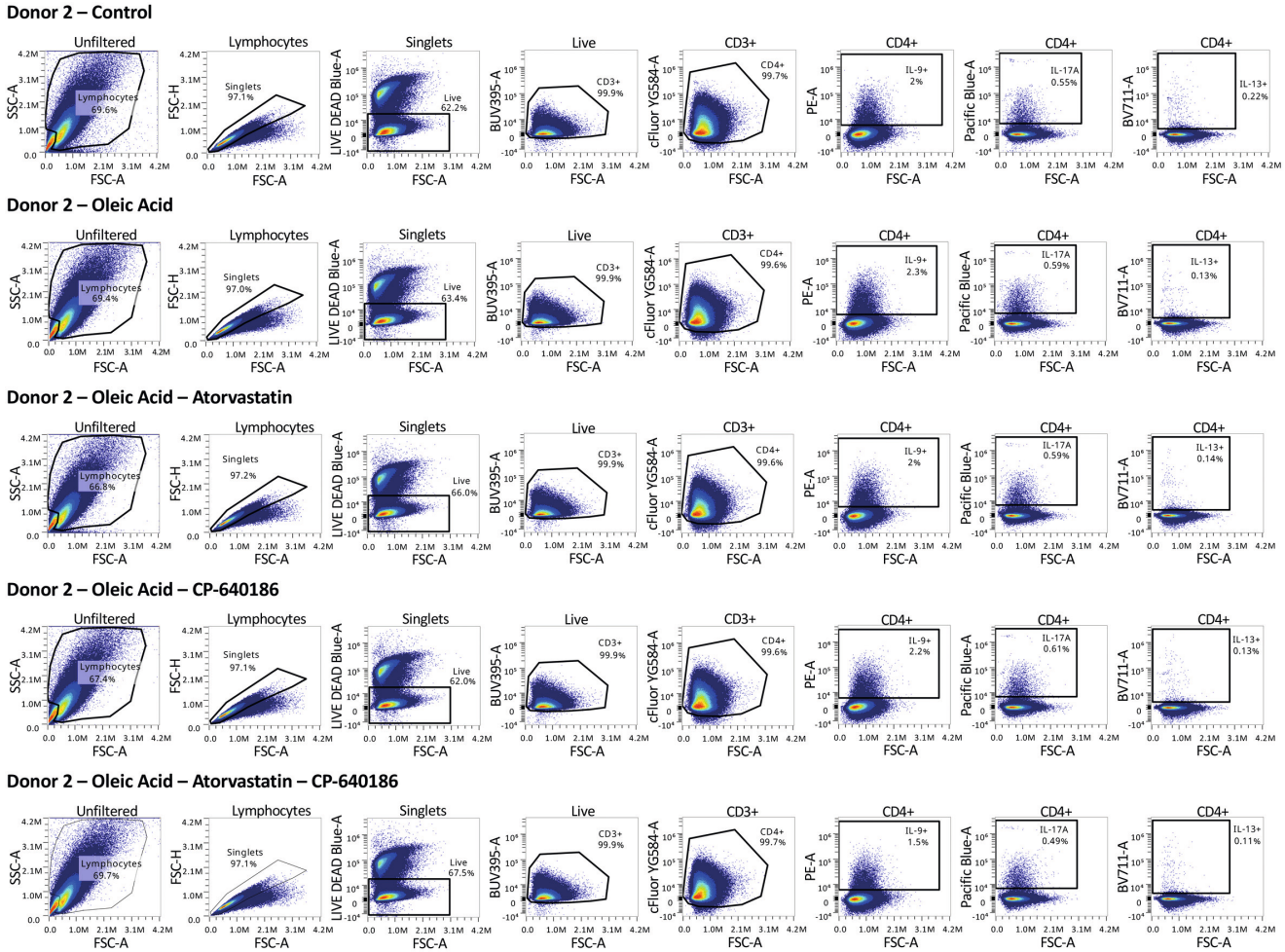

Supplemental Fig. 17 (partial) | Gating strategy for the inhibitor spectral cytometry analysis of activated CD4⁺ T cells pre-exposed to oleic acid with or without metabolic inhibitors, n = 3. Gating strategy is the same for all 3 donors analyzed and includes gates set for all markers measured. Gating strategy for 2 different donors and 5 different exposures are shown here, the rest of the figure can be found in the online supplement: https://doi.org/10.1016/j.isci.2024.109496.

Supplemental Table 1 | Changes in gene expression and $CD4^+$ T cell markers due to oleic acid pre-exposure.

Supplemental Table 1 | (a) (partial) Upregulated differentially expressed genes in order of significance along with their Ensembl ID, gene symbol, UniProt ID, base mean, log2 fold change, log2 fold change at 0.5h, log2 fold change at 3h, log2 fold change at 24h, log2 fold change at 48h, log2 fold change at 72h, p value, and adjusted p value (FDR). The log2FoldChange at specific time points were used to create the heatmap and the UniProt ID was used for Path-MAP in PathBank. Top 30 most significantly expressed genes are shown here, the rest of the table can be found in the online supplement: https://doi.org/10.1016/j.isci.2024.109496.

Order	Ensembl ID	Gene Symbol	UniProt	baseMean	log2FC	log2FC 0.5h	log2FC 3h	log2FC 24h	log2FC 48h	log2FC 72h	P value	P_{FDR}
1	ENSG00000110090	*CPT1A*	P50416	3804.649	-0.066	-0.067	2.669	2.897	3.095	3.228	0	0
2	ENSG00000178537	*SLC25A20*	O43772	931.641	0.064	0.062	2.254	1.491	1.662	1.715	0	0
3	ENSG00000072778	*ACADVL*	P49748	8010.624	0.057	0.057	0.270	0.739	0.791	0.875	5.190E-260	2.237E-256
4	ENSG00000167315	*ACAA2*	P42765	905.165	0.067	0.060	0.972	0.757	0.821	0.812	3.568E-206	1.153E-202
5	ENSG00000163162	*RNF149*	Q8NC42	5125.409	0.047	0.047	0.226	0.360	0.409	0.406	2.302E-111	5.955E-108
6	ENSG00000171503	*ETFDH*	Q16134	801.658	0.111	0.109	0.641	0.721	0.772	0.840	4.397E-97	9.477E-94
7	ENSG00000166575	*TMEM135*	Q86UB9	403.428	-0.053	-0.065	0.390	0.822	0.936	0.995	9.506E-82	1.756E-78
8	ENSG00000145860	*RNF145*	Q96MT1	5873.733	-0.112	-0.115	-0.176	0.379	0.421	0.361	9.517E-65	1.539E-61
9	ENSG00000143110	*C1orf162*	Q8NEQ5	2052.143	0.231	0.228	0.485	0.349	0.437	0.380	2.701E-60	3.881E-57
10	ENSG00000184602	*SNN*	O75324	2253.209	-0.096	-0.095	-0.036	0.351	0.416	0.356	4.913E-57	6.354E-54
11	ENSG00000167851	*CD300A*	Q9UGN4	573.914	0.102	0.105	0.381	0.443	0.555	0.498	1.443E-45	1.697E-42
12	ENSG00000147872	*PLIN2*	Q99541	1591.102	-0.005	-0.009	0.183	0.211	0.403	0.400	6.864E-41	7.397E-38
13	ENSG00000004799	*PDK4*	Q16654	5.514	3.381	3.071	4.328	5.433	4.714	3.357	8.302E-41	8.258E-38

[continued on next page]

Supplemental Table 1 *[continued]*

Order	Ensembl ID	Gene Symbol	UniProt	baseMean	log2FC	log2FC 0.5h	log2FC 3h	log2FC 24h	log2FC 48h	log2FC 72h	P value	P_{FDR}
14	ENSG00000122378	*PRXL2A*	Q9BRX8	387.115	0.148	0.151	0.090	0.303	0.383	0.445	6.621E-39	6.116E-36
15	ENSG00000072310	*SREBF1*	P36956	964.618	0.052	0.051	-0.319	0.301	0.527	0.665	2.790E-38	2.405E-35
16	ENSG00000172059	*KLF11*	O14901	578.566	0.199	0.193	0.469	0.787	0.829	0.740	2.566E-37	2.074E-34
17	ENSG00000111684	*LPCAT3*	Q6P1A2	720.001	0.004	-0.002	0.495	0.288	0.431	0.416	7.622E-34	5.798E-31
18	ENSG00000177479	*ARIH2*	O95376	6202.269	-0.008	-0.010	0.220	0.130	0.157	0.192	2.752E-28	1.977E-25
19	ENSG00000113161	*HMGCR*	P04035	2667.317	-0.037	-0.032	0.121	0.343	0.528	0.474	9.134E-28	6.217E-25
20	ENSG00000087157	*PGS1*	Q32NB8	2240.393	0.052	0.053	0.172	0.170	0.210	0.155	3.379E-26	2.185E-23
21	ENSG00000099194	*SCD*	O00767	452.316	-0.042	-0.025	0.353	0.633	1.341	1.301	6.064E-25	3.734E-22
22	ENSG00000278540	*ACACA*	Q13085	944.923	-0.093	-0.093	-0.079	0.329	0.387	0.313	1.338E-23	7.864E-21
23	ENSG00000153395	*LPCAT1*	Q8NF37	3186.515	-0.058	-0.059	-0.054	0.298	0.316	0.270	2.971E-23	1.671E-20
24	ENSG00000164211	*STARD4*	Q96DR4	712.106	0.016	0.015	0.419	0.324	0.516	0.496	3.675E-23	1.980E-20
25	ENSG00000104823	*ECH1*	Q13011	1348.019	0.115	0.108	0.288	0.245	0.310	0.324	4.264E-23	2.206E-20
26	ENSG00000198911	*SREBF2*	Q12772	8317.191	-0.009	-0.009	0.132	0.227	0.471	0.408	1.458E-21	6.985E-19
27	ENSG00000186480	*INSIG1*	O15503	2865.535	-0.010	-0.007	0.169	0.249	0.531	0.554	4.234E-21	1.956E-18
28	ENSG00000130164	*LDLR*	P01130	2737.906	-0.051	-0.055	0.327	0.448	0.989	0.885	4.431E-21	1.976E-18
29	ENSG00000112972	*HMGCS1*	Q01581	1968.928	-0.021	-0.022	0.225	0.313	0.519	0.424	9.547E-21	4.115E-18
30	ENSG00000116133	*DHCR24*	Q15392	1436.170	-0.078	-0.078	0.216	0.446	0.860	0.715	5.054E-20	2.108E-17

Supplemental Table 1 | (b) (partial) Downregulated differentially expressed genes in order of significance along with their Ensembl ID, gene symbol, UniProt ID, base mean, log2 fold change, log2 fold change at 0.5h, log2 fold change at 3h, log2 fold change at 24h, log2 fold change at 48h, log2 fold change at 72h, p value, and adjusted p value (FDR). The log2FoldChange at specific time points were used to create the heatmap and the UniProt ID was used for Path-MAP in PathBank. Top 30 most significantly expressed genes are shown here, the rest of the table can be found in the online supplement: https://doi.org/10.1016/j.isci.2024.109496.

Order	Ensembl ID	Gene Symbol	UniProt	baseMean	log2FC	log2FC 0.5h	log2FC 3h	log2FC 24h	log2FC 48h	log2FC 72h	P value	P_{FDR}
1	ENSG00000125637	*PSD4*	Q8NDX1	7753.592	0.002	0.003	-0.066	-0.213	-0.215	-0.294	2.682E-22	1.334E-19
2	ENSG00000166913	*YWHAB*	P31946	16988.864	-0.006	-0.008	0.000	-0.137	-0.104	-0.109	1.123E-15	3.459E-13
3	ENSG00000074370	*ATP2A3*	Q93084	8314.894	0.027	0.027	-0.063	-0.187	-0.189	-0.194	1.915E-13	4.586E-11
4	ENSG00000167460	*TPM4*	P67936	4348.318	0.003	0.001	0.049	-0.152	-0.189	-0.157	5.491E-13	1.255E-10
5	ENSG00000158435	*CNOT11*	Q9UKZ1	3021.238	0.019	0.019	-0.065	-0.123	-0.121	-0.129	8.453E-12	1.562E-09
6	ENSG00000119714	*GPR68*	Q15743	556.312	-0.080	-0.079	-0.236	-0.283	-0.362	-0.439	3.278E-11	5.729E-09
7	ENSG00000158856	*DMTN*	Q08495	527.740	0.025	0.026	-0.050	-0.249	-0.233	-0.217	2.851E-10	4.552E-08
8	ENSG00000102144	*PGK1*	P00558	9599.530	0.019	0.015	-0.008	-0.126	-0.099	-0.101	4.516E-10	6.876E-08
9	ENSG00000108654	*DDX5*	P17844	53321.550	-0.012	-0.013	-0.051	-0.119	-0.172	-0.207	4.519E-10	6.876E-08
10	ENSG00000183688	*RFLNB*	Q8N5W9	4685.097	0.010	0.009	-0.082	-0.162	-0.179	-0.241	4.641E-10	6.979E-08
11	ENSG00000131236	*CAP1*	Q01518	12576.054	-0.027	-0.029	-0.067	-0.137	-0.099	-0.100	1.042E-09	1.481E-07
12	ENSG00000172215	*CXCR6*	O00574	270.089	0.046	0.045	-0.094	-0.364	-0.386	-0.621	1.587E-09	2.147E-07
13	ENSG00000115091	*ACTR3*	P61158	8483.351	-0.001	-0.004	0.005	-0.114	-0.097	-0.140	2.746E-09	3.586E-07
14	ENSG00000070831	*CDC42*	P60953	9857.088	-0.016	-0.018	-0.028	-0.075	-0.109	-0.137	2.997E-09	3.876E-07

[continued on next page]

Supplemental Table 1 | (b) (partial) *[continued]*

Order	Ensembl ID	Gene Symbol	UniProt	baseMean	log2FC	log2FC 0.5h	log2FC 3h	log2FC 24h	log2FC 48h	log2FC 72h	P value	P_{FDR}
15	ENSG00000102158	*MAGT1*	Q9H0U3	1961.500	-0.003	-0.004	0.025	-0.095	-0.144	-0.173	3.736E-09	4.784E-07
16	ENSG00000142875	*PRKACB*	P22694	6088.499	-0.016	-0.018	-0.078	-0.080	-0.147	-0.195	4.829E-09	6.063E-07
17	ENSG00000160791	*CCR5*	P51681	445.160	-0.016	-0.015	-0.063	-0.275	-0.288	-0.297	5.118E-09	6.364E-07
18	ENSG00000075624	*ACTB*	P60709	90701.100	0.062	0.055	0.094	-0.176	-0.152	-0.168	1.135E-08	1.346E-06
19	ENSG00000197043	*ANXA6*	P08133	12140.502	0.030	0.031	-0.070	-0.201	-0.154	-0.139	1.230E-08	1.446E-06
20	ENSG00000167986	*DDB1*	Q16531	7313.881	-0.008	-0.008	-0.023	-0.111	-0.073	-0.088	1.322E-08	1.527E-06
21	ENSG00000044574	*HSPA5*	P11021	10108.431	-0.002	-0.004	0.049	-0.056	-0.125	-0.189	2.223E-08	2.457E-06
22	ENSG00000223501	*VPS52*	Q8N1B4	3308.603	0.010	0.010	-0.021	-0.081	-0.082	-0.119	3.427E-08	3.724E-06
23	ENSG00000182944	*EWSR1*	Q01844	13959.893	0.022	0.022	-0.024	-0.090	-0.102	-0.098	4.940E-08	5.237E-06
24	ENSG00000143549	*TPM3*	P06753	12626.672	0.017	0.014	-0.025	-0.093	-0.066	-0.079	5.965E-08	6.272E-06
25	ENSG00000072818	*ACAP1*	Q15027	14390.199	0.055	0.054	-0.039	-0.050	-0.112	-0.126	6.646E-08	6.821E-06
26	ENSG00000128340	*RAC2*	P15153	10806.212	0.042	0.040	-0.074	-0.139	-0.139	-0.162	9.966E-08	9.914E-06
27	ENSG00000198176	*TFDP1*	Q14186	1798.488	-0.028	-0.028	-0.010	-0.144	-0.137	-0.187	1.484E-07	1.443E-05
28	ENSG00000143870	*PDIA6*	Q15084	3458.824	0.043	0.040	-0.002	-0.027	-0.096	-0.185	2.079E-07	1.948E-05
29	ENSG00000138071	*ACTR2*	P61160	15672.838	-0.061	-0.063	0.022	-0.108	-0.107	-0.133	2.356E-07	2.176E-05
30	ENSG00000120798	*NR2C1*	P13056	1981.007	-0.016	-0.016	0.063	0.054	-0.073	-0.156	3.371E-07	3.027E-05

Supplemental Table 1 | (c) Transcription factors, extracellular markers, and intracellular markers measured in non-activated $CD4^+$ T cell after pre-exposure to oleic acid. Values are shown as a percent of the parent, n = 8.

Donor	Exposure	$CD127^{low}$ $CD25^{hi}$ $FoxP3^+$	$CD25^+$	$PD1^+$	$CTLA4^+$	$CD27^+$	$CD38^+$	$Tbet^+$	$GATA3^+$	$IL\text{-}4^+$	$IL\text{-}5^+$	$IL\text{-}13^+$	$IL\text{-}9^+$	$IL\text{-}17A^+$	$IL\text{-}21^+$	$IL\text{-}22^+$	$TNF\alpha^+$	$IFN\gamma^+$	$IL\text{-}10^+$
1	Control	0.619	4.210	1.010	28.10	0.934	38.90	0.271	0.059	0.047	0.017	0.057	0.103	0.160	0.033	0.016	0.200	1.070	0.021
1	Oleic Acid	0.501	5.540	1.980	30.10	0.925	42.10	0.869	0.103	0.069	0.057	0.087	0.284	0.193	0.070	0.041	0.225	1.530	0.056
2	Control	0.380	1.750	0.401	42.60	0.104	33.40	0.058	0.027	0.046	0.026	0.026	0.034	0.257	0.043	0.082	1.130	1.360	0.027
2	Oleic Acid	0.195	1.520	0.331	42.60	0.041	29.90	0.056	0.011	0.042	0.027	0.020	0.030	0.264	0.051	0.070	1.080	1.580	0.028
3	Control	0.903	5.080	2.620	39.30	1.730	31.40	0.813	0.147	0.068	0.103	0.049	0.242	0.178	0.159	0.073	0.812	3.650	0.102
3	Oleic Acid	0.437	2.950	0.747	38.90	0.888	29.40	0.072	0.016	0.045	0.072	0.031	0.028	0.184	0.064	0.027	0.872	4.220	0.058
4	Control	0.786	2.180	1.340	42.40	0.484	27.50	0.051	0.023	0.045	0.070	0.036	0.016	0.121	0.094	0.031	0.748	4.390	0.061
4	Oleic Acid	0.445	1.890	1.130	43.90	0.258	24.90	0.048	0.019	0.040	0.075	0.024	0.017	0.099	0.125	0.038	0.845	5.490	0.096
5	Control	2.350	5.090	0.646	12.20	0.166	47.80	0.011	0.024	0.015	0.002	0.030	0.010	0.081	0.041	0.005	0.007	0.103	0.005
5	Oleic Acid	2.280	5.350	0.547	12.50	0.099	47.90	0.035	0.022	0.020	0.009	0.020	0.014	0.084	0.055	0.003	0.013	0.088	0.005
6	Control	7.770	7.380	1.780	23.00	0.284	37.40	0.023	0.036	0.016	0.007	0.066	0.012	0.075	0.038	0.006	0.011	0.231	0.005
6	Oleic Acid	6.210	7.120	1.640	22.80	0.255	37.60	0.018	0.024	0.021	0.049	0.051	0.006	0.117	0.047	0.003	0.007	0.240	0.003
7	Control	0.798	1.310	0.638	13.40	0.227	51.10	0.016	0.024	0.020	0.002	0.015	0.010	0.086	0.044	0.007	0.005	0.030	0.003
7	Oleic Acid	0.452	1.210	0.572	13.00	0.142	51.20	0.033	0.017	0.019	0.009	0.018	0.010	0.056	0.039	0.008	0.012	0.028	0.004
8	Control	4.540	5.990	1.740	16.30	1.800	38.80	0.039	0.021	0.020	0.009	0.022	0.013	0.080	0.042	0.005	0.011	0.067	0.006
8	Oleic Acid	3.800	6.230	1.500	16.40	1.450	39.70	0.039	0.019	0.018	0.015	0.025	0.015	0.079	0.049	0.004	0.014	0.075	0.004

Supplemental Table 1 | (d) Transcription factors, extracellular markers, and intracellular markers measured in activated $CD4^+$ T cell after pre-exposure to oleic acid. The concentration of oleic acid was 30µg/mL. Values are shown as a percent of the parent, n = 8.

Donor	Exposure	$CD127^{low}$ $CD25^{hi}$ $FoxP3^+$	$CD25^+$	$PD1^+$	$CTLA4^+$	$CD27^+$	$CD38^+$	$Tbet^+$	$GATA3^+$	$IL\text{-}4^+$	$IL\text{-}5^+$	$IL\text{-}13^+$	$IL\text{-}9^+$	$IL\text{-}17A^+$	$IL\text{-}21^+$	$IL\text{-}22^+$	$TNF\alpha^+$	$IFN\gamma^+$	$IL\text{-}10^+$
1	Control	7.120	72.20	60.40	66.50	14.60	52.30	0.421	0.629	0.018	0.023	0.059	0.680	0.292	0.208	0.117	0.648	2.770	0.124
1	Oleic Acid	6.960	81.40	67.10	70.30	14.00	54.70	0.427	0.930	0.023	0.037	0.089	1.440	0.595	0.362	0.148	1.040	3.840	0.203
2	Control	4.560	62.80	55.30	80.30	2.140	54.20	0.213	1.470	0.041	0.055	0.067	0.595	0.302	0.520	0.219	2.640	4.010	0.138
2	Oleic Acid	5.980	67.50	58.00	80.30	1.440	51.40	0.244	1.780	0.019	0.097	0.115	0.889	0.389	0.828	0.304	2.610	4.600	0.150
3	Control	9.610	68.10	60.70	66.90	4.580	58.40	0.513	1.020	0.019	0.039	0.094	0.563	0.361	0.322	0.189	1.730	8.310	0.144
3	Oleic Acid	11.20	69.80	60.50	68.10	2.760	53.50	0.807	1.470	0.066	0.078	0.219	1.110	0.633	0.438	0.180	2.160	8.850	0.213
4	Control	6.860	59.90	54.20	71.80	1.850	53.00	0.415	0.698	0.022	0.104	0.158	1.040	0.181	0.475	0.104	1.740	13.20	0.151
4	Oleic Acid	8.570	60.20	53.20	69.70	1.400	50.10	0.539	0.905	0.018	0.119	0.320	2.010	0.322	0.743	0.139	2.100	13.40	0.217
5	Control	6.270	79.10	66.60	80.00	6.090	49.90	1.690	1.850	0.039	0.103	0.047	2.110	0.350	0.217	0.032	0.610	1.530	0.130
5	Oleic Acid	7.070	79.60	68.10	79.30	5.580	45.30	1.540	3.320	0.046	0.134	0.077	3.360	0.456	0.250	0.032	0.682	1.670	0.144
6	Control	9.420	85.40	76.70	80.00	2.250	60.90	1.490	1.480	0.093	0.244	0.245	3.060	1.250	0.585	0.118	1.580	3.100	0.245
6	Oleic Acid	10.50	85.30	75.10	79.50	1.660	52.90	1.090	1.390	0.080	0.245	0.199	3.660	1.410	0.544	0.115	1.630	2.810	0.250
7	Control	3.660	84.40	75.80	88.30	15.30	72.40	0.726	0.952	0.035	0.146	0.051	0.559	0.186	0.247	0.030	0.570	0.703	0.121
7	Oleic Acid	4.470	80.90	70.30	86.70	12.70	63.90	0.725	1.370	0.045	0.168	0.077	0.736	0.205	0.229	0.030	0.776	0.823	0.112
8	Control	12.00	85.30	79.70	82.20	4.720	72.80	2.780	0.434	0.135	0.332	0.264	1.960	0.868	0.594	0.124	1.640	4.200	0.392
8	Oleic Acid	13.30	85.10	79.30	82.20	3.550	70.00	2.690	0.450	0.134	0.390	0.378	2.690	1.090	0.600	0.132	1.580	4.490	0.327

Supplemental Table 1 | (e) Coexpression analysis of various $CD4^+$ T cell markers in activated $CD4^+$ T cells after pre-exposure to oleic acid. The concentration of oleic acid was 30µg/mL. Values are shown as a percent of the parent, n = 8.

Donor	Exposure	$IFNy^+$ OR TNF^+	$IFNy^+$ AND $TNFα^+$	$IL\text{-}5^+$ OR $IL\text{-}4^+$ OR $IL\text{-}13^+$	$IL\text{-}13^+$ AND $IL\text{-}4^+$ AND $IL\text{-}5^+$	$IL\text{-}5^+$ OR $IL\text{-}4^+$ OR $IL\text{-}13^+$ AND $IL\text{-}9^+$	$PD1^+$ AND $CTLA4^+$	$PD1^+$ OR $CTLA4^+$
1	Control	3.22	0.20	0.09	0	0.020	44.9	82.1
1	Oleic Acid	4.54	0.34	0.15	0	0.020	50.2	87.3
2	Control	5.89	0.76	0.16	0	0.005	45.2	90.3
2	Oleic Acid	6.32	0.89	0.22	0.001	0.020	48.2	90.1
3	Control	9.30	0.73	0.15	0	0.006	43.6	84.1
3	Oleic Acid	10.1	0.95	0.35	0	0.010	43.4	85.1
4	Control	14.0	0.96	0.27	0.002	0.020	40.3	85.7
4	Oleic Acid	14.4	1.09	0.42	0	0.040	39.3	83.7
5	Control	2.03	0.10	0.18	0.0009	0.010	55.1	91.4
5	Oleic Acid	2.22	0.13	0.23	0	0.040	56.1	91.4
6	Control	4.33	0.34	0.50	0.004	0.050	64.0	92.7
6	Oleic Acid	4.07	0.36	0.45	0.001	0.040	62.5	92.1
7	Control	1.20	0.07	0.22	0	0.007	68.4	95.6
7	Oleic Acid	1.48	0.12	0.27	0.0009	0.007	62.5	94.5
8	Control	5.44	0.39	0.64	0.003	0.030	67.4	94.4
8	Oleic Acid	5.66	0.42	0.77	0.001	0.060	67.3	94.2

Supplemental Table 1 | (e) continued

Donor	Exposure	PD1$^+$ AND CTLA4$^+$ AND CD38$^+$	PD1$^+$ AND CTLA4$^+$ AND CD38$^+$ AND IFNy$^+$ OR TNFα$^+$	PD1$^+$ AND CTLA4$^+$ AND CD38$^+$ AND IL-5$^+$ OR IL-4$^+$ OR IL-13$^+$	PD1$^+$ AND CTLA4$^+$ AND CD38$^+$ AND IL-9$^+$	IFNy$^+$ OR TNFα$^+$ AND IL-9$^+$
1	Control	33.4	1.73	0.05	0.35	0.16
1	Oleic Acid	34.2	2.32	0.07	0.72	0.32
2	Control	38.2	3.76	0.10	0.40	0.21
2	Oleic Acid	36.9	3.78	0.12	0.54	0.31
3	Control	37.7	5.88	0.08	0.44	0.19
3	Oleic Acid	33.6	5.66	0.21	0.68	0.31
4	Control	34.1	7.84	0.18	0.63	0.6
4	Oleic Acid	31.9	7.78	0.28	1.25	1.12
5	Control	36.2	0.84	0.08	0.84	0.24
5	Oleic Acid	32.9	0.80	0.09	1.00	0.40
6	Control	45.3	2.56	0.27	1.62	0.47
6	Oleic Acid	38.2	2.00	0.19	1.43	0.53
7	Control	60.3	0.87	0.16	0.42	0.05
7	Oleic Acid	51.0	0.94	0.18	0.48	0.09
8	Control	58.5	4.15	0.46	1.53	0.40
8	Oleic Acid	56.4	4.17	0.5	2.02	0.46

Supplemental Table 1 | (f) Transcription factors, extracellular markers, and intracellular markers measured in non-activated $CD4^+$ T cell after pre-exposure to oleic acid. The concentration of oleic acid was 28µg/mL. Values are shown as a percent of the parent, n = 8. In order to calculate the fold change of $CD127^{low}CD25^{hi}FoxP3^+$ for D10, D11 and D12 add a "1" to each value for that donor.

Donor	Exposure	$CD127^{low}$ $CD25^{hi}$ $FoxP3^+$	$CD25^+$	$PD1^+$	$CTLA4^+$	$CD27^+$	$CD38^+$	$Tbet^+$	$GATA3^+$	$IL\text{-}4^+$	$IL\text{-}13^+$	$IL\text{-}9^+$	$IL\text{-}17A^+$	$IL\text{-}21^+$	$IL\text{-}22^+$	$TNF\alpha^+$	$IFN\gamma^+$	$IL\text{-}10^+$
10	Control	0.000	2.210	0.470	22.30	2.050	7.250	0.002	0.041	0.003	0.002	0.006	0.195	0.022	0.011	5.410	0.009	0.003
10	Oleic Acid	0.046	2.560	0.512	24.80	1.830	8.020	0.003	0.020	0.005	0.002	0.002	0.216	0.024	0.014	7.120	0.005	0.004
11	Control	0.000	2.000	0.240	23.00	0.328	8.700	0.007	0.026	0.003	0.001	0.006	0.573	0.023	0.037	5.390	0.008	0.002
11	Oleic Acid	0.000	2.750	0.316	24.30	0.459	10.80	0.002	0.038	0.002	0.002	0.007	0.653	0.028	0.038	7.510	0.010	0.005
12	Control	0.000	1.150	0.646	16.20	0.656	8.410	0.008	0.006	0.003	0.001	0.002	0.120	0.019	0.020	3.810	0.008	0.002
12	Oleic Acid	0.000	1.690	0.718	22.20	0.439	7.160	0.018	0.005	0.003	0.001	0.005	0.155	0.030	0.023	5.620	0.007	0.004
13	Control	41.70	3.160	0.790	47.50	0.387	1.890	0.021	0.009	0.008	0.004	0.094	0.920	0.026	0.289	21.20	0.116	0.011
13	Oleic Acid	45.00	3.230	0.741	47.30	0.324	1.890	0.032	0.015	0.010	0.004	0.103	1.020	0.031	0.359	19.80	0.378	0.011
14	Control	21.90	2.040	0.217	29.10	0.312	6.550	0.019	0.011	0.003	0.002	0.100	0.192	0.030	0.346	11.30	0.057	0.006
14	Oleic Acid	16.20	2.360	0.208	30.80	0.228	7.080	0.021	0.018	0.002	0.005	0.095	0.226	0.027	0.273	13.10	0.066	0.007
15	Control	31.20	1.480	0.095	44.10	0.569	4.830	0.013	0.017	0.005	0.002	0.072	0.146	0.023	0.239	5.550	0.049	0.005
15	Oleic Acid	27.50	1.460	0.095	43.30	0.500	4.310	0.017	0.017	0.005	0.003	0.077	0.155	0.027	0.210	5.860	0.110	0.005
16	Control	11.80	2.930	0.226	29.20	1.480	7.880	0.033	0.018	0.031	0.006	0.037	0.271	0.051	0.034	6.090	0.023	0.004
16	Oleic Acid	9.710	2.720	0.246	33.30	0.660	6.880	0.025	0.009	0.019	0.002	0.021	0.407	0.027	0.031	7.590	0.016	0.003
17	Control	5.990	4.520	0.552	21.60	0.537	11.70	0.280	0.018	0.021	0.006	0.022	0.808	0.032	0.027	11.30	0.015	0.004
17	Oleic Acid	7.450	4.520	0.542	26.40	0.382	12.30	0.254	0.015	0.021	0.004	0.025	0.992	0.029	0.033	15.60	0.020	0.002

Supplemental Table 1 | (g) Transcription factors, extracellular markers, and intracellular markers measured in activated $CD4^+$ T cell after pre-exposure to oleic acid. The concentration of oleic acid was 28µg/mL. Values are shown as a percent of the parent, n = 8. In order to calculate the fold change of $CD127^{low}CD25^{hi}FoxP3^+$ for D11 and D12 add a "1" to each value for that donor.

Donor	Exposure	$CD127^{low}$ $CD25^{hi}$ $FoxP3^+$	$CD25^+$	$PD1^+$	$CTLA4^+$	$CD27^+$	$CD38^+$	$Tbet^+$	$GATA3^+$	$IL\text{-}4^+$	$IL\text{-}13^+$	$IL\text{-}9^+$	$IL\text{-}17A^+$	$IL\text{-}21^+$	$IL\text{-}22^+$	$TNF\alpha^+$	$IFN\gamma^+$	$IL\text{-}10^+$
10	EtOH	0.003	60.60	58.10	59.50	10.40	53.40	0.287	0.700	0.003	0.013	0.831	0.394	3.380	0.069	1.540	2.680	0.258
10	Oleic Acid	0.001	59.90	55.00	55.90	7.230	45.90	0.341	1.060	0.003	0.009	0.986	0.319	2.750	0.044	0.967	1.860	0.160
11	EtOH	0.000	64.90	56.20	51.90	8.930	50.90	0.349	0.840	0.008	0.016	1.190	0.389	2.510	0.079	1.270	1.370	0.188
11	Oleic Acid	0.001	62.20	52.30	52.10	7.220	46.40	0.624	1.300	0.009	0.027	1.680	0.420	2.610	0.082	1.700	1.960	0.213
12	EtOH	0.000	64.20	57.80	69.80	14.20	53.50	0.370	0.613	0.003	0.030	0.816	0.133	2.580	0.082	1.400	1.890	0.123
12	Oleic Acid	0.002	63.50	54.20	65.20	9.220	49.10	0.435	1.000	0.004	0.024	1.190	0.137	2.240	0.069	0.896	2.040	0.134
13	EtOH	6.680	80.00	71.10	61.00	4.350	65.60	1.980	2.590	0.013	0.021	3.340	1.130	1.360	0.845	7.170	8.580	0.612
13	Oleic Acid	6.280	77.20	68.20	62.10	4.760	62.70	2.020	3.480	0.024	0.035	3.800	1.030	1.240	0.848	6.550	9.090	0.738
14	EtOH	5.560	72.50	61.60	62.90	6.150	61.40	1.020	1.220	0.010	0.034	1.030	0.596	1.000	0.658	6.830	4.720	0.801
14	Oleic Acid	5.400	71.20	60.00	59.70	5.690	57.70	0.927	2.190	0.014	0.036	1.170	0.616	0.905	0.615	4.700	4.540	0.764
15	EtOH	3.130	72.60	61.50	67.50	13.60	65.70	1.100	5.310	0.016	0.038	0.522	0.181	0.803	0.325	1.800	2.640	0.431
15	Oleic Acid	3.430	73.80	62.10	62.60	11.90	66.20	1.480	6.490	0.019	0.046	0.700	0.196	0.764	0.379	1.550	2.560	0.493
16	EtOH	3.810	86.60	77.30	70.50	18.70	71.00	1.510	4.780	0.205	0.240	0.402	0.507	0.571	0.143	2.020	0.859	0.047
16	Oleic Acid	4.840	82.40	70.90	64.00	13.80	59.00	1.030	4.820	0.158	0.232	0.574	0.546	0.372	0.140	1.670	0.669	0.042
17	EtOH	4.030	84.30	66.30	52.70	7.390	71.10	7.480	0.292	0.154	0.172	1.740	1.540	0.870	0.188	17.10	8.240	0.043
17	Oleic Acid	4.940	79.00	57.60	50.90	4.700	61.60	8.920	0.483	0.100	0.179	2.440	1.430	0.736	0.131	16.00	8.890	0.049

Supplemental Table 1 | (h) Intracellular markers measured in activated $CD4^+$ T cell after pre-exposure either oleic acid, oleic acid + atorvastatin, oleic acid + CP-640186, or oleic acid + atorvastatin + CP-640186. The concentration of oleic acid was 30µg/mL, atorvastatin was 10µM, and CP-640186 was 20µM. The donor numbers are labeled respectively of the donors used in the previous experiments. Values are shown as a percent of the parent, n = 3.

Donor	Exposure	Inhibitor	IL-9$^+$	IL-17A$^+$	IL-13$^+$
2	Control	None	2.000	0.555	0.222
2	Oleic Acid	None	2.280	0.588	0.127
2	Oleic Acid	Atorvastatin	2.030	0.585	0.138
2	Oleic Acid	CP-640186	2.170	0.615	0.126
2	Oleic Acid	Atorvastatin + CP-640186	1.480	0.486	0.115
5	Control	None	2.630	0.526	0.103
5	Oleic Acid	None	3.870	0.683	0.136
5	Oleic Acid	Atorvastatin	2.560	0.528	0.080
5	Oleic Acid	CP-640186	2.250	0.659	0.106
5	Oleic Acid	Atorvastatin + CP-640186	1.840	0.580	0.106
6	Control	None	4.630	1.950	0.287
6	Oleic Acid	None	5.520	2.480	0.365
6	Oleic Acid	Atorvastatin	4.020	1.970	0.271
6	Oleic Acid	CP-640186	3.350	1.800	0.283
6	Oleic Acid	Atorvastatin + CP-640186	2.750	1.470	0.317

CHAPTER 4

EPA induces anti-inflammatory transcriptomics in T cells, implicating a triglyceride-independent pathway for cardiovascular risk reduction

Nathalie A. Reilly[1,2], Koen F. Dekkers[1], Jeroen Molenaar[1], Sinthuja Arumugam[1], Thomas B. Kuipers[1,3], Yavuz Ariyurek[4], Marten A. Hoeksema[5], J. Wouter Jukema[2,6], and Bastiaan T. Heijmans[1]

[1] *Molecular Epidemiology, Department of Biomedical Data Sciences, Leiden, the Netherlands.*
[2] *Department of Cardiology, Leiden, the Netherlands.*
[3] *Sequencing Analysis Support Core, Department of Biomedical Data Sciences, Leiden, the Netherlands.*
[4] *Leiden Genome Technology Center, Department of Human Genetics, Leiden, The Netherlands.*
[5] *Department of Medical Biochemistry, Amsterdam UMC, location University of Amsterdam, The Netherlands.*
[6] *Netherlands Heart Institute, Utrecht, The Netherlands.*

BioRxiv, (2024).
Accepted in JACC: Basic to Translational Science

Abstract

Background: A twice-daily dose of highly purified eicosapentaenoic acid (EPA) reduces the risk of atherosclerotic cardiovascular disease among patients with high triglycerides and either known cardiovascular disease or those at high risk for developing it. However, the process by which EPA exerts its beneficial effects remains poorly understood.

Objectives: We show that EPA can induce an anti-inflammatory transcriptional profile in non-activated $CD4^+$ T cells.

Methods: Non-activated $CD4^+$ T cells from 8 different donors were exposed to 100μM EPA, oleic acid, palmitic acid, or control. RNA and ATAC-sequencing were performed after 48h of exposure to determine changes in the transcriptomic and epigenetic landscape of the exposed cells as compared to control.

Results: We find that EPA-exposed $CD4^+$ T cells downregulate immune response-related genes, such as *HLA-DRA*, *CD69*, and *IL2RA*, while upregulating genes involved in oxidative stress prevention, such as *NQO1*. Furthermore, transcription footprint analysis based on ATAC-sequencing reveals downregulation of GATA3 and PU.1, key transcription factors in T_H2 and T_H9 differentiation, and upregulation of REV-ERB, an antagonist of T_H17 differentiation. By in parallel examining T cell responses to oleic acid, a monounsaturated fatty acid, and palmitic acid, a saturated fatty acid, we find that both the intensity of the transcriptomic response and the involvement of anti-inflammatory pathways is highly specific for EPA.

Conclusions: Thus, EPA can induce an anti-inflammatory transcriptomic landscape in $CD4^+$ T cells, a process that may contribute to the unexpectedly strong beneficial effects of EPA on the risk of atherosclerotic cardiovascular disease in clinical trials.

Highlights

- The mechanism by which EPA reduces the risk of ASCVD in clinical trials remains unclear.
- EPA can induce an anti-inflammatory transcriptomic landscape in non-activated $CD4^+$ T cells *in vitro*.
- T cell reactions to palmitic and oleic acid reveal EPA's unique anti-inflammatory transcriptomic response
- Examining T-cells during IPE interventions may reveal insights into EPA's benefits independent of triglyceride reduction.

Graphical abstract

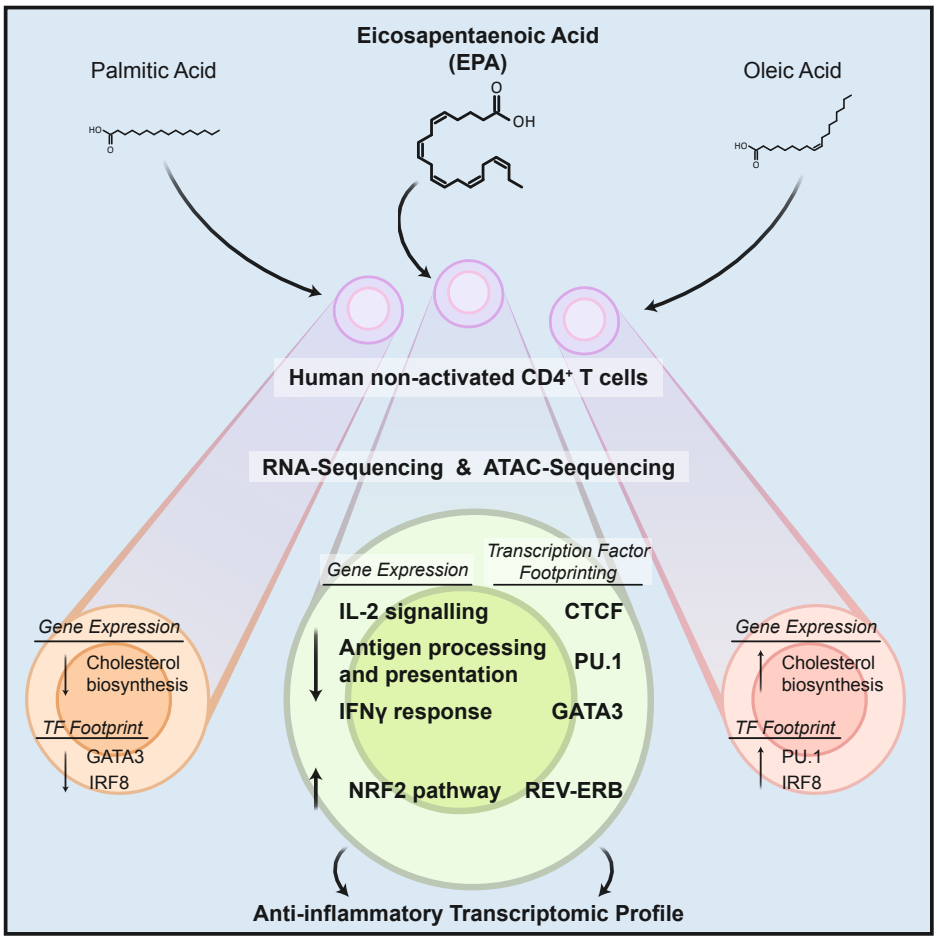

Introduction

The risk of atherosclerotic cardiovascular disease (ASCVD) persists despite therapies that effectively control blood cholesterol levels including statins and PCSK9 inhibitors[1-3]. This residual risk has been attributed, in part, to elevated triglyceride levels in blood[4]. Nevertheless, most triglyceride influencing therapies, such as fibrates or niacin, have little cardiovascular benefit[5-9]. However, there is one triglyceride lowering drug that was found to strongly reduce ASCVD risk, namely, icosapent ethyl (IPE), which in the body is metabolized to eicosapentaenoic acid (EPA), a polyunsaturated fatty acid. The REDUCE-IT trial showed that patients who received 4g of IPE administered as 2g twice daily was superior to placebo in reducing triglycerides, cardiovascular events, and cardiovascular death among patients with high triglycerides and either known cardiovascular disease or those at high risk for developing it, and who were already on statin therapy with relatively well-controlled low density lipoprotein (LDL) levels[10]. The results of the trial and its interpretation has been much debated in literature[11, 12]. In particular, it remains largely unknown how EPA exerts its beneficial effects, and only limited studies have been carried out in model membranes or by examining whole blood[13-15].

Atherosclerosis is regarded as a lipid-driven immune disease[16]. As such, the majority of immune cells in the atherosclerotic plaque are T cells, of which half are $CD4^+$[17, 18]. Furthermore, $CD4^+$ T cells aggravate atherosclerosis in established mouse models[19, 20]. Therefore, the study of $CD4^+$ T cells is a promising route to further understanding ASCVD and investigating how EPA can influence these cells can indicate a potential mechanism underlying the beneficial effects of EPA on atherosclerosis. Interestingly, EPA was suggested to have anti-inflammatory properties as indicated by a reduction in $CD4^+$ T cell proliferation, decreased differentiation towards T helper 1 (T_H1) and T helper 17 (T_H17), and increased or no effect on differentiation towards T helper 2 (T_H2) and T regulatory (T_{reg}) cells[21]. However, these studies were largely carried out in mouse models, or investigated *in vitro* during T cell activation, under polarizing conditions, or by measuring general T cell markers[22-28]. Thus, the effects of EPA on T cells remain incompletely understood and, in particular, it is unknown whether EPA can affect human $CD4^+$ T cells in a non-activated state, as they occur in the circulation and where the primary interaction with EPA takes place.

We aimed to further elucidate the effects of EPA on $CD4^+$ T cells by performing transcriptomic analysis on non-activated exposed cells. Furthermore, we assessed the specificity of the effects of EPA by exposing cells to two other fatty acids of different saturation, oleic acid (OA), a monounsaturated fatty acid, and palmitic acid (PA), a saturated fatty acid. To do so, we performed RNA and ATAC-sequencing on non-activated $CD4^+$ T cells exposed to EPA, OA, PA, or control after 48h exposure. We show that EPA leads to a marked downregulation of many anti-inflammatory genes in non-activated $CD4^+$ T cells as compared to control. The pronounced and specific effects on the transcriptomics landscape contrasted with the relatively modest effects of OA and PA.

Methods

Peripheral blood $CD4^+$ T cell isolation and culture conditions

$CD4^+$ T cell isolation and fatty acid exposure model were based on our previously described *in vitro* model with minor changes[29]. To obtain non-activated $CD4^+$ T cells, peripheral blood mononuclear cells (PBMCs) were isolated from 8 different buffy coats of anonymous blood bank donors (Sanquin, Amsterdam, The Netherlands) by Ficoll paque (Apotheek LUMC, 97902861) gradient centrifugation. All donors provided written informed consent in accordance with the protocol of the local institutional review board, the Medical Ethics committee of Sanquin blood supply in accordance with the Declaration of Helsinki. The sex of the cells could not be determined due to the anonymity of the donors. However, RNA sequencing showed that, of 8 donors sequenced, 6 were female and 2 were male, which was accounted for during the statistical analysis by correcting for donor effect. Next, $CD4^+$ T cells were purified from the PBMCs using lyophilized human anti-$CD4^+$ magnetically labeled microbeads (Miltenyi, 130-097-048) scaling the manufacturer's instructions to ⅓ of the recommended volumes. $CD4^+$ T cell purity was assessed on an LSR-II instrument at the Leiden University Medical Center Flow Cytometry Core Facility (https://www.lumc.nl/research/facilities/fcf/) with the BD FACSDiva™ v9.0 software (BD Biosciences). Cells were stained with anti-CD3-PE (BD Biosciences, 345765), anti-CD4-APC (BD Biosciences, 345771), anti-CD8-FITC (BD Biosciences, 555634), and anti-CD14-PEcy7 (BD Biosciences, 560919) and resuspended in 1% paraformaldehyde (Apotheek LUMC, 120810-001) to fix the cells prior to acquisition. Purity was >98% for all donors.

Prior to fatty acid exposure, ~$1*10^8$ isolated cells were cultured overnight to allow the cells to return to a resting state after the stress of the isolation procedure. This was done in T75 flasks (Greiner Bio-One, 658-175) at a density of ~$2.5*10^6$ cells/mL in 5% fetal calf serum (FCS) (Bodinco BDC, 16941) DMEM (Dulbecco's Modified Eagle's Serum (Sigma, 05796), 1% Pen-Strep (Lonza, DE17-602E), 1% GlutaMAX-1 (100x) (Gibco, 35050-038)) medium supplemented with 50 IU/mL IL-2 (Peprotech, 200-02) and incubated at 37°C under 5% CO_2. To keep the cells in a non-activated state, no additional stimulus was added. Any $CD4^+$ T cells not used directly after the isolation were kept in DMEM supplemented with 30% FCS, 1% Pen-Strep, 1% GlutaMAX-1, and 20% Dimethyl Sulfoxide (DMSO) (WAK-Chemie Medical GmbH, WAK-DMSO-10) medium at a density of ~$25*10^6$ cells/mL, and stored in liquid nitrogen.

Next, non-activated $CD4^+$ T cells were cultured with either EPA (Cayman, 90110), OA (Sigma, O1383), PA (Cayman, 10006627), or control for 48 hours at 37°C under 5% CO_2. The cells were exposed for 48h based off previous findings when establishing our previously described *in vitro* model[29]. To this end, $CD4^+$ T cells from each donor were plated in a 24 wells plate (density of ~$3.5*10^6$ cells/well) in 2mL 5% FCS DMEM for each condition (Fig. 1a). Cells were cultured in medium containing FCS to ensure cell viability during culture and to be more comparable to physiological conditions of the circulation where other lipids are also present. To assess the additional EPA, OA, or PA stimulus to the non-activated $CD4^+$ T cells due to FCS in the culture

medium, an FCS sample was measured via the Shotgun Lipidomics Assistant (SLA) method[30] to estimate the fraction of fatty acids in the sample. The sample was prepped as previously described[31] but with two modifications, a starting volume of 25µL FCS and 600µL MTBE was added instead of 575µL during the first extraction. Free EPA was 0.02µg/mL and EPA as components of larger molecules including cholesterol esters and sphingolipids was 0.13 µg/mL. Free OA was 0.29µg/mL and OA as components of larger molecules including cholesterol esters and sphingolipids was 4.93µg/mL. Free PA was 0.23µg/mL and PA as components of larger molecules including cholesterol esters and sphingolipids was 3.45µg/mL.

PA was dissolved in HPLC grade ethanol (Fisher Scientific, 64-17-5) to a final concentration of 5mg/mL to create a stock solution. The stock solution was vortexed briefly, sonicated in a sonicator (Branson, 2800) for 15 min, and heated for 15 min at 45°C. A small portion of the stock was extracted into a glass HPLC vial (Agilent Technologies, 5182-0714) to a final concentration of 5,000µg/mL. EPA and OA were dissolved from their stock in HPLC grade ethanol to a final concentration of 25,000 and 30,000µg/mL, respectively. The HPLC grade EtOH was then evaporated before the fatty acids were complexed to fatty acid-free (FAF) bovine serum albumin (BSA) (Sigma, A7030) in a 2% FAF BSA DMEM mixture (Dulbecco's Modified Eagle's Serum, 2% FAF BSA, 1% Pen-Strep, 1% GlutaMAX-1 (100x)) to a concentration of 151.25µg/mL for EPA, 141.25µg/mL for OA, and 128.2µg/mL for PA. Complexing fatty acids to BSA mimics physiological conditions as fatty acids are also bound to albumin in the human circulations[32]. Each fatty acid was further diluted to the final concentrations of 100µM (30.25µg/mL for EPA, 28.25µg/mL for OA, and 25.64µg/mL for PA) upon addition to the cells. The concentration tested was kept equal to ensure the cells were exposed the same amount of fatty acid particles and not influenced by concentration differences. Fatty acid stocks were stored under argon gas at -20°C to avoid oxidation.

As a control, HPLC grade EtOH was evaporated in a glass HPLC vial before adding 2% FAF BSA DMEM medium and added to the cells. The amount of 2% FAF BSA DMEM added to the wells was equal for each condition to keep the volumes equivalent. The $CD4^+$ T cells were cultured for 48h at 37°C under 5% CO_2. After exposure, the cells were washed and $1*10^5$ cells were used directly for ATAC sequencing preparation. Cells from the same donors for which ATAC sequencing was performed were later thawed from liquid nitrogen and exposed to the fatty acids as described previously. After 48h exposure, the cells were washed and $3*10^6$ cells were flash frozen in liquid nitrogen and stored at -80°C for RNA isolations. Cell viability and diameter were measured by Via1-Cassette™ (Chemometec, 941-0012) on a NucleoCounter® NC-200™ (Chemometec, 900-0200) and found to be > 95% and on average 9µm for each condition.

RNA isolation

To isolate total RNA for RNA sequencing and RT-qPCR, RNA was extracted from the cell samples using the Quick-RNA Microprep Kit (Zymo, R1050) according to manufacturer's instructions. The RNA was quantified using a Qubit® 2.0 Fluorometer (Q32866) with the Qubit® RNA BR Assay Kit (Thermofisher, Q10211) according to manufacturer's instructions. The RNA was placed over a second Zymo-Spin IC Column, washed, and a second DNase treatment performed to

remove any residual DNA contamination from the samples. RNA integrity (RIN) values of the samples were on average 7.8 SE 0.1 as determined using an Agilent 2100 Bioanalyzer Instrument (G2939BA) with the Agilent RNA 6000 Nano Reagents (Agilent, 5067-1511). RNA was divided into two samples and stored at -80°C, 1µg for RNA sequencing and the rest for cDNA synthesis and RT-qPCR measurements.

Real time-quantitative PCR

To measure the expression of *CPT1A* in all the cell samples, cDNA was synthesized with 200ng of the stored RNA using the Transcriptor First Strand cDNA Synthesis Kit (Roche, 04897030001) according to the manufacturer's instructions. Quantitative real time PCR's for *CPT1A* (Thermofisher, Hs00912671_m1, 4331182) were performed using the TaqMan™ Fast Advanced Master Mix (Thermofisher, 4444557) with 10ng cDNA per reaction on a QuantStudio 6 Real-Time PCR system (Applied Biosystems). All RT-qPCR reactions were performed in triplicate and outliers were removed if the Ct value measured differed more than 0.5% from the mean. Relative gene expression levels (-ΔCt) were calculated using the average of Ct values of *RPL13A* (Thermofisher, Hs03043887_gH, 4448892) and *SDHA* (Thermofisher, Hs00188166_m1, 4453320) as internal controls[33]. The fold change was determined using the $2^{-\Delta\Delta Ct}$ method, using the control as the reference. All statistical analyses were performed in R. Data are expressed as mean of the relative fold change and standard error. The reported P values were determined by applying a paired two-tailed student's T test. P values < 0.05 were considered to be statistically significant.

RNA sequencing analysis

RNA sequencing (RNA-seq) was performed to determine the differences in the transcriptome of control versus fatty acid exposed non-activated $CD4^+$ T cells across time. The RNA from each of the samples was sent for sequencing (Macrogen, Amsterdam, NL). RNA-sequencing libraries were prepared from 200ng RNA using the Illumina Truseq stranded mRNA library prep (Illumina, 20020594) with a poly A selection. Both whole-transcriptome amplification and sequencing library preparations were performed in two 96-well plates with 26 samples in one plate and 6 in another. Quality control steps were included to determine total RNA quality and quantity, the optimal number of PCR preamplification cycles, and fragment size selection. No samples were eliminated from further downstream steps. Barcoded libraries were divided across two plates with 26 samples in one and 6 in the other and sequenced separately. Barcoded libraries were sequenced to a read depth of 20 million reads using the Novaseq 6000 (Illumina) to generate 100 base pair paired-end reads.

FastQ files are analyzed using the RNAseq pipeline (v5.0.0) from BioWDL (https://zenodo.org/record/5109461), developed by SASC (LUMC). The pipeline performed preprocessing on the FastQ files (including quality control, quality trimming, and adapter clipping), read mapping, and expression quantification. *FastQC* (v0.11.9) is used to check raw reads and *Cutadapt* (v2.10) to perform adapter clipping. Reads are mapped to a reference genome (Ensembl v105) using *STAR aligner* (v2.7.5a), and with *HTSeq Count* (v0.12.4) the number of assigned reads to genes per sample is determined.

Based on Ensembl gene biotype annotation, we included only protein coding genes for further downstream analysis (19,991 genes in total). We used the Bioconductor package *DESeq2*[34] (v1.40.2) to test whether EPA, OA, or PA had an effect on gene expression as compared to the control. *DESeq2* fits a generalized linear model (GLM) assuming the negative binomial distribution for the counts. The model expresses the logarithm of the average of the counts in terms of one or more predictors. In this case, we used three models that had one of the fatty acids, subject identifier, and batch as predictors each. By including the subject identifier and batch in the models, we account for the dependence between measurements within the same subject and between different batches of sequencing[34]. Lowly expressed genes, i.e. that did not have at least a count of 1 in half of the samples per fatty acid and control, were removed, resulting in 12,938 genes for EPA, 12,949 genes for OA, and 12,971 genes for PA. The Benjamini-Hochberg procedure was used to correct for multiple testing at a false discovery rate (FDR) of 5%.

Differentially expressed genes per fatty acid were divided into upregulated or downregulated based on the log2 fold change values. 10 human pathway databases (BioPlanet 2019, WikiPathways 2019 Human, KEGG 2019 Human, Elsevier Pathway Collection, BioCarta 2015, Reactome 2016, HumanCyc 2016, NCI-Nature 2016, Panther 2016 and MSigDB Hallmark 2020) were queried using gene symbols, with 904 of 1170 queried genes for EPA, 51 of 60 queried genes for OA, and 26 of 33 queried genes for PA, present in at least 1 database. The identified clusters were then mapped for pathway enrichment using *clusterProfiler*[35] (v4.8.3) with the background set to the 12,938 expressed genes for EPA, 12,949 expressed genes for OA, and 12,971 expressed genes for PA as determined above. Multiple testing correction using the Benjamini-Hochberg method at 5% FDR was performed over the combined results from the 10 databases. Pathways that included highly similar gene sets were grouped (Jaccard index > 0.7) and only the most significantly enriched pathway per group was retained.

ATAC sequencing analysis

Post-exposure, the $1*10^5$ cells were taken off for ATAC sequencing and placed into DNA LoBind 1.5mL tubes (Eppendorf, 2231000945). The cells were washed 3x in ice cold buffered natrium chloride (PBS; pH 7.4; Fresen, 15360679). The samples were then handed off to the Leiden Genome Technology Center for library generation. The ATAC-sequencing libraries were generated using the Omni-ATAC protocol[36]. Briefly, the nuclei were isolated by lysing the cells in ATAC-Resuspension Buffer (RSB) (0.1% NP40 (Thermofisher, 85124), 0.1% Tween-20 (Thermofisher, 28320), and 0.01% digitonin (Promega, G9441)) for 3 min on ice. After washing the nuclei with 1mL wash buffer (RSB and 0.1% Tween) the nuclei were centrifuged for 10min at 4°C. After removing the supernatant, carefully avoiding the pelleted nuclei, the nuclei were resuspended in PBS. The nuclei were counted and normalized to 25,000 cells using the TC20 cell counter (BioRad, 1450102). The nuclei were combined with 25µL 2x TD buffer (TrisHCl pH 7.5 (Thermofisher, 15567027), NaCl (Thermofisher, A57006) and MgCl2 (Thermofisher, AM9530G)), 2µL Tn5 enzyme (Tn5 enzyme (Illumina, 15027865) and TD Tagment DNA Buffer (Illumina, 15027866)), 0.5µL 1% digitonin, 0.5µL 10% Tween-20 up to a volume of 50µL. The reaction was incubated at 37°C for 30min and then purified using AMPure Beads (Beckman Coulter, A63881) with a ratio of 1.8x and

eluted in 10µL of EB (10mM Tris-HCl). The PCR was done using 2x Kapa HiFi Master mix (Roche, 09420398001) with the barcoded primers described in the Omni-ATAC protocol. After the PCR, the products were dual size selected using AMpure beads, first using 0.4x, followed directly by 1.2x. The ATAC-sequencing libraries were checked on the Femto Pulse (Agilent, M5330AA) and pooled equimolar for sequencing. No samples were eliminated from further downstream steps.

Barcoded libraries were sent for sequencing (Macrogen, Amsterdam, NL). An additional round of quality control was performed and the samples were then pooled and divided across one lane. Barcoded libraries were sequenced to a read depth of 30 million 150 base pair paired-end reads using the Novaseq 6000 (Illumina).

FastQ files were analyzed using the ChIP-seq pipeline from BioWDL (https://github.com/biowdl/ChIP-seq), developed by SASC (LUMC). The pipeline performed preprocessing on the FastQ files (including quality control, quality trimming, and adapter clipping), read mapping, and peak calling. *FastQC* (v0.11.9) is used to check raw reads and *Cutadapt* (v2.10) to perform adapter clipping. Reads are mapped to a reference genome (Encode GRCh38) using *BWA aligner* (v0.7.17), and *MACS2* (v2.1.2) was used to perform the peakcalling. These peak files were then processed using R (v4.3.0). Using *DiffBind* (v3.10.0), reads in the BAM files were counted for each peak. Next, the read counts per peak for each sample were merged to create one table containing all peaks and read counts of all the samples combined. *De novo* motif analysis was then performed using HOMER[37].

Data availability

The data supporting the findings of this study are available within the article and its Supplementary information files. All other data including the raw files are available at the Gene Expression Omnibus repository, accession GEO (main combined submission: GSE254749, RNA sequencing submission: GSE254695, and ATAC sequencing submission: GSE254468).

Results

Transcriptomic analysis of EPA exposed non-activated CD4+ T cells

Non-activated CD4+ T cells from 8 different donors were each exposed to 100µM EPA, OA, PA, or control for 48h (Fig. 1a). Exposure did not affect cell viability or diameter (Supp. Fig. 1a and b). To confirm a response by the cells due to the fatty acid exposure, the expression of *CPT1A*, the rate limiting enzyme in β-fatty acid oxidation, was measured. *CPT1A* expression increased as compared to control (EPA: 12.4-fold, SE 1.9 ($p < 0.001$); OA: 19.5-fold, SE 3.0 ($p < 0.001$); PA: 11.3-fold, SE 2.2 ($p < 0.003$); Fig. 1b). This signifies a consistent response to EPA, OA, and PA exposure.

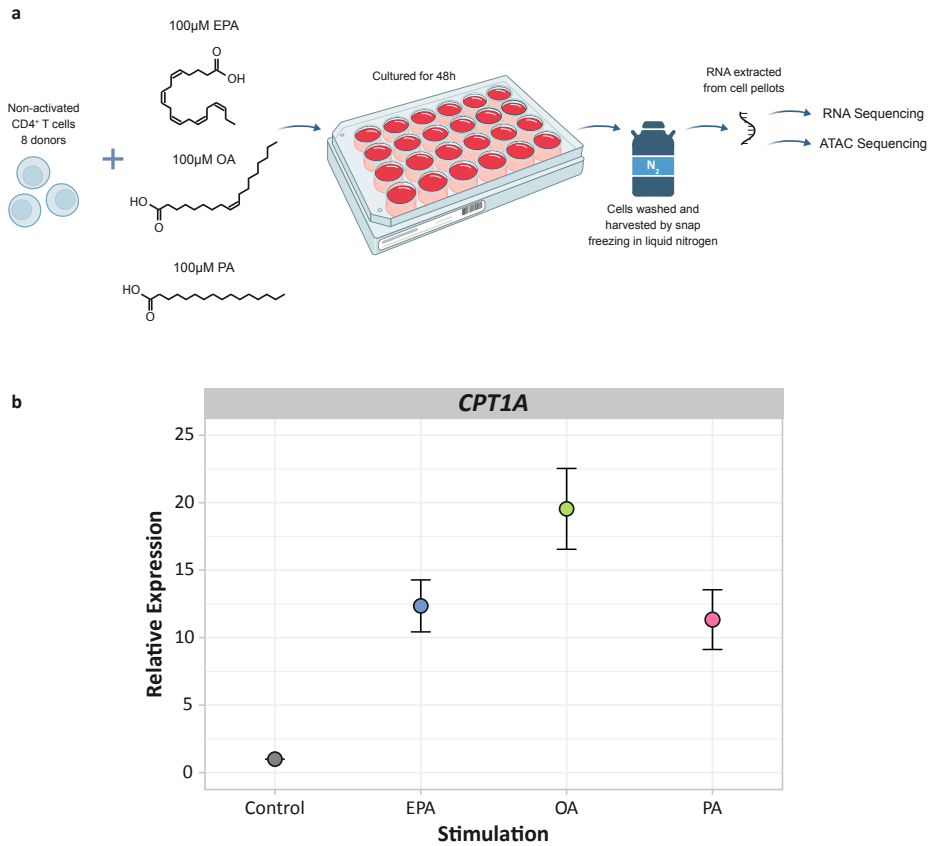

Fig. 1 | Experimental set up and *in vitro* model verification. (a) Experimental set up for RNA and ATAC sequencing of EPA, OA, and PA exposed non-activated CD4⁺ T cells, n = 8. **(b)** Dot plot showing the relative expression of *CPT1A* after 48h of fatty acid exposure as a confirmation of the *in vitro* model by RT-qPCR. Values are colored by fatty acid. On average *CPT1A* was upregulated 12.4 SE 1.9 fold for EPA ($p < 0.001$), 19.5 SE 3.0 fold for OA ($p < 0.001$), and 11.3 SE 2.2 fold for PA ($p < 0.003$), n = 8. Abbreviations, EPA = eicosapentaenoic acid, h = hours, OA = oleic acid, PA = palmitic acid.

Next, we studied the transcriptomic response of CD4⁺ T cells to EPA, OA, and PA as compared to control using RNA-seq. The transcriptional response was compared to the control condition for each fatty acid. The number of differentially expressed genes (DEGs) and effect sizes were markedly larger for EPA, than for OA and PA (Fig. 2a) and there was limited overlap between the DEGs of each fatty acid (Fig. 2b). EPA induced 1170 DEGs ($P_{FDR} < 0.05$), 723 of which were downregulated and 447 of which were upregulated (Supp. Table 1a and b). In contrast, OA induced 60 DEGs ($P_{FDR} < 0.05$; 13 downregulated and 47 upregulated; Supp. Table 1c and d). PA induced found 33 DEGs ($P_{FDR} < 0.05$; 15 downregulated and 18 upregulated; Supp. Table 1e and f). Despite the high specificity of the transcriptional response of each fatty acid, 4 genes were upregulated upon exposure of all three fatty acids. These genes were involved in β-fatty acid oxidation (*CPT1A*, *SLC25A20*, *ACADVL*, and *ACAA2*) in line with a generic cellular response to fatty acid exposure regardless of the fatty acid type (Supp. Table 1g).

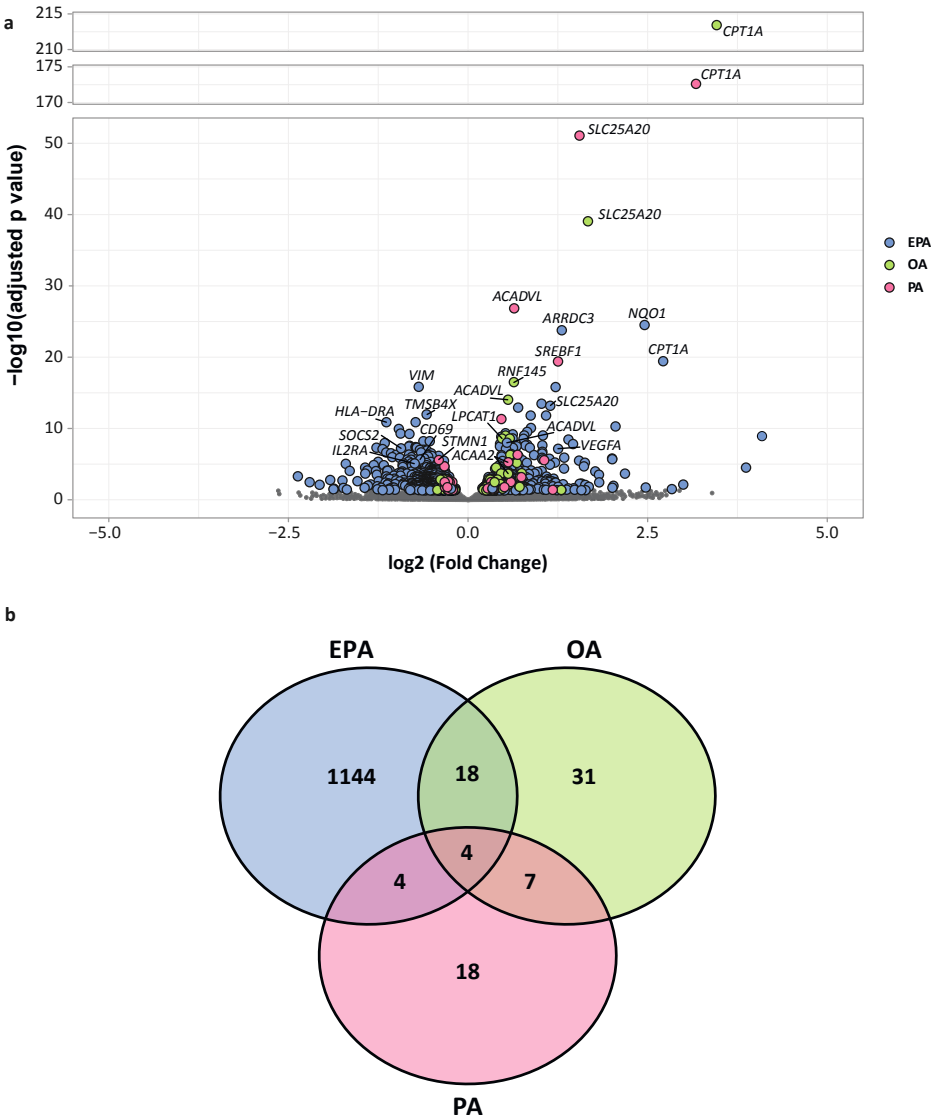

Fig. 2 | EPA, OA, and PA exposure in non-activated CD4⁺ T cells induces changes in transcriptomics. (a) Volcano plot showing the gene expression of non-activated CD4⁺ T cells exposed to either EPA, OA, or PA. All 19,991 protein coding genes are shown for each fatty acid. DEGs are colored by fatty acid and denoted by a larger size. Non-significant genes are shown in grey and denoted by a smaller size. Log2 fold change is used to show the direction of gene expression. **(b)** Venn diagram showing the unique response of non-activated CD4⁺ T cells to each fatty acid. Values are colored by fatty acid. There are 6 DEGs overlapping between all three fatty acids, 18 DEGs overlapping between EPA and OA, 4 DEGs overlapping between EPA and PA, and 7 DEGs overlapping between OA and PA. Abbreviations, EPA = eicosapentaenoic acid, OA = oleic acid, PA = palmitic acid.

We focused on the marked transcriptomic response of $CD4^+$ T cells to EPA. Firstly, we analyzed the 723 downregulated genes in EPA exposed non-activated $CD4^+$ T cells. The top three DEGs were *VIM* (vimentin), *TMSB4X* (thymosin beta 4 X-linked) and *HLA-DRA* (major histocompatibility complex, class II, DR alpha). *VIM* and *TMSB4X* both encode structures involved in the makeup of the cytoskeleton. HLA-DRA plays a central role in the immune response by presenting peptides to T cells. Remarkably, many other immune response genes were also downregulated, including *SOCS2* (suppressor of cytokine signaling 2), *CD69* (CD69 molecule), and *IL2RA* (interleukin 2 receptor subunit alpha). SOCS2 is a negative regulator of cytokine receptor signaling, particularly of IGF1R, an Insulin-Like Growth Factor whose expression is associated with the development of T_H17 over T_{reg} subsets. CD69 plays an integral part in T cell activation, and IL2RA is an important regulator of T cell differentiation. A strong downregulation of immune-related processes was confirmed by a formal analysis of enriched biological processes. In particular, interleukin (IL)-2 signaling pathway ($P_{FDR} < 0.001$; 110 DEGs), antigen processing and presentation ($P_{FDR} < 0.001$; 27 DEGs), and interferon gamma response ($P_{FDR} < 0.001$; 47 DEGs) were enriched (Fig. 3a; Supp. Table 1h). This indicates that EPA reduces immune related gene expression in non-activated $CD4^+$ T cells.

Secondly, we analyzed the 447 upregulated genes in EPA exposed non-activated $CD4^+$ T cells. The top three DEGs were *NQO1* (NAD(P)H quinone dehydrogenase 1), *ARRDC3* (arrestin domain containing 3) and *CPT1A*. NQO1 is involved in protecting cells against oxidative stress, which can be caused by lipid peroxidation and *ARRDC3* encodes a regulator of G protein-mediated signaling. Another gene of interest that was upregulated was *VEGFA* (vascular endothelial growth factor A). The enzyme encoded by this gene is a proangiogenic molecule known to be involved in creating immunosuppressive environments. This immunosuppressive profile was further supported by a formal analysis of enriched biological processes, which showed upregulation of the NRF2 pathway ($P_{FDR} < 0.001$; 20 DEGs; Fig. 3b; Supp. Table 1i). This pathway is the most important pathway for protecting cells against oxidative stress and has been shown to be involved in anti-inflammatory responses. Overall, these results suggests that EPA exposure can alter gene expression in non-activated T cells towards an anti-inflammatory profile by decreasing immune response related genes and increasing protective genes such as those in the NRF2 pathway.

Next, we investigated whether specific transcription factors may underlie the differential gene expression. To do this, we examined the enrichment of transcription factor binding motifs in loci that were more closed (down) versus more open (up) as determined by ATAC-sequencing. The top EPA downregulated motifs included CTCF, GATA3, RUNX1, and PU.1 (Fig. 3c; Supp. Table 1j). CTCF is a master regulator of chromatin looping and moreover, involved in effector cell differentiation[38, 39]. GATA3 and PU.1 are the key transcription factors for the development of T_H2 and T_H9 cells, respectively[40, 41]. RUNX1 is necessary for T cell maturation, knock outs of this transcription factor results in phenotypically and functionally immature T cells[42]. We next examined the enrichment of transcription factor binding motifs in upregulated versus downregulated genes. EPA upregulated motifs included, REV-ERB, TCF7, and FOXA1 (Fig. 3d; Supp. Table 1k). REV-ERB is an antagonist of RORγt, the key transcription factor for the development of T_H17 cells[43]. TCF7 plays a role in the regulation of autoinflammatory T cell responses[44]. FOXA1

is involved in giving T_{reg} cells their suppressive properties[45]. These results further suggest that non-activated CD4$^+$ T cells may decrease their ability to induce an immune response or effector T cell profile after EPA exposure.

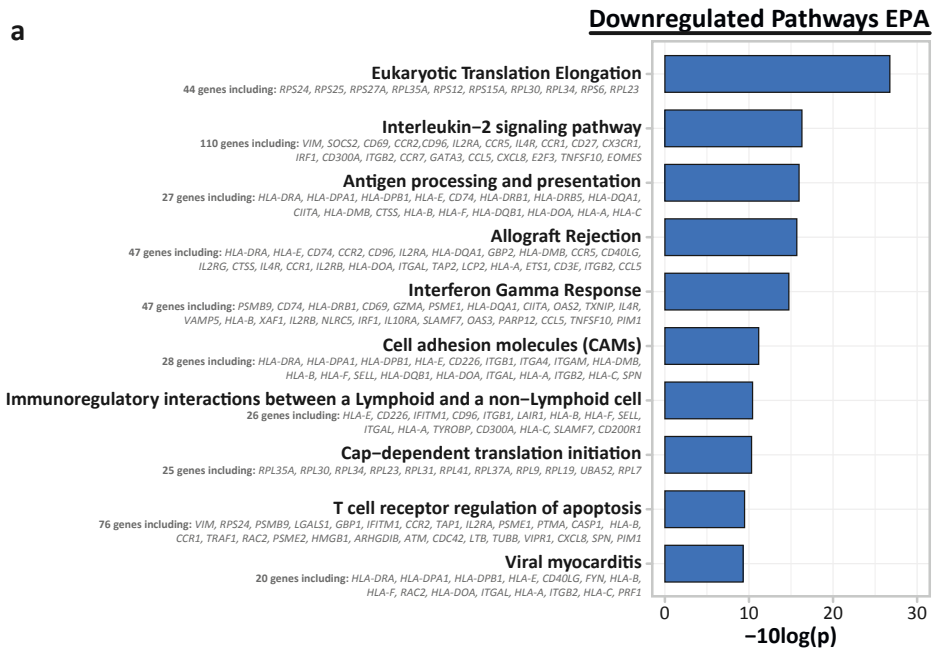

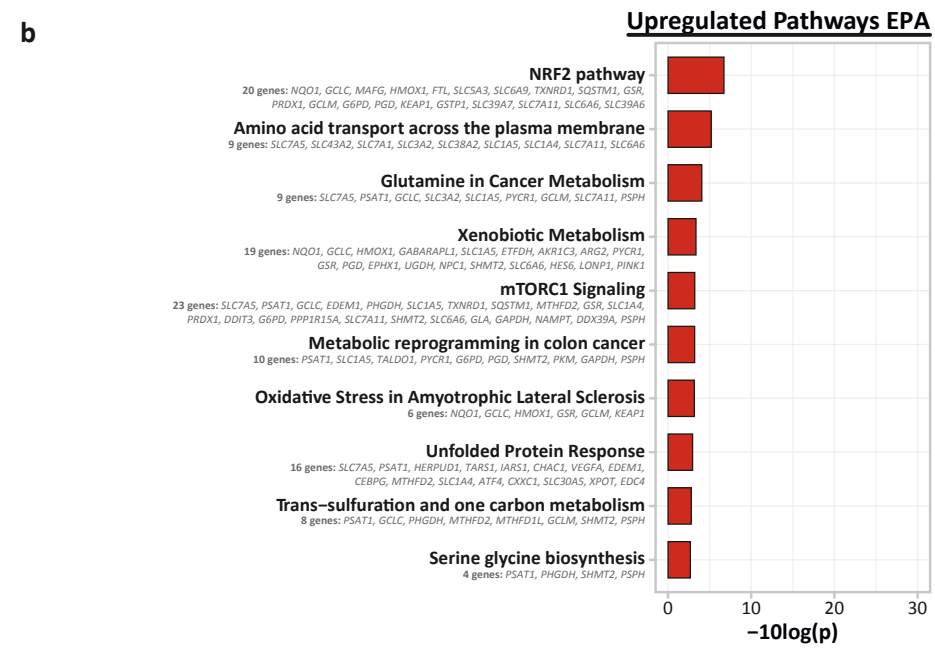

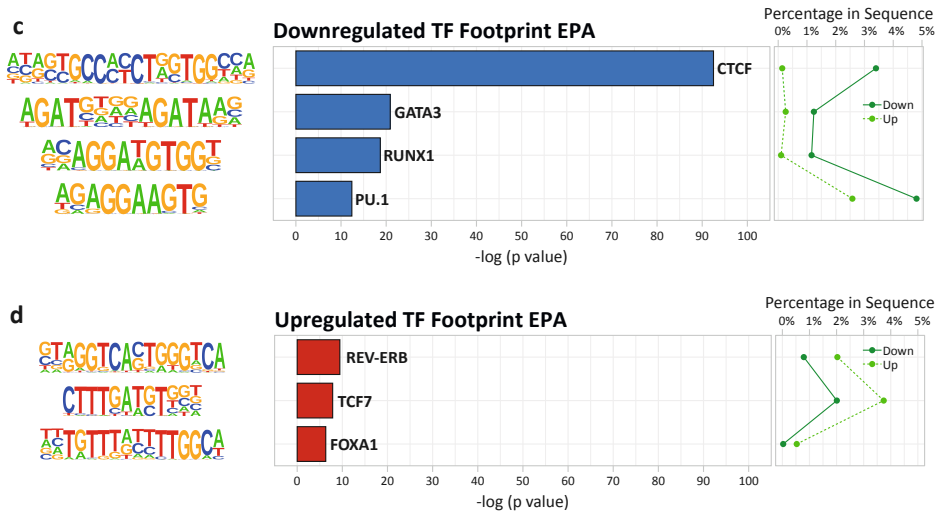

Fig. 3 | Up- and downregulated pathways and transcription factors in EPA-exposed non-activated CD4⁺ T cells. (a) Pathway enrichment analysis of all downregulated EPA DEGs generated using *clusterProfiler* using 10 human pathway databases. Top 10 enrichments are shown. **(b)** Pathway enrichment analysis of all upregulated EPA DEGs generated using *clusterProfiler* using 10 human pathway databases. Top 10 enrichments are shown. **(c)** Known motif analysis on promotors of down versus upregulated EPA ATAC peaks. Enrichment of transcription factor binding motifs was performed using HOMER. 4 motifs are shown with supplementing information on p-value, percentage of genes in upregulated gene set and percentage of genes in downregulated gene set, transcription factor name, -log(p-value), and percentage in sequence. **(d)** Known motif analysis on promotors of up versus downregulated EPA ATAC peaks. Enrichment of transcription factor binding motifs was performed using HOMER. 4 motifs are shown with supplementing information on p-value, percentage of genes in upregulated gene set and percentage of genes in downregulated gene set, transcription factor name, -log(p-value), and percentage in sequence. Abbreviations, EPA = eicosapentaenoic acid, TF = transcription factor.

Transcriptomic analysis of OA and PA exposed non-activated CD4⁺ T cells

Non-activated CD4⁺ T cells were also exposed to either OA or PA and differential gene expression was measured. In line with our previous experiments, we found that OA exposure lead to the downregulation of endogenous peptide antigen presentation (*HSPA5* and *PDIA3*; $P_{FDR} < 0.001$; 2 DEGs), electron transport chain and oxidative phosphorylation activity (*NDUFA12*, *NDUFB4*, and *ATP5F1C*; $P_{FDR} < 0.001$; 3 DEGs) and upregulation of cholesterol biosynthesis (*HMGCR*, *HMGCS1* and *DHCR24*; $P_{FDR} < 0.001$; 4 DEGs; Supp. Fig. 2a and b; Supp. Table 1l and m) related genes. Exposure to PA induced an opposite response, with the downregulation of cholesterol biosynthesis pathway (*HMGCR* and *SQLE*; $P_{FDR} < 0.05$; 2 DEGs), and upregulated beta fatty acid oxidation (*CPT1A*, *SLC25A20*, and *ACADVL*; $P_{FDR} < 0.001$; 3 DEGs; Supp. Fig. 2c and d; Supp. Table 1n and o) related genes. Thus, the changes in the transcriptome of OA and PA exposed cells seem to have a greater effect on genes involved in cellular metabolism, particularly cholesterol metabolism, as compared to EPA.

The transcriptional responses observed were in line with the results of ATAC-sequencing based transcription factor footprint analysis. For OA only three motifs were downregulated including RAR:RXR, a motif known to play a part in the development of T_{reg} over T_H17 cells (Supp. Fig. 3a;

Supp. Table 1p). OA upregulated motifs included PU.1, as was found previously[29] as well as IRF8, which is also involved in T_H9 differentiation (Supp. Fig. 3b; Supp. Table 1q). PA downregulated motifs included IRF8 and GATA3 (Supp. Fig. 3c; Supp. Table 1r) and upregulated motifs included REV-ERB (Supp. Fig. 3d; Supp. Table 1s). OA and PA showed reversed effects on cholesterol metabolism processes which were mirrored in opposite associations with transcription factor binding motifs, indicating fatty-acid specific responses in non-activated $CD4^+$ T cells.

Discussion

IPE, the highly purified form of EPA, has been associated with reduced triglycerides, cardiovascular events, and cardiovascular death in individuals with relatively well controlled LDL levels, even when corrected for placebo response in the mineral oil control group, LDL, and C-reactive protein (CRP) in the REDUCE-IT trial[10, 46-49]. The trials outcomes and interpretation have been widely debated and the mechanisms by which EPA exerts its beneficial effects remains incompletely understood[11, 12]. We show that EPA exposure can already produce distinct changes in T cells prior to activation by decreasing the expression of immune response genes and increasing the expression of genes involved in oxidative stress protection. This is further supported by changes in transcription factor binding sites in our ATAC-sequencing motif analysis, indicating a change in the epigenetic landscape of EPA exposed T cells. Furthermore, we show that EPA induces a unique response in non-activated $CD4^+$ T cells as two other fatty acids of varying degrees of saturation, OA and PA, generated a smaller yet distinct effect on gene expression profiles in T cells as compared to control. Our findings imply that different fatty acids in the circulation can induce diverse effects on T cell transcriptomics, and that specifically EPA exposure may poise T cells to have clearer anti-inflammatory responses. These results underscore a potential mechanism by which EPA may mitigate ASCVD risk, suggesting its anti-inflammatory impact on T cells as a contributing factor. This is particularly noteworthy as T cells comprise over half of the immune cell population within atherosclerotic plaques[17, 18].

Our results show that EPA exposure, but not OA nor PA, leads to a strong downregulation of immune response related genes. Particularly, genes involved in antigen processing and presentation were downregulated in EPA exposed cells, denoted by, amongst others, the decreased expression of 14 different HLA genes. This gene group is crucial in inducing immune responses[50] and has also been found to be associated with T cell activation and effector memory phenotype in $CD4^+$ T cells[51]. In addition, genes involved in IL-2 signaling were also downregulated, which is required for T cell activation[52]. Downregulation of genes in these pathways suggests that EPA exposed T cells may have a reduced ability to initiate an immune response, a key component of inflammatory responses in atherosclerotic plaques[53]. This result can support the finding that higher plasma EPA levels are associated with lower CVD risk in humans[54]. Furthermore, genes involved in pro-inflammatory pathways, such as interferon gamma response were downregulated in EPA exposed cells. IFNγ is primarily produced by pro-inflammatory T cell subset, T_H1 cells, which have also been found to decrease upon EPA exposure[27, 55-57]. Moreover, the key transcription

factors in T_H2 and T_H9 differentiation, GATA3 and PU.1, were also found to be decreased in our motif analysis. While T_H2 cells have inconclusive effects on ASCVD, T_H9 cells have been shown to aggravate it[58-60]. Thus, EPA exposure decreased genes involved in immune response and pro-inflammatory pathways as well as suggests a reduced ability for key T cell differentiation transcription factors to bind.

In further support of EPA's anti-inflammatory properties on non-activated $CD4^+$ T cells, we found that genes involved in the NRF2 pathway were upregulated upon EPA exposure. This pathway mainly functions in preventing oxidative stress in cells by activating genes involved in detoxification and removal of reactive oxygen species[61]. However, the NRF2 pathway has also been shown to aid in the anti-inflammatory responses of macrophages[62] and has been suggested as a beneficial pleiotropic effect of statins[63], as oxidative stress has been found to be a risk factor for ASCVD[64]. We also found an increased footprint for the transcription factors REV-ERB, TCF7, and FOXA1. These transcription factors are each involved in regulating T cell responses and generating a more anti-inflammatory T cell profile[43-45]. Overall, these data indicate that non-activated $CD4^+$ T cells can already acquire an anti-inflammatory transcriptomic profile, which may play a role in the anti-inflammatory properties observed of EPA in clinical trials.

EPA has a distinct effect on $CD4^+$ T cells. This is observed by our analysis of the effects of OA and PA on non-activated $CD4^+$ T cells. The number of DEGs and effect sizes were smaller upon OA and PA exposure and distinctly different. Interestingly, OA and PA each had opposed effects on cholesterol biosynthesis related genes, with OA upregulating and PA downregulating genes in this pathway. Upregulation of cholesterol biosynthesis has been related to the development of T_H17 cells by controlling RORγt activity, the key transcription factor in T_H17 differentiation[65, 66]. This observation can be further supported by OA downregulating the RAR:RXR motif, which is involved in generating T_{reg} cells over T_H17 and PA upregulating REV-ERB[43, 67]. The results of OA exposure also show the robustness of our approach as our findings here match what was found previously by our group[29]. These data suggest that our model is robust and each fatty acid induces its own unique response in non-activated $CD4^+$ T cells.

Conclusion

In conclusion, our data points to the fact that EPA produces a strong and specific anti-inflammatory transcriptional profile in non-activated $CD4^+$ T cells comprised of both the downregulation of immune related genes and the upregulation of antioxidant genes. This profile is supported by transcription factor motif analysis and by the analysis of two other fatty acids of varying degrees of saturation. Our results contribute to the debate of how EPA exerts beneficial effects in human ASCVD. Our study gives an indication that the beneficial effects observed of EPA, as asserted in clinical trials, can already start in the circulation by inducing an anti-inflammatory transcriptional profile in non-activated T cells with potentially anti-atherosclerotic properties.

Limitations of the study

We show that EPA exposure has beneficial anti-inflammatory effects on non-activated $CD4^+$ T cells. This is relevant because T cells are largely non-activated in the circulation and it is in the circulation where T cells will encounter EPA when individuals are treated with IPE to reduce ASCVD risk. Nevertheless, our results are in line with experiments on activated T cells, which showed that EPA exposure decreased proliferation[22-26], decreased T_H1 and T_H17 populations[27, 28], and had no effect on or increased T_H2 and T_{reg} populations[26-28]. Therefore, the encounter with EPA in a non-activated state may induce transcriptomic changes that influence the functional changes post-activation. Furthermore, our use of non-activated $CD4^+$ T cells with no additional selection towards naïve, effector, memory, or specific T helper subsets, as well as in culture medium containing other lipids more closely represents the diversity of T cells and environment of the circulation in which EPA exposure takes place. Additionally, we utilized OA and PA, two fatty acids of varying degrees of saturation to establish the distinct effects of EPA. Nevertheless, this does not rule out that other fatty acids may have marked effects on non-activated $CD4^+$ T cells as well[21]. A final limitation of our study is that we have employed an *in vitro* model and the effects of EPA on T cells *in vivo* should be studied in the context of trials of IPE. However, in mouse models, EPA supplementation has also been shown to reduce cholesterol levels[68], whereas, in humans, the effects of EPA on ASCVD risk were independent of LDL lowering[47]. Therefore, using a validated *in vitro* model provides valuable insights to study the effects of EPA on human $CD4^+$ T cells.

Translational perspectives

We report that EPA induces an anti-inflammatory transcriptomic profile in non-activated $CD4^+$ T cells. This observation is important to better understand the mechanism through which EPA reduces cardiovascular disease risk in studies such as the REDUCE-IT trial. The REDUCE-IT trial showed that intervention with IPE, which the body metabolizes to EPA, reduces the risk of cardiovascular events and death in patients with high triglycerides. The findings of this trial have sparked considerable debate in the literature as the results appeared to occur irrespective of the attained triglyceride level after one year[10-12]. Testing T cells from individuals undergoing IPE interventions can provide additional insights into how EPA exerts its beneficial effects independent of triglyceride reduction.

Acknowledgements
The authors' work is supported by the Dutch CardioVascular Alliance (The Dutch Heart Foundation, Dutch Federation of University Medical Centers, the Netherlands Organization for Health Research and Development, and the Royal Netherlands Academy of Sciences) for the GENIUSII project Generating the Best Evidence-Based Pharmaceutical Targets for Atherosclerosis (CVON2017-20).

Author contributions
B.T.H and J.W.J conceived the project. N.A.R. designed and conducted the experiments, analyzed the results, and drafted the manuscript. K.F.D. designed the analysis model and analyzed the RNA sequencing data. J.M. designed and performed *in vitro* model and prepped samples for ATAC sequencing. S. A. designed and performed *in vitro* model and prepped samples for RNA sequencing. T.K. aligned the RNA and ATAC sequencing data. Y.A. performed the ATAC sequencing library preparation. M.A.H. performed and analyzed the transcription factor footprint analysis. All authors contributed to the writing of the manuscript.

Competing interests
The authors declare no competing interests.

References

1 Lawler, P. R. *et al.* Targeting cardiovascular inflammation: next steps in clinical translation. *Eur. Heart J.* **42**, 113-131, (2021).

2 Sabatine, M. S. *et al.* Evolocumab and clinical outcomes in patients with cardiovascular disease. *N. Engl. J. Med.* **376**, 1713-1722, (2017).

3 Schade, D. S. & Eaton, R. P. Residual cardiovascular risk—is inflammation the primary cause? *World J. Cardiovasc. Dis.* **08**, 59-69, (2018).

4 Lawler, P. R. *et al.* Real-world risk of cardiovascular outcomes associated with hypertriglyceridaemia among individuals with atherosclerotic cardiovascular disease and potential eligibility for emerging therapies. *Eur. Heart J.* **41**, 86-94, (2020).

5 The ACCORD Study Group. Effects of intensive blood-pressure control in type 2 diabetes mellitus. *N. Engl. J. Med.* **362**, 1575-1585, (2010).

6 Keech, A. *et al.* Effects of long-term fenofibrate therapy on cardiovascular events in 9795 people with type 2 diabetes mellitus (the FIELD study): randomised controlled trial. *Lancet* **366**, 1849-1861, (2005).

7 Das Pradhan, A. *et al.* Triglyceride lowering with pemafibrate to reduce cardiovascular risk. *N. Engl. J. Med.* **387**, 1923-1934, (2022).

8 The AIM-HIGH Investigators. Niacin in patients with low HDL cholesterol levels receiving intensive statin therapy. *N. Engl. J. Med.* **365**, 2255-2267, (2011).

9 The HPS2-THRIVE Collaborative Group *et al.* Effects of extended-release niacin with laropiprant in high-risk patients. *N. Engl. J. Med.* **371**, 203-212, (2014).

10 Bhatt, D. L. *et al.* Cardiovascular risk reduction with icosapent ethyl for hypertriglyceridemia. *N. Engl. J. Med.* **380**, 11-22, (2019).

11 Kastelein, J. J. P. & Stroes, E. S. G. FISHing for the miracle of eicosapentaenoic acid. *N. Engl. J. Med.* **380**, 89-90, (2019).

12 Steg, P. G. & Bhatt, D. L. The reduction in cardiovascular risk in REDUCE-IT is due to eicosapentaenoic acid in icosapent ethyl. *Eur. Heart J.* **42**, 4865-4866, (2021).

13 Mason, R. P., Jacob, R. F., Shrivastava, S., Sherratt, S. C. R. & Chattopadhyay, A. Eicosapentaenoic acid reduces membrane fluidity, inhibits cholesterol domain formation, and normalizes bilayer width in atherosclerotic-like model membranes. *Biochim. Biophys. Acta* **1858**, 3131-3140, (2016).

14 Tsunoda, F. *et al.* Effects of oral eicosapentaenoic acid versus docosahexaenoic acid on human peripheral blood mononuclear cell gene expression. *Atherosclerosis* **241**, 400-408, (2015).

15 Vors, C. *et al.* Inflammatory gene expression in whole blood cells after EPA vs. DHA supplementation: results from the ComparED study. *Atherosclerosis* **257**, 116-122, (2017).

16 Wolf, D. & Ley, K. Immunity and inflammation in atherosclerosis. *Circ. Res.* **124**, 315-327, (2019).

17 Fernandez, D. M. *et al.* Single-cell immune landscape of human atherosclerotic plaques. *Nat. Med.* **25**, 1576-1588, (2019).

18 Depuydt, M. A. *et al.* Microanatomy of the human atherosclerotic plaque by single-cell transcriptomics. *Circ. Res.* **127**, 1437-1455, (2020).

19 Zhou, X., Robertson, A. K., Hjerpe, C. & Hansson, G. K. Adoptive transfer of CD4+ T cells reactive to modified low-density lipoprotein aggravates atherosclerosis. *Arterioscler. Thromb. Vasc. Biol.* **26**, 864-870, (2006).

20 Zhou, X., Nicoletti, A., Elhage, R. & Hansson, G. K. Transfer of CD4+ T cells aggravates atherosclerosis in immunodeficient apolipoprotein E knockout mice. *Circulation* **102**, 2919-2922, (2000).

21 Reilly, N. A., Lutgens, E., Kuiper, J., Heijmans, B. T. & Wouter Jukema, J. Effects of fatty acids on T cell function: role in atherosclerosis. *Nat. Rev. Cardiol.* **18**, 824–837, (2021).

22 Fan, Y. Y. *et al.* Remodelling of primary human CD4+ T cell plasma membrane order by n-3 PUFA. *Br. J. Nutr.* **119**, 163-175, (2018).

23 Gorjão, R., Cury-Boaventura, M. F., de Lima, T. M. & Curi, R. Regulation of human lymphocyte proliferation by fatty acids. *Cell Biochem. Funct.* **25**, 305-315, (2007).

24 Ly, L. H., Smith, R., Switzer, K. C., Chapkin, R. S. & McMurray, D. N. Dietary eicosapentaenoic acid modulates CTLA-4 expression in murine CD4+ T-cells. *Prostaglandins Leukot. Essent. Fatty Acids* **74**, 29-37, (2006).

25 Jolly, C. A., Jiang, Y. H., Chapkin, R. S. & McMurray, D. N. Dietary (n-3) polyunsaturated fatty acids suppress murine lymphoproliferation, interleukin-2 secretion, and the formation of diacylglycerol and ceramide. *J. Nutr.* **127**, 37–43, (1997).

26 Merzouk, S. A. *et al.* N-3 polyunsaturated fatty acids modulate in-vitro T cell function in type I diabetic patients. *Lipids* **43**, 485-497, (2008).

27 Bi, X. *et al.* ω-3 polyunsaturated fatty acids ameliorate type 1 diabetes and autoimmunity. *J. Clin. Invest.* **127**, 1757-1771, (2017).

28 Monk, J. M., Hou, T. Y., Turk, H. F., McMurray, D. N. & Chapkin, R. S. n3 PUFAs reduce mouse CD4+ T-cell ex vivo polarization into Th17 cells. *J. Nutr.* **143**, 1501-1508, (2013).

29 Reilly, N. A. *et al.* Oleic acid triggers metabolic rewiring of T cells poising them for T helper 9 differentiation. *iScience* **27**, 109496, (2024).

30 Su, B. *et al.* A DMS shotgun lipidomics workflow application to facilitate high-throughput, comprehensive lipidomics. *J. Am. Soc. Mass Spectrom.* **32**, 2655-2663, (2021).

31 Ghorasaini, M. *et al.* Congruence and complementarity of differential mobility spectrometry and NMR spectroscopy for plasma lipidomics. *Metabolites* **12**, 1030, (2022).

32 van der Vusse, G. J. Albumin as fatty acid transporter. *Drug Metab. Pharmacokinet.* **24**, 300-307, (2009).

33 Ledderose, C., Heyn, J., Limbeck, E. & Kreth, S. Selection of reliable reference genes for quantitative real-time PCR in human T cells and neutrophils. *BMC Res. Notes* **4**, 427, (2011).

34 Love, M. I., Huber, W. & Anders, S. Moderated estimation of fold change and dispersion for RNA-seq data with DESeq2. *Genome Biol.* **15**, 550, (2014).

35 Yu, G., Wang, L. G., Han, Y. & He, Q. Y. clusterProfiler: an R package for comparing biological themes among gene clusters. *OMICS* **16**, 284-287, (2012).

36 Corces, M. R. *et al.* An improved ATAC-seq protocol reduces background and enables interrogation of frozen tissues. *Nat. Methods* **14**, 959-962, (2017).

37 Heinz, S. *et al.* Simple combinations of lineage-determining transcription factors prime cis-regulatory elements required for macrophage and B cell identities. *Mol. Cell* **38**, 576-589, (2010).

38 Phillips, J. E. & Corces, V. G. CTCF: master weaver of the genome. *Cell* **137**, 1194-1211, (2009).

39 Zhao, X., Zhu, S., Peng, W. & Xue, H. H. The interplay of transcription and genome topology programs T cell development and differentiation. *J. Immunol.* **209**, 2269-2278, (2022).

40 Nakayama, T. *et al.* Th2 cells in health and disease. *Annu. Rev. Immunol.* **35**, 53-84, (2017).

41 Angkasekwinai, P. Th9 cells in allergic disease. *Curr. Allergy Asthma Rep.* **19**, 29, (2019).

42 Hsu, F. C. *et al.* An essential role for the transcription factor Runx1 in T cell maturation. *Sci. Rep.* **6**, 23533, (2016).

43 Mosure, S. A., Wilson, A. N. & Solt, L. A. Targeting nuclear receptors for Th17-mediated inflammation: REV-ERBerations of circadian rhythm and metabolism. *Immunometabolism* **4**, (2022).

44 Mammadli, M., Suo, L., Sen, J. M. & Karimi, M. TCF-1 is required for CD4 T cell persistence functions during alloimmunity. *Int. J. Mol. Sci.* **24**, 4326, (2023).

45 Liu, Y. *et al.* FoxA1 directs the lineage and immunosuppressive properties of a novel regulatory T cell population in EAE and MS. *Nat. Med.* **20**, 272-282, (2014).

46 Olshansky, B. *et al.* Mineral oil: safety and use as placebo in REDUCE-IT and other clinical studies. *Eur. Heart J. Suppl.* **22**, 34-48, (2020).

47 Sharretts, J. Endocrinologic and metabolic drugs advisory committee meeting. *FDA Briefing Document* (2019).

48 Briefing Document Vascepa®. *Endocrinologic and metabolic drugs adisory committee* **FDA**, (2019).

49 Assessment report Vazkepa. *Committee for Medicinal Products for Human Use* **EMA**, (2021).

50 Klein, J. & Sato, A. The HLA system. *N. Engl. J. Med.* **343**, 702-709, (2000).

51 Tippalagama, R. *et al.* HLA-DR marks recently divided antigen-specific effector CD4 T cells in active tuberculosis patients. *J. Immunol.* **207**, 523-533, (2021).

52 Chapman, N. M., Boothby, M. R. & Chi, H. Metabolic coordination of T cell quiescence and activation. *Nat. Rev. Immunol.* **20**, 55-70, (2020).

53 Grivel, J. C. *et al.* Activation of T lymphocytes in atherosclerotic plaques. *Arterioscler. Thromb. Vasc. Biol.* **31**, 2929-2937, (2011).

54 de Oliveira Otto, M. C. *et al.* Circulating and dietary omega-3 and omega-6 polyunsaturated fatty acids and incidence of CVD in the multi-ethnic study of atherosclerosis. *J. Am. Heart Assoc.* **2**, 000506, (2013).

55 Zhang, P., Smith, R., Chapkin, R. S. & McMurray, D. N. Dietary (n-3) polyunsaturated fatty acids modulate murine Th1/Th2 balance toward the Th2 pole by suppression of Th1 development. *J. Nutr.* **135**, 1745–1751, (2005).

56 Zhang, P. *et al.* Dietary fish oil inhibits antigen-specific murine Th1 cell development by suppression of clonal expansion. *J. Nutr.* **136**, 2391–2398, (2006).

57 Switzer, K. C., McMurray, D. N., Morris, J. S. & Chapkin, R. S. (n-3) Polyunsaturated fatty acids promote activation-induced cell death in murine T lymphocytes. *J. Nutr.* **133**, 496–503, (2003).

58 Zhang, W. *et al.* IL-9 aggravates the development of atherosclerosis in ApoE2/2 mice. *Cardiovasc. Res.* **106**, 453-464, (2015).

59 Gregersen, I. *et al.* Increased systemic and local interleukin 9 levels in patients with carotid and coronary atherosclerosis. *PLoS One* **8**, 72769, (2013).

60 Li, Q. *et al.* Increased Th9 cells and IL-9 levels accelerate disease progression in experimental atherosclerosis. *Am. J. Transl. Res.* **9**, 1335-1343, (2017).

61 Nguyen, T., Nioi, P. & Pickett, C. B. The Nrf2-antioxidant response element signaling pathway and its activation by oxidative stress. *J. Biol. Chem.* **284**, 13291-13295, (2009).

62 Wang, L. & He, C. Nrf2-mediated anti-inflammatory polarization of macrophages as therapeutic targets for osteoarthritis. *Front. Immunol.* **13**, 967193, (2022).

63 Mansouri, A. *et al.* Antioxidant effects of statins by modulating Nrf2 and Nrf2/HO-1 signaling in different diseases. *J. Clin. Med.* **11**, 1313, (2022).

64 Batty, M., Bennett, M. R. & Yu, E. The role of oxidative stress in atherosclerosis. *Cells* **11**, 3843, (2022).

65 Kanno, T., Nakajima, T., Miyako, K. & Endo, Y. Lipid metabolism in Th17 cell function. *Pharmacol. Ther.* **245**, 108411, (2023).

66 Kidani, Y. & Bensinger, S. J. Reviewing the impact of lipid synthetic flux on Th17 function. *Curr. Opin. Immunol.* **46**, 121-126, (2017).

67 Takeuchi, H. *et al.* Retinoid X receptor agonists modulate Foxp3+ regulatory T cell and Th17 cell differentiation with differential dependence on retinoic acid receptor activation. *J. Immunol.* **191**, 3725-3733, (2013).

68 Laguna-Fernandez, A. *et al.* ERV1/ChemR23 signaling protects against atherosclerosis by modifying oxidized low-density lipoprotein uptake and phagocytosis in macrophages. *Circulation* **138**, 1693-1705, (2018).

Supplemental information

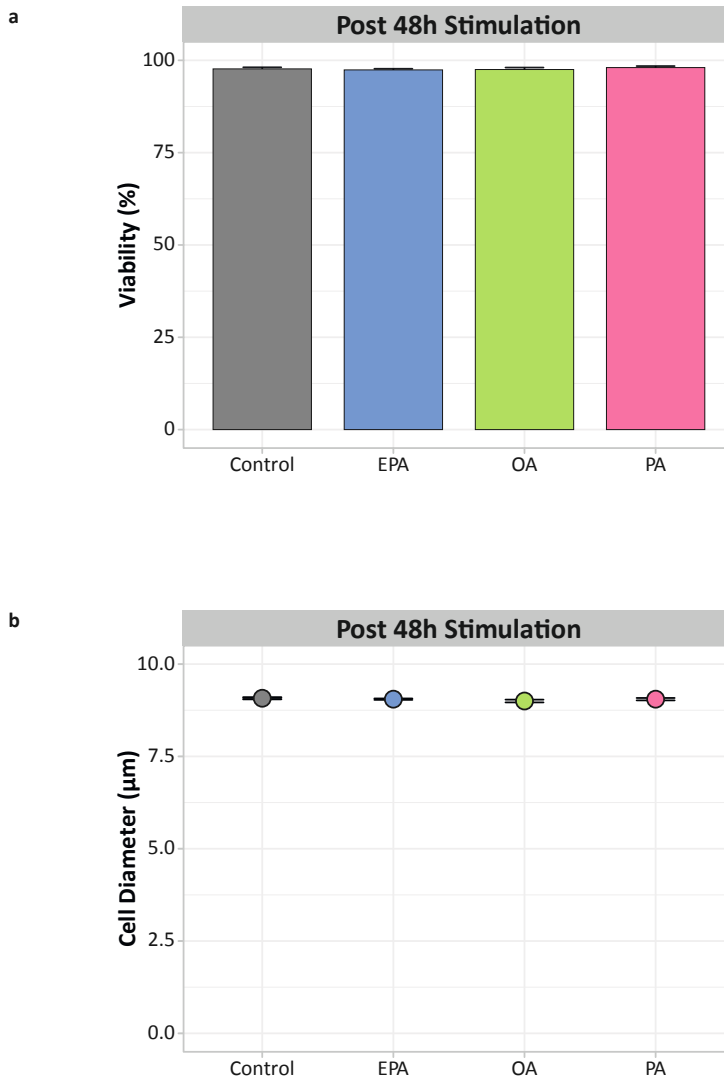

Supplemental Fig. 1 | Verification of viability and cell diameter post-exposure for RNA sequencing. (a) Bar plot showing the average cell viability and standard error in percent, as determined by Via1-Cassette™ on a NucleoCounter® NC-200™. On average the cell viability of control exposed cells was 97.7 SE 0.4%, EPA exposed cells was 97.4 SE 0.3% ($p > 0.05$), OA exposed cells was 97.5 SE 0.5% ($p > 0.05$), and PA exposed cells was 98.0 SE 0.4% ($p > 0.05$) at 48h. Thus, there was no effect on $CD4^+$ T cell viability after 48h exposure, n = 8. **(b)** Dot plot showing the average cell diameter and standard error in µm, as determined by Via1-Cassette™ on a NucleoCounter® NC-200™. On average the cell diameter of control exposed cells was 9.1 SE 0.03µm, EPA exposed cells was 9.1 SE 0.02µm ($p > 0.05$), OA exposed cells was 9.0 SE 0.04µm ($p > 0.05$), and PA exposed cells was 9.1 SE 0.03µm ($p > 0.05$) at 48h. Thus, there was no effect on $CD4^+$ T cell diameter after 48h exposure, n = 8. Abbreviations, EPA = eicosapentaenoic acid, h = hours, OA = oleic acid, PA = palmitic acid.

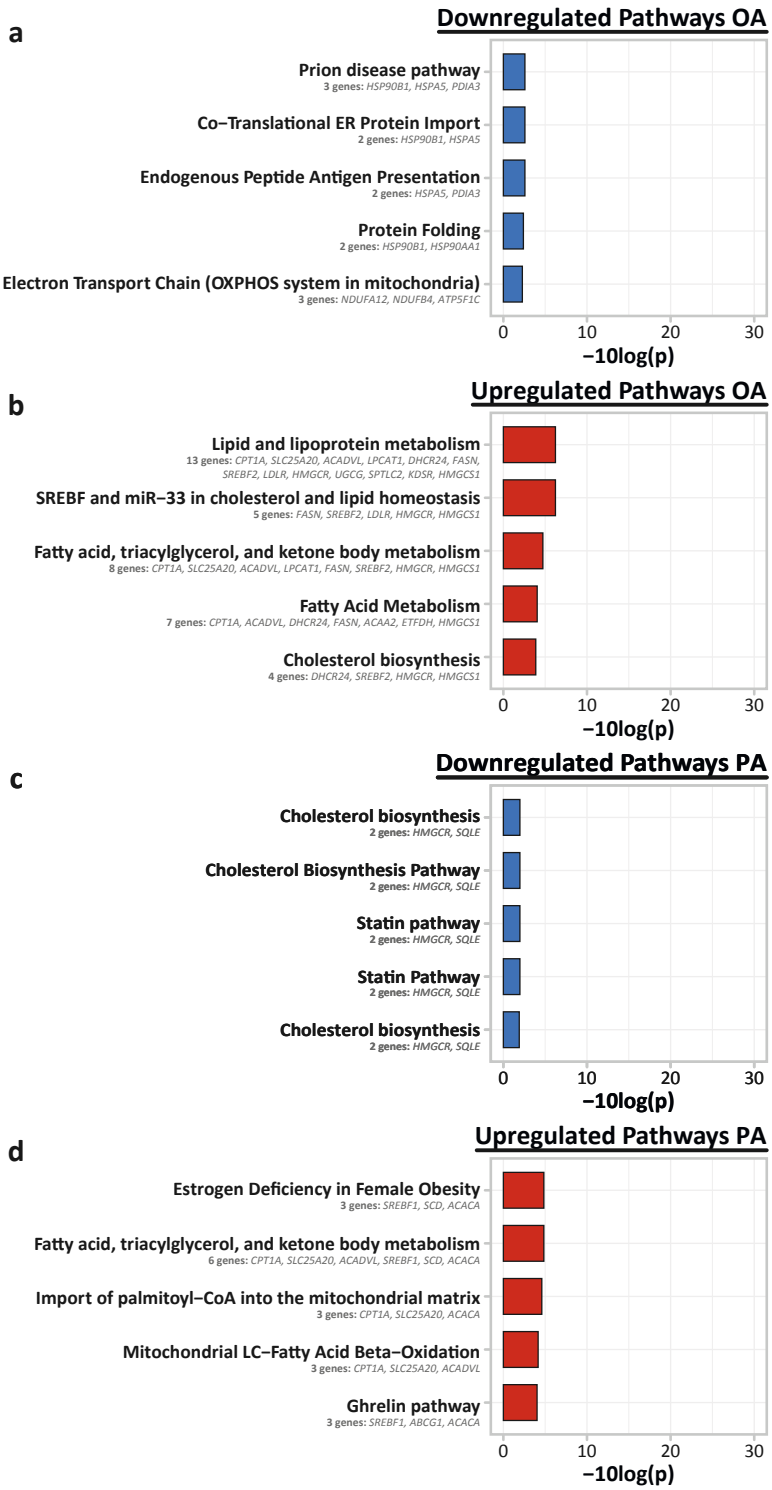
a
Downregulated Pathways OA
Prion disease pathway
3 genes: HSP90B1, HSPA5, PDIA3
Co–Translational ER Protein Import
2 genes: HSP90B1, HSPA5
Endogenous Peptide Antigen Presentation
2 genes: HSPA5, PDIA3
Protein Folding
2 genes: HSP90B1, HSP90AA1
Electron Transport Chain (OXPHOS system in mitochondria)
3 genes: NDUFA12, NDUFB4, ATP5F1C
0
10
20
30
−10log(p)
b
Upregulated Pathways OA
Lipid and lipoprotein metabolism
13 genes: CPT1A, SLC25A20, ACADVL, LPCAT1, DHCR24, FASN, SREBF2, LDLR, HMGCR, UGCG, SPTLC2, KDSR, HMGCS1
SREBF and miR–33 in cholesterol and lipid homeostasis
5 genes: FASN, SREBF2, LDLR, HMGCR, HMGCS1
Fatty acid, triacylglycerol, and ketone body metabolism
8 genes: CPT1A, SLC25A20, ACADVL, LPCAT1, FASN, SREBF2, HMGCR, HMGCS1
Fatty Acid Metabolism
7 genes: CPT1A, ACADVL, DHCR24, FASN, ACAA2, ETFDH, HMGCS1
Cholesterol biosynthesis
4 genes: DHCR24, SREBF2, HMGCR, HMGCS1
0
10
20
30
−10log(p)
c
Downregulated Pathways PA
Cholesterol biosynthesis
2 genes: HMGCR, SQLE
Cholesterol Biosynthesis Pathway
2 genes: HMGCR, SQLE
Statin pathway
2 genes: HMGCR, SQLE
Statin Pathway
2 genes: HMGCR, SQLE
Cholesterol biosynthesis
2 genes: HMGCR, SQLE
0
10
20
30
−10log(p)
d
Upregulated Pathways PA
Estrogen Deficiency in Female Obesity
3 genes: SREBF1, SCD, ACACA
Fatty acid, triacylglycerol, and ketone body metabolism
6 genes: CPT1A, SLC25A20, ACADVL, SREBF1, SCD, ACACA
Import of palmitoyl–CoA into the mitochondrial matrix
3 genes: CPT1A, SLC25A20, ACACA
Mitochondrial LC–Fatty Acid Beta–Oxidation
3 genes: CPT1A, SLC25A20, ACADVL
Ghrelin pathway
3 genes: SREBF1, ABCG1, ACACA
0
10
20
30
−10log(p)

Supplemental Fig. 2 | Up- and downregulated pathways in PA and OA-exposed non-activated $CD4^+$ T cells. **(a)** Pathway enrichment analysis of all downregulated OA DEGs generated using *clusterProfiler* using 10 human pathway databases. Top 5 enrichments are shown. **(b)** Pathway enrichment analysis of all upregulated OA DEGs generated using *clusterProfiler* using 10 human pathway databases. Top 5 enrichments are shown. **(c)** Pathway enrichment analysis of all downregulated PA DEGs generated using *clusterProfiler* using 10 human pathway databases. Top 5 enrichments are shown. **(d)** Pathway enrichment analysis of all upregulated PA DEGs generated using *clusterProfiler* using 10 human pathway databases. Top 5 enrichments are shown. Abbreviations, OA = oleic acid, PA = palmitic acid.

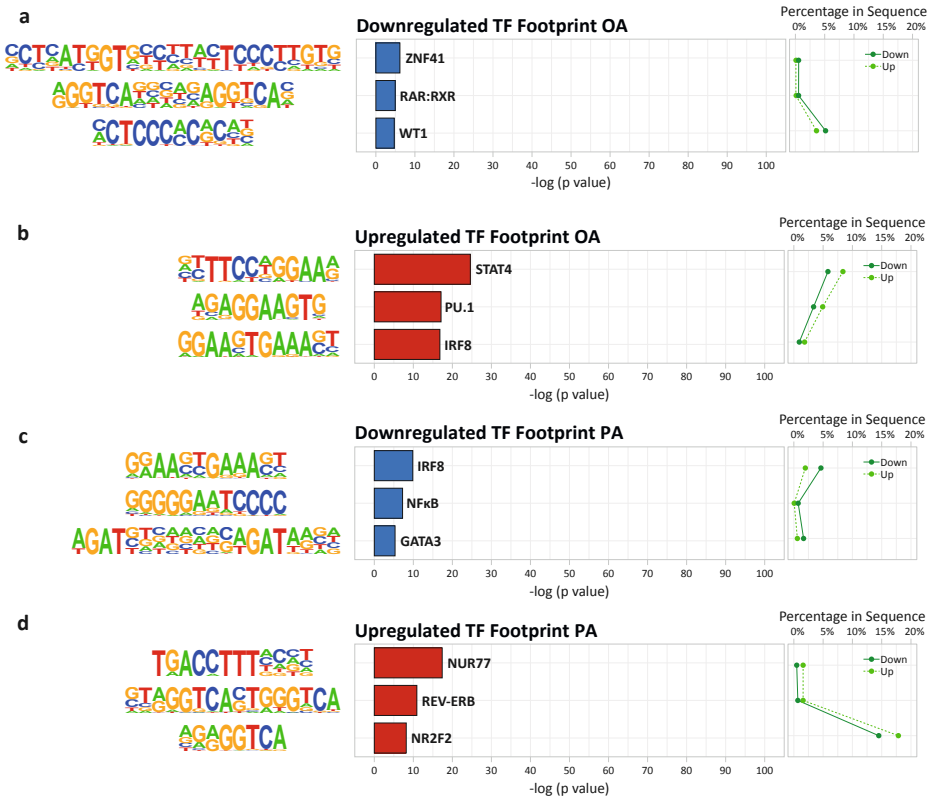

Supplemental Fig. 3 | Up- and downregulated transcription factors in PA and OA-exposed non-activated CD4+ T cells. (a) Known motif analysis on promotors of down versus upregulated OA ATAC peaks. Enrichment of transcription factor binding motifs was performed using HOMER. 3 motifs are shown with supplementing information on p-value, percentage of genes in upregulated gene set and percentage of genes in downregulated gene set, transcription factor name, -log(p-value), and percentage in sequence. **(b)** Known motif analysis on promotors of up versus downregulated OA ATAC peaks. Enrichment of transcription factor binding motifs was performed using HOMER. 4 motifs are shown with supplementing information on p-value, percentage of genes in upregulated gene set and percentage of genes in downregulated gene set, transcription factor name, -log(p-value), and percentage in sequence. **(c)** Known motif analysis on promotors of down versus upregulated PA ATAC peaks. Enrichment of transcription factor binding motifs was performed using HOMER. 3 motifs are shown with supplementing information on p-value, percentage of genes in upregulated gene set and percentage of genes in downregulated gene set, transcription factor name, -log(p-value), and percentage in sequence. **(d)** Known motif analysis on promotors of up versus downregulated PA ATAC peaks. Enrichment of transcription factor binding motifs was performed using HOMER. 4 motifs are shown with supplementing information on p-value, percentage of genes in upregulated gene set and percentage of genes in downregulated gene set, transcription factor name, -log(p-value), and percentage in sequence. Abbreviations, OA = oleic acid, PA = palmitic acid, TF = transcription factor.

Supplemental Table 1 | Changes in gene expression and $CD4^+$ T cell markers due to EPA, PA, or OA exposure.

Supplemental Table 1 | (a) (partial) Downregulated DEGs for EPA exposed non-activated $CD4^+$ T cells in order of significance along with their Ensembl ID, gene symbol, UniProt ID, base mean, log2 fold change, log fold change standard error, p value, and adjusted p value (FDR). Top 30 most significantly expressed genes are shown here.

Order	Ensembl ID	Gene Symbol	UniProt	baseMean	log2FC	log2FC SE	P value	P_{FDR}
1	ENSG00000026025	*VIM*	P08670	10461.483	-0.686	0.075	4.44E-20	1.44E-16
2	ENSG00000205542	*TMSB4X*	P62328	48176.611	-0.577	0.072	7.52E-16	1.08E-12
3	ENSG00000204287	*HLA-DRA*	P01903	633.049	-1.137	0.147	1.27E-14	1.32E-11
4	ENSG00000138326	*RPS24*	P62847	18476.569	-0.730	0.095	1.33E-14	1.32E-11
5	ENSG00000231389	*HLA-DPA1*	P20036	417.419	-0.963	0.130	1.43E-13	1.16E-10
6	ENSG00000026950	*BTN3A1*	O00481	2825.734	-0.939	0.131	7.52E-13	5.12E-10
7	ENSG00000106952	*TNFSF8*	P32971	1146.126	-0.816	0.114	9.00E-13	5.83E-10
8	ENSG00000034510	*TMSB10*	P63313	16350.584	-0.622	0.092	1.37E-11	6.08E-09
9	ENSG00000118181	*RPS25*	P62851	30745.712	-0.533	0.079	1.41E-11	6.08E-09
10	ENSG00000223865	*HLA-DPB1*	P04440	318.848	-1.159	0.174	2.74E-11	1.11E-08
11	ENSG00000186470	*BTN3A2*	P78410	3097.909	-0.814	0.125	7.80E-11	2.65E-08
12	ENSG00000240065	*PSMB9*	P28065	851.254	-0.822	0.127	1.09E-10	3.44E-08
13	ENSG00000111801	*BTN3A3*	O00478	2129.494	-0.732	0.114	1.32E-10	4.08E-08
14	ENSG00000100097	*LGALS1*	P09382	476.452	-0.723	0.113	1.68E-10	4.93E-08
15	ENSG00000204592	*HLA-E*	P13747	21754.754	-0.713	0.112	1.76E-10	4.96E-08
16	ENSG00000255150	*EID3*	Q8N140	109.010	-1.274	0.200	1.76E-10	4.96E-08
17	ENSG00000120833	*SOCS2*	O14508	272.816	-0.932	0.147	2.27E-10	6.12E-08
18	ENSG00000160856	*FCRL3*	Q96P31	201.018	-1.190	0.189	3.06E-10	7.76E-08
19	ENSG00000019582	*CD74*	P04233	2645.553	-0.622	0.099	3.92E-10	9.74E-08
20	ENSG00000008517	*IL32*	P24001	4786.915	-0.671	0.107	4.11E-10	1.00E-07
21	ENSG00000185880	*TRIM69*	Q86WT6	867.798	-0.572	0.092	5.10E-10	1.22E-07
22	ENSG00000131981	*LGALS3*	P17931	568.618	-0.653	0.107	9.88E-10	2.28E-07
23	ENSG00000113088	*GZMK*	P49863	365.982	-1.139	0.187	1.02E-09	2.31E-07

[continued on next page]

Supplemental Table 1 | (a) (partial) *[continued]*

Order	Ensembl ID	Gene Symbol	UniProt	baseMean	log2FC	log2FC SE	P value	P_{FDR}
24	ENSG00000107736	*CDH23*	Q9H251	268.652	-1.072	0.177	1.35E-09	3.02E-07
25	ENSG00000243335	*KCTD7*	Q96MP8	1002.502	-0.512	0.085	1.40E-09	3.07E-07
26	ENSG00000114737	*CISH*	Q9NSE2	599.263	-0.822	0.137	2.18E-09	4.55E-07
27	ENSG00000196126	*HLA-DRB1*	P01911	300.924	-1.002	0.168	2.43E-09	5.00E-07
28	ENSG00000130755	*GMFG*	O60234	3215.210	-0.548	0.092	2.54E-09	5.14E-07
29	ENSG00000143947	*RPS27A*	P62979	45091.864	-0.408	0.069	3.60E-09	6.96E-07
30	ENSG00000101608	*MYL12A*	P19105	7915.620	-0.504	0.086	3.78E-09	7.19E-07

Supplemental Table 1 | (b) (partial) Upregulated DEGs for EPA exposed non-activated CD4+ T cells in order of significance along with their Ensembl ID, gene symbol, UniProt ID, base mean, log2 fold change, log fold change standard error, p value, and adjusted p value (FDR). Top 30 most significantly expressed genes are shown here.

Order	Ensembl ID	Gene Symbol	UniProt	baseMean	log2FC	log2FC SE	P value	P_{FDR}
1	ENSG00000181019	*NQO1*	P15559	346.693	2.457	0.218	2.37E-29	3.07E-25
2	ENSG00000113369	*ARRDC3*	Q96B67	3175.559	1.305	0.118	2.59E-28	1.68E-24
3	ENSG00000110090	*CPT1A*	P50416	603.707	2.716	0.270	8.52E-24	3.68E-20
4	ENSG00000103257	*SLC7A5*	Q01650	1346.098	1.219	0.133	5.98E-20	1.55E-16
5	ENSG00000115758	*ODC1*	P11926	1660.221	1.023	0.120	1.56E-17	3.37E-14
6	ENSG00000178537	*SLC25A20*	O43772	267.897	1.144	0.136	3.55E-17	6.57E-14
7	ENSG00000090861	*AARS1*	P49588	4381.327	0.697	0.084	7.34E-17	1.19E-13
8	ENSG00000135069	*PSAT1*	Q9Y617	1488.575	1.086	0.136	1.18E-15	1.53E-12
9	ENSG00000001084	*GCLC*	P48506	1258.380	0.872	0.109	1.31E-15	1.54E-12
10	ENSG00000167703	*SLC43A2*	Q8N370	169.252	2.053	0.273	5.60E-14	5.17E-11
11	ENSG00000125534	*PPDPF*	Q9H3Y8	1332.610	0.876	0.118	9.86E-14	8.50E-11
12	ENSG00000172613	*RAD9A*	Q99638	820.146	0.823	0.113	3.95E-13	3.01E-10
13	ENSG00000139514	*SLC7A1*	P30825	1604.807	0.522	0.073	6.51E-13	4.68E-10

[continued on next page]

Supplemental Table 1 | (b) (partial) *[continued]*

Order	Ensembl ID	Gene Symbol	UniProt	baseMean	log2FC	log2FC SE	P value	P_{FDR}
14	ENSG00000051108	*HERPUD1*	Q15011	1950.929	0.623	0.087	1.07E-12	6.59E-10
15	ENSG00000197063	*MAFG*	O15525	646.794	1.042	0.148	1.68E-12	9.53E-10
16	ENSG00000116852	*KIF21B*	O75037	5536.202	0.782	0.111	1.69E-12	9.53E-10
17	ENSG00000100292	*HMOX1*	P09601	118.300	4.091	0.583	2.20E-12	1.19E-09
18	ENSG00000198830	*HMGN2*	P05204	4201.608	0.462	0.066	2.80E-12	1.45E-09
19	ENSG00000113407	*TARS1*	P26639	3883.418	0.621	0.090	4.95E-12	2.46E-09
20	ENSG00000162413	*KLHL21*	Q9UJP4	1585.720	0.772	0.112	5.78E-12	2.77E-09
21	ENSG00000168003	*SLC3A2*	P08195	5743.672	1.397	0.204	7.76E-12	3.58E-09
22	ENSG00000072778	*ACADVL*	P49748	3071.367	0.541	0.081	2.37E-11	9.91E-09
23	ENSG00000196305	*IARS1*	P41252	3525.848	0.446	0.067	3.64E-11	1.43E-08
24	ENSG00000128965	*CHAC1*	Q9BUX1	266.899	1.461	0.221	4.02E-11	1.53E-08
25	ENSG00000082898	*XPO1*	O14980	4845.018	0.824	0.126	5.09E-11	1.88E-08
26	ENSG00000139112	*GABARAPL1*	Q9H0R8	821.575	1.034	0.158	6.32E-11	2.27E-08
27	ENSG00000087086	*FTL*	P02792	23835.068	0.800	0.123	6.97E-11	2.44E-08
28	ENSG00000134294	*SLC38A2*	Q96QD8	5627.146	0.676	0.104	9.33E-11	3.10E-08
29	ENSG00000166986	*MARS1*	P56192	5359.986	0.444	0.069	1.00E-10	3.24E-08
30	ENSG00000198743	*SLC5A3*	P53794	1939.433	0.860	0.135	1.66E-10	4.93E-08

Supplemental Table 1 | (c) Downregulated DEGs for OA exposed non-activated $CD4^+$ T cells in order of significance along with their Ensembl ID, gene symbol, UniProt ID, base mean, log2 fold change, log fold change standard error, p value, and adjusted p value (FDR).

Order	Ensembl ID	Gene Symbol	UniProt	baseMean	log2FC	log2FC SE	P value	P_{FDR}
1	ENSG00000205542	*TMSB4X*	P62328	53784.953	-0.300	0.063	1.93E-06	0.00146
2	ENSG00000166598	*HSP90B1*	P14625	9262.938	-0.336	0.071	2.02E-06	0.00146
3	ENSG00000044574	*HSPA5*	P11021	5535.011	-0.382	0.081	2.19E-06	0.00149
4	ENSG00000184752	*NDUFA12*	Q9UI09	1467.880	-0.347	0.082	2.55E-05	0.01178
5	ENSG00000111348	*ARHGDIB*	P52566	18341.064	-0.224	0.057	9.10E-05	0.03021

[continued on next page]

Supplemental Table 1 | (c) *[continued]*

Order	Ensembl ID	Gene Symbol	UniProt	baseMean	log2FC	log2FC SE	P value	P_{FDR}
6	ENSG00000065518	*NDUFB4*	O95168	923.826	-0.345	0.090	0.000119	0.03589
7	ENSG00000167004	*PDIA3*	P30101	5053.715	-0.275	0.072	0.000135	0.03820
8	ENSG00000034510	*TMSB10*	P63313	18121.778	-0.287	0.076	0.000146	0.03951
9	ENSG00000265972	*TXNIP*	Q9H3M7	19375.847	-0.185	0.049	0.000150	0.03973
10	ENSG00000145050	*MANF*	P55145	661.685	-0.427	0.113	0.000159	0.04114
11	ENSG00000111481	*COPZ1*	P61923	1920.473	-0.221	0.060	0.000207	0.04787
12	ENSG00000165629	*ATP5F1C*	P36542	1803.183	-0.277	0.075	0.000211	0.04787
13	ENSG00000080824	*HSP90AA1*	P07900	12647.574	-0.264	0.072	0.000222	0.04787

Supplemental Table 1 | (d) (partial) Upregulated DEGs for OA exposed non-activated CD4+ T cells in order of significance along with their Ensembl ID, gene symbol, UniProt ID, base mean, log2 fold change, log fold change standard error, p value, and adjusted p value (FDR). Top 30 most significantly expressed genes are shown here.

Order	Ensembl ID	Gene Symbol	UniProt	baseMean	log2FC	log2FC SE	P value	P_{FDR}
1	ENSG00000110090	*CPT1A*	P50416	893.439	3.460	0.110	2.87E-218	3.71E-214
2	ENSG00000178537	*SLC25A20*	O43772	352.353	1.669	0.121	1.34E-43	8.65E-40
3	ENSG00000145860	*RNF145*	Q96MT1	2335.306	0.638	0.068	7.35E-21	3.17E-17
4	ENSG00000072778	*ACADVL*	P49748	3128.902	0.557	0.064	2.87E-18	9.28E-15
5	ENSG00000143110	*C1orf162*	Q8NEQ5	1332.128	0.522	0.072	3.78E-13	9.78E-10
6	ENSG00000153395	*LPCAT1*	Q8NF37	1527.598	0.473	0.067	1.35E-12	2.59E-09
7	ENSG00000184602	*SNN*	O75324	905.754	0.581	0.082	1.40E-12	2.59E-09
8	ENSG00000116133	*DHCR24*	Q15392	474.003	0.588	0.093	3.08E-10	4.98E-07
9	ENSG00000169710	*FASN*	P49327	866.664	0.680	0.116	4.68E-09	6.74E-06
10	ENSG00000198911	*SREBF2*	Q12772	3184.981	0.390	0.070	2.37E-08	3.07E-05
11	ENSG00000102032	*RENBP*	P51606	250.558	0.747	0.142	1.57E-07	0.000184
12	ENSG00000130164	*LDLR*	P01130	1013.144	0.461	0.088	1.87E-07	0.000202
13	ENSG00000167315	*ACAA2*	P42765	483.439	0.558	0.108	2.23E-07	0.000222

[continued on next page]

Supplemental Table 1 | (d) (partial) *[continued]*

Order	Ensembl ID	Gene Symbol	UniProt	baseMean	log2FC	log2FC SE	P value	P_{FDR}
14	ENSG00000166575	*TMEM135*	Q86UB9	161.166	0.722	0.146	7.39E-07	0.000683
15	ENSG00000167106	*FAM102A*	Q5T9C2	7915.593	0.290	0.060	1.43E-06	0.001236
16	ENSG00000103249	*CLCN7*	P51798	1764.038	0.411	0.086	1.88E-06	0.001456
17	ENSG00000069424	*KCNAB2*	Q13303	4855.716	0.308	0.065	2.30E-06	0.001489
18	ENSG00000113161	*HMGCR*	P04035	913.374	0.369	0.081	5.52E-06	0.003402
19	ENSG00000198355	*PIM3*	Q86V86	716.562	0.450	0.102	1.05E-05	0.006197
20	ENSG00000171503	*ETFDH*	Q16134	301.259	0.553	0.127	1.41E-05	0.007922
21	ENSG00000140526	*ABHD2*	P08910	1283.746	0.291	0.068	1.70E-05	0.009194
22	ENSG00000174903	*RAB1B*	Q9H0U4	2107.877	0.334	0.078	1.95E-05	0.010094
23	ENSG00000106266	*SNX8*	Q9Y5X2	144.357	0.710	0.168	2.40E-05	0.011780
24	ENSG00000079432	*CIC*	Q96RK0	2107.033	0.347	0.082	2.53E-05	0.011780
25	ENSG00000163162	*RNF149*	Q8NC42	1907.621	0.340	0.081	3.02E-05	0.013471
26	ENSG00000161011	*SQSTM1*	Q13501	3912.137	0.262	0.063	3.26E-05	0.014059
27	ENSG00000172059	*KLF11*	O14901	161.305	0.718	0.174	3.65E-05	0.015237
28	ENSG00000158470	*B4GALT5*	O43286	294.347	0.478	0.120	6.72E-05	0.026870
29	ENSG00000011021	*CLCN6*	P51797	556.903	0.388	0.098	6.85E-05	0.026870
30	ENSG00000113163	*CERT1*	Q9Y5P4	911.346	0.347	0.088	7.53E-05	0.028490

Supplemental Table 1 | (e) Downregulated DEGs for PA exposed non-activated $CD4^+$ T cells in order of significance along with their Ensembl ID, gene symbol, UniProt ID, base mean, log2 fold change, log fold change standard error, p value, and adjusted p value (FDR).

Order	Ensembl ID	Gene Symbol	UniProt	baseMean	log2FC	log2FC SE	P value	P_{FDR}
1	ENSG00000117632	*STMN1*	P16949	1324.856	-0.407	0.067	1.44E-09	2.68E-06
2	ENSG00000163659	*TIPARP*	Q7Z3E1	2383.237	-0.329	0.058	1.57E-08	2.04E-05
3	ENSG00000153395	*LPCAT1*	Q8NF37	1166.324	-0.276	0.058	2.38E-06	0.00257
4	ENSG00000113161	*HMGCR*	P04035	726.112	-0.325	0.070	3.58E-06	0.00328
5	ENSG00000118816	*CCNI*	Q14094	4732.443	-0.218	0.047	3.99E-06	0.00328

[continued on next page]

Supplemental Table 1 | (e) *[continued]*

Order	Ensembl ID	Gene Symbol	UniProt	baseMean	log2FC	log2FC SE	P value	P_{FDR}
6	ENSG00000145741	*BTF3*	P20290	10617.724	-0.255	0.056	4.30E-06	0.00328
7	ENSG00000006451	*RALA*	P11233	1137.560	-0.283	0.067	2.66E-05	0.01724
8	ENSG00000145860	*RNF145*	Q96MT1	1666.498	-0.287	0.069	2.81E-05	0.01733
9	ENSG00000187109	*NAP1L1*	P55209	12784.530	-0.322	0.077	3.00E-05	0.01768
10	ENSG00000128989	*ARPP19*	P56211	1868.746	-0.278	0.067	3.43E-05	0.01932
11	ENSG00000104549	*SQLE*	Q14534	334.452	-0.364	0.090	4.68E-05	0.02427
12	ENSG00000117592	*PRDX6*	P30041	1454.171	-0.211	0.053	7.87E-05	0.03518
13	ENSG00000153283	*CD96*	P40200	6532.967	-0.210	0.054	0.000104	0.04298
14	ENSG00000130741	*EIF2S3*	P41091	5440.858	-0.211	0.055	0.000107	0.04298
15	ENSG00000125868	*DSTN*	P60981	923.114	-0.270	0.070	0.000109	0.04298

Supplemental Table 1 | (f) Upregulated DEGs for PA exposed non-activated $CD4^+$ T cells in order of significance along with their Ensembl ID, gene symbol, UniProt ID, base mean, log2 fold change, log fold change standard error, p value, and adjusted p value (FDR).

Order	Ensembl ID	Gene Symbol	UniProt	baseMean	log2FC	log2FC SE	P value	P_{FDR}
1	ENSG00000110090	*CPT1A*	P50416	709.522	3.173	0.112	1.88E-177	2.44E-173
2	ENSG00000178537	*SLC25A20*	O43772	328.362	1.552	0.099	1.28E-55	8.30E-52
3	ENSG00000072778	*ACADVL*	P49748	3226.461	0.642	0.055	3.26E-31	1.41E-27
4	ENSG00000072310	*SREBF1*	P36956	748.306	1.252	0.125	1.23E-23	3.99E-20
5	ENSG00000143110	*C1orf162*	Q8NEQ5	1302.359	0.464	0.058	1.83E-15	4.76E-12
6	ENSG00000111684	*LPCAT3*	Q6P1A2	415.027	0.690	0.109	2.26E-10	4.89E-07
7	ENSG00000160179	*ABCG1*	P45844	158.548	1.060	0.176	1.75E-09	2.84E-06
8	ENSG00000167315	*ACAA2*	P42765	486.997	0.560	0.095	3.79E-09	5.47E-06
9	ENSG00000166575	*TMEM135*	Q86UB9	164.063	0.743	0.148	5.64E-07	0.000665
10	ENSG00000149428	*HYOU1*	Q9Y4L1	2099.100	0.321	0.069	3.85E-06	0.003283
11	ENSG00000099194	*SCD*	O00767	183.550	0.595	0.129	4.11E-06	0.003283

[continued on next page]

Supplemental Table 1 | (f) *[continued]*

Order	Ensembl ID	Gene Symbol	UniProt	baseMean	log2FC	log2FC SE	P value	P_{FDR}
12	ENSG00000196155	*PLEKHG4*	Q58EX7	674.104	0.305	0.072	2.22E-05	0.015991
13	ENSG00000182871	*COL18A1*	P39060	687.338	0.507	0.120	2.49E-05	0.016984
14	ENSG00000278540	*ACACA*	Q13085	410.104	0.359	0.088	4.54E-05	0.024270
15	ENSG00000141524	*TMC6*	Q7Z403	9025.505	0.274	0.068	5.20E-05	0.025954
16	ENSG00000079432	*CIC*	Q96RK0	2111.939	0.362	0.091	7.28E-05	0.034997
17	ENSG00000182095	*TNRC18*	O15417	1055.115	0.343	0.087	7.56E-05	0.035038
18	ENSG00000155090	*KLF10*	Q13118	39.296	1.179	0.302	9.28E-05	0.040127

Supplemental Table 1 | (g) Table showing additional information on the genes that overlap between the different fatty acids. Information on Gene Symbol, Ensembl ID, chromosome location, log2 fold change of that gene in each specific fatty acid, p value of that gene in each specific fatty acid, adjusted p value of that gene in each specific fatty acid, and whether the direction of gene expression is the same in each fatty acid is included.

Overlapping Genes	Ensembl ID	log2FC EPA	log2FC OA	log2FC PA	P value EPA	P value OA	P value PA	P_{FDR} EPA	P_{FDR} OA	P_{FDR} PA	Direction Same
Overlapping Genes EPA vs OA vs PA											
CPT1A	ENSG00000110090	2.716	3.460	3.173	8.52E-24	2.87E-218	1.88E-177	3.68E-20	3.71E-214	2.44E-173	Yes Up
SLC25A20	ENSG00000178537	1.144	1.669	1.552	3.55E-17	1.34E-43	1.28E-55	6.57E-14	8.65E-40	8.30E-52	Yes Up
ACADVL	ENSG00000072778	0.541	0.557	0.642	2.37E-11	2.87E-18	3.26E-31	9.91E-09	9.28E-15	1.41E-27	Yes Up
ACAA2	ENSG00000167315	0.340	0.558	0.560	0.00177	2.23E-07	3.79E-09	0.02553	0.00022	5.47E-06	Yes Up
Overlapping Genes EPA vs OA											
TMSB4X	ENSG00000205542	-0.577	-0.300		7.52E-16	1.93E-06		1.08E-12	0.00146		Yes Down
PPDPF	ENSG00000125534	0.876	0.298		9.86E-14	0.00017		8.50E-11	0.04178		Yes Up
TMSB10	ENSG00000034510	-0.622	-0.287		1.37E-11	0.00015		6.08E-09	0.03951		Yes Down
CLCN7	ENSG00000103249	0.599	0.411		1.76E-09	1.88E-06		3.74E-07	0.00146		Yes Up
ETFDH	ENSG00000171503	0.758	0.553		1.98E-08	1.41E-05		2.84E-06	0.00792		Yes Up
SQSTM1	ENSG00000161011	0.618	0.262		4.20E-08	3.26E-05		5.49E-06	0.01406		Yes Up
RENBP	ENSG00000102032	0.716	0.747		8.37E-06	1.57E-07		0.00042	0.00018		Yes Up
PIM3	ENSG00000198355	0.479	0.450		2.24E-05	1.05E-05		0.00091	0.00620		Yes Up

[continued on next page]

Supplemental Table 1 | (g) *[continued]*

Overlapping Genes	Ensembl ID	log2FC EPA	log2FC OA	log2FC PA	P value EPA	P value OA	P value PA	P_{FDR} EPA	P_{FDR} OA	P_{FDR} PA	Direction Same
TXNIP	ENSG00000265972	-0.278	-0.185		2.93E-05	0.00015		0.00113	0.03973		Yes Down
CLCN6	ENSG00000011021	0.522	0.388		4.06E-05	6.85E-05		0.00147	0.02687		Yes Up
FLCN	ENSG00000154803	0.348	0.260		4.13E-05	9.78E-05		0.00149	0.03165		Yes Up
AMDHD2	ENSG00000162066	0.537	0.482		0.00012	8.14E-05		0.00352	0.02849		Yes Up
PPP1R15A	ENSG00000087074	0.459	0.344		0.00023	0.00022		0.00547	0.04787		Yes Up
HSP90B1	ENSG00000166598	-0.305	-0.336		0.00035	2.02E-06		0.00764	0.00146		Yes Down
ARHGDIB	ENSG00000111348	-0.247	-0.224		0.00067	9.10E-05		0.01230	0.03021		Yes Down
SNX8	ENSG00000106266	0.576	0.710		0.00124	2.40E-05		0.01963	0.01178		Yes Up
ATXN2L	ENSG00000168488	0.264	0.254		0.00133	0.00022		0.02050	0.04787		Yes Up
HSPA5	ENSG00000044574	-0.237	-0.382		0.00197	2.19E-06		0.02764	0.00149		Yes Down
Overlapping Genes EPA vs PA											
CD96	ENSG00000153283	-0.419		-0.210	6.55E-08		0.00010	7.70E-06		0.04298	Yes Down
TNRC18	ENSG00000182095	0.355		0.343	0.00012		7.56E-05	0.00353		0.03504	Yes Up
PLEKHG4	ENSG00000196155	-0.417		0.305	0.00128		2.22E-05	0.02012		0.01599	No EPA Down PA Up

[continued on next page]

Supplemental Table 1 | (g) *[continued]*

Overlapping Genes	Ensembl ID	log2FC EPA	log2FC OA	log2FC PA	P value EPA	P value OA	P value PA	P_{FDR} EPA	P_{FDR} OA	P_{FDR} PA	Direction Same
COL18A1	ENSG00000182871	-0.565		0.507	0.00196		2.49E-05	0.02757		0.01698	Yes Up
Overlapping Genes OA vs PA											
RNF145	ENSG00000145860		0.638	-0.287		7.35E-21	2.81E-05		3.17E-17	0.01733	No OA Up PA Down
C1orf162	ENSG00000143110		0.522	0.464		3.78E-13	1.83E-15		9.78E-10	4.76E-12	Yes Up
LPCAT1	ENSG00000111684		0.473	0.690		1.35E-12	2.26E-10		2.59E-09	4.89E-07	Yes Up
TMEM135	ENSG00000166575		0.722	0.743		7.39E-07	5.64E-07		0.00068	0.00067	Yes Up
HMGCR	ENSG00000113161		0.369	-0.325		5.52E-06	3.58E-06		0.00340	0.00328	No OA Up PA Down
CIC	ENSG00000079432		0.347	0.362		2.53E-05	7.28E-05		0.01178	0.03500	Yes Up
KLF10	ENSG00000155090		1.297	1.179		0.00017	9.28E-05		0.04178	0.04013	Yes Up

Supplemental Table 1 | (h) (partial) Pathway enrichment analysis of all downregulated EPA DEGs generated using *clusterProfiler* using 10 human pathway databases. Enriched pathways are shown with information on which group that term clusters into based on the Jaccard index > 0.70, pathway term, number of DEGs that overlap with that databases gene set for that pathway, p value, adjusted p value, number of DEGs in that pathway that were upregulated, number of DEGs in that pathway that were downregulated, and gene names of all DEGs included in that pathway. Only the top term of the first 20 groups are shown here.

Group	Term	Overlap	P value	Adjusted P value	Up-regulated	Down-regulated	Genes
1	Eukaryotic translation elongation	44/85	7.47E-31	1.75E-27	0	44	*RPS24, RPS25, RPS27A, RPL35A, RPS12, RPS15A, RPL30, RPL34, RPS6, RPL23, RPS29, RPL31, RPS7, RPS21, RPS20, RPS23, RPS8, RPS13, RPL21, RPL37, RPL23A, RPL11, RPS27, RPL32, RPL27, RPS3A, EEF1B2, RPL39, RPL38, RPL12, RPL4, RPL10A, RPL41, RPL37A, RPL9, RPL5, RPL24, RPL6, RPL19, UBA52, RPS11, RPL7, RPS18, RPS14*
2	Interleukin-2 signaling pathway	110/728	3.38E-19	5.02E-17	0	110	*VIM, BTN3A1, BTN3A2, BTN3A3, SOCS2, GZMK, CISH, CD69, GBP1, CCR2, DPP4, TAP1, TRIB2, GZMA, CD96, IL2RA, RPS6, S100A11, ITGAM, AIF1, CD52, DENND2D, PTGER2, CASP1, RNF144A, NELL2, FCER1G, NCR3, RPL21, S100A4, MEOX1, CCR5, CD40LG, CTSO, ADTRP, GZMM, MAL, VNN2, CD2, FYN, IL2RG, CTSS, APOBEC3G, IL4R, MT2A, CYP1A1, LITAF, VAMP5, RGS10, SELL, RBM3, CCR1, TNFRSF1B, IL2RB, NMT2, KCNN4, BTG1, LAT, HEMGN, PDCD4, MLLT3, CD27, LCP2, NKG7, AHNAK, GNLY, ETS1, ACP5, CX3CR1, RAB33A, TBCD, FLOT1, PDE7A, TNFRSF25, IRF1, IFIT1, CD300A, ITGB2, MDFIC, BCL2, ADAM19, TRIM21, TAGLN2, LTB, CCR7, NLRP1, PTPRC, CTSZ, SORL1, TXK, PARP8, TTN, SLA2, GATA3, SAMHD1, CCL5, AP3M2, IQGAP2, FCGBP, CXCL8, SPN, E2F3, TNFSF10, CAMK2N1, CTSH, SIT1, JAK3, PIM1, PRF1, EOMES*
3	Antigen processing and presentation	27/54	7.67E-19	1.10E-16	0	27	*HLA-DRA, HLA-DPA1, HLA-DPB1, PSMB9, HLA-E, CD74, HLA-DRB1, B2M, TAP1, PSME1, HLA-DRB5, HLA-DQA1, CIITA, HLA-DMB, CD8A, CTSS, PSMB8, HLA-B, HLA-F, CD4, HLA-DQB1, HLA-DOA, PSME2, TAP2, HLA-A, HLA-C, HSPA5*
4	Allograft rejection	47/172	1.47E-18	2.03E-16	0	47	*HLA-DRA, HLA-E, CD74, B2M, CCR2, TAP1, GZMA, CD96, IL2RA, KRT1, HLA-DQA1, GBP2, HLA-DMB, CD8A, CCR5, CD40LG, FYB1, RPS3A, CD2, IL2RG, CTSS, IL4R, RPL39, CAPG, CD3D, CCR1, IL2RB, CD4, HLA-DOA, CRTAM, ITGAL, TAP2, ST8SIA4, LCP2, HLA-A, RPL9, ETS1, DARS1, CD3E, ITGB2, LTB, CFP, PTPRC, CCL5, NLRP3, SIT1, PRF1*

[continued on next page]

Supplemental Table 1 | (h) (partial) *[continued]*

Group	Term	Overlap	P value	Adjusted P value	Up-regulated	Down-regulated	Genes
5	Interferon Gamma Response	47/181	1.39E-17	1.80E-15	0	47	*PSMB9, CD74, HLA-DRB1, B2M, CD69, TAP1, GZMA, PSME1, HLA-DQA1, CIITA, CASP1, SAMD9L, OAS2, TXNIP, IL4R, MT2A, SRI, VAMP5, PSMB8, HLA-B, XAF1, IL2RB, BTG1, NLRC5, PSME2, ST8SIA4, LCP2, HLA-A, ZBP1, IRF1, IFIT1, TRIM21, IL10RA, TRIM14, PNP, SLAMF7, OAS3, PARP12, CFH, SAMHD1, CCL5, TNFSF10, FGL2, ST3GAL5, PIM1, RTP4, SP110*
6	Cell adhesion molecules (CAMs)	28/84	6.41E-14	6.94E-12	0	28	*HLA-DRA, HLA-DPA1, HLA-DPB1, HLA-E, HLA-DRB1, CD226, ITGB1, ITGA4, ITGAM, HLA-DRB5, HLA-DQA1, HLA-DMB, CD8A, CD40LG, CD2, HLA-B, HLA-F, SELL, CD4, HLA-DQB1, HLA-DOA, ITGAL, HLA-A, PECAM1, ITGB2, HLA-C, PTPRC, SPN*
7	Immunoregulatory interactions between a lymphoid and a non-lymphoid cell	26/77	3.63E-13	3.73E-11	0	26	*HLA-E, B2M, CD226, IFITM1, CD96, ITGB1, ITGA4, LAIR1, NCR3, CD8A, CD40LG, CD3D, HLA-B, HLA-F, SELL, HCST, CRTAM, ITGAL, HLA-A, TYROBP, CD3E, CD300A, ITGB2, HLA-C, SLAMF7, CD200R1*
8	Cap-dependent translation initiation	25/72	5.04E-13	4.92E-11	0	25	*RPL35A, RPL30, RPL34, RPL23, RPL31, RPL21, RPL37, RPL23A, RPL11, RPL32, RPL27, RPL39, RPL38, RPL12, RPL4, RPL10A, RPL41, RPL37A, RPL9, RPL5, RPL24, RPL6, RPL19, UBA52, RPL7*
9	T cell receptor regulation of apoptosis	76/529	3.50E-12	3.34E-10	0	76	*VIM, RPS24, PSMB9, LGALS1, GBP1, IFITM1, CCR2, TAP1, IL2RA, PSME1, PTMA, RPL23, RPS29, S100A6, RPS20, CASP1, GADD45B, FCER1G, S100A4, RPL37, MCL1, CCR5, CD40LG, MAL, APOL3, RPS3A, CD2, CYBB, PSMB8, HLA-B, CCR1, TNFRSF1B, TRAF1, HLA-DQB1, RAC2, BTG1, ITGAL, RPL10A, PSME2, RPL41, RCBTB2, HSP90B1, TRAF5, PDE7A, HMGB1, TNFRSF25, CD3E, IRF1, ARHGDIB, CLIC5, ITGB2, BCL2, ATM, CDC42, RPL6, LTB, CCR7, NLRP1, PTPRC, RHOH, PNP, TUBB, HSPA5, GATA3, CCL5, IQGAP2, VIPR1, CXCL8, SPN, S100A10, NLRP3, CNBP, DYNLL1, PIM1, RPS14, SH3BGRL*
10	Viral myocarditis	20/50	5.29E-12	4.93E-10	0	20	*HLA-DRA, HLA-DPA1, HLA-DPB1, HLA-E, HLA-DRB1, HLA-DRB5, HLA-DQA1, HLA-DMB, CD40LG, FYN, HLA-B, HLA-F, HLA-DQB1, RAC2, HLA-DOA, ITGAL, HLA-A, ITGB2, HLA-C, PRF1*

[continued on next page]

Supplemental Table 1 | (h) (partial) *[continued]*

Group	Term	Overlap	P value	Adjusted P value	Up-regulated	Down-regulated	Genes
11	Interferon gamma signaling	24/76	1.53E-11	1.28E-09	0	24	*HLA-DRA, HLA-DPA1, HLA-DPB1, HLA-E, HLA-DRB1, B2M, GBP1, HLA-DRB5, HLA-DQA1, CIITA, GBP2, OAS2, GBP5, MT2A, HLA-B, HLA-F, HLA-DQB1, HLA-A, IRF1, TRIM21, HLA-C, CAMK2G, TRIM14, OAS3*
12	Immune system	127/1169	9.49E-11	7.04E-09	0	127	*HLA-DRA, HLA-DPA1, HLA-DPB1, PSMB9, HLA-E, SOCS2, CD74, IL32, TRIM69, LGALS3, CISH, HLA-DRB1, RPS27A, B2M, GBP1, CD226, IFITM1, CCR2, TAP1, CD96, IL2RA, ITGB1, ITGA4, PSME1, NEFL, ITGAM, HLA-DRB5, HLA-DQA1, CIITA, GBP2, TNFSF12, CASP1, HLA-DMB, LAIR1, TNFSF13B, FCER1G, NCR3, CD8A, OAS2, CD40LG, CTSO, GZMM, FYN, TLR5, IL2RG, TXNIP, CTSS, C5AR2, GBP5, P2RX7, MT2A, PTPRJ, CYBB, PSMB8, CD3D, CALM1, HLA-B, HLA-F, SELL, XAF1, TNFRSF1B, GRAP2, IL2RB, HCST, CD4, HLA-DQB1, CNKSR2, LAT, HLA-DOA, CRTAM, ITGAL, NLRC5, CD27, PSME2, TAP2, LCP2, HLA-A, TYROBP, SYNGAP1, MYLIP, HSP90B1, PEBP1, EDAR, ZBP1, HMGB1, TNFRSF25, CD3E, IRF1, ATP6V0E2, IFIT1, CD300A, ITGB2, BCL2, CDC42, TRIM21, HLA-C, CFL1, LTB, THEM4, CAMK2G, ARRB1, NLRP1, PTPRC, TRIM14, SLAMF7, RPS6KA5, ARPC2, TXK, ARPC3, HSPA5, OAS3, FGF9, UBA52, CFH, SAMHD1, UBE2F, FCN1, NUP37, NLRP3, CD200R1, CTSH, AIM2, SKP1, DYNLL1, JAK3, RPS6KA1, BTLA*
13	Phosphorylation of CD3 and TCR zeta chains	12/19	1.14E-10	8.28E-09	0	12	*HLA-DRA, HLA-DPA1, HLA-DPB1, HLA-DRB1, HLA-DRB5, HLA-DQA1, PTPRJ, CD3D, CD4, HLA-DQB1, CD3E, PTPRC*
14	Formation of the ternary complex, and subsequently, the 43S complex	18/49	3.31E-10	2.29E-08	0	18	*RPS24, RPS25, RPS27A, RPS12, RPS15A, RPS6, RPS29, RPS7, RPS21, RPS20, RPS23, RPS8, RPS13, RPS27, RPS3A, RPS11, RPS18, RPS14*
15	Asthma	11/17	4.81E-10	3.16E-08	0	11	*HLA-DRA, HLA-DPA1, HLA-DPB1, HLA-DRB1, HLA-DRB5, HLA-DQA1, HLA-DMB, FCER1G, CD40LG, HLA-DQB1, HLA-DOA*
16	Acute phase in atopic dermatitis	14/30	7.29E-10	4.71E-08	0	14	*IL2RA, MAF, FCER1G, CD40LG, FYN, IL2RG, IL4R, CD3D, IL2RB, CD4, CD3E, PTPRC, GATA3, JAK3*

[continued on next page]

Supplemental Table 1 | (h) (partial) *[continued]*

Group	Term	Overlap	P value	Adjusted P value	Up-regulated	Down-regulated	Genes
17	$CD8^+$ naive T-cell -> $CD4^+$ naive T-cell surface expression markers	15/35	7.87E-10	5.01E-08	0	15	*CD69, IL2RA, CCR5, CD40LG, IL4R, SELL, CD4, ITGAL, CD27, HLA-A, PECAM1, CCR7, PTPRC, BTLA, PRF1*
18	Hematopoietic cell lineage	20/70	5.53E-09	3.12E-07	0	20	*HLA-DRA, HLA-DPA1, HLA-DPB1, HLA-DRB1, IL2RA, ITGA4, ITGAM, HLA-DRB5, HLA-DQA1, HLA-DMB, CD8A, MS4A1, CD2, IL4R, CD3D, CD4, HLA-DQB1, HLA-DOA, CD3E, GP5*
19	Disease	70/553	7.92E-09	4.35E-07	0	70	*RPS24, RPS25, PSMB9, RPS27A, B2M, RPL35A, LYZ, RPS12, RPS15A, IGFBP4, PSME1, RPL30, RPL34, RPS6, RPL23, RPS29, RPL31, RPS7, RPS21, RPS20, RPS23, RPS8, RPS13, RPL21, RPL37, CCR5, RPL23A, RPL11, RPS27, RPL32, RPL27, RPS3A, FYN, APOBEC3G, RPL39, CYBB, RPL38, PSMB8, CALM1, RPL12, CD4, NMT2, IGFBP3, RPL4, RPL10A, PSME2, RPL41, HLA-A, RPL37A, HSP90B1, PPIA, RPL9, PDIA6, ATP6V0E2, RPL5, CDC42, RPL24, RPL6, THEM4, RPL19, HSPA5, FGF9, UBA52, RPS11, CXCL8, NUP37, RPL7, SKP1, RPS18, RPS14*
20	Interferon alpha response	23/93	8.59E-09	4.65E-07	0	23	*PSMB9, CD74, B2M, IFITM1, TAP1, PSME1, GBP2, CASP1, SAMD9L, LPAR6, TXNIP, IL4R, PSMB8, SELL, PSME2, IRF1, TRIM21, HLA-C, TRIM14, PARP12, LAMP3, RTP4, SP110*

Supplemental Table 1 | (i) (partial) Pathway enrichment analysis of all upregulated EPA DEGs generated using *clusterProfiler* using 10 human pathway databases. Enriched pathways are shown with information on which group that term clusters into based on the Jaccard index > 0.70, pathway term, number of DEGs that overlap with that databases gene set for that pathway, p value, adjusted p value, number of DEGs in that pathway that were upregulated, number of DEGs in that pathway that were downregulated, and gene names of all DEGs included in that pathway. Only the top term of the 19 groups are shown here.

Group	Term	Overlap	P value	Adjusted P value	Up-regulated	Down-regulated	Genes
1	NRF2 pathway	20/86	6.08E-11	1.90E-07	20	0	*NQO1, GCLC, MAFG, HMOX1, FTL, SLC5A3, SLC6A9, TXNRD1, SQSTM1, GSR, PRDX1, GCLM, G6PD, PGD, KEAP1, GSTP1, SLC39A7, SLC7A11, SLC6A6, SLC39A6*
2	Amino acid transport across the plasma membrane	9/18	6.40E-09	6.65E-06	9	0	*SLC7A5, SLC43A2, SLC7A1, SLC3A2, SLC38A2, SLC1A5, SLC1A4, SLC7A11, SLC6A6*
3	Glutamine in cancer metabolism	9/24	1.40E-07	8.73E-05	9	0	*SLC7A5, PSAT1, GCLC, SLC3A2, SLC1A5, PYCR1, GCLM, SLC7A11, PSPH*
4	Xenobiotic metabolism	19/136	1.12E-06	0.00044	19	0	*NQO1, GCLC, HMOX1, GABARAPL1, SLC1A5, ETFDH, AKR1C3, ARG2, PYCR1, GSR, PGD, EPHX1, UGDH, NPC1, SHMT2, SLC6A6, HES6, LONP1, PINK1*
5	mTORC1 signaling	23/195	1.77E-06	0.00061	23	0	*SLC7A5, PSAT1, GCLC, EDEM1, PHGDH, SLC1A5, TXNRD1, SQSTM1, MTHFD2, GSR, SLC1A4, PRDX1, DDIT3, G6PD, PPP1R15A, SLC7A11, SHMT2, SLC6A6, GLA, GAPDH, NAMPT, DDX39A, PSPH*
6	Metabolic reprogramming in colon cancer	10/40	2.03E-06	0.00063	10	0	*PSAT1, SLC1A5, TALDO1, PYCR1, G6PD, PGD, SHMT2, PKM, GAPDH, PSPH*
7	Oxidative stress in amyotrophic lateral sclerosis	6/12	2.47E-06	0.00070	6	0	*NQO1, GCLC, HMOX1, GSR, GCLM, KEAP1*
8	Unfolded protein response	16/110	4.67E-06	0.00112	16	0	*SLC7A5, PSAT1, HERPUD1, TARS1, IARS1, CHAC1, VEGFA, EDEM1, CEBPG, MTHFD2, SLC1A4, ATF4, CXXC1, SLC30A5, XPOT, EDC4*
9	Trans-sulfuration and one carbon metabolism	8/28	7.44E-06	0.00166	8	0	*PSAT1, GCLC, PHGDH, MTHFD2, MTHFD1L, GCLM, SHMT2, PSPH*

[continued on next page]

Supplemental Table 1 | (i) (partial) *[continued]*

Group	Term	Overlap	P value	Adjusted P value	Up-regulated	Down-regulated	Genes
10	Serine glycine biosynthesis	4/5	1.08E-05	0.00207	4	0	*PSAT1, PHGDH, SHMT2, PSPH*
11	Oxidative stress, all-trans-retinal and lipofuscin toxicity in AMD	6/15	1.21E-05	0.00210	6	0	*NQO1, HMOX1, VEGFA, GCLM, KEAP1, HIF1A*
12	SLC-mediated transmembrane transport	19/164	1.84E-05	0.00302	19	0	*SLC7A5, SLC43A2, SLC7A1, SLC3A2, SLC38A2, SLC5A3, SLC1A5, SLC6A9, CTNS, SLC12A7, SLCO3A1, SLC1A4, SLC35A2, NUP153, SLC39A7, SLC7A11, SLC6A6, SLC30A5, SLC39A6*
13	Glutathione metabolism	8/38	8.33E-05	0.01039	8	0	*ODC1, GCLC, CHAC1, GSR, GCLM, G6PD, PGD, GSTP1*
14	Amino acid biosynthesis and interconversion (transamination)	5/14	0.00013	0.01424	5	0	*PSAT1, PHGDH, PYCR1, GPT2, PSPH*
15	mTOR signaling activation by amino acids	8/41	0.00015	0.01581	8	0	*SLC7A5, SLC3A2, SLC1A5, FNIP1, SESN2, FLCN, ATF4, PPP1R15A*
16	Reactive oxygen species pathway	8/45	0.00029	0.02914	8	0	*NQO1, GCLC, FTL, TXNRD1, GSR, PRDX1, GCLM, G6PD*
17	Ferroptosis	7/35	0.00033	0.03089	7	0	*GCLC, HMOX1, SLC3A2, FTL, SAT2, GCLM, SLC7A11*
18	Protein nuclear import and export	5/17	0.00036	0.03293	5	0	*XPO1, NXF1, RCC1, NUP153, XPOT*
19	Metabolic reprogramming in cancer: overview	9/59	0.00040	0.03507	9	0	*PSAT1, PHGDH, SLC1A5, PYCR1, SHMT2, PKM, GAPDH, HIF1A, PSPH*

Supplemental Table 1 | (j) (partial) Known motif analysis on promotors of down versus upregulated EPA ATAC peaks. Enriched transcription factors are shown in order of significance. Enrichment of transcription factor binding motifs was performed using HOMER. Information on rank, motif, name of transcription factor, p value, log p value, q value (Benjamini), number of target sequences with motif, number of background sequences with motif, percent of targets sequences with motif, and percent of background sequences with motif. Top 20 significant transcription factors are shown here.

Rank	Motif	Name	P value	q value (Benjamini)	# TS with Motif	# BG with Motif	% TS with Motif	% BG with Motif
1		CTCF	1.00E-40	0	41.00	0.90	3.40%	0.14%
2		BORIS	1.00E-32	0	35.00	1.00	2.90%	0.15%
3		OCT:OCT	1.00E-22	0	172.0	42.90	14.27%	6.38%
4		KLF10	1.00E-15	0	110.0	26.30	9.13%	3.92%
5		GRE	1.00E-13	0	35.00	4.80	2.90%	0.72%
6		X-box	1.00E-13	0	19.00	1.60	1.58%	0.24%
7		GRE	1.00E-09	0	21.00	2.90	1.74%	0.43%
8		ARE	1.00E-09	0	29.00	4.30	2.41%	0.64%
9		GATA3	1.00E-09	0	15.00	1.70	1.24%	0.26%
10		ETS:RUNX	1.00E-08	0	14.00	0.60	1.16%	0.10%

[continued on next page]

Supplemental Table 1 | (j) (partial) *[continued]*

Rank	Motif	Name	P value	q value (Benjamini)	# TS with Motif	# BG with Motif	% TS with Motif	% BG with Motif
11		RFX1	1.00E-07	0	27.00	4.40	2.24%	0.66%
12		ETV2	1.00E-07	0	111.0	36.30	9.21%	5.40%
13		RFX2	1.00E-07	0	13.00	1.00	1.08%	0.15%
14		ZFP57	1.00E-07	0	13.00	1.60	1.08%	0.24%
15		BRN1	1.00E-06	0	68.00	19.70	5.64%	2.94%
16		GATA2	1.00E-06	0	95.00	32.00	7.88%	4.75%
17		ETV4	1.00E-06	0	101.0	34.60	8.38%	5.15%
18		PSE	1.00E-05	0.0001	97.00	33.50	8.05%	4.98%
19		PGR	1.00E-05	0.0001	43.00	11.80	3.57%	1.75%
20		PU.1	1.00E-05	0.0001	58.00	17.30	4.81%	2.58%

Supplemental Table 1 | (k) (partial) Known motif analysis on promotors of up versus downregulated EPA ATAC peaks. Enriched transcription factors are shown in order of significance. Enrichment of transcription factor binding motifs was performed using HOMER. Information on rank, motif, name of transcription factor, p value, log p value, q value (Benjamini), number of target sequences with motif, number of background sequences with motif, percent of targets sequences with motif, and percent of background sequences with motif. Top 20 significant transcription factors are shown here.

Rank	Motif	Name	P value	q value (Benjamini)	# TS with Motif	# BG with Motif	% TS with Motif	% BG with Motif
1		AP-2α	1.00E-12	0	74.00	34.10	7.91%	3.08%
2		THRb	1.00E-08	0	438.0	413.5	46.84%	37.39%
3		E2F4	1.00E-08	0	14.00	3.00	1.50%	0.27%
4		OCT4:SOX17	1.00E-05	0.0002	17.00	5.30	1.82%	0.48%
5		E2F1	1.00E-05	0.0003	8.00	0.00	0.86%	0.00%
6		ZIC	1.00E-05	0.0005	88.00	64.50	9.41%	5.84%
7		PBX3	1.00E-05	0.0005	21.00	8.90	2.25%	0.81%
8		AR	1.00E-05	0.0005	399.0	396.4	42.67%	35.85%
9		ZNF136	1.00E-04	0.0007	12.00	3.60	1.28%	0.32%
10		REV-ERB	1.00E-04	0.0034	19.00	8.80	2.03%	0.79%

[continued on next page]

Supplemental Table 1 | (k) (partial) *[continued]*

Rank	Motif	Name	P value	q value (Benjamini)	# TS with Motif	# BG with Motif	% TS with Motif	% BG with Motif
11		STAT4	1.00E-03	0.0071	98.00	80.30	10.48%	7.26%
12		TR4	1.00E-03	0.0088	6.00	1.30	0.64%	0.12%
13		GLI3	1.00E-03	0.0088	15.00	6.70	1.60%	0.61%
14		MYB	1.00E-03	0.0088	141.0	125.2	15.08%	11.32%
15		MYNN	1.00E-03	0.0088	27.00	16.00	2.89%	1.44%
16		ZSCAN22	1.00E-03	0.0088	10.00	3.90	1.07%	0.35%
17		THRa	1.00E-03	0.0092	72.00	56.50	7.70%	5.11%
18		TCF7	1.00E-03	0.0092	35.00	22.20	3.74%	2.01%
19		TGIF1	1.00E-03	0.0101	318.0	320.4	34.01%	28.98%
20		HNF4a	1.00E-03	0.0118	49.00	35.40	5.24%	3.20%

Supplemental Table 1 | (l) (partial) Pathway enrichment analysis of all downregulated OA DEGs generated using *clusterProfiler* using 10 human pathway databases. Enriched pathways are shown with information on which group that term clusters into based on the Jaccard index > 0.70, pathway term, number of DEGs that overlap with that databases gene set for that pathway, p value, adjusted p value, number of DEGs in that pathway that were upregulated, number of DEGs in that pathway that were downregulated, and gene names of all DEGs included in that pathway. Only the top term of the 11 groups are shown here.

Group	Term	Overlap	P value	Adjusted P value	Up-regulated	Down-regulated	Genes
1	Prion disease pathway	3/33	9.94E-06	0.00264	0	3	*HSP90B1, HSPA5, PDIA3*
2	Co-translational ER protein import	2/6	2.48E-05	0.00264	0	2	*HSP90B1, HSPA5*
3	Endogenous peptide antigen presentation	2/6	2.48E-05	0.00264	0	2	*HSPA5, PDIA3*
4	Protein folding	2/13	0.00013	0.00401	0	2	*HSP90B1, HSP90AA1*
5	Electron transport chain (OXPHOS system in mitochondria)	3/87	0.00019	0.00534	0	3	*NDUFA12, NDUFB4, ATP5F1C*
6	ER stress (unfolded protein response)	2/31	0.00076	0.01277	0	2	*HSPA5, HSP90AA1*
7	Proteins involved in myocardial ischemia	3/161	0.00113	0.01639	0	3	*TMSB4X, TXNIP, HSP90AA1*
8	Apoptotic keratinocytes clearance recession in systemic lupus erythematosus	2/38	0.00114	0.01639	0	2	*HSP90B1, TXNIP*
9	Complex I biogenesis	2/49	0.00189	0.02438	0	2	*NDUFA12, NDUFB4*
10	Response to elevated platelet cytosolic calcium	2/56	0.00246	0.02878	0	2	*TMSB4X, HSPA5*
11	T cell receptor regulation of apoptosis	4/529	0.00414	0.03977	0	4	*HSP90B1, HSPA5, ARHGDIB, HSP90AA1*

Supplemental Table 1 | (m) (partial) Pathway enrichment analysis of all upregulated OA DEGs generated using *clusterProfiler* using 10 human pathway databases. Enriched pathways are shown with information on which group that term clusters into based on the Jaccard index > 0.70, pathway term, number of DEGs that overlap with that databases gene set for that pathway, p value, adjusted p value, number of DEGs in that pathway that were upregulated, number of DEGs in that pathway that were downregulated, and gene names of all DEGs included in that pathway. Only the top term of the first 20 groups are shown here.

Group	Term	Overlap	P value	Adjusted P value	Up-regulated	Down-regulated	Genes
1	Lipid and lipoprotein metabolism	13/372	2.86E-09	5.90E-07	13	0	*CPT1A, SLC25A20, ACADVL, LPCAT1, DHCR24, FASN, SREBF2, LDLR, HMGCR, UGCG, SPTLC2, KDSR, HMGCS1*
2	SREBF and miR-33 in cholesterol and lipid homeostasis	5/15	3.57E-09	5.90E-07	5	0	*FASN, SREBF2, LDLR, HMGCR, HMGCS1*
3	Fatty acid, triacylglycerol, and ketone body metabolism	8/148	1.90E-07	1.88E-05	8	0	*CPT1A, SLC25A20, ACADVL, LPCAT1, FASN, SREBF2, HMGCR, HMGCS1*
4	Fatty acid metabolism	7/133	1.45E-06	8.99E-05	7	0	*CPT1A, ACADVL, DHCR24, FASN, ACAA2, ETFDH, HMGCS1*
5	Cholesterol biosynthesis	4/23	2.61E-06	0.00013	4	0	*DHCR24, SREBF2, HMGCR, HMGCS1*
6	srebp control of lipid synthesis	3/7	2.68E-06	0.00013	3	0	*SREBF2, LDLR, HMGCS1*
7	mTORC1 signaling	7/194	1.77E-05	0.00063	7	0	*DHCR24, LDLR, HMGCR, SQSTM1, HMGCS1, PPP1R15A, INSIG1*
8	Androgen response	5/86	3.30E-05	0.00102	5	0	*DHCR24, HMGCR, ABHD2, HMGCS1, INSIG1*
9	Mitochondrial LC-fatty acid beta-oxidation	3/16	4.17E-05	0.00122	3	0	*CPT1A, SLC25A20, ACADVL*
10	TNF-α signaling via NF-κB	6/169	8.24E-05	0.00227	6	0	*SNN, LDLR, SQSTM1, B4GALT5, KLF10, PPP1R15A*
11	HNF3B pathway	3/23	0.00013	0.00263	3	0	*CPT1A, ACADVL, HMGCS1*

[continued on next page]

Supplemental Table 1 | (m) (partial) *[continued]*

Group	Term	Overlap	P value	Adjusted P value	Up-regulated	Down-regulated	Genes
12	Proteins involved in non-alcoholic fatty liver disease	5/115	0.00013	0.00263	5	0	*CPT1A, FASN, SREBF2, LDLR, INSIG1*
13	Ceramide *de novo* biosynthesis	2/6	0.00028	0.00479	2	0	*SPTLC2, KDSR*
14	Fatty acid metabolism	3/33	0.00039	0.00563	3	0	*CPT1A, ACADVL, ACAA2*
15	Import of palmitoyl-CoA into the mitochondrial matrix	2/7	0.00039	0.00563	2	0	*CPT1A, SLC25A20*
16	Mevalonate pathway	2/7	0.00039	0.00563	2	0	*HMGCR, HMGCS1*
17	Estrogen response early	5/147	0.00042	0.00591	5	0	*FASN, FAM102A, ABHD2, UGCG, KLF10*
18	Synthesis of UDP-N-acetyl-glucosamine	2/8	0.00051	0.00688	2	0	*RENBP, AMDHD2*
19	Sphingolipid metabolism	3/40	0.00068	0.00869	3	0	*UGCG, SPTLC2, KDSR*
20	Oncostatin M	5/167	0.00075	0.00883	5	0	*DHCR24, LDLR, HMGCR, HMGCS1, KLF10*

Supplemental Table 1 | (n) Pathway enrichment analysis of all downregulated PA DEGs generated using *clusterProfiler* using 10 human pathway databases. Enriched pathways are shown with information on which group that term clusters into based on the Jaccard index > 0.70, pathway term, number of DEGs that overlap with that databases gene set for that pathway, p value, adjusted p value, number of DEGs in that pathway that were upregulated, number of DEGs in that pathway that were downregulated, and gene names of all DEGs included in that pathway.

Group	Term	Overlap	P value	Adjusted P value	Up-regulated	Down-regulated	Genes
1	Cholesterol biosynthesis	2/10	7.41E-05	0.01047	0	2	*HMGCR, SQLE*
2	Cholesterol biosynthesis pathway	2/15	0.00017	0.01047	0	2	*HMGCR, SQLE*
3	Statin pathway	2/16	0.00020	0.01047	0	2	*HMGCR, SQLE*
4	Statin pathway	2/16	0.00020	0.01047	0	2	*HMGCR, SQLE*
5	Cholesterol biosynthesis	2/22	0.00038	0.01255	0	2	*HMGCR, SQLE*
6	Cholesterol biosynthesis	2/23	0.00041	0.01255	0	2	*HMGCR, SQLE*
7	Superpathway of cholesterol biosynthesis	2/23	0.00041	0.01255	0	2	*HMGCR, SQLE*
8	Activation of gene expression by SREBF (SREBP)	2/42	0.00138	0.03683	0	2	*HMGCR, SQLE*

Supplemental Table 1 | (o) (partial) All significant pathway enrichment analysis of all upregulated PA DEGs generated using *clusterProfiler* using 10 human pathway databases. Enriched pathways are shown with information on which group that term clusters into based on the Jaccard index > 0.70, pathway term, number of DEGs that overlap with that databases gene set for that pathway, p value, adjusted p value, number of DEGs in that pathway that were upregulated, number of DEGs in that pathway that were downregulated, and gene names of all DEGs included in that pathway. Only the top term of the first 20 groups are shown here.

Group	Term	Overlap	P value	Adjusted P value	Up-regulated	Down-regulated	Genes
1	Estrogen deficiency in female obesity	3/6	6.12E-08	1.44E-05	3	0	*SREBF1, SCD, ACACA*
2	Fatty acid, triacylglycerol, and ketone body metabolism	6/175	1.37E-07	1.44E-05	6	0	*CPT1A, SLC25A20, ACADVL, SREBF1, SCD, ACACA*
3	Import of palmitoyl-CoA into the mitochondrial matrix	3/10	3.66E-07	2.52E-05	3	0	*CPT1A, SLC25A20, ACACA*
4	Mitochondrial LC-fatty acid beta-oxidation	3/16	1.70E-06	6.94E-05	3	0	*CPT1A, SLC25A20, ACADVL*
5	Ghrelin pathway	3/19	2.93E-06	9.31E-05	3	0	*SREBF1, ABCG1, ACACA*
6	Fatty acid biosynthesis	3/22	4.64E-06	0.00011	3	0	*ACAA2, SCD, ACACA*
7	Liver X receptor pathway	2/5	2.28E-05	0.00028	2	0	*SREBF1, SCD*
8	Import of palmitoyl-CoA into the mitochondrial matrix	2/7	4.77E-05	0.00055	2	0	*CPT1A, SLC25A20*
9	reversal of insulin resistance by leptin	2/8	6.36E-05	0.00063	2	0	*CPT1A, ACACA*
10	AMPK related catabolism deceleration in glucose insufficiency	2/8	6.36E-05	0.00063	2	0	*SREBF1, ACACA*
11	HNF3B pathway	2/23	0.00057	0.00345	2	0	*CPT1A, ACADVL*
12	RORA activates circadian expression	2/25	0.00067	0.00400	2	0	*CPT1A, SREBF1*
13	Fatty acyl-CoA biosynthesis	2/31	0.00103	0.00580	2	0	*SCD, ACACA*

[continued on next page]

Supplemental Table 1 | (o) (partial) *[continued]*

Group	Term	Overlap	P value	Adjusted P value	Up-regulated	Down-regulated	Genes
14	Circadian rhythm related genes	3/135	0.00109	0.00599	3	0	*CPT1A, SREBF1, KLF10*
15	PPAR signaling pathway	2/40	0.00172	0.00895	2	0	*CPT1A, SCD*
16	Activation of chaperones by IRE1 alpha	2/45	0.00217	0.01072	2	0	*ACADVL, HYOU1*
17	Oleate biosynthesis	1/3	0.00470	0.01975	1	0	*SCD*
18	Metabolism	6/1142	0.00520	0.02155	6	0	*CPT1A, ACADVL, LPCAT3, ABCG1, ACAA2, ACACA*
19	Beta-oxidation of myristoyl-CoA to lauroyl-CoA	1/4	0.00626	0.02451	1	0	*ACADVL*
20	VEGFR -> CTNND signaling	1/4	0.00626	0.02451	1	0	*COL18A1*

Supplemental Table 1 | (p) Known motif analysis on promotors of down versus upregulated OA ATAC peaks. All enriched transcription factors are shown in order of significance. Enrichment of transcription factor binding motifs was performed using HOMER. Information on rank, motif, name of transcription factor, p value, log p value, q value (Benjamini), number of target sequences with motif, number of background sequences with motif, percent of targets sequences with motif, and percent of background sequences with motif.

Rank	Motif	Name	P value	q value (Benjamini)	# TS with Motif	# BG with Motif	% TS with Motif	% BG with Motif
1		ZNF41	1.00E-02	0.9003	5.00	6.40	0.54%	0.10%
2		RAR:RXR	1.00E-02	1	5.00	8.30	0.54%	0.13%
3		WT1	1.00E-02	1	48.00	228.8	5.15%	3.60%

Supplemental Table 1 | (q) (partial) Known motif analysis on promotors of up versus downregulated OA ATAC peaks. Enriched transcription factors are shown in order of significance. Enrichment of transcription factor binding motifs was performed using HOMER. Information on rank, motif, name of transcription factor, p value, log p value, q value (Benjamini), number of target sequences with motif, number of background sequences with motif, percent of targets sequences with motif, and percent of background sequences with motif. Top 23 significant transcription factors are shown here.

Rank	Motif	Name	P value	q value (Benjamini)	# TS with Motif	# BG with Motif	% TS with Motif	% BG with Motif
1		Twist	1.00E-20	0	49.00	2.70	1.28%	0.30%
2		ZIC3	1.00E-20	0	217.0	25.40	5.68%	2.85%
3		GLI2	1.00E-20	0	109.0	9.00	2.85%	1.01%
4		PAX5	1.00E-17	0	33.00	1.80	0.86%	0.20%
5		EHF	1.00E-16	0	456.0	71.30	11.94%	8.01%
6		GFY	1.00E-11	0	26.00	0.00	0.68%	0.00%
7		Duxbl	1.00E-11	0	25.00	1.20	0.65%	0.13%
8		ZSCAN22	1.00E-10	0	35.00	2.50	0.92%	0.28%
9		RXR	1.00E-10	0	442.0	75.80	11.58%	8.51%
10		STAT4	1.00E-10	0	320.0	51.80	8.38%	5.82%
11		AP-2α	1.00E-10	0	313.0	50.30	8.20%	5.65%

[continued on next page]

Supplemental Table 1 | (q) (partial) *[continued]*

Rank	Motif	Name	P value	q value (Benjamini)	# TS with Motif	# BG with Motif	% TS with Motif	% BG with Motif
12		OCT4:SOX17	1.00E-09	0	48.00	4.50	1.26%	0.50%
13		PTF1A	1.00E-09	0	1198.0	240.9	31.38%	27.06%
14		ZNF692	1.00E-08	0	93.00	11.50	2.44%	1.29%
15		PPARα	1.00E-08	0	412.0	72.20	10.79%	8.11%
16		ELF4	1.00E-08	0	351.0	60.70	9.19%	6.82%
17		DMC1	1.00E-08	0	21.00	0.00	0.55%	0.00%
18		RUNX2	1.00E-08	0	370.0	64.60	9.69%	7.26%
19		Nur77	1.00E-07	0	59.00	6.20	1.55%	0.69%
20		ETS1	1.00E-07	0	118.0	16.70	3.09%	1.87%
21		SMAD4	1.00E-07	0	600.0	113.1	15.72%	12.70%
22		PU.1	1.00E-07	0	188.0	30.00	4.92%	3.37%
23		IRF8	1.00E-07	0	70.00	8.30	1.83%	0.93%

Supplemental Table 1 | (r) Known motif analysis on promotors of down versus upregulated PA ATAC peaks. All enriched transcription factors are shown in order of significance. Enrichment of transcription factor binding motifs was performed using HOMER. Information on rank, motif, name of transcription factor, p value, log p value, q value (Benjamini), number of target sequences with motif, number of background sequences with motif, percent of targets sequences with motif, and percent of background sequences with motif.

Rank	Motif	Name	P value	q value (Benjamini)	# TS with Motif	# BG with Motif	% TS with Motif	% BG with Motif
1		IRF8	1.00E-04	0.022	25.00	27.00	4.62%	1.96%
2		PBX3	1.00E-03	0.143	18.00	19.10	3.33%	1.38%
3		NFkB	1.00E-03	0.143	4.00	0.80	0.74%	0.06%
4		ZNF382	1.00E-03	0.143	4.00	0.90	0.74%	0.06%
5		ETS:E-box	1.00E-02	0.143	11.00	9.20	2.03%	0.67%
6		GATA2	1.00E-02	0.147	48.00	79.60	8.87%	5.77%
7		NKX3-2	1.00E-02	0.185	174.0	369.4	32.16%	26.78%
8		GATA3	1.00E-02	0.234	9.00	8.20	1.66%	0.60%
9		IRF2	1.00E-02	0.234	9.00	8.80	1.66%	0.64%
10		p63	1.00E-02	0.234	25.00	37.00	4.62%	2.68%
11		ZNF264	1.00E-02	0.234	34.00	54.70	6.28%	3.97%

[continued on next page]

Supplemental Table 1 | (r) *[continued]*

Rank	Motif	Name	P value	q value (Benjamini)	# TS with Motif	# BG with Motif	% TS with Motif	% BG with Motif
12		ZNF317	1.00E-02	0.234	6.00	5.00	1.11%	0.36%
13		GATA4	1.00E-02	0.234	67.00	125.9	12.38%	9.12%
14		GATA1	1.00E-02	0.237	41.00	70.20	7.58%	5.09%
15		IRF3	1.00E-02	0.242	20.00	28.20	3.70%	2.04%
16		TLX	1.00E-02	0.253	25.00	38.70	4.62%	2.80%
17		FOXM1	1.00E-02	0.253	72.00	139.5	13.31%	10.11%
18		NFY	1.00E-02	0.253	48.00	86.70	8.87%	6.28%
19		ELF4	1.00E-02	0.253	53.00	97.10	9.80%	7.04%

Supplemental Table 1 | (s) (partial) Known motif analysis on promotors of up versus downregulated PA ATAC peaks. All enriched transcription factors are shown in order of significance. Enrichment of transcription factor binding motifs was performed using HOMER. Information on rank, motif, name of transcription factor, p value, log p value, q value (Benjamini), number of target sequences with motif, number of background sequences with motif, percent of targets sequences with motif, and percent of background sequences with motif. Top 20 significant transcription factors are shown here.

Rank	Motif	Name	P value	q value (Benjamini)	# TS with Motif	# BG with Motif	% TS with Motif	% BG with Motif
1		PITX1	1.00E-09	0	30.00	3.10	2.16%	0.57%
2		ZBTB12	1.00E-08	0	63.00	11.80	4.54%	2.19%
3		HOXC9	1.00E-07	0	95.00	20.30	6.84%	3.75%
4		Pdx1	1.00E-07	0	183.0	47.10	13.17%	8.74%
5		Nur77	1.00E-07	0	22.00	2.70	1.58%	0.49%
6		HOXA1	1.00E-05	0.0001	37.00	6.90	2.66%	1.27%
7		DR4	1.00E-05	0.0003	32.00	5.20	2.30%	0.97%
8		CHOP	1.00E-04	0.0008	46.00	9.60	3.31%	1.77%
9		REV-ERB	1.00E-04	0.0009	22.00	3.70	1.58%	0.68%
10		EBF	1.00E-04	0.0012	17.00	2.90	1.22%	0.53%

[continued on next page]

Supplemental Table 1 | (s) (partial) *[continued]*

Rank	Motif	Name	P value	q value (Benjamini)	# TS with Motif	# BG with Motif	% TS with Motif	% BG with Motif
11		COUP-TFII	1.00E-04	0.0012	230.0	69.50	16.56%	12.88%
12		IRF:BATF	1.00E-04	0.0033	16.00	2.50	1.15%	0.46%
13		MEF2B	1.00E-03	0.0036	171.0	51.00	12.31%	9.45%
14		PBX2	1.00E-03	0.0037	153.0	44.30	11.02%	8.21%
15		PAX5	1.00E-03	0.0046	53.00	12.80	3.82%	2.38%
16		ZNF415	1.00E-03	0.0067	75.00	19.60	5.40%	3.62%
17		SOX9	1.00E-03	0.0067	112.0	31.20	8.06%	5.79%
18		STAT4	1.00E-03	0.0067	130.0	37.40	9.36%	6.92%
19		COUP-TFII	1.00E-03	0.0067	248.0	78.20	17.85%	14.50%
20		PBX1	1.00E-03	0.0074	10.00	0.00	0.72%	0.00%

CHAPTER 5

Insights into the role of triglycerides and T cells in cardiovascular risk: T cells of patients with moderate hypertriglyceridemia have a pro-inflammatory transcriptomic profile

Nathalie A. Reilly[1,4*], Janneke W.C.M. Mulder[2*], Koen F. Dekkers[1], Thomas B. Kuipers[1,3], Leonie C. van Vark-van der Zee[5], Monique T. Mulder[5], Jeanine E. Roeters van Lennep[2], J. Wouter Jukema[4,6], and Bastiaan T. Heijmans[1]

[1] *Molecular Epidemiology, Department of Biomedical Data Sciences, Leiden University Medical Centre, The Netherlands,*
[2] *Department of Internal Medicine, Erasmus MC Cardiovascular Institute, University Medical Centre Rotterdam, Rotterdam, The Netherlands,*
[3] *Sequencing Analysis Support Core, Department of Biomedical Data Sciences,*
[4] *Department of Cardiology, Leiden University Medical Centre, The Netherlands,*
[5] *Department of Internal Medicine, Division of Pharmacology, Vascular and Metabolic Diseases, Erasmus University Medical Centre, Rotterdam, The Netherlands, and*
[6] *Netherlands Heart Institute, Utrecht, The Netherlands.*
[*] *These authors contributed equally to this work*

Abstract

Background and aims: The role of triglycerides and T cells in atherosclerosis, the underlying cause of cardiovascular disease (CVD), is increasingly recognized. Moderately elevated triglycerides have emerged as a causal risk factor of CVD, while T cells are the most prominent immune cell type in the atherosclerotic plaque. Studies in mice and *in vitro* indicate that triglycerides can affect T cell function. Here, we characterize differences in T cells across control and patient groups with distinct triglyceride levels either due to genetic or secondary causes using the transcriptome as a functional read-out.

Methods: We enrolled patients with primary (genetically determined, n=13) and secondary (due to a secondary cause, n=14) moderate hypertriglyceridemia and compared them to controls (n=15). Additionally, we enrolled patients with rare genetic conditions, namely primary severe hypertriglyceridemia (n=3) or hypotriglyceridemia (n=4). From all participants (n=49), we purified $CD4^+$ and $CD8^+$ T cells and extracted RNA for RNA sequencing.

Results: $CD4^+$ T cells of patients with primary moderate hypertriglyceridemia displayed a pro-inflammatory transcriptomic profile ($P_{FDR}<0.05$), including an upregulated interleukin-6 receptor (*IL6R*) expression, a subunit of the IL-6 receptor complex that is causally linked to CVD. The profile was mirrored in $CD8^+$ T cells from these patients and also present in both T cell types from secondary moderate hypertriglyceridemia patients, albeit less pronounced. In accordance, the transcriptomic differences were reversed in patients with hypo- and absent in patients with severe hypertriglyceridemia.

Conclusions: Elevated triglycerides may contribute to CVD by promoting a pro-inflammatory response in T cells.

Graphical abstract

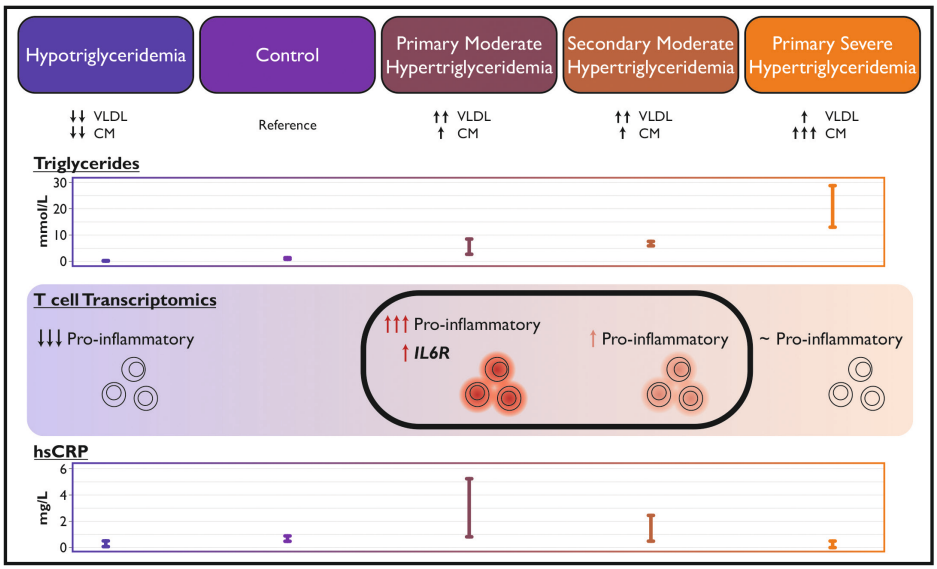

Key Question: What are the differences in T cells across control and patient groups with distinct triglyceride levels either due to genetic or secondary causes using the transcriptome as a functional read-out?

Key Finding: T cells of patients carrying mutations resulting in moderately elevated triglyceride levels show an increased expression of pro-inflammatory genes as compared with controls. Effects in patients with secondary, hypotriglyceridemia and severe hyperglyceridaemia were consistent, reversed and absent, respectively.

Take-home Message: Patients with moderately elevated triglyceride levels have T cells with pro-inflammatory characteristics, a finding that sheds new light on the role of triglycerides in cardiovascular disease.

Introduction

Triglyceride levels in individuals may range from lowered (hypotriglyceridemia, <0.5mmol/L) to normal (0.8–2.0mmol/L) to elevated (hypertriglyceridemia, >2.0mmol/L). Moderate hypertriglyceridemia, between the range of 2–10mmol/L, has been associated, through genome-wide association studies[1-4], with an increased risk of cardiovascular disease (CVD)[5-9], which Mendelian randomization[10-14] studies have indicated to be a causal effect. In accordance, individuals with hypotriglyceridemia were indicated to be at a lower risk for developing CVD[15, 16]. Interestingly, the risk of CVD is no longer increased in individuals with severe hypertriglyceridemia (>10mmol/L), because triglycerides are then stored in chylomicrons which cannot cross the arterial wall[17]. The differences in triglyceride levels can be attributed to primary genetic factors (e.g. pathogenic mutations in *MTTP* or *LPL*) or secondary outcomes of conditions like diabetes[18]. However, the precise pathophysiology of CVD in those with altered triglyceride levels remains poorly understood.

Triglycerides in the circulation are mostly contained within triglyceride-rich lipoproteins (TGRLs), which have also been found as a causal risk factor for CVD[19, 20]. However, CVD, and the main underlying cause thereof, atherosclerosis, develop due to the interplay between lipids, the immune system, and the vascular wall[21]. As such, emerging evidence underscores a significant role not only of triglycerides, but also of the immune system in its pathogenesis[22, 23]. In particular, T cells have been found to make up over half the immune cells in atherosclerotic plaques, of which half are $CD4^+$ and half are $CD8^+$ [24, 25]. Moreover, the biologically functional components of triglycerides, fatty acids, have already been found to substantially impact T cell functionality[26-28]. In patients with hypertriglyceridemia, T cells are exposed to excess triglycerides contained in TGRLs in the circulation. Therefore, the study of patients with primary hyper- or hypotriglyceridemia can shed light on how moderately elevated triglyceride levels can contribute to atherosclerotic disease through interactions with the immune system *in vivo*.

Here, we compare $CD4^+$ and $CD8^+$ T cells derived from patients with varying levels of triglycerides from both primary and secondary causes as compared to a control group using the transcriptome as a functional read-out. We show that patients of moderately elevated triglycerides levels have T cells characterized by a pro-inflammatory transcriptomic profiles shedding light on an unexplored pathway relevant to atherosclerosis and CVD.

Methods

Participant selection and data collection

Participants were enrolled in one of five groups, being control (defined as no known abnormal triglyceride levels and no fibrate use and/or triglyceride levels between 0.8–2.0mmol/L), primary moderate hypertriglyceridemia (a confirmed pathogenic mutation in the *LPL*, *APOC2*, *APOA5*, *LMF1*, *GPIHBP1*, or *APOE2/APOE2* gene and the most recent measured triglyceride level >3.0mmol/L), secondary moderate hypertriglyceridemia (due to a secondary cause, such as diabetes or lifestyle

factors including obesity and excessive alcohol use and the most recent measured triglyceride level >3.0mmol/L), primary severe hypertriglyceridemia (two confirmed pathogenic mutations in the *LPL*, *APOC2*, *APOA5*, *LMF1*, or *GPIHBP1* gene leading to familial hyperchylomicronaemia syndrome (FCS) and the most recent measured triglyceride level >13.0mmol/L), and hypotriglyceridemia group (a pathogenic mutation in the *MTTP* or *APOB* gene resulting in a hypobetalipoproteinaemia or abetalipoproteinaemia phenotype and the most recent measured triglyceride level <0.56mmol/L).

The exclusion criteria were as follows: 1) below the age of 18 years, 2) presence of an infection at the time of blood drawing (e.g. COVID-19), 3) medical history or current treatment for any condition that could impact the immune system at the time of participation (e.g. ongoing treatment for malignancy or immunotherapy), and 4) unwillingness or inability to provide informed consent. For the control group, an additional exclusion criterion was applied in cases where triglyceride levels were unknown, with a threshold set at 2.0mmol/L for the triglyceride levels measured in the sample.

The local ethical board of Erasmus MC in Rotterdam, The Netherlands, approved and assigned a waiver for this study (MEC-2021-0596). Patients were consecutively recruited after informed consent was given at the lipid clinic of the Erasmus MC in Rotterdam, The Netherlands, between March 2022 and December 2022. We included 15, 13, and 14 participants for the control, primary, and secondary moderate hypertriglyceridemia groups respectively (Table 1). However, because FCS and abetalipoproteinemia are very rare conditions, we included 3 and 4 participants in the primary severe hypertriglyceridemia and hypotriglyceridemia group, respectively (Table 1). At the time of inclusion, additional data, including sex, age, BMI, smoking, medication (particularly lipid-lowering therapy), diet, and medical history, were collected. In total, 36mL of fasted whole blood was collected per individual in anticoagulant citrate phosphate dextrose adenine (CPDA) tubes (Greiner Bio-One, 455056) and transported to the Leiden University Medical Centre (LUMC) in Leiden, The Netherlands (Fig. 1).

Plasma and peripheral blood isolation

To obtain plasma and peripheral blood mononuclear cells (PBMCs) from the patients, whole blood samples in the CPDA tubes were transferred into a 50mL tube (Starlab Group, E1450-0200) and spun down at 350g for 10min to isolate the plasma. 1.8mL plasma was collected into a 2mL Sarstedt Microtube (Sarstedt, 72.730.009 and 65.716.002) and stored at -80°C for lipid profiling, see below. Whole blood was mixed and diluted 1:1 in PBMC isolation buffer (buffered natrium chloride (PBS; pH 7.4; Fresen, 15360679), 2% Alburex (CLS Behring GmbH, C1309/490)). To obtain peripheral blood mononuclear cells (PBMCs), freshly collected and diluted whole blood was filtered by Ficoll paque (Pharmacy LUMC, 97902861) gradient centrifugation using Leucosep tubes (Greiner Bio-One, 227290). Cells were washed in PBMC isolation buffer. An additional red blood cell lysis step was carried out using red blood cell lysis buffer (MilliQ water, 0.15M NH_4Cl (Merck Millipore, 101145), 1mM $KHCO_3$ (Merck Millipore, 104854), and 0.1mM Na_2 EDTA (Sigma Aldrich, E5134)). Cell viability was measured by trypan blue (Sigma Aldrich, T8154) exclusion using a 0.0025mm^2 haemocytometer (Bürker-Turk Bright Line, 0640211).

Cell sorting and harvesting

To obtain $CD4^+$ and $CD8^+$ T cells, PBMCs were resuspended in FACS buffer (PBS and 0.4% Alburex) and labelled with live dead (Invitrogen, L34964), anti-CD3-PE (BD Biosciences, 555340), anti-CD4-APC (BD Biosciences, 555349), anti-CD8-FITC (BD Biosciences, 555634), anti-CD14-Alexa Fluor® 700 (BD Biosciences, 557923), and anti-CD19-BV786 (BD Biosciences, 563325). PBMCs were sorted into $CD4^+$ T cells, $CD8^+$ T cells, $CD14^+$ monocytes, and $CD19^+$ B cells using the CytoFLEX SRT Benchtop cell sorter (Beckman Coulter, Brea, CA, USA) at the LUMC Flow Cytometry Core Facility (https://www.lumc.nl/research/facilities/fcf/) with the CytExpert SRT v1.0.3.10011 software (Beckman Coulter). Cells were collected in 5% fetal calf serum (FCS) (Bodinco BDC, 16941) DMEM (Dulbecco's Modified Eagle's Serum (Sigma, 05796), 1% Pen-Strep (Lonza, DE17-602E), 1% GlutaMAX-1 (100x) (Gibco, 35050-038)). Post-sorting cell purity was assessed on the CytoFLEX SRT Benchtop cell sorter and shown to be on average 97.2 SE 0.3% for $CD4^+$ T cells and 97.0 SE 0.4% for $CD8^+$ T cells (Supp. Fig. 1a and b).

The cells were subsequently washed in PBS and cell viability and diameter were measured by Via1-Cassette™ (Chemometec, 941-0012) on a NucleoCounter® NC-200™ (Chemometec, 900-0200) and found to be on average 97.4 SE 0.2% and 9.3 SE 0.02µm for $CD4^+$ T cells and 96.8 SE 0.4% and 9.5 SE 0.04µm for $CD8^+$ T cells (Supp. Fig. 1c, d, e and f). A maximum of 2 million cells were harvested by flash freezing in liquid nitrogen and stored at -80°C for RNA isolations. Any additional cells were kept in DMEM supplemented with 30% FCS, 1% Pen-Strep, 1% GlutaMAX-1, and 20% Dimethyl Sulfoxide (DMSO) (WAK-Chemie Medical GmbH, WAK-DMSO-10) medium at a density of ~$25*10^6$ cells/mL, and stored in cryogenic tubes (Greiner Bio-One, 126263) in liquid nitrogen.

Plasma measurements

Plasma samples of the patients were used to determine lipid concentrations, measure high sensitivity C-reactive protein (hsCRP), and profile lipoproteins. Lipid levels, including triglycerides, total cholesterol, LDL-cholesterol, HDL-cholesterol, apolipoprotein (Apo)A-I, and ApoB were measured using standard laboratory techniques. LDL-cholesterol, HDL-cholesterol, total cholesterol and triglycerides were measured with an enzymatic photometric analysis. ApoB and ApoA-I were measured by photometric measurement of antigen-antibody reaction. Lipoprotein (a) [Lp(a)] and hsCRP concentrations were measured using a particle-enhanced immunoturbidimetric assay. All kits were from DiaSys Diagnostic systems GmbH, Holzheim Germany (Diagnostic System #171399910930 and #170459910930 respectively; DiaSys Diagnostic System, GmbH, Holzheim, Germany). This method is largely independent of Apo(a) KIV repeat number. A Mann-Whitney U test was used to determine whether the differences in hsCRP were significantly higher or lower in the patient groups as compared to the control group. Next, chylomicron, VLDL, IDL, LDL, and HDL were isolated using density gradient ultracentrifugation according to the Proudfoot protocol[29, 30]. The cholesterol and triglyceride content of these particles was determined using a Selectra E (DDS Diagnostic system, Istanbul, Turkey), according to the manufacturer's instructions.

RNA isolation

To isolate total RNA for RNA sequencing, RNA was extracted from the cell samples using the Zymo Quick-DNA/RNA Microprep Plus Kit (Zymo Research, D7005) according to manufacturer's instructions. The RNA was quantified using a Qubit® 2.0 Fluorometer (Q32866) with the Qubit® RNA BR Assay Kit (Thermofisher, Q10211) according to manufacturer's instructions. RNA integrity (RIN) was determined using an Agilent 2100 Bioanalyzer Instrument (G2939BA) with the Agilent RNA 6000 Nano Reagents (Agilent, 5067-1511), RIN values were on average 9.7 (SD, 0.6) for $CD4^+$ T cell samples and 9.0 (SD, 0.8) for $CD8^+$ T cell samples. The minimum RNA yield was 160ng and 160ng to 1µg was stored at -80°C for RNA sequencing.

RNA sequencing analysis

RNA sequencing (RNA-seq) was performed to determine the differences in the transcriptome of $CD4^+$ and $CD8^+$ T cells of individuals with primary or secondary moderate hypertriglyceridemia, primary severe hypertriglyceridemia, hypotriglyceridemia, or none (control). The RNA from each of the samples was sent for sequencing (Macrogen, Amsterdam, The Netherlands). RNA-seq libraries were prepared from 200ng RNA using the Illumina Truseq stranded mRNA library prep (Illumina, 20020594) with a poly A selection. Both whole-transcriptome amplification and sequencing library preparations were performed in two 96-well plates with 53 samples in one plate and 45 in another. Quality control steps were included to determine total RNA quality and quantity, the optimal number of PCR preamplification cycles, and fragment size selection. For 48 of the 49 $CD4^+$ and 43 of 49 $CD8^+$ T cell samples, RNA-seq data passed quality control. The samples that did not pass the quality control included 2 control samples, one from $CD4^+$ and one from $CD8^+$ T cells, 1 primary moderate sample from $CD8^+$ T cells and 4 secondary moderate samples from $CD8^+$ T cells. Barcoded libraries were divided across 4 lanes and sequenced separately. Barcoded libraries were sequenced to a read depth of 30 million reads using the Novaseq 6000 (Illumina) to generate 150 base pair paired-end reads.

FastQ files are analysed using the RNAseq pipeline (v5.0.0) from BioWDL (https://zenodo.org/record/5109461), developed by SASC (LUMC). The pipeline performed pre-processing on the FastQ files (including quality control, quality trimming, and adapter clipping), read mapping, and expression quantification. *FastQC* (v0.11.9) is used to check raw reads and *Cutadapt* (v2.10) to perform adapter clipping. Reads are mapped to a reference genome (Ensembl v105) using *STAR aligner* (v2.7.5a), and with *HTSeq Count* (v0.12.4) the number of assigned reads to genes per sample is determined.

Based on count distribution of the sequenced sample it was opted to exclude 1 control and 1 primary severe hypertriglyceridemia sample from the $CD4^+$ T cell analysis as well as 2 control, 1 secondary moderate hypertriglyceridemia, and 1 primary severe hypertriglyceridemia sample in the $CD8^+$ T cell analysis. Based on Ensembl gene biotype annotation, we included only protein coding genes of chromosomes 1-22 for further downstream analysis (19,111 genes in total). We further filtered the background of each group to contain only the counts where at least half of the raw counts per group had a count of 1. Then, for each comparison, only genes were kept that were

expressed in both the control and experimental group, leaving 13,377 expressed genes for primary moderate, 13,386 expressed genes for secondary moderate, 13,421 expressed genes for primary severe, and 13,466 expressed genes for hypotriglyceridemia in the $CD4^+$ T cell analysis, as well as 12,575 expressed genes for primary moderate, 12,671 expressed genes for secondary moderate, 12,396 expressed genes for primary severe, 12,407 expressed genes for hypotriglyceridemia in the $CD8^+$ T cell analysis. We used the Bioconductor package *DESeq2*[31] (v1.42.0) to test whether primary moderate, secondary moderate, primary severe, or hypotriglyceridemia had an effect on gene expression as compared to the control per cell type, $CD4^+$ and $CD8^+$. *DESeq2* fits a generalized linear model (GLM) assuming the negative binomial distribution for the counts. The model expresses the logarithm of the average of the counts in terms of one or more predictors. In this case, we used four models that had one of the groups, sex, and age as predictors each. By including sex and age in the models, we account for the dependence between measurements within the same sex and between different ages of the participants[31]. The Benjamini-Hochberg procedure was manually used to correct for multiple testing and a false discovery rate (FDR) <0.05 was considered statistically significant.

In order to determine whether the similarities in direction of effect sizes of the DEGs in the primary moderate $CD4^+$ T cells expressed in the other $CD4^+$ and $CD8^+$ T cells groups was significant, a binomial test was used. This determines the probability of a particular outcome across a certain number of trials (n=39 DEGs), where there are precisely two possible outcomes (up or down). In order to identify distinct gene expression patterns in the data, the log2 fold change of the DEGs of the $CD4^+$ and $CD8^+$ primary moderate and secondary moderate groups were plotted in heatmaps using *ComplexHeatmap*[32] (v2.18.0). Differentially expressed genes per group were divided into upregulated or downregulated based on the log2 fold change values. 10 human pathway databases (BioPlanet 2019, WikiPathways 2023 Human, KEGG 2021 Human, Elsevier Pathway Collection, BioCarta 2016, Reactome 2022, HumanCyc 2016, NCI-Nature 2016, Panther 2016 and MSigDB Hallmark 2020) were queried using gene symbols. 331 of 406 queried genes for hypotriglyceridemia in $CD8^+$ T cells present in at least 1 database. The identified clusters were then mapped for pathway enrichment using *clusterProfiler*[33] (v4.10.0). The background was set to the 8,799 expressed genes for hypotriglyceridemia in the $CD8^+$ T cells. This was based on at least half of the raw counts per group and control having a count of 1, the gene being expressed in both comparison groups, and the independent filtering of *DESeq2*. Multiple testing using the Benjamini-Hochberg method at 5% FDR was performed over the combined results from the 10 databases. Pathways that included highly similar gene sets were grouped (Jaccard index > 0.7) and only the most significantly enriched pathway per group was retained.

Results

We generated transcriptomic profiles of $CD4^+$ and $CD8^+$ cells for 47 participants (19 (40.4%) women, median age 53 [37-60] years, BMI 26.1 [23.7-29.6] kg/m^2, 10 (21.3%) current smokers) (Table 1). Six patients in the primary moderate hypertriglyceridemia group (n=13) had an *APOE2/*

APOE2 genotype, six an *LPL* mutation, and one patient had a pathogenic *APOA5* mutation. The causes of hypertriglyceridemia in the secondary moderate group (n=14) were diabetes mellitus type 2 (8 (57.1%)) and/or lifestyle related factors (6 (42.9%)). Both patients in the primary severe hypertriglyceridemia group had *LPL/LPL* mutations. In the hypotriglyceridemia group (n=4), 3 patients had a causative *MTTP/MTTP* mutation and 1 patient had an *APOB* variant. The participants included 14 controls. Twenty-five (53.2%) participants used lipid-lowering therapy. None of the participants in the control, primary severe, or hypotriglyceridemia group had a recorded medical history of cardiovascular disease.

Measured triglyceride levels exhibited an increasing trend from the hypotriglyceridemia group (range 0.1–0.3mmol/L), controls (median 1.3 [0.8–1.4] mmol/L), primary moderate group (median 5.2 [2.7–8.5] mmol/L), secondary moderate group (median 6.8 [5.9–7.6] mmol/L), to the primary severe group (range 13.0–28.8 mmol/L; Supp. Fig. 2). A similar trend was observed for chylomicron cholesterol and chylomicron triglycerides (Table 1). The lipoprotein profiles of each participant per group are shown in Supp. Fig. 2.

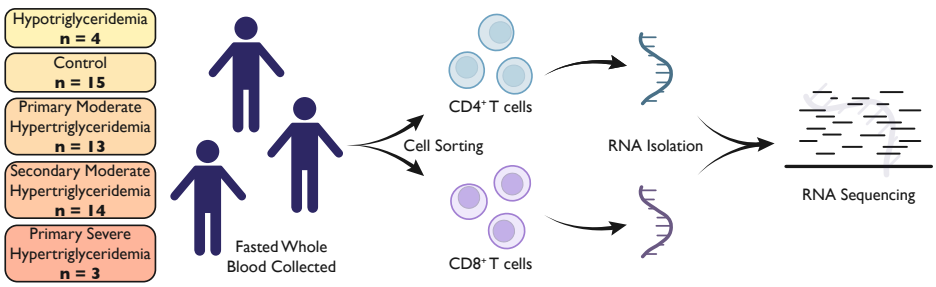

Fig. 1 | Experimental setup. Experimental setup for RNA sequencing of isolated $CD4^+$ and $CD8^+$ T cells derived from participants with primary or secondary moderate hypertriglyceridemia, primary severe hypertriglyceridemia, hypotriglyceridemia, or control.

Moderate hypertriglyceridemia induced transcriptomic effects on $CD4^+$ and $CD8^+$ T cells

In order to discover whether moderately elevated triglycerides have an effect on T cell gene expression, RNA sequencing was performed on $CD4^+$ and $CD8^+$ T cells isolated from individuals with primary moderate and secondary moderate hypertriglyceridemia. Gene expression differences in each cell type, $CD4^+$ and $CD8^+$, from both groups, primary and secondary moderate, were compared to $CD4^+$ and $CD8^+$ T cells isolated from the control group, respectively. This allowed us to discern between the effects of moderately elevated triglyceride exposure on $CD4^+$ and $CD8^+$ T cells separately.

We first focused on the transcriptomic profile in T cells from patients with primary moderate hypertriglyceridemia as compared with that in controls. The most prominent difference in transcriptomic profile was observed in $CD4^+$ T cells, in which 39 differentially expressed genes (DEGs) were found (P_{FDR}<0.05; Supp. Table. 1a), 19 (48.7%) of which were upregulated.

Table 1 | Participant characteristics. Participant characteristics in total and per group, including lipid levels and high sensitivity CRP at the time of inclusion. Participant characteristics in total and per group, including lipid levels and high sensitivity CRP at the time of inclusion. Continuous data shown as median [IQR] or in case of n < 5 as minimum-maximum. Categorical data are provided in count (%). BMI = body mass index, PCSK9 = proprotein convertase subtilisin/kexin type 9, TIA = transient ischemic attack. Remnants = total cholesterol - LDL cholesterol - HDL cholesterol.

	Total	Control	Primary Moderate Hypertriglyceridemia	Secondary Moderate Hypertriglyceridemia	Primary Severe Hypertriglyceridemia	Primary Hypotriglyceridemia
N	47	14	13	14	2	4
General Characteristics						
Age	53 [37-60]	48 [36-59]	56 [47-60]	56 [53-64]	34 [34-34]	26 [25-33]
Sex, female	19 (40.4%)	8 (57.1%)	3 (23.1%)	5 (35.7%)	0	3 (75.0%)
BMI, kg/m2	26.1 [23.7-29.6]	24.3 [22.4-25.8]	27.5 [26.0-30.1]	28.5 [27.6-31.5]	25.6 [23.3-28.0]	21.2 [20.0-23.0]
Smoking (ever)	19 (40.4%)	1 (7.1%)	8 (61.5%)	7 (50%)	2 (100%)	1 (25.0%)
Smoking (current)	10 (21.3%)	0	5 (38.5%)	3 (21.4%)	1 (50.0%)	1 (25.0%)
Diabetes mellitus type 2	14 (29.8%)	0	6 (46.2%)	8 (57.1%)	0	0
Lipid-Lowering Therapy						
Statin	18 (38.3%)	1 (7.1%)	8 (61.5%)	9 (64.3%)	0	0
High intensity statin	8 (17.0%)	0	3 (23.1%)	5 (35.7%)	0	0
Ezetimibe	7 (14.9%)	0	4 (30.8%)	3 (21.4%)	0	0
Fibrate	8 (17.0%)	0	4 (30.8%)	4 (28.6%)	0	0
PCSK9 Inhibitor	4 (8.5%)	0	1 (7.7%)	3 (21.4%)	0	0

[continued on next page]

Table 1 | Participant characteristics. *[continued]*

	Total	Control	Primary Moderate Hypertriglyceridemia	Secondary Moderate Hypertriglyceridemia	Primary Severe Hypertriglyceridemia	Primary Hypotriglyceridemia
Medical History						
Pancreatitis	7 (14.9%)	0	2 (15.4%)	3 (21.4%)	2 (100%)	0
Cardiovascular Disease	9 (19.1%)	0	2 (15.4%)	7 (50.0%)	0	0
Myocardial infarction	3 (6.4%)	0	1 (7.7%)	2 (14.3%)	0	0
Ischemic Stroke or TIA	2 (4.3%)	0	0	2 (14.3%)	0	0
Laboratory Levels in mmol/L						
Triglycerides	3.2 [1.4-6.9]	1.3 [0.8-1.4]	5.2 [2.7-8.5]	6.8 [5.9-7.6]	13.0-28.8	0.1-0.3
Total cholesterol	4.9 [4.0-5.4]	5.0 [4.5-5.1]	4.8 [4.1-5.8]	4.9 [4.2-5.6]	9.0-11.5	2.0-2.8
LDL-cholesterol	1.9 [1.0-3.0]	3.1 [2.7-3.9]	1.7 [1.1-2.4]	1.6 [1.1-2.9]	0.0-0.0	0.1-0.9
HDL-cholesterol	1.06 [0.85-1.31]	1.37 [1.18-1.58]	0.84 [0.81-1.06]	0.97 [0.89-1.08]	0.44-1.23	0.64-1.14
Apolipoprotein A1, g/L	0.95 [0.84-1.09]	1.09 [1.00-1.14]	0.93 [0.83-0.97]	1.00 [0.88-1.09]	0.36-0.54	0.37-0.89
Apolipoprotein B, g/L	0.78 [0.59-0.94]	0.86 [0.68-1.02]	0.74 [0.54-0.91]	0.84 [0.74-1.08]	0.01-0.71	0.01-0.24
Lipoprotein(a), g/L	0.05 [0.02-0.23]	0.07 [0.03-0.12]	0.06 [0.01-0.13]	0.16 [0.03-0.44]	0.00-0.02	0.01-0.04
High sensitivity CRP, mg/L	0.82 [0.43-1.48]	0.75 [0.48-0.89]	1.55 [0.82-5.24]	1.09 [0.49-2.45]	0.00-0.50	0.15-0.51
Chylomicrons cholesterol	0.029 [0.007-0.387]	0.007 [0.002-0.011]	0.165 [0.021-0.682]	0.263 [0.166-0.388]	4.119-8.812	0.000-0.001
Chylomicrons triglyceride	0.143 [0.030-1.199]	0.028 [0.010-0.034]	0.503 [0.113-1.905]	1.028 [0.616-1.412]	11.300-13.615	0.001-0.022
Remnants	1.40 [0.34-2.25]	0.10 [0.00-0.31]	1.55 [1.46-2.31]	2.16 [1.94-2.42]	7.72-11.10	0.77-1.21

Most notably, this included *ILR6* which encodes a subunit of the interleukin 6 (IL-6) receptor complex and plays an important role in the immune response[34] (Fig. 2a). The effects of IL-6 on $CD4^+$ T cells include stimulating T cell survival and proliferation as well as promoting T_H2 and T_H17 differentiation[35]. Furthermore, a Mendelian randomization study of *IL6R* constituted the first evidence for a causal role of inflammation in coronary heart disease[36]. A pro-inflammatory expression profile of $CD4^+$ T cells of primary moderate patients was further indicated by the upregulation of the genes *NCOR1, DOCK8,* and *LPAR6*. *NCOR1* has been shown to aid the function of T_H1 and T_H17 effector cells[37], *DOCK8* is necessary for T cell migration, survival, and immune responses[38], and *LPAR6* has been shown to contribute to T cell activation and effector cell function[39]. On the other hand, genes that were found to be downregulated in $CD4^+$ T cells included *MLF2* and *MMP14*. *MLF2* is a negative regulator of p53, a transcription factor required for T cell homeostasis[40, 41] and *MMP14* expression has been related to surface MHC shedding and immune evasion[42]. These findings contribute to the suggested pro-inflammatory transcriptional profile by downregulating genes involved in T cell regulation. Many of the DEGs had a function in inflammation, however we also identified DEGs involved in other processes. Particularly, genes involved in fatty acid metabolism (*SLC25A34* and *IDH3B*), the cytoskeleton (*KRT10, B4GALT4, SPTAN1,* and *MICAL3*), as well as translation and posttranslational modifications (*PARP4, EIF4B,* and *PABPN1*) were also found. Finally, *APOE* was downregulated, a finding which is likely a direct effect of the mutation carried by a subgroup of patients rather than a downstream effect of elevated triglycerides.

In $CD8^+$ T cells, only 2 DEGs were found in the primary moderate group, which were both upregulated (Supp. Table 1b). These two genes were *NFE2L3* and *MAST1*. *NFE2L3* encodes a transcription factor involved in binding antioxidant response elements and increased expression of this gene has been correlated to effector $CD8^+$ T cells[43]. *MAST1* encodes a protein that associates with microtubules. In the secondary moderate group, no differential expression was observed as compared with controls except for one gene in $CD8^+$ cells, namely *COLQ*, which encodes a subunit of a collagen-like molecule (Supp. Table 1c).

Although the individual DEGs observed for the two T cells and patient groups were different, the patterns of differential expression when combining all DEGs observed across analysis were remarkably similar (Fig. 2b; n=42). Additionally, we found that the effect sizes observed in $CD4^+$ cells of patients with primary moderate hypertriglyceridemia (n=39) matched in direction for 87% of the genes in primary moderate $CD8^+$ cells ($P_{binomial}<0.001$), and 98% of the genes in the secondary moderate $CD4^+$ cells ($P_{binomial}<0.001$), of which 19% and 24%, respectively, were also nominally significant.

To corroborate the pro-inflammatory transcription profiles of T cells, we measured hsCRP levels. As compared to controls (median, 0.75 [0.48-0.89] mg/L), hsCRP levels were particularly higher among patients with primary moderate hypertriglyceridemia (median 1.55 [0.82–5.24] mg/L; P=0.029) and to a lesser extent among patient with secondary hypertriglyceridemia (median 1.09 [0.49–2.45] mg/L; P=0.265; Table 1).

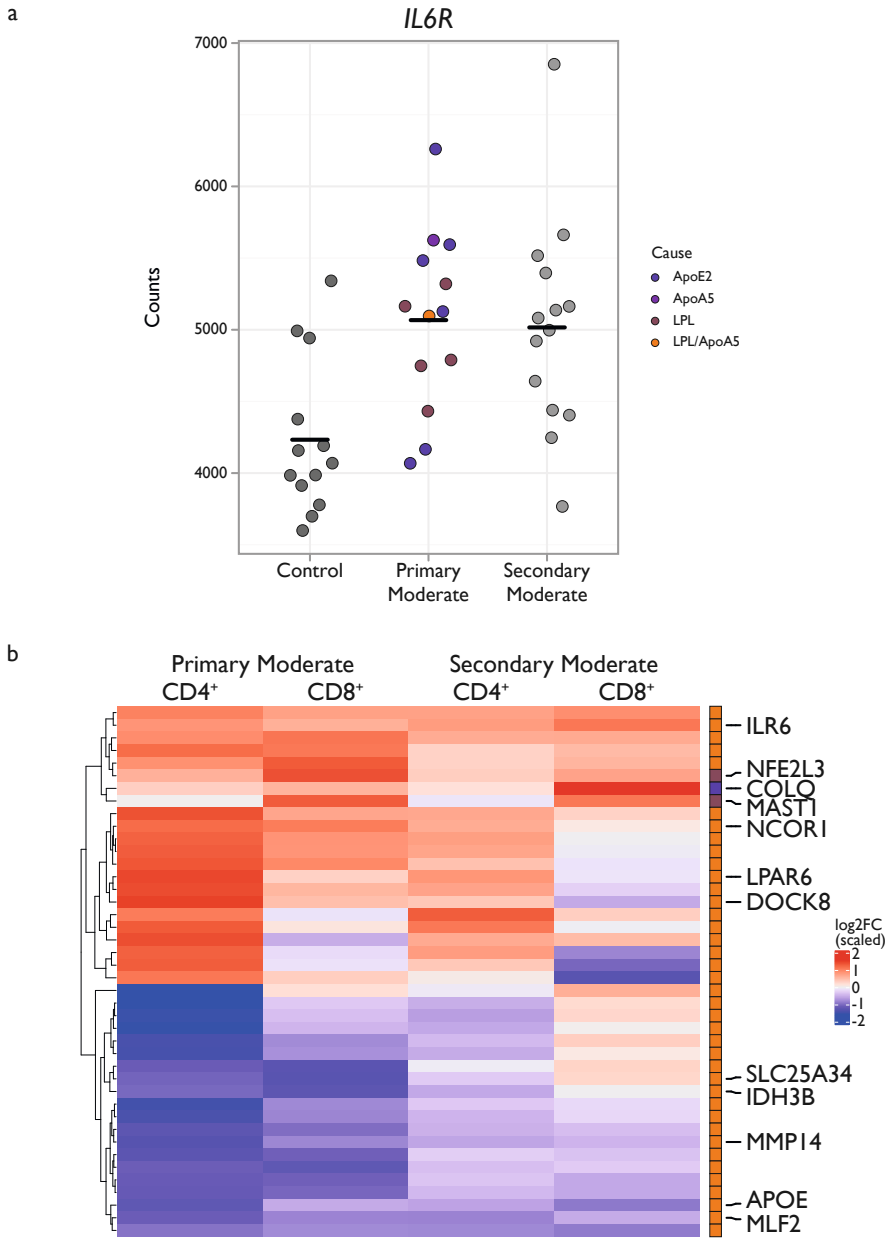

Fig. 2 | (a) Dot plot of the raw count data for the gene *IL6R* in $CD4^+$ T cells for the control, primary moderate, and secondary moderate groups. Dots are coloured by cause of hypertriglyceridemia. **(b)** Differentially expressed genes (DEGs) in $CD4^+$ and $CD8^+$ T cells from primary and secondary moderate groups as compared to the control group. Heatmap obtained from the *DESeq2* analysis resulting in 42 DEGs ($P_{FDR} < 0.05$). DEGs are clustered based on effect sizes. Bar on the right indicates the group in which the gene is differentially expressed (blue = $CD4^+$ primary moderate, orange = $CD8^+$ primary moderate, and green = $CD8^+$ secondary moderate. Genes of interest are labelled, $CD4^+$ T cells primary moderate n = 13, $CD8^+$ T cells primary moderate n = 12, $CD4^+$ T cells secondary moderate n = 14, and $CD8^+$ T cells secondary moderate n = 9.

Primary severe hypertriglyceridemia and hypotriglyceridemia induced transcriptomic effects on CD4⁺ and CD8⁺ T cells

We also enrolled a small number of participants with primary hypotriglyceridemia (n=4) and primary severe hypertriglyceridemia (n=2). In the hypotriglyceridemia group, we would expect opposite effects on the transcription profile in T cells. Indeed, for the 39 DEGs of the primary moderate CD4⁺ T cell group, 30 genes in CD4⁺ and 32 genes in CD8⁺ T cells showed the opposite effect size, 77% and 82%, respectively ($P_{binomial}$<0.001). Although triglycerides levels are very high in the primary severe group, this patient population is not considered to be at increased risk of CVD because the extreme triglyceride levels are mostly transported in chylomicrons[17]. This was reflected in that little to no difference in effect sizes was observed in the 39 DEGs of the primary moderate CD4⁺ T cell group. Specifically, 24 genes in the primary severe CD4⁺ group and 15 genes in primary severe CD8⁺ group showed the same effect size, 62% and 39%, respectively ($P_{binomial}$>0.05). In fact, the primary severe CD8⁺ group was more similar to the hypotriglyceridemia CD8⁺ group in direction of effect sizes with 27 genes or 69% going in the same direction ($P_{binomial}$<0.05). This result was visualized by plotting the effect sizes of the DEGs of the primary moderate and secondary moderate groups (n=42) in each of the groups and cell types tested (Fig. 3).

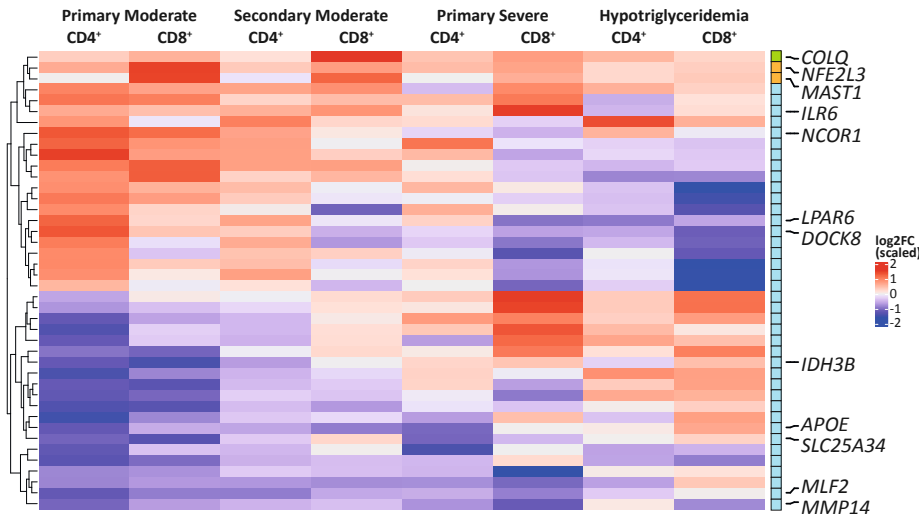

Fig. 3 | Differentially expressed genes (DEGs) in CD4⁺ and CD8⁺ T cells from primary and secondary moderate groups as compared to the control group. Heatmap shows the expression of the aforementioned DEGs in the CD4⁺ and CD8⁺ T cells from primary severe hypertriglyceridemia and hypotriglyceridemia groups as well. Heatmap obtained from the *DESeq2* analysis resulting in 42 DEGs (P_{FDR}<0.05). DEGs are clustered based on effect sizes. Genes of interest are labelled, CD4⁺ T cells primary moderate n=13, CD8⁺ T cells primary moderate n=12, CD4⁺ T cells secondary moderate n=14, CD8⁺ T cells secondary moderate n=9, CD4⁺ T cells primary severe n=2, CD8⁺ T cells primary severe n=2, CD4⁺ T cells hypotriglyceridemia n=4, and CD8⁺ T cells hypotriglyceridemia n=4.

Next, we further explored the associations of severely elevated and reduced triglycerides with CD4⁺ and CD8⁺ T cell gene expression as compared to the control. The primary severe group showed no DEGs in CD4⁺ T cells and 4 DEGs in CD8⁺ T cells that were unique to this group and

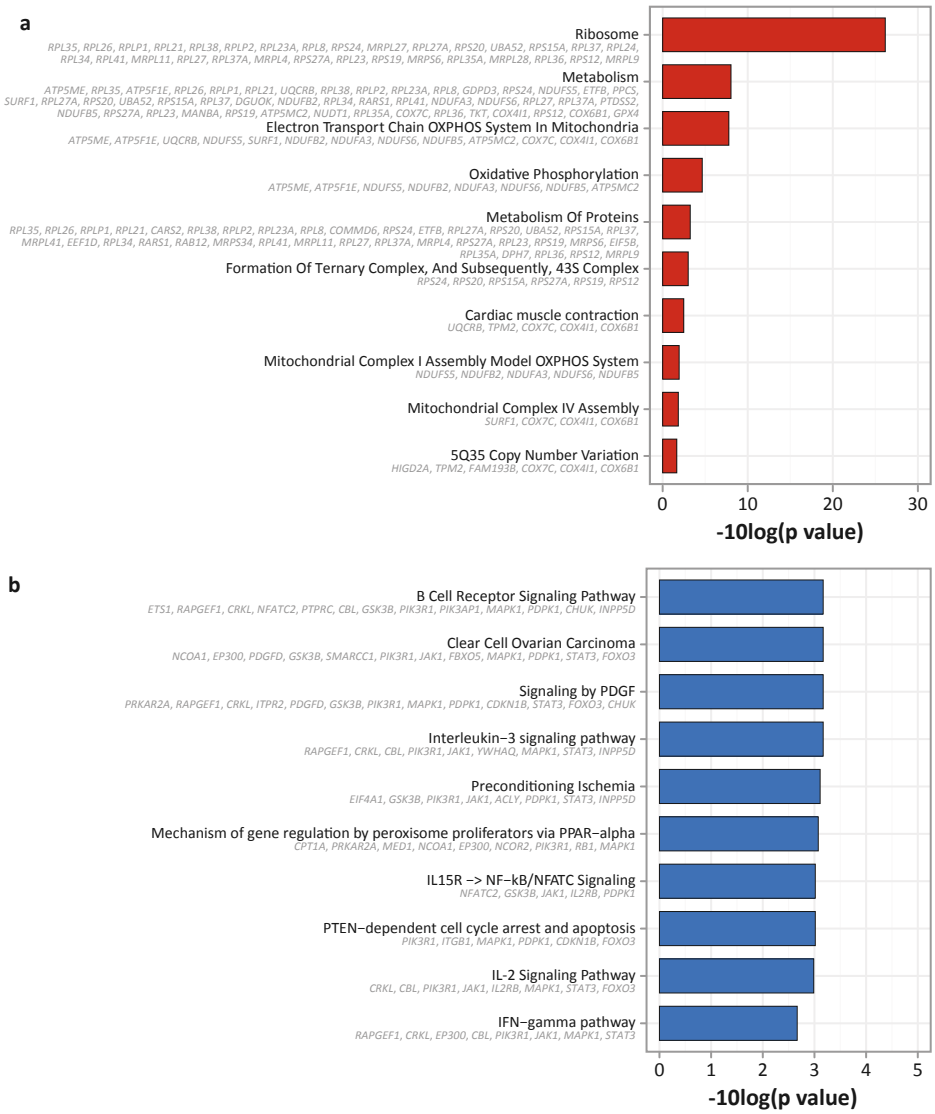

Fig. 4 | Pathway enrichment analysis of DEGs in the CD8⁺ T cells hypotriglyceridemia group. (a) Pathway enrichment analysis of all upregulated CD8⁺ T cell hypotriglyceridemia group DEGs generated using *clusterProfiler* using 10 human pathway databases. Top 10 enrichments are shown. **(b)** Pathway enrichment analysis of all downregulated CD8⁺ T cell hypotriglyceridemia group DEGs generated using *clusterProfiler* using 10 human pathway databases. Top 10 enrichments are shown.

downregulated (Supp. Table 1d). Strikingly, the hypotriglyceridemia group showed 66 DEGs in CD4⁺ T cells and 406 DEGs in CD8⁺ T cells (Supp. Table 1e and f). DEGs of CD4⁺ T cells showed upregulation of fatty acid and cholesterol biosynthesis and transport genes (*SCD*, *DHCR24*, and *LDLR*) as well as downregulation of pro-inflammatory T cell differentiation and immune response genes (*ETS1* and *CD84*). In CD8⁺ T cells, a formal analysis of enriched biological processes

showed 15 upregulated pathways (Fig. 4a; Supp. Table 1g) and 203 downregulated pathways (Fig. 4b; Supp. Table 1h). Upregulated pathways contained the ribosome (including *RPL35, RPL26, RPLP1,* and *RPL21*) and oxidative phosphorylation (including *ATP5ME, NDUFA3,* and *NDUFS6*). Downregulated pathways included B cell signalling (including *ETS1, NFATC2, GSK3B,* and *PIK3AP1*), IL-2 signalling (including *CRKL, JAK1, IL2RB,* and *STAT3*) and IFNγ pathway (including *RAPGEF1, EP300, PIK3R1,* and *MAPK1*).

As compared to controls (median, 0.75 [0.48-0.89] mg/L), hsCRP levels were not elevated among patients with primary severe hypertriglyceridemia (min-max 0-0.50mg/L; P=0.15) and decreased in hypotriglyceridemia (min-max 0.15-0.51mg/L; P=0.025; Table 1).

Discussion

Triglycerides and T cells have re-emerged as risk factors for atherosclerosis and CVD[22, 23]. However, whether triglycerides can affect T cell responses, which may contribute to atherosclerosis and CVD development, remains unknown. We studied patients with hypertriglyceridemia as a natural experiment of *in vivo* exposure to elevated triglyceride levels to determine the interaction between triglycerides and T cells. We found that transcriptomic landscapes of T cells markedly depended on the levels of circulating triglycerides. Specifically, we found that moderately elevated triglyceride levels, between 2.7–8.5mmol/L associated with a pro-inflammatory transcriptomic profile, while decreased triglyceride levels, between 0.1–0.3mmol/L associated with an anti-inflammatory transcriptomic profile, in both $CD4^+$ and $CD8^+$ T cells. Furthermore, we observed stronger effects among patients with primary moderate than with secondary moderate hypertriglyceridemia, possibly reflecting the persistent exposure to elevated triglycerides in patients with a genetic cause of the disorder. These results were reflected in high-sensitivity CRP levels, which were elevated more strongly in primary than secondary moderate patients. Our findings imply that moderately elevated triglycerides may induce a pro-inflammatory response in circulating T cells, which is attenuated in severely elevated and reversed in depleted triglyceride environments.

Moderately elevated triglyceride levels between 2–10mmol/L are associated with a higher risk of CVD[6]. We found that these levels of triglycerides also associated with a pro-inflammatory transcriptomic profile in T cells, specifically in $CD4^+$ T cells. $CD4^+$ T cells are generally thought to be pro-atherogenic, where depletion of $CD4^+$ T cells is atheroprotective[44], while addition of these cells aggravated atherosclerosis in an *Apoe*$^{-/-}$ mouse model[45, 46]. We found increased expression of multiple pro-inflammatory and pro-atherogenic genes such as *IL6R, NCOR1, DOCK8,* and *LPAR6,* in purified $CD4^+$ T cells from the primary moderate patients. The profile was also detectable in $CD8^+$ T cells, although not significantly. While the role of $CD8^+$ T cells in atherosclerosis has not yet been established[47, 48], the proportion of this cell type is enriched in atherosclerotic plaques as compared with the circulation[25]. These results suggest that $CD4^+$ T cells, and to a lesser extent $CD8^+$ T cells, are influenced by triglycerides to establish a pro-inflammatory phenotype, that may play role in T cell-mediated effects of triglycerides on atherosclerosis and CVD.

The pro-inflammatory transcriptomics profile discovered in the T cells of the primary moderate group was largely reproduced in both the transcriptomic profiles of the $CD4^+$ and $CD8^+$ T cells of secondary moderate patients. This was further reflected in the levels of high sensitivity CRP measured in both the primary and secondary moderate groups. Both groups showed increased levels of high sensitivity CRP above normal, but the levels were higher in the primary moderate group than in the secondary moderate group. Thus, our findings point to the consistent upregulation of pro-inflammatory transcriptomic profile in $CD4^+$ and $CD8^+$ T cells associated with moderately elevated triglyceride levels.

We also compared the results to T cells derived from patients with primary severe hypertriglyceridemia (>13mmol/L) and hypotriglyceridemia (<0.3mmol/L). However, because the mutations that lead to these disorders are very rare, only a small number of participants could be included. Nevertheless, we observed that in the primary severe group, the pro-inflammatory transcriptomic profile dissipates. The gene expression patterns here less closely resembled that of the moderately elevated groups, and very few genes were differentially expressed in both $CD4^+$ and $CD8^+$ T cells. In individuals with severe hypertriglyceridemia, excess triglycerides are stored in chylomicrons. Unlike smaller lipoproteins such as VLDL, chylomicrons have a limited ability to penetrate the arterial wall and typically have a relatively short lifespan in circulation, with a half-life of approximately 5min[17, 49]. Additionally, chylomicrons follow a route through the lymphatic system before entering circulation, while VLDL and other TGRLs are directly synthesized and released into circulation by the liver[50, 51]. Therefore, one possible explanation could be that chylomicrons may have fewer interactions with endothelial cells and the arterial wall, potentially resulting in reduced inflammatory responses in T cells.

On the contrary, T cells derived from the hypotriglyceridemia group expressed an anti-inflammatory transcriptional landscape, with pathways such as B cell signalling, IL-2 signalling, and IFNγ pathway being downregulated. Furthermore, the gene expression patterns of the hypotriglyceridemia group were opposite that of the primary and secondary moderate groups. Hypotriglyceridemia has been suggested to be atheroprotective[15, 16], which is supported by the anti-inflammatory transcriptional profile induced in T cells derived from these patients.

Conclusions

We report that circulating triglycerides are associated with T cell transcriptional landscapes that match the hypothesized pro-inflammatory effects of triglyceride levels and T cells in atherosclerosis and CVD[5-9, 52, 53]. Where patients with elevated triglycerides within the range of 2–10mmol/L, known to be atherogenic, associated with pro-inflammatory effects in T cells, but the effect dissipated above this range, known to be less atherogenic, and reversed in diminished triglyceride levels, thought to be atheroprotective. In conclusion, our findings stipulate that triglycerides may influence circulating T cells to promote the expression of a pro- or anti-inflammatory transcriptional landscape. The implication of this finding for atherosclerosis and CVD pathogenesis warrants further investigation.

Limitations of the study

To our knowledge, this is the first study investigating T cell transcriptomics over the full spectrum of triglyceride levels. Although the results of this study are based on a relatively small and heterogenous sample size, they do provide a meaningful comparison and insight into how different circulating levels of triglycerides might influence the immune system around it, particularly T cells. Furthermore, our use of individuals with hyper- and hypotriglyceridemia due to defined genetic mutations provides a natural *in vivo* exposure, which allowed us to study the effects in human T cells.

Translational perspectives

We report that patients with moderately elevated triglycerides have T cells with pro-inflammatory characteristics, including a higher interleukin-6 receptor expression, and increased levels of the inflammatory marker high sensitivity CRP. This observation is important to better understand why elevated triglycerides are a risk factor for CVD and helps the interpretation of the unexpectedly high benefit of triglyceride-lowering treatment using icosapent ethyl in the REDUCE-IT trial. Also, it suggests that this patient group at risk of CVD may benefit from anti-inflammatory treatments like canakinumab (CANTOS trial) and colchicine (COLCOT trial), or in the future, novel treatment like the interleukin-6 inhibitor ziltivekimab.

Acknowledgements
The authors' work is supported by the Dutch CardioVascular Alliance (The Dutch Heart Foundation, Dutch Federation of University Medical Centres, the Netherlands Organization for Health Research and Development, and the Royal Netherlands Academy of Sciences) for the GENIUSII project Generating the Best Evidence-Based Pharmaceutical Targets for Atherosclerosis (CVON2017-20).

Author contributions
B.T.H, J.W.J, and J.R.v.L. conceived the project. N.A.R. and J.M. designed and conducted the experiments, analysed the results, and drafted the manuscript. K.F.D. designed the analysis model and analysed the RNA sequencing data. T.B.K. aligned the RNA sequencing data. L.C.V-Z. and M.T.M. performed the plasma measurements including the analysis of the lipoprotein profiling. All authors contributed to the writing of the manuscript.

Competing interests
The authors declare no competing interests.

Data availability statement
Upon reasonable request, it can be expected that specific anonymous data will be shared to a qualified researcher.

References

1 Teslovich, T. M. *et al.* Biological, clinical and population relevance of 95 loci for blood lipids. *Nature* **466**, 707-713, (2010).

2 Schunkert, H. *et al.* Large-scale association analysis identifies 13 new susceptibility loci for coronary artery disease. *Nat. Genet.* **43**, 333-338, (2011).

3 Willer, C. J. *et al.* Discovery and refinement of loci associated with lipid levels. *Nat. Genet.* **45**, 1274-1283, (2013).

4 Do, R. *et al.* Common variants associated with plasma triglycerides and risk for coronary artery disease. *Nat. Genet.* **45**, 1345-1352, (2013).

5 Peng, J., Luo, F., Ruan, G., Peng, R. & Li, X. Hypertriglyceridemia and atherosclerosis. *Lipids Health Dis.* **16**, 233, (2017).

6 Nordestgaard, B. G. & Varbo, A. Triglycerides and cardiovascular disease. *Lancet* **384**, 626-635, (2014).

7 Puri, R. *et al.* Non-HDL cholesterol and triglycerides: implications for coronary atheroma progression and clinical events. *Arterioscler. Thromb. Vasc. Biol.* **36**, 2220-2228, (2016).

8 Zafrir, B., Jubran, A., Hijazi, R. & Shapira, C. Clinical features and outcomes of severe, very severe, and extreme hypertriglyceridemia in a regional health service. *J. Clin. Lipidol.* **12**, 928-936, (2018).

9 Arca, M. *et al.* Association of hypertriglyceridemia with all-cause mortality and atherosclerotic cardiovascular events in a low-risk italian population: the TG-REAL retrospective cohort analysis. *J. Am. Heart Assoc.* **9**, 015801, (2020).

10 Jørgensen, A. B. *et al.* Genetically elevated non-fasting triglycerides and calculated remnant cholesterol as causal risk factors for myocardial infarction. *Eur. Heart J.* **34**, 1826-1833, (2013).

11 Triglyceride Coronary Disease Genetics Consortium and Emerging Risk Factors Collaboration. Triglyceride-mediated pathways and coronary disease: collaborative analysis of 101 studies. *Lancet* **375**, 1634-1639, (2010).

12 Varbo, A. *et al.* Remnant cholesterol as a causal risk factor for ischemic heart disease. *J. Am. Coll. Cardiol.* **61**, 427-436, (2013).

13 Varbo, A., Benn, M., Tybjaerg-Hansen, A. & Nordestgaard, B. G. Elevated remnant cholesterol causes both low-grade inflammation and ischemic heart disease, whereas elevated low-density lipoprotein cholesterol causes ischemic heart disease without inflammation. *Circulation* **128**, 1298-1309, (2013).

14 Holmes, M. V. *et al.* Mendelian randomization of blood lipids for coronary heart disease. *Eur. Heart J.* **36**, 539-550, (2015).

15 Dron, J. S. & Hegele, R. A. Genetics of triglycerides and the risk of atherosclerosis. *Curr. Atheroscler. Rep.* **19**, 31, (2017).

16 Thomsen, M., Varbo, A., Tybjaerg-Hansen, A. & Nordestgaard, B. G. Low nonfasting triglycerides and reduced all-cause mortality: a mendelian randomization study. *Clin. Chem.* **60**, 737-746, (2014).

17 Varbo, A. & Nordestgaard, B. G. Remnant cholesterol and triglyceride-rich lipoproteins in atherosclerosis progression and cardiovascular disease. *Arterioscler. Thromb. Vasc. Biol.* **36**, 2133-2135, (2016).

18 Brunzell, J. D. Hypertriglyceridemia. *N. Engl. J. Med.* **357**, 1009-1017, (2007).

19 Nordestgaard, B. G. Triglyceride-rich lipoproteins and atherosclerotic cardiovascular disease new insights from epidemiology, genetics, and biology. *Circ. Res.* **118**, 547-563, (2016).

20 Budoff, M. Triglycerides and triglyceride-rich lipoproteins in the causal pathway of cardiovascular disease. *Am. J. Cardiol.* **118**, 138-145, (2016).

21 Jebari-Benslaiman, S. *et al.* Pathophysiology of atherosclerosis. *Int. J. Mol. Sci.* **23**, (2022).

22 Sandesara, P. B., Virani, S. S., Fazio, S. & Shapiro, M. D. The forgotten lipids: triglycerides, remnant cholesterol, and atherosclerotic cardiovascular disease risk. *Endocr. Rev.* **40**, 537-557, (2019).

23 Saigusa, R., Winkels, H. & Ley, K. T cell subsets and functions in atherosclerosis. *Nat. Rev. Cardiol.* **17**, 387-401, (2020).

24 Depuydt, M. A. *et al.* Microanatomy of the human atherosclerotic plaque by single-cell transcriptomics. *Circ. Res.* **127**, 1437-1455, (2020).

25 Fernandez, D. M. *et al.* Single-cell immune landscape of human atherosclerotic plaques. *Nat. Med.* **25**, 1576-1588, (2019).

26 Kersten, S. Triglyceride metabolism under attack. *Cell Metab.* **25**, 1209-1210, (2017).

27 Kersten, S. Physiological regulation of lipoprotein lipase. *Biochim. Biophys. Acta* **1841**, 919-933, (2014).

28 Reilly, N. A., Lutgens, E., Kuiper, J., Heijmans, B. T. & Wouter Jukema, J. Effects of fatty acids on T cell function: role in atherosclerosis. *Nat. Rev. Cardiol.* **18**, 824–837, (2021).

29 Proudfoot, J. M. *et al.* HDL is the major lipoprotein carrier of plasma F2-isoprostanes. *J. Lipid Res.* **50**, 716-722, (2009).

30 Versmissen, J. *et al.* Familial hypercholesterolaemia: cholesterol efflux and coronary disease. *Eur. J. Clin. Invest.* **46**, 643-650, (2016).

31 Love, M. I., Huber, W. & Anders, S. Moderated estimation of fold change and dispersion for RNA-seq data with DESeq2. *Genome Biol.* **15**, 550, (2014).

32 Gu, Z., Eils, R. & Schlesner, M. Complex heatmaps reveal patterns and correlations in multidimensional genomic data. *Bioinformatics* **32**, 2847-2849, (2016).

33 Yu, G., Wang, L. G., Han, Y. & He, Q. Y. clusterProfiler: an R package for comparing biological themes among gene clusters. *OMICS* **16**, 284-287, (2012).

34 Tanaka, T., Narazaki, M. & Kishimoto, T. IL-6 in inflammation, immunity, and disease. *Cold Spring Harb. Perspect. Biol.* **6**, 016295, (2014).

35 Dienz, O. & Rincon, M. The effects of IL-6 on CD4 T cell responses. *Clin. Immunol.* **130**, 27-33, (2009).

36 Interleukin-6 Receptor Mendelian Randomisation Analysis Consortium *et al.* The interleukin-6 receptor as a target for prevention of coronary heart disease: a mendelian randomisation analysis. *Lancet* **379**, 1214-1224, (2012).

37 Hainberger, D. *et al.* NCOR1 orchestrates transcriptional landscapes and effector functions of CD4+ T cells. *Front. Immunol.* **11**, 579, (2020).

38 Kearney, C. J., Randall, K. L. & Oliaro, J. DOCK8 regulates signal transduction events to control immunity. *Cell Mol. Immunol.* **14**, 406-411, (2017).

39 He, J., Meng, M. & Wang, H. A novel prognostic biomarker LPAR6 in hepatocellular carcinoma via associating with immune infiltrates. *J. Clin. Transl. Hepatol.* **10**, 90-103, (2022).

40 Fang, D. *et al.* MLF2 negatively regulates P53 and promotes colorectal carcinogenesis. *Adv. Sci.* **10**, 2303336, (2023).

41 Madapura, H. S. *et al.* p53 contributes to T cell homeostasis through the induction of pro-apoptotic SAP. *Cell Cycle* **11**, 4563-4569, (2012).

42 Liu, G., Atteridge, C. L., Wang, X., Lundgren, A. D. & Wu, J. D. The membrane type matrix metalloproteinase MMP14 mediates constitutive shedding of MHC class I chain-related molecule A independent of A disintegrin and metalloproteinases. *J. Immunol.* **184**, 3346-3350, (2010).

43 Zhang, Q. *et al.* NFE2L3 as a potential functional gene regulating immune microenvironment in human kidney cancer. *Biomed. Res. Int.* **2022**, 9085186, (2022).

44 Zhou, X., Robertson, A. K., Rudling, M., Parini, P. & Hansson, G. K. Lesion development and response to immunization reveal a complex role for CD4 in atherosclerosis. *Circ. Res.* **96**, 427-434, (2005).

45 Zhou, X., Robertson, A. K., Hjerpe, C. & Hansson, G. K. Adoptive transfer of CD4+ T cells reactive to modified low-density lipoprotein aggravates atherosclerosis. *Arterioscler. Thromb. Vasc. Biol.* **26**, 864-870, (2006).

46 Zhou, X., Nicoletti, A., Elhage, R. & Hansson, G. K. Transfer of CD4+ T cells aggravates atherosclerosis in immunodeficient apolipoprotein E knockout mice. *Circulation* **102**, 2919-2922, (2000).

47 van Duijn, J., Kuiper, J. & Slutter, B. The many faces of CD8+ T cells in atherosclerosis. *Curr. Opin. Lipidol.* **29**, 411-416, (2018).

48 Cochain, C. & Zernecke, A. Protective and pathogenic roles of CD8+ T cells in atherosclerosis. *Basic Res. Cardiol.* **111**, 71, (2016).

49 Nakajima, K. *et al.* Postprandial lipoprotein metabolism: VLDL vs chylomicrons. *Clin. Chim. Acta* **412**, 1306-1318, (2011).

50 Dash, S., Xiao, C., Morgantini, C. & Lewis, G. F. New insights into the regulation of chylomicron production. *Annu. Rev. Nutr.* **35**, 265-294, (2015).

51 Xiao, C., Hsieh, J., Adeli, K. & Lewis, G. F. Gut-liver interaction in triglyceride-rich lipoprotein metabolism. *Am. J. Physiol. Endocrinol. Metab.* **301**, 429-446, (2011).

52 Ketelhuth, D. F. & Hansson, G. K. Adaptive response of T and B cells in atherosclerosis. *Circ. Res.* **118**, 668-678, (2016).

53 Aukrust, P. *et al.* The complex role of T-cell-based immunity in atherosclerosis. *Curr. Atheroscler. Rep.* **10**, 236–243, (2008).

Supplemental information

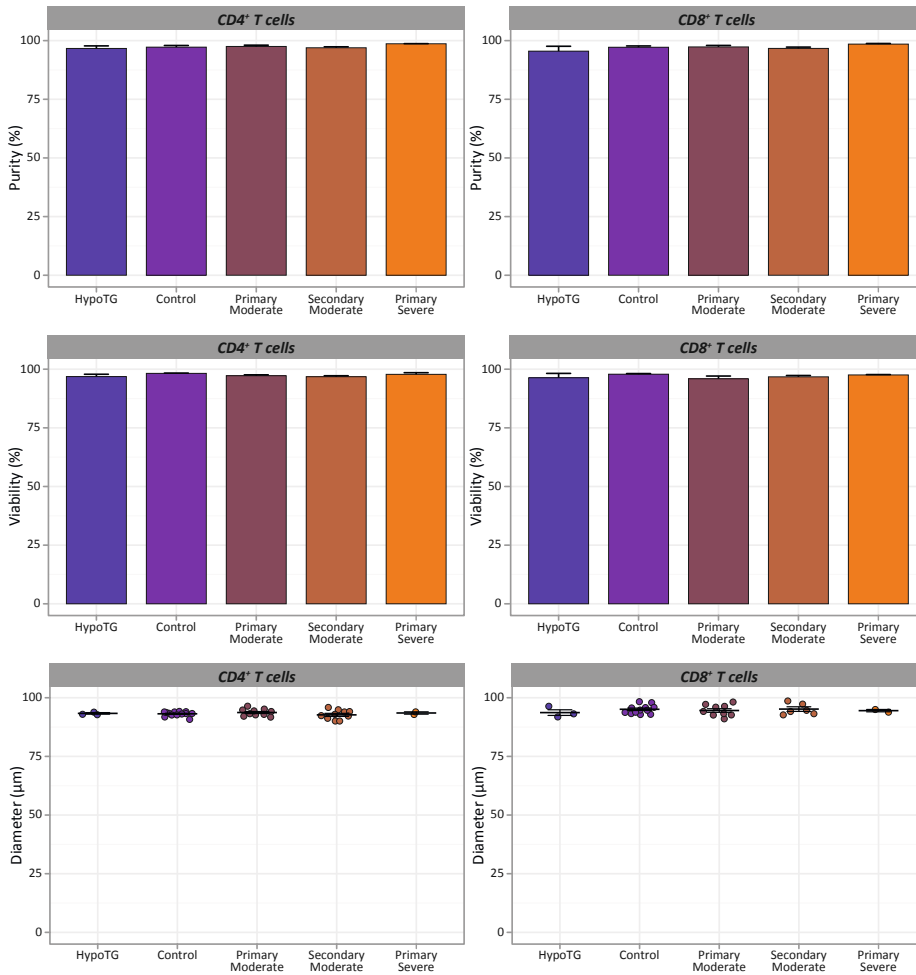

Supplemental Fig. 1 | Cell purity, viability, and diameter post-sorting. (a) Bar plot showing the average cell purity and standard error in percent of $CD4^+$ T cells isolated from each group as determined by the CytoFLEX SRT Benchtop cell sorter. On average the cell purity of $CD4^+$ T cells was 97.2 SE 0.7% for the control group, 97.5 SE 0.6% for the primary moderate group, 97.0 SE 0.4 for the secondary moderate group, 98.7 SE 0.1% for the primary severe, and 96.7 SE 1.1% for the hypotriglyceridemia group. **(b)** Bar plot showing the average cell purity and standard error in percent of $CD8^+$ T cells isolated from each group as determined by the CytoFLEX SRT Benchtop cell sorter. On average the cell purity of $CD8^+$ T cells was 97.2 SE 0.6% for the control group, 97.3 SE 0.6% for the primary moderate group, 96.7 SE 0.6 for the secondary moderate group, 98.5 SE 0.3% for the primary severe, and 95.5 SE 2.1% for the hypotriglyceridemia group. **(c)** Bar plot showing the average viability and standard error in percent, as determined by Via1-Cassette™ on a NucleoCounter® NC-200™ of $CD4^+$ T cells post-sorting per group. On average the cell viability of $CD4^+$ T cells was 98.2 SE 0.1% for the control group, 97.2 SE 0.4% for the primary moderate group, 96.8 SE 0.4% for the secondary moderate group, 97.8 SE 0.7% for the primary severe, and 96.9 SE 1.0% for the hypotriglyceridemia group. **(d)** Bar plot showing the average viability and standard error in percent, as determined by Via1-Cassette™ on a NucleoCounter® NC-200™ of $CD8^+$ T cells post-sorting per group. On average the cell viability of $CD8^+$ T

cells was 97.9 SE 0.3% for the control group, 95.9 SE 1.2% for the primary moderate group, 96.7 SE 0.6% for the secondary moderate group, 97.6 SE 0.2% for the primary severe, and 96.4 SE 1.9% for the hypotriglyceridemia group. **(e)** Dot plot showing the average cell diameter and standard error in µm, as determined by Via1-Cassette™ on a NucleoCounter® NC-200™ of $CD4^+$ T cells post-sorting per group. On average the cell diameter of $CD4^+$ T cells was 9.3 SE 0.03µm for the control group, 9.4 SE 0.04µm for the primary moderate group, 9.3 SE 0.07µm for the secondary moderate group, 9.4 SE 0.05µm for the primary severe, and 9.3 SE 0.03µm for the hypotriglyceridemia group. **(f)** Dot plot showing the average cell diameter and standard error in µm, as determined by Via1-Cassette™ on a NucleoCounter® NC-200™ of $CD8^+$ T cells post-sorting per group. On average the cell diameter of $CD8^+$ T cells was 9.5 SE 0.05µm for the control group, 9.5 SE 0.08µm for the primary moderate group, 9.5 SE 0.10µm for the secondary moderate group, 9.5 SE 0.05µm for the primary severe, and 9.4 SE 0.12µm for the hypotriglyceridemia group.

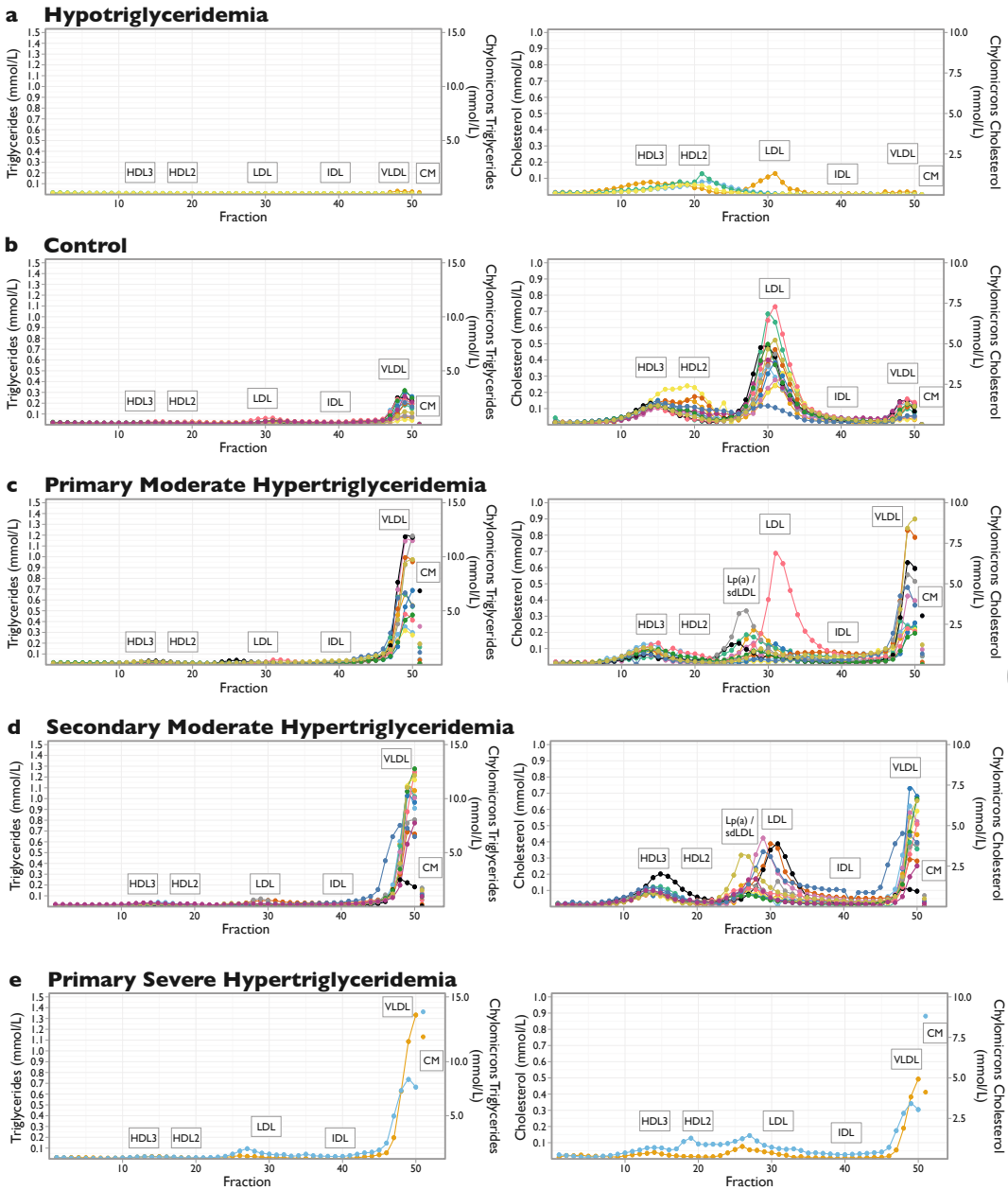

Supplemental Fig. 2 | Lipoprotein profiles per individual. Triglycerides are in the lefthand figures and cholesterol in the righthand figures of the **(a)** hypotriglyceridemia, **(b)** control, **(c)** primary moderate hypertriglyceridemia, **(d)** secondary moderate hypertriglyceridemia, and **(e)** primary severe hypertriglyceridemia group. Chylomicrons are depicted as separate values.

Supplemental Table 1 | Changes in gene expression in $CD4^+$ and $CD8^+$ T cells derived from patients with hypertriglyceridemia or hypotriglyceridemia.

Supplemental Table 1 | (a) DEGs for $CD4^+$ T cells from primary moderate hypertriglyceridemia group in order of significance along with their Ensembl ID, gene symbol, UniProt ID, base mean, log2 fold change, log fold change standard error, p value, and adjusted p value (FDR).

Order	Ensembl ID	Gene Symbol	UniProt	baseMean	Log2FC	Log2FC SE	P value	P_{FDR}
1	ENSG00000069329	*VPS35*	Q96QK1	1310.900	0.348	0.067	2.17E-07	0.002
2	ENSG00000141027	*NCOR1*	O75376	2275.859	0.334	0.071	2.30E-06	0.011
3	ENSG00000154165	*GPR15*	P49685	656.740	2.143	0.471	5.36E-06	0.011
4	ENSG00000089693	*MLF2*	Q15773	2214.182	-0.251	0.054	3.10E-06	0.011
5	ENSG00000169021	*UQCRFS1*	P47985	1370.786	-0.345	0.076	6.05E-06	0.011
6	ENSG00000175390	*EIF3F*	O00303	9104.610	-0.217	0.048	5.11E-06	0.011
7	ENSG00000107099	*DOCK8*	Q8NF50	4372.962	0.464	0.107	1.44E-05	0.016
8	ENSG00000123104	*ITPR2*	Q14571	1040.976	0.361	0.084	1.63E-05	0.016
9	ENSG00000131558	*EXOC4*	Q96A65	821.362	0.266	0.062	1.73E-05	0.016
10	ENSG00000125245	*GPR18*	Q14330	238.422	-0.966	0.224	1.65E-05	0.016
11	ENSG00000162910	*MRPL55*	Q7Z7F7	826.591	-0.290	0.066	1.22E-05	0.016
12	ENSG00000186395	*KRT10*	P13645	616.223	-0.324	0.074	1.12E-05	0.016
13	ENSG00000175536	*LIPT2*	A6NK58	161.772	-0.643	0.151	1.93E-05	0.017
14	ENSG00000121578	*B4GALT4*	O60513	891.611	-0.404	0.095	2.22E-05	0.018
15	ENSG00000110200	*ANAPC15*	P60006	765.260	-0.206	0.049	2.45E-05	0.018
16	ENSG00000185591	*SP1*	P08047	2182.606	0.304	0.073	3.07E-05	0.022
17	ENSG00000205413	*SAMD9*	Q5K651	1599.738	0.438	0.107	4.41E-05	0.028
18	ENSG00000126005	*MMP24OS*	A0A0U1RRL7	1002.648	-0.306	0.075	4.18E-05	0.028
19	ENSG00000159377	*PSMB4*	P28070	4855.277	-0.226	0.056	5.22E-05	0.031
20	ENSG00000144840	*RABL3*	Q5HYI8	676.009	0.287	0.072	6.11E-05	0.032
21	ENSG00000160712	*IL6R*	P08887	4629.771	0.291	0.073	6.16E-05	0.032
22	ENSG00000111786	*SRSF9*	Q13242	2738.199	-0.137	0.034	5.85E-05	0.032
23	ENSG00000198064	*NPIPB13*	A6NJU9	62.888	0.865	0.217	6.79E-05	0.033

[continued on next page]

Supplemental Table 1 | (a) *[continued]*

Order	Ensembl ID	Gene Symbol	UniProt	baseMean	Log2FC	Log2FC SE	P value	P_{FDR}
24	ENSG00000139679	*LPAR6*	P43657	2493.899	0.672	0.169	7.29E-05	0.034
25	ENSG00000125835	*SNRPB*	P14678	2318.209	-0.251	0.063	7.45E-05	0.034
26	ENSG00000162461	*SLC25A34*	Q6PIV7	123.128	-0.499	0.126	7.72E-05	0.034
27	ENSG00000157227	*MMP14*	P50281	38.752	-0.736	0.187	8.24E-05	0.035
28	ENSG00000130203	*APOE*	P02649	31.750	-0.839	0.214	9.03E-05	0.036
29	ENSG00000102699	*PARP4*	Q9UKK3	1744.975	0.352	0.091	0.00011	0.041
30	ENSG00000063046	*EIF4B*	P23588	29254.798	-0.285	0.074	0.00011	0.041
31	ENSG00000100836	*PABPN1*	Q86U42	1088.730	-0.271	0.070	0.00011	0.041
32	ENSG00000177311	*ZBTB38*	Q8NAP3	1667.448	0.405	0.106	0.00014	0.045
33	ENSG00000178440	*TIMM23B-AGAP6*		18.591	1.063	0.279	0.00014	0.045
34	ENSG00000197694	*SPTAN1*	Q13813	7831.595	0.293	0.077	0.00014	0.045
35	ENSG00000101365	*IDH3B*	O43837	2118.595	-0.197	0.052	0.00014	0.045
36	ENSG00000177570	*SAMD12*	Q8N8I0	306.832	0.736	0.195	0.00016	0.049
37	ENSG00000182134	*TDRKH*	Q9Y2W6	300.104	0.368	0.098	0.00017	0.049
38	ENSG00000092068	*SLC7A8*	Q9UHI5	139.980	-2.390	0.633	0.00016	0.049
39	ENSG00000243156	*MICAL3*	Q7RTP6	296.014	0.698	0.186	0.00017	0.049

Supplemental Table 1 | (b) DEGs for $CD8^+$ T cells from primary moderate hypertriglyceridemia group in order of significance along with their Ensembl ID, gene symbol, UniProt ID, base mean, log2 fold change, log fold change standard error, p value, and adjusted p value (FDR).

Order	Ensembl ID	Gene Symbol	UniProt	baseMean	Log2FC	Log2FC SE	P value	P_{FDR}
1	ENSG00000050344	*NFE2L3*	Q9Y4A8	131.314	1.551	0.300	2.28E-07	0.003
2	ENSG00000105613	*MAST1*	Q9Y2H9	14.915	4.616	1.001	4.00E-06	0.025

Supplemental Table 1 | (c) DEGs for $CD8^+$ T cells from secondary moderate hypertriglyceridemia group in order of significance along with their Ensembl ID, gene symbol, UniProt ID, base mean, log2 fold change, log fold change standard error, p value, and adjusted p value (FDR).

Order	Ensembl ID	Gene Symbol	UniProt	baseMean	Log2FC	Log2FC SE	P value	P_{FDR}
1	ENSG00000206561	*COLQ*	Q9Y215	566.855	1.374	0.294	2.96E-06	0.037

Supplemental Table 1 | (d) DEGs for $CD8^+$ T cells from primary severe group in order of significance along with their Ensembl ID, gene symbol, UniProt ID, base mean, log2 fold change, log fold change standard error, p value, and adjusted p value (FDR).

Order	Ensembl ID	Gene Symbol	UniProt	baseMean	Log2FC	Log2FC SE	P value	P_{FDR}
1	ENSG00000080493	*SLC4A4*	Q9Y6R1	246.560	-1.657	0.342	1.26E-06	0.016
2	ENSG00000109756	*RAPGEF2*	Q9Y4G8	722.977	-1.454	0.316	4.08E-06	0.025
3	ENSG00000169554	*ZEB2*	O60315	3472.877	-1.738	0.398	1.28E-05	0.042
4	ENSG00000189190	*ZNF600*	Q6ZNG1	2194.249	-1.463	0.336	1.34E-05	0.042

Supplemental Table 1 | (e) (partial) DEGs for $CD4^+$ T cells from hypotriglyceridemia group in order of significance along with their Ensembl ID, gene symbol, UniProt ID, base mean, log2 fold change, log fold change standard error, p value, and adjusted p value (FDR). Top 30 most significantly expressed genes are shown here.

Order	Ensembl ID	Gene Symbol	UniProt	baseMean	Log2FC	Log2FC SE	P value	P_{FDR}
1	ENSG00000099194	*SCD*	O00767	167.515	2.360	0.398	2.90E-09	3.60E-05
2	ENSG00000136541	*ERMN*	Q8TAM6	354.683	1.060	0.185	9.65E-09	5.99E-05
3	ENSG00000116133	*DHCR24*	Q15392	220.084	1.602	0.286	2.11E-08	8.75E-05
4	ENSG00000144152	*FBLN7*	Q53RD9	277.620	-0.650	0.124	1.44E-07	0.00045
5	ENSG00000198064	*NPIPB13*	A6NJU9	64.361	1.456	0.289	4.67E-07	0.00116
6	ENSG00000186166	*CENATAC*	Q86UT8	1448.013	0.615	0.132	3.16E-06	0.00654
7	ENSG00000075292	*ZNF638*	Q14966	3579.615	0.495	0.110	7.34E-06	0.00757
8	ENSG00000104133	*SPG11*	Q96JI7	2772.839	0.378	0.085	8.53E-06	0.00757

[continued on next page]

Supplemental Table 1 | (e) (partial) *[continued]*

Order	Ensembl ID	Gene Symbol	UniProt	baseMean	Log2FC	Log2FC SE	P value	P_{FDR}
9	ENSG00000115239	*ASB3*	Q9Y575	484.747	0.547	0.122	7.75E-06	0.00757
10	ENSG00000150401	*DCUN1D2*	Q6PH85	394.946	0.494	0.109	6.39E-06	0.00757
11	ENSG00000160447	*PKN3*	Q6P5Z2	83.384	1.032	0.227	5.76E-06	0.00757
12	ENSG00000196757	*ZNF700*	Q9H0M5	666.493	0.795	0.179	8.37E-06	0.00757
13	ENSG00000221914	*PPP2R2A*	P63151	1330.896	0.406	0.089	5.28E-06	0.00757
14	ENSG00000117298	*ECE1*	P42892	3252.266	-0.377	0.083	6.16E-06	0.00757
15	ENSG00000100055	*CYTH4*	Q9UIA0	4291.201	0.381	0.088	1.47E-05	0.01139
16	ENSG00000116350	*SRSF4*	Q08170	2338.237	0.499	0.115	1.42E-05	0.01139
17	ENSG00000185946	*RNPC3*	Q96LT9	1394.700	-0.620	0.143	1.56E-05	0.01139
18	ENSG00000108474	*PIGL*	Q9Y2B2	1201.827	-0.340	0.079	1.67E-05	0.01152
19	ENSG00000204178	*MACO1*	Q8N5G2	889.374	0.334	0.079	2.08E-05	0.01292
20	ENSG00000111276	*CDKN1B*	P46527	7866.116	-0.559	0.131	2.00E-05	0.01292
21	ENSG00000103222	*ABCC1*	P33527	2898.805	-0.272	0.065	2.57E-05	0.01443
22	ENSG00000115705	*TPO*	P07202	18.123	-3.135	0.746	2.62E-05	0.01443
23	ENSG00000258728	*ENSG 00000258728*		701.586	-0.627	0.149	2.67E-05	0.01443
24	ENSG00000106077	*ABHD11*	Q8NFV4	275.336	0.538	0.129	3.07E-05	0.01464
25	ENSG00000110628	*SLC22A18*	Q96BI1	299.581	1.153	0.277	3.06E-05	0.01464
26	ENSG00000139624	*CERS5*	Q8N5B7	959.383	0.499	0.120	3.18E-05	0.01464
27	ENSG00000206418	*RAB12*	Q6IQ22	450.507	0.567	0.136	3.18E-05	0.01464
28	ENSG00000121542	*SEC22A*	Q96IW7	252.048	0.448	0.108	3.58E-05	0.01588
29	ENSG00000170260	*ZNF212*	Q9UDV6	324.595	0.739	0.181	4.33E-05	0.01791
30	ENSG00000240053	*LY6G5B*	Q8NDX9	197.842	-0.464	0.113	4.30E-05	0.01791

Supplemental Table 1 | (f) (partial) DEGs for $CD8^+$ T cells from hypotriglyceridemia group in order of significance along with their Ensembl ID, gene symbol, UniProt ID, base mean, log2 fold change, log fold change standard error, p value, and adjusted p value (FDR). Top 30 most significantly expressed genes are shown here.

Order	Ensembl ID	Gene Symbol	UniProt	baseMean	Log2FC	Log2FC SE	P value	P_{FDR}
1	ENSG00000084112	*SSH1*	Q8WYL5	1657.780	-0.803	0.146	3.54E-08	0.00031
2	ENSG00000110090	*CPT1A*	P50416	1258.597	-1.728	0.326	1.12E-07	0.00049
3	ENSG00000139514	*SLC7A1*	P30825	702.125	-0.709	0.136	1.74E-07	0.00051
4	ENSG00000172493	*AFF1*	P51825	2084.541	-0.726	0.144	4.93E-07	0.00108
5	ENSG00000204472	*AIF1*	P55008	988.474	1.423	0.289	8.56E-07	0.00116
6	ENSG00000166446	*CDYL2*	Q8N8U2	292.277	-1.258	0.257	9.86E-07	0.00116
7	ENSG00000177311	*ZBTB38*	Q8NAP3	1843.038	-1.181	0.242	1.05E-06	0.00116
8	ENSG00000178502	*KLHL11*	Q9NVR0	423.669	-1.461	0.298	9.68E-07	0.00116
9	ENSG00000160218	*TRAPPC10*	P48553	2748.232	-0.805	0.167	1.34E-06	0.00131
10	ENSG00000172428	*COPS9*	Q8WXC6	659.556	0.642	0.134	1.59E-06	0.00140
11	ENSG00000114302	*FAAH*	P13861	1122.716	-0.785	0.167	2.73E-06	0.00210
12	ENSG00000135272	*MDFIC*	Q9P1T7	1620.508	-0.767	0.164	2.87E-06	0.00210
13	ENSG00000060237	*WNK1*	Q9H4A3	5648.666	-0.605	0.130	3.41E-06	0.00231
14	ENSG00000040199	*PHLPP2*	Q6ZVD8	406.036	-0.903	0.199	5.53E-06	0.00257
15	ENSG00000109452	*INPP4B*	O15327	1429.090	-0.974	0.213	4.88E-06	0.00257
16	ENSG00000111252	*SH2B3*	Q9UQQ2	1498.342	-0.561	0.124	5.84E-06	0.00257
17	ENSG00000125686	*MED1*	Q15648	1683.447	-0.759	0.167	5.66E-06	0.00257
18	ENSG00000133657	*ATP13A3*	Q9H7F0	1044.678	-0.958	0.211	5.40E-06	0.00257
19	ENSG00000134954	*ETS1*	P14921	26654.754	-0.683	0.149	4.57E-06	0.00257
20	ENSG00000164307	*ERAP1*	Q9NZ08	2230.601	-1.023	0.224	4.88E-06	0.00257
21	ENSG00000048707	*VPS13D*	Q5THJ4	2677.249	-0.558	0.124	6.92E-06	0.00257
22	ENSG00000084676	*NCOA1*	Q15788	2543.318	-0.730	0.162	6.96E-06	0.00257
23	ENSG00000104419	*NDRG1*	Q92597	1323.154	-0.587	0.130	6.61E-06	0.00257
24	ENSG00000173706	*HEG1*	Q9ULI3	1004.858	-1.213	0.270	7.23E-06	0.00257

[continued on next page]

Supplemental Table 1 | (f) (partial) *[continued]*

Order	Ensembl ID	Gene Symbol	UniProt	baseMean	Log2FC	Log2FC SE	P value	P_{FDR}
25	ENSG00000224470	*ATXN1L*	P0C7T5	2024.319	-0.828	0.185	7.31E-06	0.00257
26	ENSG00000024862	*CCDC28A*	Q8IWP9	363.350	0.769	0.172	7.66E-06	0.00259
27	ENSG00000066294	*CD84*	Q9UIB8	2499.072	-0.823	0.184	8.09E-06	0.00264
28	ENSG00000186469	*GNG2*	P59768	3931.442	-0.851	0.192	9.67E-06	0.00304
29	ENSG00000169020	*ATP5ME*	P56385	877.665	0.634	0.144	1.06E-05	0.00310
30	ENSG00000145734	*BDP1*	A6H8Y1	1555.640	-0.910	0.206	1.03E-05	0.00310

Supplemental Table 1 | (g) (partial) Pathway enrichment analysis of all upregulated CD8⁺ T cell hypotriglyceridemia DEGs generated using *clusterProfiler* using 10 human pathway databases. Enriched pathways are shown with information on which group that term clusters into based on the Jaccard index > 0.70, pathway term, number of DEGs that overlap with that databases gene set for that pathway, p value, adjusted p value, number of DEGs in that pathway that were upregulated, number of DEGs in that pathway that were downregulated, and gene names of all DEGs included in that pathway. Only the top term of the 15 groups are shown here.

Group	Term	Overlap	P value	Adjusted P value	Up-regulated	Down-regulated	Genes
1	Ribosome	31/116	4.12E-30	6.78E-27	31	0	*RPL35, RPL26, RPLP1, RPL21, RPL38, RPLP2, RPL23A, RPL8, RPS24, MRPL27, RPL27A, RPS20, UBA52, RPS15A, RPL37, RPL24, RPL34, RPL41, MRPL11, RPL27, RPL37A, MRPL4, RPS27A, RPL23, RPS19, MRPS6, RPL35A, MRPL28, RPL36, RPS12, MRPL9*
2	Metabolism	47/1130	2.04E-10	9.34E-09	47	0	*ATP5ME, RPL35, ATP5F1E, RPL26, RPLP1, RPL21, UQCRB, RPL38, RPLP2, RPL23A, RPL8, GDPD3, RPS24, NDUFS5, ETFB, PPCS, SURF1, RPL27A, RPS20, UBA52, RPS15A, RPL37, DGUOK, NDUFB2, RPL34, RARS1, RPL41, NDUFA3, NDUFS6, RPL27, RPL37A, PTDSS2, NDUFB5, RPS27A, RPL23, MANBA, RPS19, ATP5MC2, NUDT1, RPL35A, COX7C, RPL36, TKT, COX4I1, RPS12, COX6B1, GPX4*
3	Electron transport chain OXPHOS system in mitochondria	13/79	3.76E-10	1.67E-08	13	0	*ATP5ME, ATP5F1E, UQCRB, NDUFS5, SURF1, NDUFB2, NDUFA3, NDUFS6, NDUFB5, ATP5MC2, COX7C, COX4I1, COX6B1*
4	Oxidative phosphorylation	8/46	6.86E-07	2.21E-05	8	0	*ATP5ME, ATP5F1E, NDUFS5, NDUFB2, NDUFA3, NDUFS6, NDUFB5, ATP5MC2*
5	Metabolism of proteins	38/1186	2.02E-05	0.00057	38	0	*RPL35, RPL26, RPLP1, RPL21, CARS2, RPL38, RPLP2, RPL23A, RPL8, COMMD6, RPS24, ETFB, RPL27A, RPS20, UBA52, RPS15A, RPL37, MRPL41, EEF1D, RPL34, RARS1, RAB12, MRPS34, RPL41, MRPL11, RPL27, RPL37A, MRPL4, RPS27A, RPL23, RPS19, MRPS6, EIF5B, RPL35A, DPH7, RPL36, RPS12, MRPL9*

[continued on next page]

Supplemental Table 1 | (g) (partial) *[continued]*

Group	Term	Overlap	P value	Adjusted P value	Up-regulated	Down-regulated	Genes
6	SARS-CoV-2 modulates host translation machinery	6/39	3.79E-05	0.00099	6	0	*RPS24, RPS20, RPS15A, RPS27A, RPS19, RPS12*
7	Cardiac muscle contraction	5/31	0.00014	0.00333	5	0	*UQCRB, TPM2, COX7C, COX4I1, COX6B1*
8	Mitochondrial complex I assembly model OXPHOS system	5/41	0.00053	0.01153	5	0	*NDUFS5, NDUFB2, NDUFA3, NDUFS6, NDUFB5*
9	Mitochondrial complex IV assembly	4/25	0.00069	0.01440	4	0	*SURF1, COX7C, COX4I1, COX6B1*
10	5Q35 copy number variation	6/71	0.00108	0.02198	6	0	*HIGD2A, TPM2, FAM193B, COX7C, COX4I1, COX6B1*
11	Mitochondrial translation elongation	6/73	0.00125	0.02512	6	0	*MRPL41, MRPS34, MRPL11, MRPL4, MRPS6, MRPL9*
12	Signaling by constitutively active EGFR	3/16	0.00212	0.03964	3	0	*HRAS, UBA52, RPS27A*
13	Formation pf ATP by chemiosmotic coupling	3/16	0.00212	0.03964	3	0	*ATP5ME, ATP5F1E, ATP5MC2*
14	Cellular response to chemical stress	8/142	0.00236	0.04364	8	0	*SURF1, UBA52, NUDT2, RPS27A, COX7C, TKT, COX4I1, COX6B1*
15	Modulation by Mtb of host immune system	2/5	0.00263	0.04763	2	0	*UBA52, RPS27A*

Supplemental Table 1 | (h) (partial) Pathway enrichment analysis of all downregulated CD8⁺ T cell hypotriglyceridemia DEGs generated using *clusterProfiler* using 10 human pathway databases. Enriched pathways are shown with information on which group that term clusters into based on the Jaccard index > 0.70, pathway term, number of DEGs that overlap with that databases gene set for that pathway, p value, adjusted p value, number of DEGs in that pathway that were upregulated, number of DEGs in that pathway that were downregulated, and gene names of all DEGs included in that pathway. Only the top term of the first 20 groups are shown here.

Group	Term	Overlap	P value	Adjusted P value	Up-regulated	Down-regulated	Genes
1	B cell receptor signaling pathway	13/74	3.49E-07	0.00068	0	13	*ETS1, RAPGEF1, CRKL, NFATC2, PTPRC, CBL, GSK3B, PIK3R1, PIK3AP1, MAPK1, PDPK1, CHUK, INPP5D*
2	Clear cell ovarian carcinoma	12/65	5.71E-07	0.00068	0	12	*NCOA1, EP300, PDGFD, GSK3B, SMARCC1, PIK3R1, JAK1, FBXO5, MAPK1, PDPK1, STAT3, FOXO3*
3	Signaling by PDGF	13/80	8.91E-07	0.00068	0	13	*PRKAR2A, RAPGEF1, CRKL, ITPR2, PDGFD, GSK3B, PIK3R1, MAPK1, PDPK1, CDKN1B, STAT3, FOXO3, CHUK*
4	Interleukin-3 signaling pathway	9/36	1.05E-06	0.00068	0	9	*RAPGEF1, CRKL, CBL, PIK3R1, JAK1, YWHAQ, MAPK1, STAT3, INPP5D*
5	Preconditioning ischemia	8/28	1.40E-06	0.00078	0	8	*EIF4A1, GSK3B, PIK3R1, JAK1, ACLY, PDPK1, STAT3, INPP5D*
6	Mechanism of gene regulation by peroxisome proliferators via PPARα	9/39	2.18E-06	0.00084	0	9	*CPT1A, PRKAR2A, MED1, NCOA1, EP300, NCOR2, PIK3R1, RB1, MAPK1*
7	IL15R -> NF-κB/NFATC signaling	5/9	3.17E-06	0.00096	0	5	*NFATC2, GSK3B, JAK1, IL2RB, PDPK1*
8	PTEN-dependent cell cycle arrest and apoptosis	6/15	3.35E-06	0.00096	0	6	*PIK3R1, ITGB1, MAPK1, PDPK1, CDKN1B, FOXO3*
9	IL 2 signaling pathway	8/32	4.26E-06	0.00103	0	8	*CRKL, CBL, PIK3R1, JAK1, IL2RB, MAPK1, STAT3, FOXO3*
10	IFNγ pathway	8/36	1.10E-05	0.00216	0	8	*RAPGEF1, CRKL, EP300, CBL, PIK3R1, JAK1, MAPK1, STAT3*
11	Prostate cancer	11/72	1.17E-05	0.00216	0	11	*ETS1, EP300, GSK3B, JAK1, RB1, ABCC1, RUNX3, MAPK1, PDPK1, CDKN1B, STAT3*

[continued on next page]

Supplemental Table 1 | (h) (partial) *[continued]*

Group	Term	Overlap	P value	Adjusted P value	Up-regulated	Down-regulated	Genes
12	Interleukin-7 signaling pathway	7/27	1.34E-05	0.00221	0	7	*EP300, GSK3B, PIK3R1, JAK1, MAPK1, CDKN1B, STAT3*
13	Signaling events mediated by stem cell factor receptor (c-Kit)	8/37	1.37E-05	0.00221	0	8	*SH2B3, CRKL, CBL, GSK3B, PIK3R1, PDPK1, STAT3, FOXO3*
14	ALK associated neuroblastoma	6/19	1.64E-05	0.00244	0	6	*RAPGEF1, CRKL, MAPK1, PDPK1, STAT3, FOXO3*
15	Signal transduction	63/1228	1.73E-05	0.00248	0	63	*CPT1A, PRKAR2A, PHLPP2, SH2B3, NCOA1, GNG2, RAPGEF1, WIPF1, IKZF1, REST, CRKL, ARAP2, CLIP1, LATS2, EP300, STRN, KMT2D, BMPR2, ITPR2, CBL, ARHGAP35, PDGFD, NCOR2, GSK3B, TFDP2, LLGL1, LRIG1, F2R, DOCK2, PIK3R1, ITGB1, TAB2, SLK, ACTR2, JAK1, B4GALT1, PRKCH, NOTCH2, IL2RB, ERBIN, RAPGEF2, SEPTIN7, AKAP13, YWHAQ, PIK3AP1, RUNX3, INCENP, GFOD1, MAPK1, PDPK1, CDKN1B, WASF2, KTN1, STAT3, FOXO3, DOCK9, ARHGEF3, CHUK, TNKS2, CAB39, MYH9, FASN, PIP4K2A*
16	PI3K-Akt signaling pathway	16/153	1.94E-05	0.00259	0	16	*PHLPP2, GNG2, PDGFD, GSK3B, F2R, PIK3R1, ITGB1, JAK1, IL2RB, YWHAQ, PIK3AP1, MAPK1, PDPK1, CDKN1B, FOXO3, CHUK*
17	Kit receptor signaling pathway	8/39	2.07E-05	0.00267	0	8	*CRKL, EP300, CBL, PIK3R1, MAPK1, STAT3, FOXO3, INPP5D*
18	Interleukin-3, interleukin-5 and GM-CSF signaling	7/29	2.23E-05	0.00273	0	7	*RAPGEF1, CRKL, CBL, PIK3R1, JAK1, IL2RB, INPP5D*
19	Signaling by interleukins	11/77	2.25E-05	0.00273	0	11	*RAPGEF1, CRKL, CBL, PIK3R1, TAB2, JAK1, IL2RB, MAPK1, STAT3, CHUK, INPP5D*
20	IL-2 receptor beta chain in T cell activation	8/40	2.51E-05	0.00292	0	8	*CRKL, CBL, PIK3R1, JAK1, IL2RB, RB1, MAPK1, PDPK1*

CHAPTER 6

Summary and general discussion

Summary

The pathophysiology of atherosclerosis has traditionally been understood by the interactions between macrophages, excess cholesterol laden low density lipoprotein (LDL), and the vascular wall[1]. Although these components have been extensively studied and medications like statins have successfully lowered cholesterol levels and reduced cardiovascular risk, a residual risk of cardiovascular disease (CVD) still exists[2]. Thus, it is important to consider what alternative factors might be playing a role in the pathophysiology of this disease. The aim of this thesis was to uncover how triglycerides and fatty acids interacted with and influenced T cells in the circulation and to determine whether this pre-exposure could alter the function of T cells, which could shape the role these cells play in atherosclerosis (Fig. 1).

T cells, triglycerides and fatty acids are each components of interest in further uncovering the pathophysiology of atherosclerosis. To do this, studies generally explore the role of various individual fatty acids in the context of cardiovascular outcomes, investigate how specific fatty acids influence T cell function, or examine how T cells affect atherosclerosis. Yet, there is no overall picture of the differences and commonalities between the influence of various fatty acids on T cell responses. In **Chapter 2**, we connected the findings and results of such studies in a Review to provide a generalized overview of how fatty acids, T cells, and their interactions may contribute to atherosclerosis[3]. By comparing the known effects of specific fatty acids on T cell function and the known effects of specific fatty acids on atherosclerosis, we were able to show that, by and large, the effect a fatty acid had on atherosclerosis and T cell function were similar, that the effect of fatty acids was primarily determined by the saturation level, and was similar for $CD4^+$ and $CD8^+$ T cells. Saturated fatty acids (SFAs) generally showed pro-inflammatory and pro-atherogenic effects while polyunsaturated fatty acids (PUFAs) had anti-inflammatory and atheroprotective effects. The effect of monounsaturated fatty acids (MUFAs) depended on the context of the experiment and can have both pro- and anti-inflammatory/atherogenic effects. Our review highlighted the key role for cellular metabolism in the fatty acid-induced alterations in T cell function, namely activation, proliferation and differentiation. A limitation of the studies performed so far was that they were performed during or after T cell activation, which might influence the outcomes measured as this process requires the import and use of nutrients to support cell growth and proliferation. The evaluation of current literature led us to hypothesize that the influences of fatty acids on T cells already occurs prior to activation, in a non-activated state in the circulation, which would affect the impact of T cells on the pathophysiology of atherosclerosis upon entering the plaque, where they become activated[4].

To test the hypothesis resulting from **Chapter 2**, **Chapter 3** describes the set up and use of an *in vitro* model for non-activated T cell exposure to oleic acid[5]. Oleic acid, a MUFA, is one of the most common fatty acids in the circulation[6]. The high natural abundance of this fatty acid in the circulation along with the strong effects on T cells found in previous studies make oleic acid of particular interest for further investigation[7-13]. To this end, we employed transcriptome-wide analysis of oleic acid exposed non-activated $CD4^+$ T cells. Not only have $CD4^+$ T cells been found

to aggravate atherosclerotic disease in mouse models[14, 15], but this cell type is known for its ability to differentiate into several subsets that each induce a distinct pro- or anti-inflammatory effect[16]. This makes $CD4^+$ T cells of particular investigative interest over $CD8^+$ T cells, whose role in atherosclerosis remains debated[17, 18]. We discovered that oleic acid resulted in a highly specific upregulation of cholesterol and fatty acid biosynthesis related genes and pathways. This metabolic reprogramming pre-activation resulted in increased IL-9^+ producing cells post-activation. Intriguingly, the expression of this highly pro-inflammatory cytokine was reversed when cells were exposed to the metabolic inhibitors of cholesterol and fatty acid biosynthesis during oleic acid exposure. Thus, this study supports our hypothesis from **Chapter 2**: non-activated T cells, as they occur in the circulation, can be influenced by fatty acids to become poised for preferential differentiation after activation.

Oleic acid was of interest because of its high abundance and strong effects on T cells. Yet, the interest in eicosapentaenoic acid (EPA), a PUFA, has recently increased dramatically because it was found to strongly reduce atherosclerotic CVD risk in the landmark clinical trial, REDUCE-IT[19, 20]. However, the mechanism by which EPA exerts its beneficial effects remain largely speculative. In **Chapter 4**, we test the effect of EPA on T cells to contribute understanding of the favorable outcomes observed in the REDUCE-IT trial[21]. In REDUCE-IT, patients received 4g of icosapent ethyl (IPE), a highly purified form of EPA, administered orally as 2g twice daily[22]. Upon ingestion, IPE is metabolized into EPA and absorbed into the bloodstream. Here EPA can interact with many different components of the circulation, including T cells. We employed the same *in vitro* model developed in **Chapter 3** to determine whether EPA can induce favorable transcriptomic properties in non-activated $CD4^+$ T cells. To our surprise, we observed a very strong downregulation of immune response and upregulation of antioxidant related genes through RNA sequencing. The putative effects of EPA were an order of magnitude greater than the effects we found for palmitic, a SFA, or oleic acid, a MUFA. Our data suggests that fatty acids have unique effects on non-activated T cells, as EPA, palmitic acid and oleic acid each had distinct effects on T cell transcriptomics. Our data highlights that EPA triggers a robust anti-inflammatory transcriptional profile in non-activated $CD4^+$ T cells, suggesting its potential therapeutic benefits through the modulation of immune and antioxidant genes.

In **Chapters 3** to **4**, we showed that individual fatty acids have distinct effects on T cell function *in vitro*. Yet, *in vivo*, a mix of lipids are found in the circulation, including the composite of fatty acids, triglycerides, which have reemerged as a risk factor for CVD, especially at moderately increased levels[23, 24]. Although the exact role of triglycerides in CVD is still debated, individuals with moderate hypertriglyceridemia are at an increased risk for developing CVD[25-27]. However, it remains unknown if increased triglyceride levels can also influence T cells, and whether that may play a role in the increased risk of CVD observed. In **Chapter 5**, we aimed to translate our *in vitro* findings to an *in vivo* situation by determining the influence of increased circulating triglycerides on $CD4^+$ and $CD8^+$ T cells. The addition of $CD8^+$ T cells is relevant because these cells are the T cell type whose relative abundance is most increased in plaque as compared with the circulation[28].

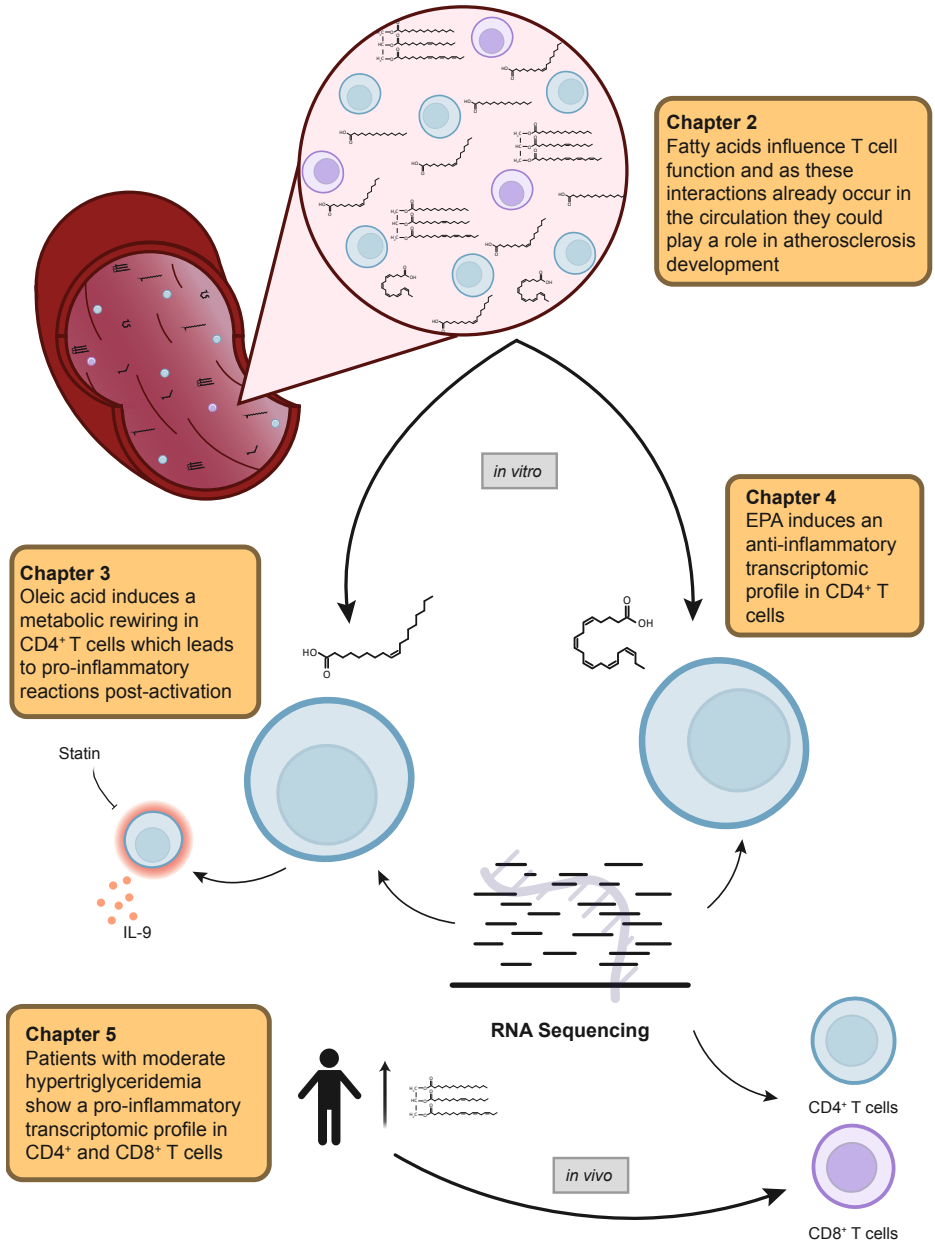

Fig. 1 | Overview of chapter progression and interrelation. This thesis starts in Chapter 2 by reviewing existing literature on the influence of fatty acids on T cells and their potential role in atherosclerosis development and progression. This chapter concludes by formulating a hypothesis that lays the groundwork for all subsequent research performed in this thesis. Chapters 3 and 4 focus on investigating the effects of a specific fatty acid on non-activated $CD4^+$ T cell transcriptomics *in vitro*. Chapter 3 additionally examines cellular function post-activation and finds that metabolic inhibitors can block the observed changes. Lastly, Chapter 5 aims to translate the *in vitro* findings to an *in vivo* context by analyzing the transcriptomic profiles of $CD4^+$ and $CD8^+$ T cells derived from patients with hypertriglyceridemia.

While the role of $CD8^+$ T cells in atherosclerosis pathogenesis remains disputed, investigating their function may offer valuable insights into how triglycerides influence T cell responses[17, 18]. We investigated patients with primary moderate and secondary moderate hypertriglyceridemia, and discovered that T cells derived from these individuals have a more pro-inflammatory transcriptomic landscape as compared to the control group. In addition, this effect was attenuated in patients with primary severe hypertriglyceridemia and reversed in hypotriglyceridemia, showing that different triglycerides levels may shape T cell transcriptomics towards a more pro- or anti-inflammatory profile. This reveals that the circulatory landscape of an individual may have profound effects on T cell function, which may influence the role these cells play in atherosclerosis and CVD.

Fatty acid induced effects on T cells

In **Chapter 2** we presented an overview of the effects that various studies have identified regarding the impact of fatty acids on T cells from experimental studies and linked these outcomes to the effects of these fatty acids on atherosclerosis as reported by epidemiological studies. In each experimental study the effect of 1–9 different fatty acids was evaluated and maximally 2 of the 4 functional outcomes: metabolism, activation, proliferation, and differentiation. The four categories defined each characterize a different aspect of the T cell immune response starting from activation and ending at differentiation, with metabolism underlying each of the other three categories[29, 30]. By determining how fatty acids influence T cells during or post-activation, we can gain an understanding of how T cells may react in the lipid rich core of the atherosclerotic plaque, where T cells are in an activated state[4]. However, the method for measuring the same functional outcome differed between studies[9-12, 31-34]. The diversity in the methods used to expose T cells to fatty acids as well as to determine T cell function, suggest a need for a standardized model of T cell fatty acid exposure. Furthermore, the lack of a consensus of what a proper control is for these types of studies, whether it is nothing, a solvent, or another fatty acid, requires careful consideration[9, 32, 35]. Most importantly, measuring T cell outcomes post-activation gives no indication of whether T cells can be influenced by fatty acids encountered in the circulation, where T cells remain in a non-activated state, and whether pre-exposure to a fatty acid can impact T cell function at a later time.

The overview created in **Chapter 2** allowed us to discern which fatty acids would be of interest for future investigation. In particular, fatty acids that have a high relative abundance in blood and those with variable or strong effects on T cell function, such as palmitic acid, oleic acid and/or EPA, were of interest[6-13, 31-34, 36-48]. Therefore, these fatty acids were chosen to continue our investigations with in **Chapter 3** and **4**. We started by investigating oleic acid in **Chapter 3**. This was because previous research found both pro- or anti-inflammatory effects of monounsaturated fatty acids, including oleic acid, despite it being one of the most abundant fatty acids in circulation[6-13]. We found that oleic acid induced a pro-inflammatory profile $CD4^+$ T cells, likely through rewiring cellular metabolic pathways pre-activation, as marked by distinct and specific changes in gene

expression. By establishing a standardized model for fatty acid T cell exposure in **Chapter 3**, we were able to extrapolate its use to investigate multiple fatty acids at once in **Chapter 4**. Here, we focused primarily on EPA because of its strong anti-inflammatory properties particularly as observed in the REDUCE-IT trial[19, 20]. It was conceivable that non-activated T cells respond to all fatty acids in a similar way, inducing changes in metabolic pathways. However, this was not the case as **Chapter 4** showed almost no changes in gene expression of metabolic pathways due to EPA exposure. Instead, immune response related genes were strongly downregulated. Oleic acid once again showed a strong upregulation of metabolic genes. Palmitic acid exposed non-activated T cells downregulated metabolic genes, and there was little overlap between differentially expressed genes (DEGs) between the three different fatty acid exposed T cells. Therefore, the specific fatty acid a T cell comes into contact with in the circulation can induce a unique response in that T cell, which may dictate the responses that T cell has upon entering the lipid environment of the atherosclerotic plaque.

Modeling triglyceride, fatty acid, and T cell interactions

We showed in **Chapter 2** that a number of different models were used to examine fatty acid effects on T cells and thus we first aimed to devise a standardized model of fatty acid T cell exposure. Although animal models are commonly used for disease modelling and have previously also been used to determine fatty acid effects on T cells, *in vivo* models such as these come with the disadvantages of cost, duration, ethics, and genetic differences that make human translation difficult[49, 50]. Instead, we developed an *in vitro* model of fatty acid T cell exposure in **Chapter 3**. Developing an *in vitro* model allowed us to use $CD4^+$ T cells derived from human subjects as well as tightly control the concentration and duration of fatty acid exposure in both **Chapter 3** and **4**. While *in vitro* models do simplify the environment and present limitations such as static conditions, limited microenvironmental factors, and absence of tissue architecture, our goal was to closely mimic the conditions of the circulation[51]. We ensured our model mimicked the conditions of the circulation by using bovine serum albumin (BSA) bound fatty acid and non-activated cells cultured in the presence of fetal calf serum (FCS). Furthermore, we were also able to establish a proper control for these types of studies. The model developed used the solvent, ethanol, in which oleic acid was diluted as the control and compares the results to medium only, this eliminates the possibility of the solvent having an effect on the T cells. For these reasons, we are confident that our model reflects the most optimal conditions to study individual fatty acid effects on T cells in the human setting. The data derived from this model are highly reliable, translational, and can aid in reducing the need for the use of animal models.

In vitro modelling allowed for a controlled fatty acid exposure to T cells. The model was designed to simplify the biological system of the circulation and aid in uncovering the specific mechanisms of actions that increased fatty acid exposure had on non-activated T cells. However, the human circulation is a complex environment that an *in vitro* model could never fully mimic. Furthermore, T cells in the circulation are exposed to a myriad of lipids, including fatty acids and triglycerides, at

the same time. Therefore, it was important to measure T cell responses to increased triglycerides *in vivo*. Instead of turning towards the use of animal models, we opted to use a human model in **Chapter 5**. This was possible because the condition of moderately elevated triglycerides exists naturally in humans, called hypertriglyceridemia[52]. This condition provides a natural exposure model to study T cell reactions to increased triglycerides. In this regard, human *in vivo* testing is possible because the T cells only needed to be collected from the blood of these individuals and no other intervention was necessary. This allowed us to investigate how circulating triglycerides could influence T cells in a human system. While our *in vivo* model could not be used to verify our *in vitro* findings and the complexity of this system did not allow us to draw causative conclusions from our analysis, it did provide a starting point from which future work can build and extrapolate.

The choice between utilizing an *in vitro* or *in vivo* model depends on the specific circumstances and the particular question being addressed. In **Chapter 3** and **4** utilizing an *in vitro* model came with the advantage of being able to isolate the impact of a specific fatty acid on $CD4^+$ T cell gene expression and function. This allowed us to draw causative conclusions as we compared what the addition of one particular substance had on T cells while the rest of the conditions remained constant. Drawing causative conclusions *in vivo* is more difficult as the complexity of the system does not allow for a direct link to be laid between exposed and not exposed individuals. However, the use of a human *in vivo* model allowed us to directly study a complex biological system. Furthermore, our *in vivo* model also allowed us to measure how prolonged exposure to elevated triglycerides can influence T cells, which is not possible *in vitro*, due to the relatively short-lived nature of T cells. Both models did allow for the inclusion of multiple concentrations of fatty acids and triglyceride levels in the analysis, although the *in vitro* model only moved forward with one concentration, while the *in vivo* model was able to compare the effects different levels of triglycerides had on T cell gene expression. By using a mix of both *in vitro* and *in vivo* models this thesis was able to better understand how lipid T cell interactions in the circulation may be able to shape immune responses in diseases such as atherosclerosis.

Identifying T cell responses via RNA sequencing

Chapter 2 showed that studies investigating the effects of fatty acids on T cells often employs functional outcomes, such as metabolism, activation, proliferation or differentiation, as the readout. However, changes to the T cell may already occur prior to the outward result, post-activation, of the fatty acid exposure. Instead, looking inward, towards what is occurring within the cell may shed a new light on the processes involved in fatty acid exposure in T cells. One place to look within the cell is towards changes in gene expression. Examining changes in gene expression allows us to pinpoint specific biological processes and key genes involved in cellular responses. Additionally, it enables us to predict subsequent alterations in cell function, as changes in gene expression typically precede functional changes in cells.

RNA sequencing has emerged as a revolutionary tool for studying changes in gene expression in the transcriptome and is one of the most cited next generation sequencing methods available[53]. This method involves sequencing the entirety of RNA in one single assay. By mapping these transcripts back to the human genome, it facilitates the identification of which genes come to expression under specific circumstances[54]. Additionally, it allows for the detection of novel features without the limitation of prior knowledge, as is necessary for methods such as real time quantitative polymerase chain reaction (RT-qPCR), which can only identify the expression of one singular chosen gene at a time[55]. We employed this technique in **Chapter 3**, **4**, and **5** to gain novel insights into T cell responses to fatty acids and triglycerides.

In **Chapter 3**, we identified 544 DEGs in non-activated $CD4^+$ T cells exposed to oleic acid across time using RNA sequencing. In doing so, we identified the upregulation of cholesterol biosynthesis and *de novo* fatty acid biosynthesis, each a key metabolic pathway in T cell activation and the development of pro-inflammatory $CD4^+$ T cell subsets[30]. What made this observation so remarkable, is that the T cells measured were not in an activated state, but rather non-activated. Thus, through RNA sequencing of non-activated $CD4^+$ T cells, we were able to predict that oleic acid exposure may induce a metabolic reprogramming in the cell, priming them for T cell activation and pro-inflammatory subset development post-activation. This line of thought was proven to be accurate as we later found increased frequencies of IL-9^+ producing $CD4^+$ T cells post-activation. Furthermore, we were able to identify similar genes in the 60 DEGs of oleic acid exposed non-activated $CD4^+$ T cells in **Chapter 4**, demonstrating the robustness of our approach. We also identified 1170 DEGs in EPA exposed and 33 DEGs in palmitic acid exposed non-activated $CD4^+$ T cells. The overlap between genes of each fatty acid exposed cell group was very small. This continues to show the unique signature each fatty acid has on $CD4^+$ T cells based on the degree of saturation, keeping in line with the conclusions drawn in **Chapter 2**. Additionally it also shows the precision of RNA sequencing as a technique. Lastly, RNA sequencing can also provide relevant information related to the *in vivo* situation as shown in **Chapter 5**, where the changes in gene expression could be mapped to deduce information about T cell profiles in different patient groups. For example, while there were no DEGs detected in patients with secondary moderate hypertriglyceridemia group, examining the expression of the primary moderate DEGs in the secondary moderate group revealed a highly similar profile between the two groups. Moreover, examining the same DEGs in the primary severe and hypotriglyceridemia group showed an attenuated and reversed, respectively, transcriptomic landscapes. Hence, RNA sequencing can provide meaningful insights into the changed biological processes upon fatty acid and triglyceride exposure, which can aid in predicting functional T cell outcomes.

DNA methylation and ATAC sequencing

The changes in transcriptomics correspond to the measured changes in function post-activation in **Chapter 3**, hinting that there may be a memory component to fatty acid exposure. However, to the best of our knowledge, no studies have delved into how a fatty acid exposure is able to

be retained by $CD4^+$ T cells. This is particularly important because the cells in **Chapter 3** and **4** were exposed to the fatty acid prior to activation. As epigenetics often underlies this type of cellular memory[56], we aimed to identify whether epigenetic processes played a role in the cellular recollection of fatty acid exposure.

First, we checked for changes in DNA methylation. This was originally performed as part of the work related to **Chapter 3**. Interestingly, no differences in methylation status between the oleic acid exposed and control conditions were found (Table 1-2) and the work was excluded upon peer review. DNA methylation entails the transfer of a methyl group onto the C5 position of the DNA base cytosine, which forms 5-methylcytosine. This inhibits transcription factor binding or recruits proteins implicated in gene repression to the DNA, limiting gene expression[57]. Thus, although epigenetic reprogramming is likely occurring in the cells, the mode of action is not via DNA methylation. However, DNA methylation is just one form of epigenetic gene regulation. Therefore, we performed Assay for Transposase-Accessible Chromatin (ATAC) sequencing on our EPA exposed non-activated $CD4^+$ T cells in **Chapter 4**. ATAC sequencing assesses genome-wide chromatin accessibility[58]. Again, no differences in open chromatin at individual regions between the EPA exposed and control conditions were detected. ATAC sequencing is done by sequencing open regions of chromatin by exposing DNA to the highly active transposase, Tn5, which preferentially inserts into open chromatin regions, which get sequenced. This method can aid in determining how chromatin packaging affects gene expression[59]. In remains unclear whether this is a true negative result or relates to limitations of the sensitivity of the method that detected >300 thousand peaks throughout the genome of uncertain functional relevance at varying sequencing depths. Alternative assays targeting other layers of epigenetic regulation may be adopted in future studies to resolve the memory component of fatty acid exposure in T cells.

Metabolic transformations during T cell activation have been found to be interconnected with epigenetics[60]. This makes the potential role of epigenetics in shaping cellular memory of interest for future investigation. Although we did not find differences in DNA methylation or open chromatin, via ATAC sequencing, there is some indication that histone acetylation may be an intriguing epigenetic modification to study. In **Chapter 3**, our RNA sequencing found increased expression of *SLC25A1*, a carrier that transports mitochondrial citrate to the cytosol. This carrier is required for cytosolic metabolism of citrate to regenerate acetyl-CoA, which becomes the main source for histone acetylation[61]. Histone acetylation is necessary not only for T cell activation, but also for T cell polarization[62]. Decreased cytosolic Acetyl-CoA production decreased histone acetylation at the *ifng* promoter and resulted in less IFNγ producing T_H1 cells[63]. Thus, it will be particularly interesting to measure histone acetylation in fatty acid exposed cells.

Table 1 | Top 10 CpGs ordered by P adjusted value. Differentially methylated CpGs in oleic acid exposed non-activated $CD4^+$ T cells. No evidence for differential DNA methylation after oleic acid exposure was observed across any time-point.

CpGs	Beta	Standard Error	T Statistic	P value	P adjusted
cg18478105	-3E-04	0.0004	-0.6571	0.51	0.95
cg14361672	-0.003	0.0026	-1.2504	0.22	0.95
cg01763666	-0.003	0.0067	-0.3766	0.71	0.95
cg02115394	-8E-04	0.0031	-0.2614	0.8	0.95
cg13417420	0.0011	0.0031	0.3553	0.72	0.95
cg26724186	0.0012	0.0012	0.9982	0.32	0.95
cg24133276	-0.002	0.0024	-0.9594	0.34	0.95
cg13773083	0.0094	0.0056	1.697	0.09	0.95
cg17236668	0.0009	0.0008	1.0411	0.3	0.95
cg19607165	-0.001	0.0033	-0.436	0.66	0.95

Table 2 | Top 10 genes ordered by P adjusted value. Differentially methylated CpGs in oleic acid exposed non-activated $CD4^+$ T cells mapped to the nearest gene. None of the top-10 differentially methylated CpGs mapped to genes were involved in metabolism or T cell function, neither did any of the nearest genes overlap with genes identified in the transcriptome analysis.

CpGs	Ensembl ID	Gene Name
cg18478105	ENSG00000149658	YTHDF1
cg14361672	ENSG00000160447	PKN3
cg01763666	ENSG00000176155	CCDC57
cg02115394	ENSG00000130177	CDC16
cg13417420	ENSG00000111276	CDKN1B
cg26724186	ENSG00000186111	PIP5K1C
cg24133276	ENSG00000123213	NLN
cg13773083	ENSG00000182698	RESP18
cg17236668	ENSG00000239857	GET4
cg19607165	ENSG00000137203	TFAP2A

Transcription factor footprinting

RNA and ATAC sequencing can also provide information on transcription factor binding. Transcription factors are proteins that control transcription, or the process of converting DNA into RNA. However, transcription factors commonly do not only bind directly to the promoter to have an effect on gene transcription, it can also bind several thousands of base pairs up- or downstream, to regulatory sequences such as enhancers or suppressors, through which it can stimulate or repress transcription[64]. Transcription factor footprinting is a technique that predicts which transcription factors may be active or inactive based on the known binding locations within the genome[65]. RNA sequencing data can resolve transcription factor binding information based on which sequences are present in the promotors of DEGs, as was done in **Chapter 3**. On the other hand, ATAC sequencing can identify likely transcription factors, based on the open chromatin segments that are sequenced, meaning it can also resolve information on transcription factor binding to enhancer and suppressor regions. In **Chapter 4**, we used the generated ATAC sequencing data to identify the downregulation of the key T_H2 and T_H9 transcription factors, GATA3 and PU.1, respectively, as well as the upregulation of the T_H17 antagonist REV-ERB, supporting the anti-inflammatory profile induced by EPA exposure. It is notable that our ATAC sequencing analysis did not yield any differentially expressed peaks, but the transcription factor footprinting did uncover results. Usually, ATAC sequencing generates a large number of differentially expressed peaks, which can be refined by focusing on peaks near transcription factors or DEGs. However, the reverse process is not feasible because changes in transcription factor binding does not necessarily imply relevance for nearby peaks. This unexpected outcome might stem from the inactive state of the exposed T cells or the quality of the ATAC sequencing. With more time, attention, and relaxed thresholds on peak calling, disparities in open chromatin could still emerge. Despite the initial negative findings from the ATAC sequencing analysis, the data could still be used to extract meaningful insights into cell function through transcription factor footprinting.

Measuring T cell functionality

Using the results of the RNA sequencing data generated in **Chapter 3**, we were able to formulate a hypothesis on the functional changes that may occur post-activation in $CD4^+$ T cells pre-exposed to oleic acid. To show these functional changes occurred post-activation, we employed several different methods to test T cell functionality. **Chapter 2** suggested that there were four facets to look at, metabolism, activation, proliferation, and differentiation. We initially investigated proliferation through a radioactive labeling-based assay[5]. We were unable to detect any differences in cellular proliferation using this method. This method utilizes a radioactive version of the DNA base thymine so that the radiolabeled thymidine is used to synthesize DNA during cell division. Thus, every cell division generates more radiolabeled thymidine, providing an overall measure of proliferation[66]. However, this method does not provide more detailed insights into proliferative capabilities such as number of cell divisions, and as such, other methods of cellular proliferation should be considered.

We next explored metabolism and activation utilizing a Seahorse bioanalyzer. Unfortunately, it proved difficult to obtain consistent results using this method. This method measures changes in oxygen consumption (OCR) and proton efflux (ECAR) in culture media as a measurement of cellular metabolism[67]. Given the distinct shift in cellular metabolism during activation from beta oxidation (oxygen consumption) to aerobic glycolysis (proton efflux), the Seahorse bioanalyzer offers the potential to quantify the rate of T cell activation and metabolic alterations[30]. However, this method is very sensitive and requires extremely controlled conditions, small changes in the pH of the medium, number of cells per well, and concentration of substrates added can all influence the results observed. Thus, the need for a large number of replicates limits the number of conditions and donors that can be measured at once, contributing to the variable results measured.

Next, we shifted our focus to the fourth facet of T cell function, differentiation. As T cells activate, they differentiate into various subsets marked by specific cytokine production and gene expression[29]. To measure cytokine production we employed an enzyme-linked immunosorbent assay (ELISA) and to measure changes in gene expression we used an RT-qPCR. Unfortunately, these methods yielded variable or nonsignificant results, making it difficult to interpret changes in T cell function. In an ELISA assay, an antigen, in this case the cytokine of interest, is anchored to a solid surface, either directly or through a capture antibody. Then, a detection antibody linked to a detectable molecule like an enzyme or a fluorophore binds to the antigen, which can be measured via a spectrophotometer[68]. An ELISA thus provides a semi-quantitative rather than an absolute measurements as it relies on standard curves for quantitation. An ELISA as well as an RT-qPCR may have difficulties measuring low abundance analytes because of its limited sensitivity and dynamic range[69]. Furthermore, ELISA's can suffer from cross reactivity with similar analytes as cells are measured in bulk samples and RT-qPCR's can suffer from amplification biases especially for low abundance transcripts[68, 70]. Both methods typically only measure one cytokine/gene at a time, which can be time-consuming and inefficient when analyzing multiple targets simultaneously[69, 70].

Finally, we adopted flow cytometry as a means of discerning T cell differentiation. This technique allows for complex mixtures of cells to be simultaneously characterized, identified, and is generally more sensitive than, for example, an ELISA. Cytometry, both traditional flow and spectral, depends on lasers to catch the scattering of light and one or more fluorescent markers that are read by detectors as single cells in solution flow passed. Thus, this technique can discern rare cell populations and low abundance cytokines with high sensitivity because it is measured at the single-cell level. Populations of cells can then be identified based on the light scattering and fluorescent properties[71]. In traditional flow cytometry, the aim is to collect the emission of a fluorochrome through one detector channel where it is expected to be excited. However, because most fluorochromes have broad emission spectra, "spill over" into another detector channel may occur, called spectral overlap, which has to be later compensated during the analysis to obtain the pure signal[72]. Instead, spectral cytometry records small segments of light, between 38–64 parameters, across the full spectrum. By recording each fluorochrome across the entire

emission spectra, a spectral fingerprint is produced. This reduces the need for compensation as each fluorochrome can be identified by its unique fingerprint and increases the number of markers which can be measured in one sample[73]. Therefore, we opted to use spectral cytometry to measure 26 different T cell markers both extra- and intracellularly as well as intranuclearly. The adoption of spectral cytometry enabled us to accurately characterize components of T cell differentiation, leveraging its ability to discern a broad range of markers simultaneously. This approach provided the stable and reproducible identification of increased IL-9$^+$ production by oleic acid pre-exposed T cells, underscoring the value of spectral cytometry in elucidating complex cellular responses.

Future directions

The experiments conducted in this thesis lay the groundwork for future investigations, particularly focusing on elucidating the relationship between triglycerides/fatty acids, T cells, and atherosclerosis. To advance our understanding, the next step involves providing mechanistic insights into how fatty acids influence T cell responses. Cellular proliferation, a crucial aspect of the adaptive immune response, was examined in **Chapter 3** using radioactive labeling. However, this method solely offers information on cell numbers without depicting proliferative capability, lacking data on the frequency of cell division. To address this gap, flow cytometry may be a valuable tool[74]. By labeling the cell membrane with a fluorescent dye, each cell division round results in signal dilution, allowing for the quantification of proliferative activity[75]. Moreover, alternative cytometry techniques like mass cytometry could provide deeper insights into T cell differentiation. Unlike conventional fluorescence-based methods, mass cytometry employs metal isotopes for cell labeling, overcoming spectral overlap issues. This approach enables the measurement of a larger number of markers in a single sample, facilitating the identification of cell subsets based on transcription factors and cytokines[76].

Single cell RNA sequencing may also offer additional insights into T cell subset development. Single cell RNA sequencing can not only identify subpopulations of T cells, but could also provide information about the genes and signaling pathways that are active or differentially expressed during subset development[77]. Moreover, to gain a full understanding of mechanistic outcomes of triglyceride/fatty acid exposure on T cells, examining protein production will be essential. Techniques that use mass spectrometry, such as shotgun proteomics may allow for high-throughput protein identification and quantification[78]. These techniques can assess whether transcriptomic changes translate into altered protein expression. Integrating these methods offers a comprehensive approach to elucidate how fatty acid exposure shapes T cell responses and provides a higher resolution of the underlying mechanisms.

Finally, translating the findings of this thesis into practice in the clinic will be important. By understanding how the various fatty acids of the circulation shape T cell responses, clinicians will be able to make more informed decisions in patient care. Understanding typical ranges of

fatty acids in the circulation allows clinicians to assess whether an individual deviates from these norms, potentially indicating either advantageous or detrimental effects based on the specific fatty acid. For instance, lower levels of oleic acid may suggest reduced risk of atherosclerosis due to decreased T_H9 cell development, and vice versa[5, 79]. This can be achieved through either standard lipid profiling or lipidomic profiling to provide information about concentrations of fatty acids in the circulation as well as in the atherosclerotic plaque[80, 81]. This will also show whether T cells might have a secondary response to a fatty acid encountered in the circulation and also in the plaque. This knowledge may also enable a more targeted approach to patient care, such as using statins to mitigate the inflammatory properties of oleic acid on T cells, thereby aiding this drugs anti-inflammatory and anti-atherogenic effects.

In order to do this, a comprehensive overview of T cells responses to fatty acids is imperative, especially considering variations in fatty acid concentrations in the circulation. This is particularly relevant for individuals with hypertriglyceridemia as triglycerides are the composite of three fatty acid chains linked by a glycerol group[25-27]. Understanding which fatty acids make up the triglycerides in an individual with hypertriglyceridemia could aid in understanding how to most effectively treat these patients. For example, boosting EPA concentrations with medications like IPE, to counteract the negative effects of more common fatty acids such as palmitic and oleic acid may mitigate inflammatory processes in T cells and aid in reducing atherosclerosis. Furthermore, analyzing T cells derived from individuals treated with IPE may offer additional insights into the beneficial outcomes observed of studies such as REDUCE-IT[19, 20].

Expanding this overview of fatty acid effects to other immune cell types, notably $CD8^+$ T cells, is crucial. $CD8^+$ T cells are the second most abundant immune cell type in circulation and their population increases in atherosclerotic plaques[28], yet their precise role in disease pathogenesis remains undefined[17, 18]. This lack of clarity may stem from how the circulatory landscape influences $CD8^+$ T cell responses. Furthermore, other immune cell types, such as monocytes, macrophages, B cells, and dendritic cells should also be investigated[1]. In doing so, an atlas could be created that elucidates how circulatory landscapes shape immune responses and, consequently, impact atherosclerosis development and progression. Thus, targeting triglycerides/fatty acids may offer beneficial effects on atherosclerosis by being able to shape anti-inflammatory responses in T cells.

Conclusion

This thesis represents a departure from previous research paradigms by delving into the intricate interplay between fatty acids and T cells, particularly focusing on their influence at earlier non-activated stages. By developing an innovative *in vitro* model, we not only unveiled the profound impact of fatty acid exposure on the transcriptomic landscape of T cells, but also revealed the consequential effects on responses post-activation. Moreover, this research attempted to bridge the gap between *in vitro* findings and real-world implications by investigating T cells from individuals with hypertriglyceridemia. While the exact mechanistic pathways remain to

be elucidated, these findings serve as a solid base from which new hypotheses can be generated and tested, suggesting that $CD4^+$ T cells are intricately molded by environmental interactions. Thus, targeting triglycerides and fatty acids may lead to beneficial effects on atherosclerosis by leveraging the anti-inflammatory properties of T cells. This work opens new avenues for exploration, advancing our understanding of the complex relationship between fatty acids and T cell dynamics, with implications for shaping our comprehension of human health and disease.

References

1 Schaftenaar, F., Frodermann, V., Kuiper, J. & Lutgens, E. Atherosclerosis: the interplay between lipids and immune cells. *Curr. Opin. Lipidol.* **27**, 209-215, (2016).

2 Sampson, U. K., Fazio, S. & Linton, M. F. Residual cardiovascular risk despite optimal LDL cholesterol reduction with statins: the evidence, etiology, and therapeutic challenges. *Curr. Atheroscler. Rep.* **14**, 1-10, (2012).

3 Reilly, N. A., Lutgens, E., Kuiper, J., Heijmans, B. T. & Wouter Jukema, J. Effects of fatty acids on T cell function: role in atherosclerosis. *Nat. Rev. Cardiol.* **18**, 824–837, (2021).

4 Grivel, J. C. *et al.* Activation of T lymphocytes in atherosclerotic plaques. *Arterioscler. Thromb. Vasc. Biol.* **31**, 2929-2937, (2011).

5 Reilly, N. A. *et al.* Oleic acid triggers metabolic rewiring of T cells poising them for T helper 9 differentiation. *iScience* **27**, 109496, (2024).

6 Bicalho, B., David, F., Rumplel, K., Kindt, E. & Sandra, P. Creating a fatty acid methyl ester database for lipid profiling in a single drop of human blood using high resolution capillary gas chromatography and mass spectrometry. *J. Chromatogr. A* **1211**, 120-128, (2008).

7 Endo, Y. *et al.* Obesity drives Th17 cell differentiation by inducing the lipid metabolic kinase, ACC1. *Cell Rep.* **12**, 1042-1055, (2015).

8 Angela, M. *et al.* Fatty acid metabolic reprogramming via mTOR-mediated inductions of PPARγ directs early activation of T cells. *Nat. Commun.* **7**, 13683, (2016).

9 Ioan-Facsinay, A. *et al.* Adipocyte-derived lipids modulate CD4+ T-cell function. *Eur. J. Immunol.* **43**, 1578-1587, (2013).

10 Moussa, M. *et al.* In vivo effects of olive oil-based lipid emulsion on lymphocyte activation in rats. *Clin. Nutr.* **19**, 49-54, (2000).

11 Passos, M. E. *et al.* Differential effects of palmitoleic acid on human lymphocyte proliferation and function. *Lipids Health Dis.* **15**, 217, (2016).

12 Hossein zade, A. *et al.* Fatty acids effect on T helper differentiation in vitro. *Int. J. Food Sci. Nutr.* **5**, (2016).

13 Miura, S. *et al.* Increased proliferative response of lymphocytes from intestinal lymph during long chain fatty acid absorption. *Immunology* **78**, 142-146, (1993).

14 Zhou, X., Robertson, A. K., Hjerpe, C. & Hansson, G. K. Adoptive transfer of CD4+ T cells reactive to modified low-density lipoprotein aggravates atherosclerosis. *Arterioscler. Thromb. Vasc. Biol.* **26**, 864-870, (2006).

15 Zhou, X., Nicoletti, A., Elhage, R. & Hansson, G. K. Transfer of CD4+ T cells aggravates atherosclerosis in immunodeficient apolipoprotein E knockout mice. *Circulation* **102**, 2919-2922, (2000).

16 Saigusa, R., Winkels, H. & Ley, K. T cell subsets and functions in atherosclerosis. *Nat. Rev. Cardiol.* **17**, 387-401, (2020).

17 Cochain, C. & Zernecke, A. Protective and pathogenic roles of CD8+ T cells in atherosclerosis. *Basic Res. Cardiol.* **111**, 71, (2016).

18 van Duijn, J., Kuiper, J. & Slutter, B. The many faces of CD8+ T cells in atherosclerosis. *Curr. Opin. Lipidol.* **29**, 411-416, (2018).

19 Bhatt, D. L. *et al.* Cardiovascular risk reduction with icosapent ethyl for hypertriglyceridemia. *N. Engl. J. Med.* **380**, 11-22, (2019).

20 Bhatt, D. L. *et al.* Effects of icosapent ethyl on total ischemic events from REDUCE-IT. *J. Am. Coll. Cardiol.* **73**, 2791-2802, (2019).

21 Reilly, N. A. *et al.* Eicosapentaenoic acid induces an anti-inflammatory transcriptomic landscape in T cells implicating a pathway independent of triglyceride lowering in cardiovascular risk reduction. *BioRxiv*, (2024).

22 Bhatt, D. L. *et al.* Rationale and design of REDUCE-IT: reduction of cardiovascular events with icosapent ethyl-intervention trial. *Clin. Cardiol.* **40**, 138-148, (2017).

23 Talayero, B. G. & Sacks, F. M. The role of triglycerides in atherosclerosis. *Curr. Cardiol. Rep.* **13**, 544-552, (2011).

24 Dron, J. S. & Hegele, R. A. Genetics of triglycerides and the risk of atherosclerosis. *Curr. Atheroscler. Rep.* **19**, 31, (2017).

25 Arca, M. *et al.* Association of hypertriglyceridemia with all-cause mortality and atherosclerotic cardiovascular events in a low-risk italian population: the TG-REAL retrospective cohort analysis. *J. Am. Heart Assoc.* **9**, 015801, (2020).

26 Toth, P. P. Triglycerides and atherosclerosis: bringing the association into sharper focus. *J. Am. Coll. Cardiol.* **77**, 3042-3045, (2021).

27 Peng, J., Luo, F., Ruan, G., Peng, R. & Li, X. Hypertriglyceridemia and atherosclerosis. *Lipids Health Dis.* **16**, 233, (2017).

28 Fernandez, D. M. *et al.* Single-cell immune landscape of human atherosclerotic plaques. *Nat. Med.* **25**, 1576-1588, (2019).

29 Smith-Garvin, J. E., Koretzky, G. A. & Jordan, M. S. T cell activation. *Annu. Rev. Immunol.* **27**, 591-619, (2009).

30 Chapman, N. M., Boothby, M. R. & Chi, H. Metabolic coordination of T cell quiescence and activation. *Nat. Rev. Immunol.* **20**, 55-70, (2020).

31 Stentz, F. B. & Kitabchi, A. E. Palmitic acid-induced activation of human T-lymphocytes and aortic endothelial cells with production of insulin receptors, reactive oxygen species, cytokines, and lipid peroxidation. *Biochem. Biophys. Res. Commun.* **346**, 721-726, (2006).

32 Haghikia, A. *et al.* Dietary fatty acids directly impact central nervous system autoimmunity via the small intestine. *Immunity* **43**, 817-829, (2015).

33 Monk, J. M., Hou, T. Y., Turk, H. F., McMurray, D. N. & Chapkin, R. S. n3 PUFAs reduce mouse CD4+ T-cell ex vivo polarization into Th17 cells. *J. Nutr.* **143**, 1501-1508, (2013).

34 Switzer, K. C., McMurray, D. N., Morris, J. S. & Chapkin, R. S. (n-3) Polyunsaturated fatty acids promote activation-induced cell death in murine T lymphocytes. *J. Nutr.* **133**, 496–503, (2003).

35 Kew, S. *et al.* Effects of oils rich in eicosapentaenoic and docosahexaenoic acids on immune cell composition and function in healthy humans. *Am. J. Clin. Nutr.* **79**, 674–681, (2004).

36 Gorjão, R., Cury-Boaventura, M. F., de Lima, T. M. & Curi, R. Regulation of human lymphocyte proliferation by fatty acids. *Cell Biochem. Funct.* **25**, 305-315, (2007).

37 Fan, Y. Y. *et al.* Remodelling of primary human CD4+ T cell plasma membrane order by n-3 PUFA. *Br. J. Nutr.* **119**, 163-175, (2018).

38 Pompos, L. J. & Fritsche, K. L. Antigen-driven murine CD4+ T lymphocyte proliferation and interleukin-2 production are diminished by dietary (n-3) polyunsaturated fatty acids. *J. Nutr.* **132**, 3293–3300, (2002).

39 Ly, L. H., Smith, R., Switzer, K. C., Chapkin, R. S. & McMurray, D. N. Dietary eicosapentaenoic acid modulates CTLA-4 expression in murine CD4+ T-cells. *Prostaglandins Leukot. Essent. Fatty Acids* **74**, 29-37, (2006).

40 Merzouk, S. A. *et al.* N-3 polyunsaturated fatty acids modulate in-vitro T cell function in type I diabetic patients. *Lipids* **43**, 485-497, (2008).

41 Jolly, C. A., Jiang, Y. H., Chapkin, R. S. & McMurray, D. N. Dietary (n-3) polyunsaturated fatty acids suppress murine lymphoproliferation, interleukin-2 secretion, and the formation of diacylglycerol and ceramide. *J. Nutr.* **127**, 37–43, (1997).

42 Collison, L. W., Collison, R. E., Murphy, E. J. & Jolly, C. A. Dietary n-3 polyunsaturated fatty acids increase T-lymphocyte phospholipid mass and acyl-CoA binding protein expression. *Lipids* **40**, 81–87, (2005).

43 McMurray, D. N., Jolly, C. A. & Chapkin, R. S. Effects of dietary n-3 fatty acids on T cell activation and T cell receptor-mediated signaling in a murine model. *J. Infect. Dis.* **182**, S103–S107, (2000).

44 Thies, F. *et al.* Dietary supplementation with γ-linolenic acid or fish oil decreases T lymphocyte proliferation in healthy older humans. *J. Nutr.* **131**, 1918–1927, (2001).

45 Bi, X. *et al.* ω-3 polyunsaturated fatty acids ameliorate type 1 diabetes and autoimmunity. *J. Clin. Invest.* **127**, 1757-1771, (2017).

46 Zhang, P., Smith, R., Chapkin, R. S. & McMurray, D. N. Dietary (n-3) polyunsaturated fatty acids modulate murine Th1/Th2 balance toward the Th2 pole by suppression of Th1 development. *J. Nutr.* **135**, 1745–1751, (2005).

47 Zhang, P. *et al.* Dietary fish oil inhibits antigen-specific murine Th1 cell development by suppression of clonal expansion. *J. Nutr.* **136**, 2391–2398, (2006).

48 Block, R. C., Harris, W. S., Reid, K. J., Sands, S. A. & Spertus, J. A. EPA and DHA in blood cell membranes from acute coronary syndrome patients and controls. *Atherosclerosis* **197**, 821-828, (2008).

49 Zaragoza, C. *et al.* Animal models of cardiovascular diseases. *J. Biomed. Biotechnol.* **2011**, 497841, (2011).

50 Getz, G. S. & Reardon, C. A. Animal models of atherosclerosis. *Arterioscler. Thromb. Vasc. Biol.* **32**, 1104–1115, (2012).

51 Saeidnia, S., Manayi, A. & Abdollahi, M. From in vitro experiments to in vivo and clinical studies; pros and cons. *Curr. Drug Discov. Technol.* **12**, 218-224, (2015).

52 Brunzell, J. D. Hypertriglyceridemia. *N. Engl. J. Med.* **357**, 1009-1017, (2007).

53 Wang, Z., Gerstein, M. & Snyder, M. RNA-seq: a revolutionary tool for transcriptomics. *Nat. Rev. Genet.* **10**, 57-63, (2009).

54 Wilhelm, B. T. & Landry, J. R. RNA-seq-quantitative measurement of expression through massively parallel RNA-sequencing. *Methods* **48**, 249-257, (2009).

55 Hitzemann, R. *et al.* Genes, behavior and next-generation RNA sequencing. *Genes Brain Behav.* **12**, 1-12, (2013).

56 D'Urso, A. & Brickner, J. H. Mechanisms of epigenetic memory. *Trends Genet.* **30**, 230-236, (2014).

57 Moore, L. D., Le, T. & Fan, G. DNA methylation and its basic function. *Neuropsychopharmacology* **38**, 23-38, (2013).

58 Sun, Y., Miao, N. & Sun, T. Detect accessible chromatin using ATAC-sequencing, from principle to applications. *Hereditas* **156**, 29, (2019).

59 Grandi, F. C., Modi, H., Kampman, L. & Corces, M. R. Chromatin accessibility profiling by ATAC-seq. *Nat. Protoc.* **17**, 1518-1552, (2022).

60 Soriano-Baguet, L. & Brenner, D. Metabolism and epigenetics at the heart of T cell function. *Trends Immunol.* **44**, 231-244, (2023).

61 Wellen, K. E. *et al.* ATP-citrate lyase links cellular metabolism to histone acetylation. *Science* **324**, 1076-1080, (2009).

62 Shyer, J. A., Flavell, R. A. & Bailis, W. Metabolic signaling in T cells. *Cell Res.* **30**, 649-659, (2020).

63 Peng, M. *et al.* Aerobic glycolysis promotes T helper 1 cell differentiation through an epigenetic mechanism. *Science* **354**, 481-484, (2016).

64 Lambert, S. A. *et al.* The human transcription factors. *Cell* **172**, 650-665, (2018).

65 Dugourd, A. & Saez-Rodriguez, J. Footprint-based functional analysis of multiomic data. *Curr. Opin. Syst. Biol.* **15**, 82-90, (2019).

66 Yadav, K., Singhal, N., Rishi, V. & Yadav, H. Cell proliferation assays. *eLS*, (2014).

67 Yoonseok, K., Winer, L. P., Rogers, G. W. & Hynes, J. Real-time detection and modulation of human T cell activation using agilent seahorse XF Hu T Cell activation assay kit. *Agilent Technologies, Inc.*, (2020).

68 Shah, K. & Maghsoudlou, P. Enzyme-linked immunosorbent assay (ELISA): the basics. *Br. J. Hosp. Med.* **77**, C98-C101, (2016).

69 Leng, S. X. *et al.* ELISA and multiplex technologies for cytokine measurement in inflammation and aging research. *J. Gerontol. A Biol. Sci. Med. Sci.* **63**, 879–884, (2008).

70 Bustin, S. & Nolan, T. Talking the talk, but not walking the walk: RT-qPCR as a paradigm for the lack of reproducibility in molecular research. *Eur. J. Clin. Invest.* **47**, 756-774, (2017).

71 McKinnon, K. M. Flow cytometry: an overview. *Curr. Protoc. Immunol.* **120**, 5.1.1-5.1.11, (2018).

72 Adan, A., Alizada, G., Kiraz, Y., Baran, Y. & Nalbant, A. Flow cytometry: basic principles and applications. *Crit. Rev. Biotechnol.* **37**, 163-176, (2017).

73 Nolan, J. P. The evolution of spectral flow cytometry. *Cytometry A* **101**, 812-817, (2022).

74 Messele, T. *et al.* Nonradioactive techniques for measurement of in vitro T-cell proliferation: alternatives to the [3H]thymidine incorporation assay. *Clin. Diagn. Lab. Immunol.* **7**, 687–692, (2000).

75 Quah, B. J. & Parish, C. R. New and improved methods for measuring lymphocyte proliferation in vitro and in vivo using CFSE-like fluorescent dyes. *J. Immunol. Methods* **379**, 1-14, (2012).

76 Ornatsky, O. *et al.* Highly multiparametric analysis by mass cytometry. *J. Immunol. Methods* **361**, 1-20, (2010).

77 Williams, J. W. *et al.* Single cell RNA sequencing in atherosclerosis research. *Circ. Res.* **126**, 1112-1126, (2020).

78 McDonald, W. H. & Yates, J. R. I. Shotgun proteomics and biomarker discovery. *Dis. Markers* **18**, 99–105, (2002).

79 Steffen, B. T., Duprez, D., Szklo, M., Guan, W. & Tsai, M. Y. Circulating oleic acid levels are related to greater risks of cardiovascular events and all-cause mortality: The Multi-Ethnic Study of Atherosclerosis. *J. Clin. Lipidol.* **12**, 1404-1412, (2018).

80 Tiyyagura, S. R. & Smith, D. A. Standard lipid profile. *Clin. Lab. Med.* **26**, 707-732, (2006).

81 Meikle, T. G., Huynh, K., Giles, C. & Meikle, P. J. Clinical lipidomics: realizing the potential of lipid profiling. *J. Lipid Res.* **62**, 100127, (2021).

CHAPTER 7

Appendix

Summary

Atherosclerosis is the primary contributor to cardiovascular disease (CVD), which remains the leading cause of death worldwide and is fundamentally driven by the interactions between lipids, the immune system, and the vascular wall. Atherosclerosis is characterized by the accumulation of fats in the blood vessel walls, which attracts immune cells that then trigger an inflammatory response. Despite the immune system's attempts to clear these fats, the inflammation persists leading to chronic inflammation. This ongoing inflammation leads to an increasing buildup of fats and immune cells, resulting in the formation of atherosclerotic plaques. When these plaques eventually rupture, it can have serious consequences such as heart attacks or strokes.

Until recently, this disease was mainly associated with cholesterol, a lipid, and macrophages, a type of immune cell that continuously takes up cholesterol in the vessel walls until a fatty atherosclerotic plaque is created. However, recent research has highlighted the importance of other factors, such as triglycerides and T cells, in the development of atherosclerosis. Excessive triglycerides in the bloodstream can cause and/or aggravate the disease when present in excess, particularly through triglyceride-rich lipoproteins. Additionally, T cells, a key component of the adaptive immune system, are also found in large numbers within atherosclerotic plaques. However, these cells and lipids are already present and interacting in the human body before they reach the site of the atherosclerotic plaque. Thus, the aim of this thesis is to better understand how triglycerides and fatty acids can influence T cells in the context of atherosclerosis.

In the human body, each cell and lipid plays an important role. In this intricate system, triglycerides are crucial building blocks that provide energy and structure to cells. Triglycerides are composed of three fatty acid molecules attached to a glycerol backbone. These lipids serve as an energy reservoir because they can be broken down by the cell, releasing the fatty components, which can then be used by cells to fuel various cellular processes. As such, fatty acids also play a crucial role in the human system. Fatty acids can be divided into saturated, monounsaturated, and polyunsaturated fatty acids. This classification is based on the number of double bonds in the chemical structure of the fatty acid: saturated fatty acids have no double bonds, monounsaturated fatty acids have one, and polyunsaturated fatty acids have two or more. Generally, saturated fatty acids are considered unhealthy, while unsaturated fatty acids are seen as healthy.

T cells are specialized immune cells that can identify and respond to their environment, including triglycerides and fatty acids. T cells in the circulation are generally in an inactive, or non-activated, state. In this state, T cells do not proliferate, do not produce cytokines, and exhibit low metabolic activity in the form of beta-oxidation. Only when stimulated by antigen-presenting cells, such as macrophages or dendritic cells, do they become activated and initiate immune responses. Once activated, T cells will proliferate, produce cytokines, and shift their metabolism to aerobic glycolysis, fatty acid biosynthesis, and cholesterol biosynthesis. However, whether the interaction with triglycerides and various fatty acids influences T cells, and whether this can lead to adverse reactions in high lipid environments, like the atherosclerotic plaque, remains unknown.

To investigate this question, this thesis employs various *in vitro*, -omics, and *in vivo* techniques. An *in vitro* experiment studies things outside of a living organism. As such, the term "in vitro" literally means "in glass", referring to experiments conducted in controlled environments such as test tubes or Petri dishes. An -omics experiment studies large amounts of biological data, such as all genes (transcriptomics), proteins (proteomics), or metabolites (metabolomics) in an organism, to provide a comprehensive overview of biological processes. An *in vivo* experiment is conducted within a living organism, such as an animal or a human. Instead of working with laboratory glassware, tests are performed directly in the body. This helps scientists understand how a treatment or substance behaves in a real biological environment. As a result, this thesis leads to a more comprehensive understanding of the impact that fatty acids and triglyceride levels have on T cell function.

First, we systematically mapped the known effects of fatty acids on T cell function and then compared these with the known effects of the same fatty acids on the development and progression of atherosclerosis. By dividing T cell function into four categories (metabolism, activation, proliferation and differentiation) we could map out the individual effects of 14 different fatty acids on T cell function. Interestingly, the way fatty acids were found to influence T cells aligned with the impact these fatty acids have been found to have on the development of atherosclerosis. However, it is important to note that these results were all found in activated T cells, and may not necessarily reflect the interactions and influences fatty acids are having on T cells in the circulation, prior to activation.

To investigate how fatty acids influence T cell function prior to activation we developed an *in vitro* model. Here, we focused on $CD4^+$ T cells, which are generally thought to play a pro-inflammatory role in CVD. These $CD4^+$ T cells were exposed to one of the most abundant fatty acids in the circulation, oleic acid, which has also been shown to be associated with an increased risk of CVD. Using our *in vitro* exposure model we examined the expression levels of thousands of genes simultaneously, via RNA sequencing. After exposing non-activated $CD4^+$ T cells to oleic acid, this transcriptomics approach revealed strong changes in T cell metabolism towards a pro-inflammatory state, as the cells increased the expression of genes related to fatty acid and cholesterol biosynthesis. This result was further validated by activating the $CD4^+$ T cells after oleic acid exposure and measuring the development of T cell subsets. The results showed that when T cells were pre-exposed to oleic acid, they were more likely to become IL-9^+ producing T cells after activation compared to T cells that were not pre-exposed. IL-9 is the hallmark cytokine of the highly pro-inflammatory T_H9 subset, which has been associated with atherosclerosis pathogenesis. Interestingly, this finding was inhibited when the cells were also exposed to statins, powerful cholesterol biosynthesis inhibitors, along with oleic acid. These findings suggest that fatty acids can influence atherosclerosis by affecting immune cells, potentially through cellular metabolism.

Expanding upon these findings, we next explored the role of other fatty acid types on $CD4^+$ T cell function. Specifically, we focused on eicosapentaenoic acid (EPA), a polyunsaturated omega-3

fatty acid. This fatty acid was used in the REDUCE-IT study, which showed that patients with hypertriglyceridemia who received EPA had reduced triglyceride levels, risk of cardiovascular events, and cardiovascular mortality compared to a placebo. Despite these results, it remains unclear how EPA provides its benefits, and there are only limited studies on these effects. We identified a strong anti-inflammatory transcriptomic profile in $CD4^+$ T cells exposed to EPA *in vitro*. We also used ATAC sequencing to identify where transcription factors, proteins that influence gene expression, bind to DNA, helping us understand why certain genes were up or down regulated in our transcriptomics results. This analysis showed that GATA3 and PU.1, which are important for the development of T_H2 and T_H9 cells, were reduced, while REV-ERB, which inhibits the development of T_H17 cells, was increased. T_H2, T_H9, and T_H17 are all subsets of $CD4^+$ T cells that have known pro-inflammatory effects in different diseases and as such, the lower expression of these subsets should be beneficial. We additionally tested palmitic acid, a saturated fatty acid, and oleic acid, a monounsaturated fatty acid, to provide a more comprehensive understanding of how fatty acid saturation might affect $CD4^+$ T cells. These results showed that the anti-inflammatory effects were unique to EPA-exposed cells, a finding that may contribute to the unexpectedly strong beneficial effects observed in studies like REDUCE-IT.

Lastly, we aimed to translate our *in vitro* findings to an *in vivo* model. Here, we leveraged a "natural experiment" design, comparing the $CD4^+$ and $CD8^+$ T cells of individuals with elevated triglyceride levels (2.7–8.5 mmol/L) due to primary, or genetic mutations to those without such mutations. This set up mimics a controlled experimental setup where the genetic variation acts as a natural intervention. We once again used RNA sequencing to determine global changes in gene expression in $CD4^+$ and $CD8^+$ T cells of individuals with and without elevated triglyceride levels. We identified a pro-inflammatory transcriptomic profile in T cells derived from individuals with elevated triglycerides. Specifically, we observed upregulation of the *IL6R* gene in $CD4^+$ T cells, a gene that encodes a cytokine causally linked to cardiovascular disease. Notably, patients with triglyceride levels between 2.7–8.5 mmol/L have an increased risk of cardiovascular disease. However, this risk diminishes when triglyceride levels exceed 10 mmol/L, as triglycerides are then primarily stored in particles called chylomicrons, which are too large to easily cross the vessel walls. Interestingly, the pro-inflammatory gene expression profile was not observed in T cells derived from patients with these extremely high triglyceride levels. Furthermore, transcriptomic differences were reversed in patients with low triglycerides (0.1–0.3 mmol/L), or hypotriglyceridemia, a condition suspected to have a protective effect against cardiovascular disease. Lastly, the pro-inflammatory gene expression profile was found in T cells from patients with secondary hypertriglyceridemia (between 2.7–8.5 mmol/L), caused by secondary factors such as diabetes, although to a lesser extent. This research suggests that elevated triglycerides may contribute to cardiovascular disease, potentially by promoting inflammation in T cells.

Collectively, this thesis departs from previous research by examining the complex interaction between fatty acids and T cells, particularly in their early, non-activated stages. The research suggests that $CD4^+$ T cells are strongly influenced by their environment and that cellular metabolism plays a crucial role in cell function. It appears that different fatty acids can have varying effects

on T cells, ranging from pro- to anti-inflammatory, and that measuring global gene expression differences can provide profound insights into the cell's state. Finally, it is suggested that targeting triglycerides and fatty acids may have beneficial effects on atherosclerosis by leveraging the anti-inflammatory properties of T cells. This work opens new avenues for further research and enhances our understanding of the intricate relationship between fatty acids and T cells, which effects on how we understand human health and disease.

Nederlandse samenvatting

Atherosclerose speelt een belangrijke rol in het ontstaan van hart- en vaatziekten, wat wereldwijd de leidende doodsoorzaak is. Atherosclerose, of in de volksmond: aderverkalking, wordt in essentie veroorzaakt door de wisselwerking tussen lipiden, het immuunsysteem en de vaatwand. Atherosclerose is een langdurige ontsteking van de vaatwand van bloedvaten. Hierbij hopen vetten zich op in de vaatwand, wat immuun cellen aantrekt die vervolgens een ontstekingsreactie in gang zetten. Ondanks de pogingen van het immuunsysteem om deze vetten op te ruimen, blijft de ontsteking aanhouden. Deze voortdurende inflammatie leidt tot een toenemende ophoping van vetten en immuuncellen, wat resulteert in de vorming van atherosclerotische plaques. Wanneer deze plaques uiteindelijk scheuren, kan dit ernstige gevolgen hebben zoals hartaanvallen of beroertes.

Tot voor kort ging bijna alle aandacht uit naar cholesterol, een lipide, en macrofagen, een type immuun cel die in de vaatwand ongeremd cholesterol blijft opnemen net zo lang totdat er een vettige atherosclerotische plaque ontstaat. Recent onderzoek heeft het belang van andere factoren, zoals triglyceriden en T cellen, als significante risicofactoren voor atherosclerose geïdentificeerd. Overtollige triglyceride in de bloedbaan kan atherosclerose veroorzaken en/of verergeren, voornamelijk via triglyceride-rijke lipoproteïnen. Daarnaast worden T cellen, een belangrijk onderdeel van het adaptieve immuunsysteem, ook in grote aantallen aangetroffen in zogenoemde atherosclerotische plaques. Echter, deze cellen en lipiden zijn al aanwezig en actief in het menselijk lichaam voordat ze de plaats van de atherosclerotische plaque bereiken. Het doel van dit proefschrift is daarom het beter begrijpen van hoe triglyceriden en vetzuren T cellen kunnen beïnvloeden in de context van atherosclerose.

In het menselijk lichaam speelt elke cel en lipide een belangrijke eigen rol. In dit systeem zijn triglyceriden cruciale bouwstenen die energie en structuur aan cellen leveren. Triglyceriden zijn opgebouwd uit drie vetzuurmoleculen die met elkaar verbonden zijn door glycerol. Triglyceriden dienen als energiereservoir aangezien ze door de cel kunnen worden afgebroken waardoor de verzuurcomponenten vrijkomen. Deze kunnen vervolgens gebruikt worden als voedingsstoffen voor diverse processen in de cel. Op deze manier spelen ook vetzuren een cruciale rol in het menselijk systeem. Vetzuren kunnen onderverdeelt worden in verzadigde, enkelvoudig onverzadigd, en meervoudig onverzadigd. Deze benaming heeft te maken met het aantal dubbele bindingen in de chemische structuur van het vetzuur, waarbij onverzadigde vetzuren geen dubbele bindingen hebben, enkelvoudig onverzadigde vetzuren er één hebben, en meervoudig onverzadigde vetzuren er twee of meer hebben. Over het algemeen worden verzadigde vetzuren als ongezond beschouwd, terwijl onverzadigde vetzuren als gezond worden gezien.

T cellen zijn gespecialiseerde immuuncellen die hun omgeving, waaronder triglyceriden en vetzuren, kunnen waarnemen en daar vervolgens op kunnen reageren. T cellen in de circulatie verkeren over het algemeen in een niet-geactiveerde stand. In deze stand prolifereren T cellen niet, produceren ze geen cytokines en vertonen ze lage metabolische activiteit in de vorm van

bèta-oxidatie. Pas wanneer ze worden gestimuleerd door antigeen-presenterende cellen, zoals macrofagen of dendritische cellen, worden ze geactiveerd en wekken ze immuun responsen op. Zodra een T cel geactiveerd is, zal deze prolifereren, cytokines produceren en zijn metabolisme omzetten naar aerobe glycolyse, vetzuur- en cholesterolbiosynthese. Het is tot nu toe nog niet bekend of T cellen beïnvloed kunnen worden door de interacties met triglyceriden en verschillende vetzuren en of dit vervolgens kan leiden tot ongewenste reacties in een omgeving met hoge lipidengehaltes, zoals een atherosclerotische plaque.

Om deze vraag te onderzoeken hebben we in dit proefschrift verschillende *in vitro*, -omics en *in vivo* technieken toegepast. Een *in vitro* experiment is een type wetenschappelijk onderzoek waarbij dingen worden bestudeerd buiten een levend organisme. Het woord "*in vitro*" betekent letterlijk "in het glas" en verwijst naar het feit dat de experimenten vaak plaatsvinden in containers, zoals reageerbuisjes of petrischalen. Een -omics experiment bestudeert grote hoeveelheden biologische gegevens, zoals alle genen (transcriptomics), eiwitten (proteomics), of metabolieten (metabolomics) in een organisme, om een uitgebreid overzicht van biologische processen te krijgen. Een *in vivo* experiment is een onderzoek dat wordt uitgevoerd binnen een levend organisme, zoals een dier of een mens. In plaats van in een laboratoriumglaswerk te werken, worden de tests direct in het lichaam gedaan. Dit helpt wetenschappers te begrijpen hoe een behandeling of stof zich gedraagt in een echte biologische omgeving. Als resultaat leidt dit proefschrift tot een meer omvattend begrip van de invloed die verzuren en triglycerideniveaus hebben op de functie van T cellen.

Ten eerste hebben we systematisch de bekende effecten van vetzuren op de functie van T cellen in kaart gebracht en hebben we dit vervolgens vergeleken met de bekende effecten van diezelfde vetzuren op de ontwikkeling en progressie van atherosclerose. Dit hebben we gedaan door eerst de functie van T cellen in vier categorieën (metabolisme, activatie, proliferatie en differentiatie) te verdelen. Hierdoor konden we de individuele effecten van 14 verschillende vetzuren op de functie van T cellen in kaart brengen. Opvallend genoeg kwam naar voren dat de manier waarop vetzuren T cellen beïnvloeden overeenkomt met de invloed die deze vetzuren hebben op de ontwikkeling van atherosclerose. Belangrijk is wel dat dit resultaat gevonden werd in geactiveerde T cellen en dat dit resultaat dus niet noodzakelijkerwijs reflecteert hoe vetzuren T cellen beïnvloeden vóór dat deze geactiveerd zijn, zoals de T cellen normaal gesproken voorkomen in de bloedbaan.

Om te onderzoeken hoe vetzuren de functie van T cellen beïnvloeden vóór dat deze geactiveerd zijn, hebben we een *in vitro* model ontwikkeld. Hierbij hebben we ons gericht op $CD4^+$ T cellen, die over het algemeen een pro-inflammatoire rol spelen in atherosclerose. Deze $CD4^+$ T cellen hebben we blootgesteld aan één van de meest voorkomende vetzuren in de circulatie, oliezuur, dat ook geassocieerd is met een verhoogd risico op hart- en vaatziekten. Door gebruik te maken van dit *in vitro* blootstellingsmodel hebben we de expressieniveaus van duizenden genen tegelijkertijd onderzocht via RNA-sequencing. Na het blootstellen van niet-geactiveerde $CD4^+$ T cellen aan oliezuur, vonden we met RNA-sequencing sterke veranderingen in het T cel metabolisme richting een pro-inflammatoire staat, doordat de cellen de expressie van genen die te maken hebben met vetzuurbiosynthese en cholesterolbiosynthese verhoogde. Dit resultaat werd verder bevestigd

door $CD4^+$ T cellen te activeren na de blootstelling aan oliezuur en de ontwikkeling van T cel subsets te meten. De resultaten lieten zien dat wanneer T cellen vooraf zijn blootgesteld aan oliezuur, ze vaker IL-9^+ producerende T cellen worden na activatie dan T cellen die niet vooraf zijn blootgesteld. IL-9 is het kenmerkende cytokine van de sterk pro-inflammatoire T_H9 subset die is geassocieerd met de verergering van atherosclerose. Interessant genoeg werd deze bevinding omgekeerd als de cellen tegelijkertijd aan de blootstelling met oliezuur ook blootgesteld werden aan statines, krachtige cholesterolbiosyntheseremmers. Deze bevindingen duiden aan dat vetzuren atherosclerose kunnen beïnvloeden door immuuncellen aan te tassen, bijvoorbeeld via cellulaire metabolisme.

Vervolgens hebben we de rol van andere vetzuurtypes op de functie van $CD4^+$ T cellen onderzocht. Specifiek hebben we ons gericht op eicosapentaeenzuur (EPA), een meervoudig omega-3 onverzadigd vetzuur. Dit vetzuur was gebruikt in de REDUCE-IT-studie, die aantoonde aan dat patiënten met hypertriglyceredemie die EPA kregen, beter waren in het verlagen van triglyceriden, cardiovasculaire gebeurtenissen en cardiovasculaire sterfte dan een placebo. Ondanks deze resultaten, is het nog steeds onduidelijk hoe EPA precies zijn voordelen biedt, en er zijn slechts beperkte studies gedaan naar deze effecten. Genexpressie levels lieten een sterke anti-inflammatoire profiel zien in de $CD4^+$ T cellen die *in vitro* zijn blootgesteld aan EPA. Om beter te begrijpen waarom bepaalde genexpressie levels verhoogd of verlaagd waren, hebben we ook ATAC-sequencing toegepast om te identificeren waar transcriptiefactoren, eiwitten die de gen activiteit reguleren, binden aan DNA. Deze analyse liet zien dat GATA3 en PU.1, die belangrijk zijn voor de ontwikkeling van T_H2- en T_H9-cellen, verminderd worden, terwijl REV-ERB, dat de ontwikkeling van T_H17-cellen tegenwerkt, verhoogd wordt. T_H2, T_H9, en T_H17 kunnen ieder een pro-inflammatoire rol spelen in verschillende ziektes, en dus is de verlaging van expressie van deze subsets gunstig. Verder hebben we ook T cellen blootgesteld aan palmitinezuur, een verzadigd vetzuur, of oliezuur, een enkelvoudig onverzadigd vetzuur om een breder begrip te krijgen van de rol van de verzadiging van vetzuren in de functie van $CD4^+$ T cellen. Deze resultaten lieten zien dat de anti-inflammatoire effecten uniek waren voor EPA blootgestelde cellen, een bevinding dat kan bijdragen aan de onverwacht sterke gunstige effecten in studies zoals REDUCE-IT.

Tot slot hebben we geprobeerd om onze *in vitro* bevindingen te vertalen naar een *in vivo* model. Hiervoor hebben we gebruik gemaakt van een "natuurlijk experiment" ontwerp, waarbij we de $CD4^+$ en $CD8^+$ T cellen van individuen met verhoogde triglycerideniveaus (2.7–8.5mmol/L) door primaire, of genetische mutaties, vergeleken met die van personen zonder dergelijke mutaties. Deze opzet bootst een gecontroleerde experimentele opstelling na waarbij genetische variatie fungeert als een natuurlijke interventie. We hebben opnieuw RNA-sequencing toegepast om globale verschillen in genexpressie te bepalen in $CD4^+$ en $CD8^+$ T cellen tussen individuen met en zonder mutaties. In de T cellen afkomstig van personen met een verhoogd triglycerideniveau vonden we genexpressie levels die een pro-inflammatoir profiel markeren. Specifiek zagen wij een op-regulatie van het gen *IL6R* in de $CD4^+$ T cellen, een gen dat een cytokine codeert die causaal verband houdt met hart- en vaatziekten. Opmerkelijk is dat patiënten met een triglyceridegehalte tussen de 2.7–8.5mmol/L een verhoogd risico op hart- en vaatziekten hebben.

Dit risico vervalt echter als het triglycerideniveau boven de 10mmol/L komt, doordat triglyceriden dan voornamelijk worden opgeslagen in deeltjes die chylomicronen heten, die te groot zijn om gemakkelijk door de vaatwand heen te kunnen passeren. Opmerkelijk genoeg kwam het pro-inflammatoir gen expressie profiel niet te voren in T cellen afgeleid van patiënten met deze extreem hoge triglyceriden. Verder werden de transcriptieverschillen omgekeerd bij patiënten met lage triglyceriden (0.1–0.3mmol/L), of hypotriglyceredemie, een aandoening dat ook verdacht wordt van een beschermend effect tegen hart- en vaat ziekte. Als laatste was het pro-inflammatoire gen expressie profiel in T cellen afgeleid van patiënten met secundaire hypertriglyceredemie (tussen de 2.7–8.5mmol/L), veroorzaakt door secundaire oorzaken zoals diabetes, wel terug gevonden, hoewel in mindere mate. Dit onderzoek wijst erop dat verhoogde triglyceriden kunnen bijdragen aan hart- en vaatziekten, potentieel door een inflammatie in T cellen te bevorderen.

Samenvattend breekt dit proefschrift met eerdere onderzoeken door te kijken naar de complexe interactie tussen vetzuren en T cellen, vooral in de vroege, niet-geactiveerde stadia. Het onderzoek suggereert dat $CD4^+$ T cellen sterk worden beïnvloed door hun omgeving en dat cel metabolisme een belangrijke rol speelt in de uiteindelijke cel functie. Het blijkt dat verschillende vetzuren uiteenlopende effecten kunnen hebben op T cellen, variërend van pro- tot anti-inflammatoir, en dat het meten van globale genexpressieverschillen diepgaande inzichten kan geven in de toestand van de cel. Tot slot wordt gesuggereerd dat het aanpakken van triglyceriden en vetzuren mogelijk gunstige effecten kan hebben op atherosclerose door de ontstekingsremmende eigenschappen van T cellen te benutten. Dit werk opent nieuwe mogelijkheden voor verder onderzoek en bevordert een beter begrip van de ingewikkelde relatie tussen vetzuren en T cellen, met implicaties voor de kennis over gezondheid en ziekte.

List of publications

1. **Reilly, N. A.**, Dekkers, K. F., Molenaar, J. M., Arumugam, S., Kuipers, T. B., Ariyurek, Y., Hoeksema, M. A., Jukema, J. W., & Heijmans, B. T. Eicosapentaenoic acid induces an anti-inflammatory transcriptomic landscape in T cells implicating a pathway independent of triglyceride lowering in cardiovascular risk reduction. *BioRxiv,* (2024).

2. **Reilly, N. A.**, Sonnet, F., Dekkers, K. F., Kwekkeboom, J. C., Sinke, L., Hilt, S., Suleiman, H. M., Hoeksema, M. A., Mei, H., van Zwet, E. W., Everts, B., Ioan-Facsinay, A., Jukema, J. W., & Heijmans, B. T. Oleic acid triggers metabolic rewiring of T cells poising them for T helper 9 differentiation. *iScience* 27, 109496, (2024).

3. **Reilly, N. A.**, Lutgens, E., Kuiper, J., Heijmans, B. T. & Jukema, J. W. Effects of fatty acids on T cell function: role in atherosclerosis. *Nat. Rev. Cardiol.* 18, 824–837, (2021).

4. Lu, M., Krutovsky, K. V., Nelson, C. D., West, J. B., **Reilly, N. A.**, & Loopstra, C. A., Association genetics of growth and adaptive traits in loblolly pine (Pinus taeda L.) using whole-exome-discovered polymorphisms. *Tree Genetics & Genomes* 13, (2017).

Curriculum Vitae

Nathalie Reilly was born on the 25th of August, 1992 in Amsterdam, The Netherlands. She moved to the United States of America when she was 12 and completed her secondary school cum laude in 2011 in Chapel Hill, North Carolina.

She then moved to Wilmington, North Carolina to obtain her bachelor's degree in Biology with a minor in Chemistry at the University of North Carolina Wilmington. During this time, she interned three times, twice in Wilmington firstly studying the genetics of bird evolution in the group of Dr. Marcel van Tuinen and secondly investigating the gut microbiome of beached whales in the group of Dr. Ryan Rhodes. She also interned as part of the PINEMAP program in College Station, Texas helping to investigate how pine forest genetics could be modified to make them more resistant to global warming in the group of Dr. Carol Loopstra. As part of this program she also taught biology to local middle school and high school students in Wilmington, North Carolina. She completed her bachelor's degree cum laude at the University of North Carolina Wilmington in 2015.

Nathalie then moved back to Amsterdam, The Netherlands to continue her education with a master's degree in Biomolecular Sciences at the Vrije Universiteit Amsterdam. As part of her training she completed two internships. First, she worked at the company BioDetection Systems researching the anti-inflammatory properties of shiitake mushroom extracts on adipocyte development. Second, her master's thesis was executed under the supervision of Dr. Jack van Loon of the Academisch Centrum Tandheelkunde Amsterdam (ACTA) and the European Space Agency (ESA) and Dr. Jessica Legradi of the Department of Environment and Health at the Vrije Universiteit Amsterdam. This internship focused on how different levels of gravity, ranging from microgravity (approaching 0g's) to hypergravity (2, 4, and 6g's) influence adipocyte metabolism in 3 different animal models (*Daphnia magna*, *Folsomia candida*, and *Nasonia vitripennis*). She completed her master's degree at the Vrije Universiteit Amsterdam in 2018.

After obtaining her Master's degree in 2018, Nathalie started her PhD at the Leiden University Medical Center at the Department of Biomedical Data Sciences, Molecular Epidemiology and the Department of Cardiology under the supervision of Prof. dr. Bas Heijmans and Prof. dr. Wouter Jukema. Here, she focused on how triglycerides and fatty acids could influence the transcriptome and epigenome of circulating T cells, in the context of atherosclerosis. The results of this research are outlined in this thesis. During her PhD, Nathalie collaborated with several research groups in The Netherlands and presented her work at national and international conferences, including

the Dutch National Lipid Day, the Rembrandt Symposium, the International Conference on ImmunoMetabolism, and Epigenomics of Common Diseases. At the Rembrandt Symposium and the Dutch National Lipid Day she won awards for her poster and oral presentations, respectively. Nathalie also received two grants during her PhD, one awarded to hire a promising master student for 6 months to start developing an exciting new project and a second one to travel to attend an international conference.

Currently, Nathalie is employed at the nuclear medicines company Curium as a Research Scientist in the Research and Development team. Here, she is working on discovering and developing cutting-edge radiopharmaceuticals to diagnose and treat diseases such as cancer.

Acknowledgements

After more than 5 years, my adventure as a PhD student has come to an end. This trajectory has taught me resilience, perseverance, and the art of navigating unexpected detours. I have learned so much and grown into the scientist I am today thanks to all the wild and wonderful experiences. So, a big shout out to myself for staying ridiculously positive, dedicated, and determined through every caffeine-fueled late night! Of course, I wouldn't be where I am today without the support of my amazing family, friends, and colleagues. Thank you all for always being there for me and encouraging me throughout this journey.

Als eerste wil ik graag mijn supervisors Prof. dr. Bas Heijmans en Prof. dr. Wouter Jukema bedanken voor de gelegenheid om mijn promotietraject binnen jullie groepen te kunnen doen en voor jullie eeuwige enthousiasme in ons onderzoeksonderwerp. Bas, jou passie voor wetenschap is aanstekelijk en ik neem die passie graag mee in mijn verdere leven. Wouter, ondanks jou drukke schema heb je altijd tijd voor mij gemaakt om bij te praten over ons onderzoek, artikelen, en leven, en dat waardeer ik ontzettend.

Next, I want to thank all my colleagues at MOLEPI and within the Epigenetics group for their support. Lucy, Jazmin, Mahnoor, Laura, Thomas, Yunfeng, and Tom you all made our group feel warm and welcome. Ilja en Pia, zoals beschreven in ons gedicht, we zijn drie erwten in een peul, Pia een zonnestraal zo helder en Ilja met een glimlach zo breed. Door jullie voelde onze kantoor als een tweede thuis, we hebben samen gelachen, gehuild, gejuicht, en gekreund, en ik zal eeuwig dankbaar zijn voor jullie vriendschap. Dani Bizzari, thanks for being my friend inside and outside of work and always being ready to go on random adventures to trampoline parks with me.

I would also like to thank all my great collaborators along the way. Andreea Ioan-Facsinay, Bart Everts, Marten Hoeksema, Joanneke Kwekkeboom, and Jeanine Roeters van Lennep, without you this research would not have been possible. Koen, je stond door de jaren heen altijd voor mijn velen vragen gereed, en je geduld en deskundigheid hebben mij en dit project enorm geholpen. Janneke, het was een plezier om samen met jou te kunnen werken aan ons hypertriglyceredemie project, we zijn samen een sterk team en dat heeft geleid naar een schitterend artikel. Rike, you jumped right into helping me even while finishing your own PhD. Your enthusiasm and expertise made you a joy to work with and I'm glad we had this opportunity to get to know each other. Prof. dr. Ingrid Meulenbelt, bedankt voor je steun en bereidbaarheid om mij te coachen, ik heb jou hulp ontzettend gewaardeerd.

Aan mijn stagiaires, Stan, Jeroen, en Sinthuja, ik vond het een ontzettende eer om zo'n leuke studenten als jullie te hebben kunnen begeleid. Ik vond het heel fijn om met jullie samen te hebben gewerkt en dat jullie erbij zijn gebleven door alle lange experimenten die ik jullie kant op gooide.

To my friends, Fernando, Vanessa, Jose, Lisette, Hester, Frédérique, Juliette, Jackie, Maddie, Onur, Sandra, Nick Stauble, and Tes thank you for always encouraging me to be the best, most nerdy version of myself.

Lieve Papa, je hebt mij geleerd dat het leven bestaat uit een beetje cultuur en een beetje plezier, en die houding heb ik mee genomen tijdens mijn PhD. Uit jouw eigen verhaal heb ik geleerd dat ik alles kan bereiken wat ik wil met een beetje moed en toewijding, dankjewel. Dear Mom, thank you for showing and teaching me what strong independent women can achieve. You've always had the remarkable ability to help people see how much they have to offer the world and for that I am endlessly grateful. Dear Brendan, your creativity motivates me to see the world in different technicolor lights. You remind me that normal is boring and that adding a little flare (or a lot) of attitude is the best way to make every day feel like a party. Dear Dani, the moon to my sun, your tireless dedication to running your own companies is immensely inspiring. You never fail to brighten my day with your ceaseless enthusiasm and empathy, thank you for walking through this life with me. Dear Oli, dear Guapo, your dedication to becoming a better version of yourself always inspires me. Thank you for rescuing me in the middle of the night when I missed the last train home because my experiments ran long and for always reminding me to go out and exercise.

Reflecting on this journey, I know that the lessons I've learned and the people I've met will stay with me and inspire me in all my coming endeavors. I'm looking towards the sunshine and I can't wait to see what the future will bring.